Development of a feasibility framework for lignite-based controlled-release fertilisers

A thesis presented in partial fulfilment of the requirements
for the degree of

Master of Philosophy
in
Engineering

at Massey University, Manawatū campus, New Zealand

Sonja G. Willemse
May 2020

Every man is guilty of all the good he did not do.

Voltaire
(1694 – 1778)

ABSTRACT

Excessive agricultural fertilisation of the essential nutrients nitrogen (N), phosphorus (P) and potassium (K) causes severe environmental damage and financial losses for farmers. The efficiency of conventional commercial fertilisers is low because nutrients are released at a faster rate than plants can uptake, resulting in surface runoff, leaching and volatilisation losses. The environmental concerns are pressing, and considerable resources are dedicated to the development of a new fertilisation strategy. The ultimate solution would be a controlled-release fertiliser that consists of a cheap and strong base material that requires simple pre-treatment, constitutes efficient controlled-release of nutrients independent of soil and environmental conditions, has soil remediating properties, and increases P bioavailability.

Literature has shown that lignite, the lowest grade coal, has the potential to act as a matrix for adsorption, but no comprehensive research has been conducted on the feasibility of such a substrate in an agricultural context. The inhomogeneity of lignite poses so far unanswered challenges, in particular the requirement of a case-by-case assessment of individual lignite types and their potential to act as a fertiliser matrix. This research provides a solution to those challenges by offering a feasibility framework that experimentally assesses which pre-treatments are required to optimise the adsorption of nutrients onto any given lignite type, in order to produce prototypes for environmentally and economically feasible lignite-based controlled-release fertilisers.

In order to maximise fertiliser efficiency, the focus is on maximising nutrient uptake by the lignite structure. In the framework, it is hypothesised that nutrient uptake can be maximised by manipulating certain properties of lignite. A case study with a local New Zealand type of lignite, Kai Point lignite, was used to develop methods that allow for the evaluation of a range of property manipulations. Parameters investigated were grinding time, solvent treatment, nutrient species, pH, temperature and initial concentration. The properties manipulated were particle size distribution, specific surface area, micro and meso pore volume and nutrient uptake capacity of lignite.

Special emphasis is placed on solvent treatment of lignite. It is proposed that choosing an appropriate solvent can induce swelling of the lignite structure in such a manner that the availability of binding sites is increased, fostering nutrient uptake and retention capacity. The results of the case study showed that the combination of particle size distribution control and the use of acetone as the swelling solvent constituted solvent swelling of Kai Point lignite, attaining a maximum of 57 % swelling. When analysing nutrient uptake capacity, it was found that under specific conditions solvent swelling can increase nutrient adsorption by almost 94 %. In the scoping experiments, a minimum nutrient-N content of 6.5 % and a maximum of 37 % is attained for Kai Point lignite.

During the case study it became apparent that the inhomogeneous nature of lignite demands a significant number of replicates to get statistically significant results in the feasibility framework. The large number of replicates is projected to make experimentation and analysis a time-consuming endeavour. In anticipation of this problem, a new rapid batch method was established for the automated gathering, processing and analysis of experimental lignite swelling data.

This research shows the potential of specific manipulations to increase the cost-efficiency and environmental benefits of lignite-based controlled release fertilisers, and provides a practical feasibility framework with methods capable of tailoring those manipulations to any type of lignite.

ACKNOWLEDGEMENTS

This research is a cooperation between Massey University and CRL Energy Ltd. and is funded by the New Zealand Ministry of Business, Innovation and Employment through the Smart Ideas - Endeavour Fund.

I would like to acknowledge the following people for their contributions to this work. Dr Nicola Brown, for her invaluable supervision and who's insight shaped this thesis into a coherent and flowing apotheosis of an eventful postgraduate research journey. Dr Luke Fullard, lecturer in mathematics, whose knowledge, expertise and relentless enthusiasm for coding and science aided in the conception of a novel image analysis tool. And Nick Look, IT Team leader of the School of Food and Advanced Technology, who came to the rescue on numerous occasions, with not only his technical expertise, but also his wit and humour, and without whom this research would have been a time consuming and daunting task.

My gratitude also goes out to the technicians in the School of Food and advanced technology. Anne-Marie Jackson, head of biotechnology labs, for her enthusiasm and remarkable capacity to provide students with all the resources necessary to conduct diligent laboratory research, while maintaining an ordered, professional and pleasant laboratory environment. Anthony Wade, electronics technician, for his help with constructing the lightbox setup and the delightful conversations. Michelle Tamehana, Kylie Evans, John Edwards and John Sykes of the School of Food and Advanced Technology, and Anja Moebis of the School of Agriculture and Environment, who's expertise greatly contributed to alleviating the task of finding the appropriate knowledge and resources to accommodate this research.

My deepest gratitude goes out to my fellow postgraduate students, my friends, who will not be named only out of consideration for their privacy. The saying *"the people make the place"* has never been truer. Their company, support and inspiration, and the interesting and amusing technical and philosophical discussions brought life to even the

most drudging, 14-hour lab-days and challenging after-hours data analyses. Their care and kindness for passing on the knowledge gained from their own positive and negative experiences during their postgraduate journey have greatly helped me navigate through the bureaucratic jungle of academia.

Lastly, I want to convey a special thanks to William Wilkinson, who has been unwavering by my side and dedicated in his support throughout this unusual postgraduate journey. His help constituted emergency Apple-related assistance, but most notably, moral support at dark times when a thesis was the least challenging aspect of our lives. His help was as crucial to the ultimate completion of this thesis as the assistance of all the university staff mentioned above combined.

GLOSSARY OF TERMS AND ABBREVIATIONS

TERM	DEFINITION
ATR-FTIR	Attenuated Total Reflectance - Fourier Transform Infrared spectroscopy; a non-destructive analytical technique used to determine the chemical bonds present in a material.
Bentonite	A montmorillonite containing silicate mineral with lamellar structure.
Brown coal	Lignite, the lowest ranked grade of coal.
CRL Energy Ltd.	An energy, minerals, and environmental research and consulting company based in Lower Hutt, New Zealand.
D_M	Mass-median diameter of wet slurry.
Electrophoretic mobility	The motion of one phase relative to an interface with a different phase under the influence of an external electric field, e.g. the motion of a particle dispersed in a fluid or of a liquid in a solid (Tadros, 2015).
FES	Flame Emission Spectrometry: analytical technique where atoms are excited in a flame, and the intensity of the emitted light is measured.
Kai Point	A subbituminous coal mine in Otago.
Humic and fulvic acids	A general name for naturally occurring, biogenic, heterogeneous organic substances that can generally be characterised as yellow to black in colour, of high molecular weight (MW), and refractory.
Lignite	The lowest ranked grade of coal, also known as brown coal.
Lithotype	A geological unit characterised by its specific lithology, its sedimentary origin and its climatic-stratigraphical position.
N_2O	A greenhouse gas that also depletes the ozone layer.
N/P/K	Nitrogen/Phosphorus/Potassium
Nitrogen (N)	An element essential for plant nutrition.
pH	A measure of how acidic/basic water is.

Phosphorus (P)	An element essential for plant nutrition.
pK_a	The negative log of the acid dissociation constant, K_a, used to indicate the strength of an acid.
Point of zero charge	Or iso-electric point, the specific pH where the surface groups are uncharged.
Potassium (K)	An element essential for plant nutrition.
Precision agriculture	Practical land management solutions through the use of leading edge precision technology tools.
Proximate analysis	Moisture, ash, volatile and fixed carbon and sulphur content of a coal sample.
PSD	Particle size distribution.
Raw lignite	Lignite as it is obtained from a mine.
Slurry	A semi liquid mixture of fine particle in liquid.
TGA	Thermogravimetric analysis.
Ultimate analysis	Quantitative analysis of a coal sample especially in terms of the elements carbon, hydrogen, sulphur, oxygen, and nitrogen, trace elements and ash.
Urea	An organic compound with the chemical formula $CO(NH_2)_2$ and a 46% nitrogen fertiliser.
UV/VIS	Ultraviolet-visible spectroscopy: fast and inexpensive analytical technique where absorbance in the UV and visible light range is measured of a solution.
PXRD	Powder X-ray diffraction; a non-destructive analytical technique used to determine the mineralogical and structural characteristics of materials.
XRF	X-ray fluorescence; a non-destructive analytical technique used to determine the elemental composition of materials.
Zeta potential	The potential difference between the static fluid layer surrounding particles and the dispersion medium.

Glossary adapted from MBIE Project Proposal for the 2017 Endeavour Fund - Smart Ideas.

TABLE OF CONTENTS

LIST OF FIGURES

LIST OF TABLES

LIST OF EQUATIONS

CHAPTER 1

INTRODUCTION

1.1 Rationale and importance of research

Fertilisers release nutrients at a rate faster than plants can uptake, causing dire environmental issues and heavy financial losses for farmers. To provide plants with sufficient quantities of essential nutrients and to obtain maximum yield, farmers resort to overfertilization (Cameron et al., 2013, Fageria and Baligar, 2005). The essential agricultural nutrients are nitrogen (N), required for the growth of leaves and stems; phosphorus (P), important for seed germination and root growth; and potassium (K), fostering flower and fruit growth.

Overfertilization has caused planet-wide shortages of nitrogen and potassium fertilisers and high prices of phosphate fertilisers (Begeman, 2018, Childers et al., 2011). Excessive fertilisation can cause fertiliser burn, also known as leaf scorch, when combined with dry and high temperature environmental conditions. It is the result of a disproportionate amount of (fertiliser) salts in the soil, causing osmotic stress and hypertonicity in plants, decreasing profit for farmers.

The real issue, however, lies with the environmental implications of overfertilization which manifest themselves at a much larger scale and higher cost (Dodds et al., 2009). The main contributor to the overfertilization problem, and thus the focus of this study, is the high reactivity and mobility of fertiliser-N (Jackson et al., 2008). Leaching and volatilisation of N cause elevated greenhouse gas emissions in the form of nitrous oxide (Vitousek et al., 1997, Ye et al., 1994, Morgan et al., 2004) and pollution of waterways. The latter results in eutrophication and drinking water contamination, along with changes and depletion in aquatic biodiversity (Hautier et al., 2009, Goulding et al., 2008).

Fertiliser-P, on the other hand, is less soluble than N and therefore less susceptible to leaching and volatilisation. This has resulted in P build-up in soil and subsequent surface runoff and subsurface drainage, contributing to eutrophication of waterways (Eastman et al., 2010, Eslamian et al., 2018). In some areas of the world the build-up of impurities found in P-fertilisers, such as fluorine (Gray, 2018), cadmium (Stafford et al., 2018), uranium (Salmanzadeh et al., 2017) and radium (Pearson et al., 2019), has caused soil contamination.

K-overfertilization is causing less environmental issues than N and P, because potassium is not very mobile, particularly in clay soils (Sardi and Csitari, 1998), and is applied in much smaller quantities than nitrogen and phosphate. Potassium does play a role with regards to the economics of fertilisation since the element is getting scarcer and thus more expensive. Potassium is often used in combined N/P/K fertilisers and accommodates for a complete fertiliser package.

A functional and economically viable method is urgently needed to control and match the nutrient release rate of fertilisers to plant requirements, and limit environmental effects that exacerbate weathering and leaching of N/P/K. While efforts have been made both by academics and industry in the form of new types of fertilisers and precision agricultural techniques, a truly sustainable, environmentally friendly, practical and cost-effective fertilisation strategy has yet to be found (Ganesapillai and Simha, 2015, Safwat and Matta, 2018). Current methods of controlling the release rate of fertilisers are organic and inorganic low-solubility compounds and physical barriers that prevent the immediate release of N/P/K. There are two types of physical barriers: coatings, encapsulating spheres or granules of nutrient species, and matrices, in which nutrients are dispersed or adsorbed. This research focusses on the development of a new type of fertiliser matrix that can be paired with state-of-the-art precision agriculture as well as conventional agricultural techniques.

Lignite, a type of low-calorific coal, also known as brown coal, has been found to possess properties that make it remarkably suited as absorbent. Though lignite has large spatial variability, the overall preferential properties are lignite's high specific surface area due to its extensive pore structure, its uneven and wide distribution range of pore sizes (Pan et al., 2019), its humic and fulvic acid content (Kiss et al., 1984), its high number of

oxygen-containing functional groups which act as binding sites (Kwiatkowska et al., 2008), its capacity to swell in volume when in contact with certain solvents (Jones et al., 1991), and lastly, the world-wide abundance of lignite (Jones, 2016b) and its low cost (Denne et al., 2009).

The preferential properties mentioned above provide lignite with unique uptake capabilities which have been studied for various applications such as NO_x and CO_2 adsorption (Vinodh et al., 2015, Sarah and Rajanikanth, 2016), copper adsorption (Ling Ong and Swanson, 1966) and the adsorption of quinoline (Xu et al., 2016). Recently, several studies have hinted that lignite can also be used in an agricultural setting to host nitrogen (Rose et al., 2016, Sun et al., 2016, Paramashivam et al., 2016, Saha et al., 2017, Saha et al., 2019). This leads to the question if the manipulation of the preferential properties of lignite (also referred to as "lignite property manipulation") can aide in the development of a lignite-based controlled-release fertiliser that is an environmentally friendly alternative to current controlled-release fertiliser strategies, used in both conventional and precision agricultural practices.

In precision agriculture, it is not desirable to produce only one type of fertiliser that contains all three essential agricultural nutrients (N/P/K) in a fixed ratio. What sets precision agriculture apart, is customisability: the specific nutritional needs of individual plants can be addressed by using robots that deliver exactly the amount of nutrients the plant requires (Brase, 2006). This type of tailored fertilisation demands fertilisers with a known quantity of only one nutrient which are used in addition to the general combined fertilisers with specific N/P/K ratios (Haneklaus and Schnug, 2006).

1.2 Scope of research

This thesis aims to provide a practical framework to examine through experimentation if a particular type of lignite is a potential candidate for a lignite-based controlled-release fertiliser and how it can be manipulated to increase nutrient adsorption. Though the experimental work in this thesis focusses on nitrogen, the framework needs be able to examine the efficacy of lignite property manipulation to foster adsorption of either N, P,

K, or a combination of the three nutrients. It is imperative that the subsequent controlled release of the adsorbed nutrients is investigated to match plant specific nutrient uptake, and the framework also needs to be able to examine which delivery type might be optimal for potential deployment in precision agriculture.

Methodical control of, and procedures for, the manipulation of the properties of lignite will be introduced and employed within the feasibility framework. The framework evaluates a range of manipulations for prototype development, such as mechanical comminution, solvent swelling, nutrient species, pH and temperature variations. In the framework, detailed methods are established and demonstrated to produce prototypes of lignite-based fertilisers.

In order to develop the abovementioned methods, this research uses Kai Point lignite (Otago, NZ, 45°28'39"S 169°18'24"E) as a case study. Due to the large spatial variability of lignite (sometimes even within quarries), the designed methodologies should be able to assess the suitability of any type of lignite as the basis for a new group of matrix-based controlled-release fertilisers, and the efficacy of property manipulations to increase nutrient adsorption.

In order to develop such a versatile feasibility framework for a potential lignite based-controlled release fertiliser, this study aims to:

1. Determine which properties and parameters are of primary importance when developing a potential lignite-based controlled-release fertiliser;
2. Provide a case study with a proof-of-concept of lignite property manipulation, solvent swelling and nutrient uptake by a type of local lignite;
3. Develop detailed methods to examine and characterise the ability of lignite property manipulation to maximise nutrient adsorption onto lignite.

While outside the scope of this research, it is essential that the proposed feasibility framework can provide tools to *in vitro* examine how the manipulation of lignite properties affects controlled-nutrient release character, and if the release occurs in a manner that competes with current (commercial) fertilisers. Next, guidelines need to be developed to evaluate the optimal delivery type (e.g. slurry, granules, pellets) of lignite-based controlled-release fertiliser prototypes, aimed at precision agriculture.

After using the proposed framework to produce prototypes with the most potential, field trials need to be conducted to compare the performance of lignite-based controlled-release fertilisers to conventional fertilisers strategies. Future larger-scale field trials should reveal what the implications are of adding lignite to the (agricultural) environment from an ecological and health and safety perspective. The field trials should be followed by an assessment of the scalability and economic feasibility of the newly designed lignite-based controlled-release fertilisers. Only after a thorough evaluation of both the environmental and economic aspects, can a truly sustainable alternative fertiliser strategy be developed.

CHAPTER 2

LITERATURE REVIEW

2.1 Background: The need for a new fertiliser strategy

Managing soil fertility has proven to be a challenge for farmers and legislators alike (Cameron et al., 2013). Nutrient losses from fertilisation and animal manure can occur through *1)* (sub)surface runoff (leaching), *2)* volatilisation and *3)* immobilisation. In many areas of the world, about 50 % of the applied nutrients are lost to the environment through leaching and volatilisation (Modolo et al., 2018, Raun et al., 2002), a visualisation of these processes is given in **Figure 1**. In cool climates, nutrient losses are less, at about 23 % (Drury, 1996). Yet, under specific circumstances, such as warm climates, periods of heavy rainfall, sandy soil or particular crops, losses as high as 94 % have been reported (Chen et al., 2008).

Most of the nutrient losses occur through volatilisation of ammonium (NH_4^+) and ammonia (NH_3), N-runoff/leaching (Shaviv, 2000) and to a lesser extent due to N-immobilisation (Trenkel, 2010a). Leaching of N to groundwater affects soil microbial and invertebrate communities, and has been found to alter root associated fungi (RAF) communities. The latter has profound aboveground implications in the form of shifting plant communities (Dean et al., 2014, Klironomos et al., 2011). Nitrogen in surface water runoff causes nitrate and ammonia toxicity for aquatic life and triggers blooms of unwanted organisms such as periphyton, macrophyte, phytoplankton and cyanobacteria (Hautier et al., 2009, PCE, 2013).

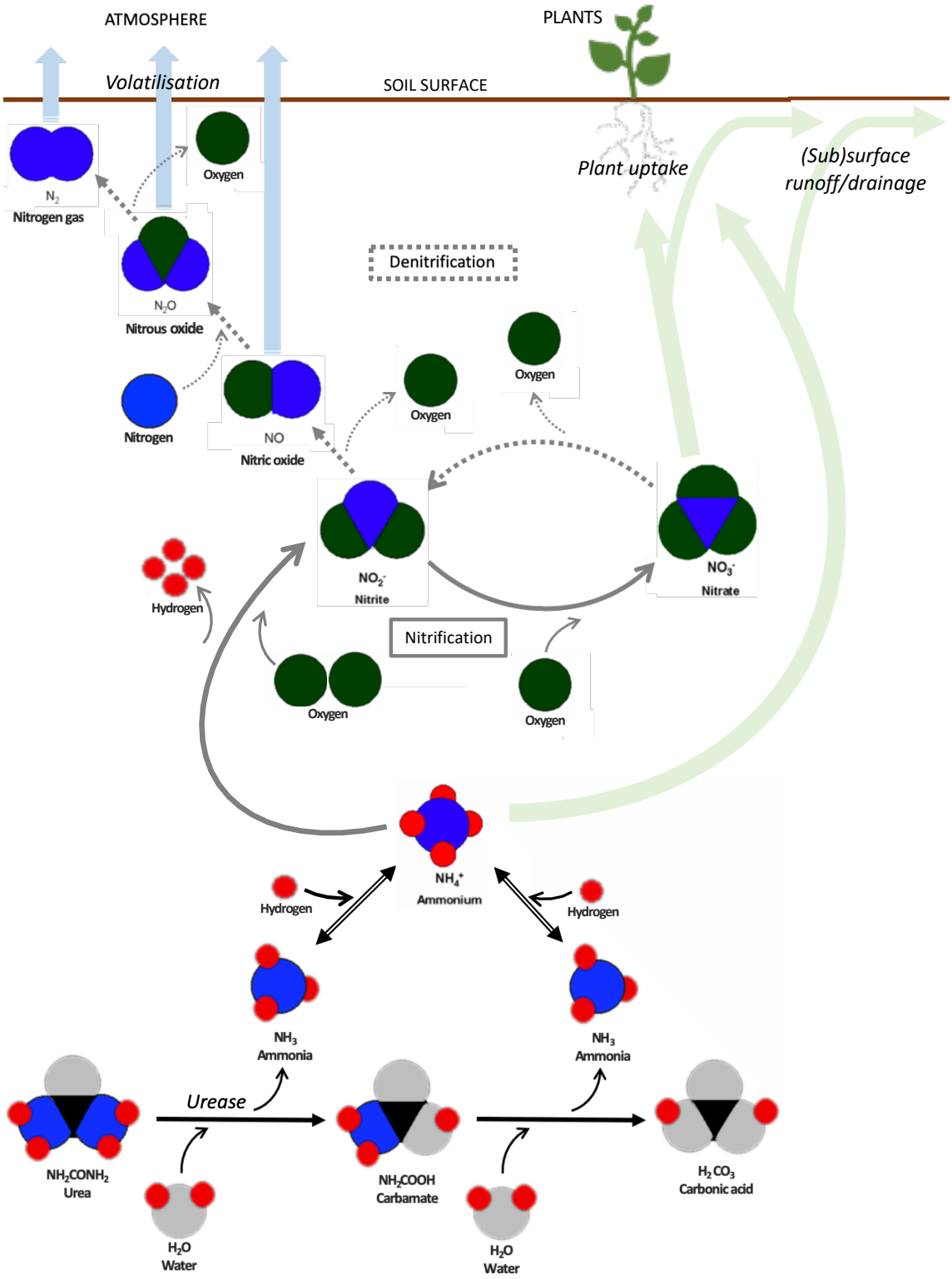

Figure 1 *Graphical representation of the pathways transforming urea via urease enzymatic activity into ammonia, followed by nitrification and denitrification, and the pathways of plant uptake and nitrogen losses through (sub)surface runoff/drainage and volatilisation.*

During volatilisation, NH_4^+ and NH_3 are nitrified and subsequently denitrified into nitric oxide (NO) and nitrous oxide (N_2O), a process visualised in **Figure 1**. Nitrous oxide is a

greenhouse gas 206 times more potent than CO_2 (Houghton et al., 1990 as cited by Morgan et al., 2004), and when released into the atmosphere it contributes to stratospheric NO, a free radical promoting the depletion of ozone (Morgan et al., 2004, Ye et al., 1994). Immobilisations of N arises when nitrogen is incorporated in the tissue of microorganisms or into complex organic molecules that resist breakdown, rendering it unavailable for plants, causing financial losses for farmers (Accoe et al., 2004).

Urea is the principal form of N-fertilisers used worldwide because of the relatively high N content (Safwat and Matta, 2018). The mechanism responsible for the hydrolysis of urea in soil is the catalytic activity of ureases (urea amidohydrolases, Enzyme Commission number 3.5.1.5), a nickel-dependent group of metalloenzymes found in fungi, plants, algae and some bacteria. Ureases are also found extracellular in soil because the organisms containing them release the enzymes upon cell death (Kafarski and Talma, 2018, Krajewska, 2009, Moraes et al., 2017). Although the enzymes have different protein structures, they all hydrolyse urea into carbamate (H_2N-COOH) and ammonia, followed by the spontaneous aqueous degradation of carbamide into carbonic acid (H_2CO_3) and another ammonia molecule (Fisher, 2014, Krajewska, 2009). Once produced, the volatile NH_3 forms a temperature and pH dependent equilibrium with the non-volatile NH_4^+ (Kafarski and Talma, 2018, Moraes et al., 2017). The pathways by which urea transforms into plant available ammonium and nitrate, and subsequently into volatile N_2O and NO, is displayed in **Figure 1**.

Over-application and accumulation of potassium-fertilisers in the soil have caused shortages of potassium (K) on the market, and several studies have been conducted on assessing the scale of this problem and possible solutions (Bai et al., 2016, Bellarby et al., 2018, Chen et al., 2017). Excessive use of phosphate (P) fertilisers has increased P fertiliser prices but moreover, results in serious environmental problems. Fertiliser-P is not as water-soluble as fertiliser-N and thus not as mobile, which has led to a build-up of P in the topsoil. Subsequent surface runoff and subsurface drainage of fertiliser-P leads to eutrophication of waterways (Eslamian et al., 2018, Eastman et al., 2010).

Common phosphate fertilisers such as reacted phosphate rock and single super phosphate contain impurities that cause soil contamination when prolonged build-up takes place (Monoharan, 1997, Gray, 2018). The impurities are uranium (^{238}U) and its decay product

radium (^{226}R) (Pearson et al., 2019), cadmium (Salmanzadeh et al., 2016, Kelliher et al., 2017, Stafford et al., 2018) and about 1 - 3 % fluorine (Gray, 2018).

Fertiliser companies have issued guidelines for farmers to reduce the possibility of fluorine induced livestock deaths. Besides impairing a variety of essential plant operations (Jha et al., 2008, Jha et al., 2009), fluorine is notorious for its high reactivity with aluminium (Stevens et al., 1997) which instigates soil acidification which in turn increases aluminium toxicity (Barceló and Poschenrieder, 2002) and decreases the bioavailability of P (Monoharan, 1997, Gray, 2018).

2.2 Slow- and controlled release fertilisers

The detrimental environmental effects of conventional fertiliser overapplication has called for a new fertilisation strategy, and this has emerged in the form of slow- and controlled release fertilisers. The two terms are wrongfully used interchangeably since there are distinct differences. Slow-release fertilisers release nutrients slower than conventional fertilisers such as urea or ammonium, but the exact speed and dynamics of the release are not known or controlled since those are subject to handling conditions and microorganism digestion activity. The latter is in turn determined by the specific soil conditions (Shaviv, 2000, Trenkel, 2010b, Thouand et al., 2011).

According to Trenkel (2010b) the European Standardization Committee (CEN) Task Force on Slow-Release Fertilisers proposed that a slow-release fertiliser must release:

- ≤ 15 % of the nutrients within 24 hours,
- ≤ 75 % of the nutrients within 28 days,
- ≥ 75 % of the nutrients within the stated release time (Kloth, 1996).

The disadvantage of slow-release fertilisers is that nutrient release rate can spike, depending on several soil parameters. For example, after harvesting, when soil microbial conditions are optimal, the nutrients are released faster and there is a heightened tendency for leaching (Liu, 2017). Controlled release fertilisers, on the other hand, are a more

effective type of fertiliser since they are not as susceptible to soil and climate conditions as slow-release fertilisers. They are manufactured with a clear understanding of the rate, pattern and extent of the nutrient release, which therefore can be predicted within certain limits (Shoji et al., 2001, Shaviv, 2005, Trenkel, 2010b).

Slow- and controlled release fertilisers can be classified as follows (Trenkel, 2010b, Shaviv, 2005):

- **(Organic-N) low solubility compounds**: they can either decompose by *1)* biological activity, such as urea formaldehyde condensation products, or *2)* (partially) chemically decompose, such as isobutylidene-diurea (IBDU, 31 % N). The disadvantage of urea formaldehyde products is that they are heavily depended on microbial activity. Isobutylidene-diurea is governed entirely by hydrolysis and thus depends on parameters such as soil moisture, soil temperature and pH (Nardi et al., 2018, Trenkel, 2010b). Commercially available examples of urea formaldehyde condensation products are ureaform and methylene ureas (Sartain, 2019).

- **Inorganic low-solubility compounds**: such as *1)* magnesium ammonium phosphate (struvite), which needs to be supplemented with an appropriate nitrogen treatment to compete with conventional ammonium phosphate fertilisers (Trenkel, 2010b, Szymanska et al., 2019), and more recently *2)* ionic co-crystals, formed by a neutral organic molecule and an inorganic salt (Braga et al., 2018, Honer et al., 2018, Honer et al., 2017).

  Co-crystal engineering focusses on the development of new materials with enhanced supramolecular characteristics. Compared to the conventional crystallisation process, organic–inorganic crystal-assembly allows for the manipulation and enhancement of solid state properties and achieves lower solubility in water, slower intrinsic dissolution rate, better thermal and photo stability, reduced hygroscopicity, lower susceptibility to biological activity and altered morphology and particle size distribution (Braga et al., 2018). Even though scale-up of the co-crystal production process has been implemented in many industries, co-crystallisation for agriculture is still in its infancy and the interactions with soil microbial organisms, and the

implications for nutrient uptake by plants and nutrient loss to the environment are yet to be explored (Braga et al., 2018, Honer et al., 2017).

- **Physical barriers that control nutrient release**: such as *1)* coatings of organic hydrophobic polymers or inorganic hydrophobic polymers, or *2)* a matrix in which the nutrient is dispersed that impedes dissolution. Because of their prevalence, both coatings and matrices will be discussed in more detail below.

2.2.1 Coatings and their disadvantages

Coatings can consist of organic hydrophobic polymers (thermoplastics or resins) or inorganic hydrophobic polymers (mineral based). Preventing the immediate release of nutrients to the soil via coating can be done according to two mechanisms: *1)* the coating can be designed to slowly dissolve over time or *2)* require the diffusion of the nutrients through a polymer membrane. Polymers have been popular in recent years but the problem with polymer coated fertilisers is that in most cases about 15 – 30 % of the nutrients will not diffuse through the membrane due to insufficient concentration gradients. Serious environmental problems can occur due to the accumulation of synthetic polymers in the soil (Shaviv, 2005, Trenkel, 2010b, Majeed et al., 2015).

Newly designed coatings therefore consist of biodegradable natural or synthetic polymer blends such as chitosan, starch, cellulose, lignin and polydopamine (Majeed et al., 2015, Chen et al., 2018). In sulphur coated urea the thickness of the coating determines the slow release character. Sulphur coatings are very brittle and if a crack is formed in the coating the urea to seeps out and the release is rapid. To prolong the release, sulphur coated urea is sometimes covered with a polymer (Trenkel, 2010b).

Disadvantages of natural coating materials are the high costs due to the complexity and labour intensity of the production process, even when using bio-based waste products such as bio-epoxy (Li et al., 2018), waste frying oil (Liu et al., 2017) or liquefied corn stover (Yang et al., 2013). This amounts in an overall cost of about 2.5-8 times higher

than conventional fertilisers (Simonne and Hutchinson, 2005, Chen et al., 2018), making them more suited for high profit crops (Davidson and Gu, 2012).

Other issues are fragility (low compressive strength) (Kusumastuti et al., 2019), and when a larger percentage of naturally occurring fibres is added to the polymer, the nutrients are released faster. The latter was observed for starch addition to polysulphone coatings. This issue has been countered by adding more layers of coating, which lengthens the fabrication process, increases production costs and reduces biodegradability (Thirmizir et al., 2011, Harmaen et al., 2016, Harmaen et al., 2018).

Lastly, although there are several categories of biodegradable polymers, all of them are subject to microbial activity and environmental conditions (e.g. erosion) for full biodegradation in order to accomplish full nutrient release (Mikkelsen, 1994, Bonhomme et al., 2003, Majeed et al., 2015). The real-world implications of these microbial and environmental factors cannot be accurately modelled or predicted and thus form a liability with regards to the accuracy and reliability of the slow-release process (Thouand et al., 2011).

2.2.2 Matrices

Besides coatings, another type of physical barrier is a matrix, which can uptake and disperse nutrients and impede dissolution. A matrix can consist of either hydrophobic materials (e.g. polyolefins or biochar) or hydrophilic materials such as hydrogels (Trenkel, 2010b). Additional to functioning as the carrier for a slow-release fertiliser, hydrogels are used to increase the water-retention capacity of the soil (Senna et al., 2015). An example of a hydrogel-based matrix is the leftover rice-g-poly (acrylic acid)/montmorillonite (LR-g-PAA/MMT) network synthesised by Zhou et al. (2018). Infused with urea, the hydrogel constituted in 33 % less N leaching than a conventional urea fertiliser.

A less intensive hydrogel production process was developed by Xiao et al. (2017), who designed a one-step method for the preparation of a starch-based superabsorbent polymer for slow fertiliser release. The developed hydrogel released 8 % of the absorbed urea after

5 days and 75 % after 40 days. Though having a simpler preparation method, the base material consisting of corn starches with different amylose/amylopectin ratios was purchased and is not an agricultural waste product as used in the study of Zhou et al. (2018). Trying to close the resource cycle through the recycling of materials is an important concept when finding solutions to the sustainability issue and will thus play an important part in solutions to the environmental and ecological challenges this world is facing (McLaughlin and Kinzelbach, 2015).

In the past few years several hydrophobic matrix-based slow-release fertilisers have been developed. Studies focussed on different aspects such as the ability to reduce N leaching, intercalation of urea vs. grinding regime, and urea release in water and soil:

- Yang et al. (2017) used a mixture of modified bentonite (a phyllosilicate mineral) and organic polymer (developed by Ni et al. (2013)). The matrix-materials were dried in an oven and sprayed into molten urea (130-135°C) at a ratio of 1:19 (= 5 % matrix). Using the matrix-based fertiliser, plant height significantly increased compared to conventional urea ($P>0.05$), maximum cumulative N leaching decreased by 19.2 %, and maximum cumulative ammonia emissions decreased by 3.2 %. Though promising, the production of this matrix-based fertiliser still has high energy consumption and is labour intensive (high overhead costs).

- Rudmin (2019) investigated the synthesis of a slow-release fertiliser based on glauconite-urea complexes, where glauconite (an iron potassium phyllosilicate) and urea were mixed in a ratio of 3:1 and subjected to various grinding times. They observed the formation of micro crystallinities with increasing grinding time and complete intercalation of urea into the glauconite after 20 minutes of grinding in a planetary mill or 60 minutes in a ring mill. Intercalation is a low temperature chemical interaction between a solid state matrix and a fluid, where a mobile species (atomic or molecular) originating from the fluid is embedded into the lattice of the host matrix if the lattice has suitable functional properties (Schollhorn, 1994).

  It must be noted that in general the grinding process has an extremely low energy efficiency (~ 1 %) and is therefore a very costly step in the production process (Tromans and Meech, 2004). To reduce the overall cost of the fertiliser, the grinding process should be minimised or eliminated where possible. Though Rudmin (2019)

explored the loading and incorporation of urea into glauconite, the nutrient release rate or effects on plant nutrient uptake or N leaching were not investigated.

- In a study by Liang et al. (2009), an agricultural-residue-based fertiliser used a wheat straw-g-poly(acrylic acid) (WS/PAA) superabsorbent to absorb urea. Urea release was tested in distilled water and soil. In water, with a urea loading of 28.3 %, about 40 % of the urea was released in 15 minutes and 95 % in 60 minutes. When testing in soil, about 60 % of the uptaken urea was released in 5 days, and 80 % in 10 days. However, plant response, ecological and environmental impact, and economic feasibility were not investigated for the wheat straw slow-release fertiliser in the study of Liang et al. (2009).

Biochar vs. low-rank coal as matrix

A porous carbon-rich material that has been under increased investigation with regards to the production of slow- and controlled released fertilisers is biochar. Lignocellulosic biomass is pyrolyzed at moderately high temperatures (350-500°C) in an oxygen-limited environment to create a black char (Lehmann et al., 2006, Meier and Faix, 1999). Though biochar can provide soil with organic matter and improve soil fertility, the nutrient content is low, and biochar with high volatile matter inhibits crop growth (Chen et al., 2018, González et al., 2015).

Most of the research involving a biochar matrix uses a polymer for encapsulation to allow for slow release, complicating the production process and thus increasing the cost (González et al., 2015, Wen et al., 2017). A study by Liu et al. (2019) used bentonite and polyvinyl alcohols to coat N-infused biochar. Liu et al. (2019) found the cumulative N-release for incubation in water was < 70 % in 42 days and 27.5 % for incubation in soil over the same time period. However, it must be noted that the newly developed biochar-based fertiliser contained only 3.8 % nitrogen. A prototype with a higher N % of 11.6 %, but no bentonite/polyvinyl alcohol coating, showed faster cumulative N release with almost 95 % released in 42 days in water and 70 % N released in soil.

The use of biochar has disadvantages since there is still an energy consuming and relatively complex fabrication process involved (Ganesapillai and Simha, 2015, Ooi et al., 2017). This makes it inherently more costly than a resource that can be taken right out

of the ground. Several researchers suggested using brown coal (lignite) in the production of slow-release fertilisers (Rose et al., 2016, Paramashivam et al., 2016), and Saha et al. (2017) proposed lignite as matrix for agricultural nitrogen. Lignite could be an interesting avenue to explore as slow-release matrix since it is a cheap, readily available, naturally occurring resource, with more than 6 billion tonnes recoverable in NZ alone (MBIE, 2015). For comparison, biochar is sold worldwide at a wide range of prices, ranging from $ 152 - $ 4000 NZD per tonne (Campbell et al., 2018), while lignite only costs about $ 60 - $ 175 NZD per tonne (Denne, 2014). Other benefits of using lignite as matrix, as well as past research exploring the potential of lignite-based controlled-release fertilisers is discussed in Chapter 2.3.

An important downside of land-application of lignite is the potential for CO_2 emissions due to the ability of microbes to incorporate lignite-carbon in their biomass (Rumpel et al. 2001). Rumpel & Kögel-Knabner (2002) found that lignite in the soil of some rehabilitated lignite mine sites contributed 24 % - 63 % of the total CO_2-C emissions in a 16-month incubation experiment. It must be noted that the incorporation of lignite in microbial biomass and the contribution of lignite to CO_2-C emissions may be strongly dependent on the lignite type, vegetation type, parent substrate for soil development, and duration of exposure of lignite to the agricultural environment. Further investigations of potential lignite contributions to soil-CO_2 emissions is needed as it could pose serious environmental risks.

2.2.3 Urease and nitrification inhibitors

Besides the actual slow- and controlled release fertilisers itself, another way to reduce the rate of nutrient availability in soil is through the use of urease and nitrification inhibitors. In soil, urea is hydrolysed by the enzyme urease to NH_3 and NH_4^+ (see **Figure 1**), that are subsequently nitrified and denitrified and constitute volatilisation losses of ammonia (Cameron et al., 2013). Urease inhibitors suppress the functionality of urease over a certain period, slowing down the hydrolysis of urea in the soil and thus reducing the resulting ammonia and ammonium volatilisation losses (Trenkel, 2010b).

Nitrification inhibitors, on the other hand, suppress the activity of *Nitrosomanas* bacteria in the soil, slowing down the oxidation of ammonium (NH_4^+) into nitrate (NO_2^-) and nitrite (NO_3^-). Preventing the formation of nitrate is important since this N-form is susceptible to denitrification and subsequent volatilisation in the form of NO, N_2O and N_2 (Rodgers, 1986, Trenkel, 2010b). An example of a commercially available fertiliser using the urease inhibitor N-(n-butyl) thiophosphoric triamide (NBPT) is SustaiN® (Summit-Quinphos, NZ).

There are, however, some disadvantages to urease and nitrification inhibitors: urease inhibitors are only effective for a short period of time (between 4-10 weeks), especially in warm conditions (Cantarella et al., 2018), and nitrification inhibitors do not prevent mineral N from entering water sources by leaching or runoff (Edmeades, 2004). The most commonly used urease inhibitor is NBPT and prevalent nitrification inhibitors are dicyandiamide (DCD), and more recently DMPP. Because of the importance of urease and nitrification inhibitors, ongoing research is dedicated to discovering and designing new varieties (Kafarski and Talma, 2018, Modolo et al., 2018). Most noticeably, Dong et al. (2009) found that urease activity is diminished by 50 % and nitrification duration is doubled by co-application of urea with lignite humic acids.

Some of the compounds that are found to inhibit urease activity in theory are less effective in an agricultural setting, as was discovered by Adhikari et al. (2018). They found that although copper and zinc reduced urease activity in soil supernatant, in soil itself copper and zinc did not have an effect on urease enzymatic action. This negative result was explained by complexation of (mainly) copper with organic carbon and clay particles present in the soil, rendering the copper-ions unavailable for complexation with urease.

2.3 The search for a new lignite-based controlled-release fertiliser

Due to the shortcomings of the above mentioned slow- and controlled release fertiliser solutions (described in Chapter 2.2), there is a need for a cheap and environmentally

friendly controlled-release fertiliser. Since coatings are often expensive and fragile, a matrix-based solution is proposed in this research. The worldwide abundance and extensive historical research available, present lignite as an excellent opportunity.

2.3.1 The potential beneficial properties of low-rank coal

Lignite (brown coal) and sub-bituminous coal are the lowest rank coals, which means the peat base material has been subjected to less pressure over tens or hundreds of millions of years than with the formation of bituminous coal and anthracite (higher-rank or "hard" coals) (Jones, 2016b), see **Figure 2** below. The specific lignite formation conditions result in a brown coloured coal with a calorific value up to 70 % lower than for the higher ranked coals (Jones, 2016b) but accounts for 23 % of the world's known coal reserves (Jones, 2016b). Lignite and sub-bituminous coals are the two subdivisions of low-rank coal and have been extensively researched in a fuel context during the past 2.5 centuries when the world's primary energy sources were coal and oil (van Krevelen, 1982, Durie, 1991). Previous research lays out the fundamentals of the properties of low-rank coal, its interaction with a multitude of solvents, and delivery methods (dried particles or coal-water slurries), which provides a good basis for utilisation, manipulation and optimisation of lignite as a matrix for a controlled-release fertiliser.

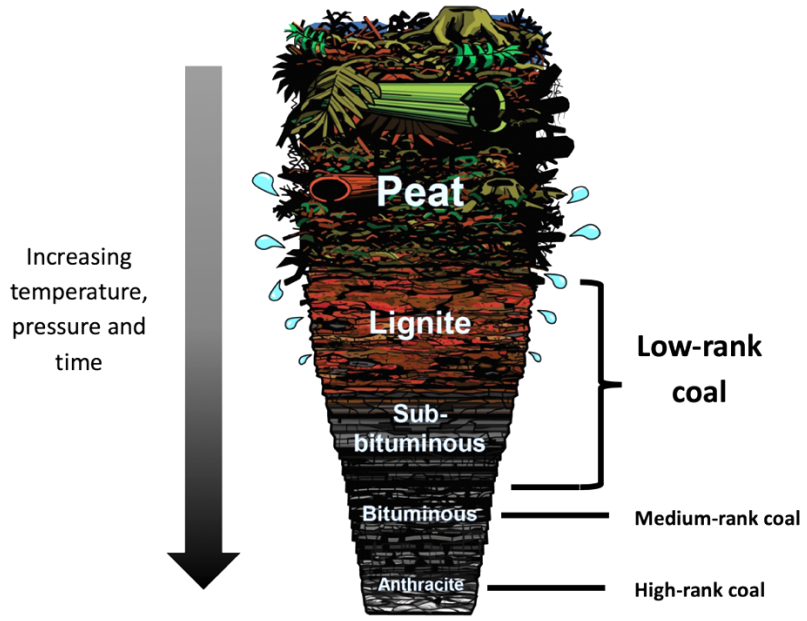

Figure 2 *Burial pressure, heat and time create peat, lignite + sub-bituminous (low-rank coal), bituminous (medium-rank coal) and anthracite (high-rank coal) consecutively. Adapted from: Greb (2019). Copyright: Kentucky Geological Survey, University of Kentucky 2019.*

There are several reasons why lignite has been proposed as adsorbent of agricultural nutrients in several previous studies: *1)* lignite is cheap (Denne, 2014), *2)* readily available (Jones, 2016b), *3)* has a high specific surface area and high porosity due to its extensive pore structure, *4)* has various pore size distributions, *5)* has a relatively high humic and fulvic acid content, and *6)* possesses a substantial amount of oxygen-containing functional groups (binding sites) (Woskoboenko et al., 1991).

In contrast to coals of higher ranks, which have lost most of their functional groups in the course of their formation, lignite, and to lesser extent sub-bituminous coal, have a complex chemical structure comprised of carboxyl and phenol side chains, alkyl and hydroxyl groups, aromatic rings, and alkyl, ether and ester linkages (Saha et al., 2017). The carboxylic acid and phenolic functional groups are of particular interest to the current research since those have been associated with NH_4^+ adsorption by lignite (Nazari et al., 2018, Tu et al., 2019). How the chemical and physical structure of low-rank coal can be manipulated to optimise nutrient ad- and desorption will be discussed in Chapter 2.4 and 2.5.

2.3.1.1 The role of humic and fulvic acids

Most of the complex structure and functional groups of lignite are due to the presence of humic acids (HAs) and fulvic acids (FAs). The existence of humic and fulvic acids has been a contentious subject for years, and it has been hypothesised that they are merely self-assambled aggregates of small compounds that can be decomposed (Lehmann & Kleber, 2015). In the scope of this work the concept of humic and fulvic acids, or humic and fulvic acids-like compounds, provides useful insights with regards to nutrient uptake by lignite. Whether or not the compounds are recalcitrant is not of vital importance, and the choice was made to use the terminology "humic and fulvic acids" to describe a group of (aggregated) componds that exhibit advantageous properties for the development of lignite-based controlled-release fertilisers.

Kiss et al. (1984) analysed several lignites and found they contained a total humic acid content (or alkali soluble fraction) of 24 – 92 %, with an average of 63 % (Woskoboenko et al., 1991). This relatively high percentage was corroborated by Huculak-Mączka et al. (2018). In nature, humic and fulvic acids play a crucial role in maintaining optimum soil quality (Piccolo, 2002b, Frimmel and Abbt-Braun, 2018), but studies have also been conducted on their capacity to form complexes with ionic compounds.

These ionic compounds can be heavy metals, allowing for contaminant remediation (Yates and Von Wandruszka, 1999, Sposito and Weber, 1986, von Wandruszka, 2000). This is of particular interest for phosphorus fertilisation because aluminium (a heavy metal) decreases the bioavailability of P. Lignite has the capacity to fix aluminium ions to its humic acid structures (Tipping et al., 1988) and thus decrease aluminium toxicity in plants and allow for better nutrient uptake (Wang et al., 1995). The ionic compounds capable of binding to humic and fulvic acids can also be organic xenobiotics, allowing for metal catalysis, resulting in inhibition of the formation of free radicals (Rice-Evans et al., 1997). This gives humic acids and fulvic acids their antioxidant properties which have been widely studied and applied in a number of scientific fields (Rice-Evans et al., 1997, de Melo et al., 2016).

Of particular interest to the current study is that complexation of ionic compounds can also be used to incorporate nutrients (Brannon and Sommers, 1985). Bosatta and Ågren

(1995) theorised that ammonia-N can be abiotically fixed to lignite's humic acid structures. However, there are other mechanisms by which lignite can uptake ionic compounds (see Chapter 2.4 and 2.5), and the extent to which humic and fulvic acids contribute to lignite's ability to uptake nutrients; and if this can be used to advance nutrient uptake, has not yet been investigated.

2.3.1.2 Humic and fulvic acids and their functional groups

Humic substances are intricate, heterogeneous molecules. They usually have a yellow to black colour and are responsible for the brown/black colour of soil (Burdick, 1965, Adey and Loveland, 2007). Humic substances are divided into two fractions: molecules that are completely soluble in aqueous solution, the fulvic acids, and molecules that are soluble in alkali media but precipitate in an acidic environment, the humic acids (Kipton et al., 1992). Fulvic acids have in recent years been described as clusters of relatively small hydrophilic molecules that remain distributed in solutions of any pH due to the ample occurrence of acid functional groups.

The size of the clusters in humic acids is determined by the prevailing hydrophobic bonds that are stabilised by intermolecular hydrogen bonds. The latter grow in numbers at lower pH and thus increase the size of the humic associations, even to the extent where precipitation of flocculants occurs at pH 1 - 2 (Piccolo, 2002a, Canellas et al., 2015). Research has stated that the functional characteristics of humic substances are attributed to electron donating methoxy groups, and phenolic and carboxylic acid groups which allow for the deprotonation of -OH and -OOH (Harvey et al., 1983, Piccolo, 2002b, Chassapis et al., 2010, Smilek et al., 2015, de Melo et al., 2016).

The importance of humic and fulvic acids for plant health is due to their crucial role in soil water retention, soil structure, biological activity, chemical bioavailability, bioaccumulation and transport of nutrients (Chassapis et al., 2010, Chen and Stevenson, 1986, Tahir et al., 2011). Research has shown that humic and fulvic acids can also be used to adsorb nutrients, particularly humic and fulvic acids derived from lignite because their oxygen-containing functional groups are 80 % comprised of carboxyl and phenol groups (Kwiatkowska et al., 2008). The high percentage of carboxylic acid and phenolic hydroxyl functional groups in humic and fulvic acids from lignite increase the cation

exchange capacity of the HA's and FA's (Debska et al., 2002, Skodras et al., 2014). Increased cation exchange capacity means increased sorption of cations (Kwiatkowska et al., 2008, Szalay, 1964) and thus more nutrient uptake. Since carboxylic and phenolic functional groups govern cation exchange capacity (Szalay, 1964, Zhang et al., 2018), the current study will aim to examine the extent to which those functional groups can be manipulated and enhanced in order to optimize nutrient adsorption by lignite.

2.3.2 Recent studies on lignite in combination with nitrogen in agriculture

The attention is on four recent studies involving the use of lignite (brown coal) in combination with a nitrogen source to reduce the environmental impact of N leaching, runoff and volatilisation. The studies entail either general lignite and N co-application, or more specific lignite - urea granulation, and experimentally assess the ability of different treatments to lower NH_3, NH_4^+, NO_3^- and N_2O losses. A thorough analysis of the used methodologies and results of the four studies is pivotal for method development, as is examining the research on scientific rigour, significance of the obtained results, and research gaps uncovered with regards to the development of a lignite-based controlled-release fertiliser. Nevertheless, the literature review focusses on identification and exploration of the theory behind the most important parameters and properties for developing lignite-based controlled-release fertilisers. The studies are therefore placed in Appendix A and referred back to in the chapter on method development. The results of the four lignite - urea studies are summarised in **Table 10** of Appendix B, and a summary of the conclusions drawn from the studies is given below.

When looking at **Table 10** it becomes apparent that even though the four studies make strong claims, the data indicates most of the results do not show a significant difference between the various tested C : N ratios. Even when comparing the losses to urea application alone, very little significant improvement is found. From their discussions, the necessity is concluded of investigating if the lignite structure can be manipulated (mechanically or chemically) to increase the availability of the carboxylic and phenolic functional groups, and thus increase the adsorption of urea-N onto lignite. From the studies it also follows that, if there is an optimum C : N ratio for the most efficient

controlled-release of N from lignite - urea fertilisers, this will need to be examined through kinetic and isothermal uptake and release studies for different types of lignite.

2.3.3 Lignite and phosphate fertilisation

In contrast to studies focussing on lignite in combination with urea, studies on lignite in combination with phosphate have not focussed on decreasing the release rate of phosphate, but instead on ensuring continuous release of a water soluble and thus bioavailable form of phosphate. Through a grinding process, Huang (2013) coated phosphate rock with lignite and found that adhesion of finer P-rock particles to larger ones was prevented by 3 – 5 % lignite addition. This process covered all P-rock particles with organic molecules from the lignite and consequently allowed for better interaction with the soil matrix. Improved interaction between the soil matrix and phosphate rock increased the amount of bio-available P (Zhang et al., 2019). This is attributed to the humic acids in lignite which significantly increase the amount of water soluble P (Wang et al., 1995). A pot cultivation test by Zhang et al. (2019) demonstrated that lignite - phosphate rock fertilisation increased not only phosphate plant uptake, but also nitrogen and potassium uptake, compared to no soil emendation or the use of conventional phosphate rock.

Besides increasing P bioavailability, there is another way lignite can be beneficial when combined with phosphate fertilisation. Zheng (2010) stated aluminium toxicity and P deficiency are the most important growth limiting factors for plants in acidic soils. When the soil pH is below 5, aluminium becomes soluble and the ions impair (P-)nutrient uptake by plant roots. Acidic soils are often high in clay minerals that bind and immobilise P, further impairing P-uptake. Lignite can bind aluminium to its humic and fulvic acid structures. This complexation decreases aluminium bioavailability, allowing for better P uptake. In addition, soil acidification is exacerbated by excessive nitrogen fertilization (Zheng, 2010), this indicates the need for a lignite-based controlled-release N fertiliser that reduces the overapplication of N, consequently mitigating soil acidification and thus increases P-fertiliser efficiency.

2.3.4. Low-rank coal-based N/P/K-combination fertiliser

In the examined body of literature no research has yet been conducted on lignite and a combination of N/P/K nutrients in the context of a controlled-release fertiliser. Previous studies with lignite have focussed on N or P fertilisation alone (see Chapter 2.3.2 and 2.3.3). Analysis of the chemical structure of nutrient-infused lignite, and kinetic and isothermal equilibrium studies with a combination of N/P/K nutrients could potentially determine the interaction effects between nutrients and lignites. Reference controlled-release N/P/K fertilisers can be found in research of Senna et al. (2015) and Wu et al. (2008). Senna et al. (2015) developed a hydrogel derived from cellulose acetate and EDTAD, containing 12 % K, 4.4 % P and 6.5 % N. Wu et al. (2008) prepared a double-coated slow-release N/P/K compound fertiliser, by coating water-soluble granular N/P/K fertiliser with chitosan and crosslinked poly (acrylic acid) / diatomite, containing 8.47 % K, 8.51 % P, and 15.77 % N.

2.4 Coal slurries

2.4.1 The necessity of coal slurries

Lignite is in essence a colloidal gel consisting of about 30 – 70 % water (depending on the base materials and formation process). The water is a structural characteristic and makes lignite notorious for its predisposition to spontaneous combustion, while the dust formed during grinding of lignite can cause explosions (Jones, 2016c, Li, 2004). These hazards were already known in the middle of the previous century when the research into coal was at its peak (Berkowitz, 1951, Veselovskii et al., 1967), but the safety issues have been under investigation ever since (Mulcahy et al., 1991, Tang and Wang, 2019).

Spontaneous combustion of lignite occurs when heat produced by low temperature oxidation in air overtakes the rate of heat loss. Moisture is a redounding factor in this process because large fluctuations in local or ambient moisture content can induce reabsorption of moisture onto lignite, producing heat of condensation or heat of wetting in the vapour state and liquid state respectively. This increase in temperature further

propels the spontaneous combustion process since the oxidation rate doubles every 10°C increase in temperature, allowing the internal temperature of the coal to increase up to the point of spontaneous combustion (Allardice, 1991, Berkowitz, 1951, Li, 2004).

This potentially dangerous tendency complicates storage and handling of lignite, therefore, to reduce the risk of spontaneous combustion or dust explosions, techniques such as hydrothermal drying, multiple-effect steam drying, the removal of harmful inorganic species, liquefaction and coal-water-slurries have been used as a tool to make coal a transportable and exportable fuel source (Mulcahy et al., 1991, Li, 2004). For the use as fertiliser, (superheated steam) drying (Rose et al., 2016) and granulation with urea (Saha et al., 2017, Saha et al., 2019) have been used to mitigate the dangers of combustion.

The use of lignite slurries (lignite + a large quantity of liquid) has, to the best of our knowledge, yet to be explored in an agricultural fertiliser context. The use of slurries will avoid the high drying costs associated with granules or pellets and will also diminish the issue with lignite particle fragility. Particle fragility comes into effect when transporting and applying the fertiliser (Rose et al., 2016). A downside of slurries is the increased (water)weight and thus increased transport cost, but this can potentially be offset by a simpler and cheaper production process and more effective nutrient delivery.

2.4.2 Coal-nutrient-slurry rheology

For practical agricultural applications, coal-slurries with nutrients should have low apparent viscosity and high stability in order to optimize the economics and safety of slurry transport and application (Vlasak and Chara, 2011). Factors influencing the rheology of coal-nutrient-slurries are solids loading, particle size distribution, particle geometry (Goudoulas et al., 2010), and interparticle forces (Sadler and Sim, 1991). The latter is affected by the type of coal and nature of adsorbed nutrient species (Tu et al., 2019), further discussed in Chapter 2.4.3 below.

Because lignite contains more oxygen functional groups than the other low-rank coal type, sub-bituminous coal, lignite should allow for more nutrient adsorption. This seems to suggest lignite is more favourable as matrix for a controlled-release fertiliser. Yet, sub-bituminous coal could have an advantage from a rheological point of view if a slurry delivery system is chosen instead of a "dry" system such as pellet or granules. In general, the maximum achievable solids loading of sub-bituminous coals is higher than that of lignites (Woskoboenko, 1991). Dependent on the lignite type, lignites can have low density, high moisture content and high wet porosity, resulting in a maximum achievable solids fraction for slurries of about 35 wt.%. Other types of lignite and bituminous coal have lower moisture content, allowing for higher solids loadings (Woskoboenko, 1991). Achieving a high solids loading while maintaining relatively low apparent viscosity is a crucial step in maximizing the nutrient concentration of a slurry and allows for fertiliser and resource efficiency optimization.

Besides density, moisture content and wet porosity, another major factor in determining apparent viscosity is particle size distribution. Yavuz and Kucukbayrak (1998) found there is an optimum mean particle diameter that results in minimal apparent viscosity of the slurry. For their type of lignite (Yozgat- Sorgun, Turkey), 47 μm was the preferred mean particle diameter. Yavuz and Kucukbayrak (1998) also found that polysized particle size distributions increase slurry stability compared to monosized particle size distributions. Buranasrisak and Narasingha (2012) found that a bimodal particle size distribution can yield a higher maximum loading than a mono- or multimodal distribution.

Particle size distributions of coal are usually altered by mechanical comminution (grinding). Mentioned in Chapter 2.2.2, grinding is an extremely costly and energy inefficient process that should be minimized to reduce fertiliser cost (Tromans and Meech, 2004). In order to find the preferred, yet minimal, amount of grinding required, the effects of mechanical comminution on coal characteristics such as particle size distribution, specific surface area, and micro and meso pore volume needs to be understood and are further discussed in Chapter 2.4.3 below.

2.4.3 The effects of mechanical comminution

The lignite structure consists of molecules such as fulvic acids (MW ~300), humic acids and its macromolecule derivatives (MW ~1000 and ~30.000 respectively), and a wide range of much larger plant residues (Woskoboenko et al., 1991). **Figure 3** below shows the mass fraction of the particle size distributions (as spherical equivalent diameter) of the molecules in Victorian brown coal after alkali digestion (peptization): about 1 % is between ~ 0.1 - 0.5 nm (fulvic acids), about 23 % is between ~ 0.5 - 2 nm (humic acids and its oligomers), only 8 % is between ~ 5 nm - 1 µm thus constituting a large gap, and the majority of the particles, about 68 %, are between ~ 1 - 3 µm (relatively small xylitic fragments) and ~ 3 µm and up (larger plant residues). Plant residue particles can take on considerable sizes and Camier (1977), as referenced by Woskoboenko et al. (1991), found that particles the size of roots, branches and even tree trunks as large as 10 m had been preserved as lignite.

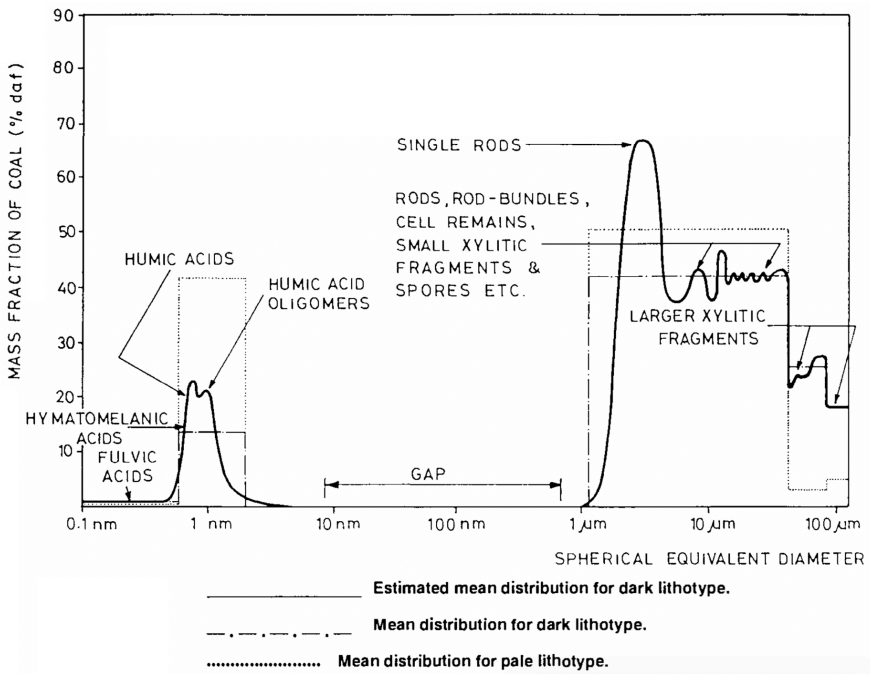

Figure 3 *Particle size distributions of the different constituents of Victorian brown coal after alkali digestion for a light and dark lithotype. Adapted from: Camier (1977) by Woskoboenko et al. (1991) in: Durie (1991). Copyright: Butterworth-Heinemann Ltd. 1991.*

Mechanical comminution is the process of reducing the particle size of large lignite particles by grinding, which is done in conjunction with a liquid to prevent dust explosions. When a sufficient amount of liquid is added, a lignite slurry is created. The shapes and sizes of the particles produced during grinding are determined by the number

of pores, cracks, organic-to-organic and mineral-to-organic interfaces present in the lignite. The larger plant residue particles manifest themselves in a large variety of sizes, structures and compositions. This produces a vastly polysized particle size distribution (Woskoboenko et al., 1991) that depends on the grinding technique employed (Rubiera et al., 1999).

Mechanical comminution of lignite is an important step in converting raw lignite into a suitable form for fuel (Eisele, 2013) or fertiliser matrix and, as mentioned earlier in Chapter 2.4.2, it is an important parameter in the rheology of lignite slurries. Woskoboenko et al. (1991) noted that grinding of coal changes the physical structure but not the chemical rank. The grinding process increases the density and compressive strength of lignite and decreases the Hardgrove grindability (Johns, 1989). Hardgrove grindability is a unitless index that gives information on how much energy is consumed by a pulveriser to process a particular coal relative to a reference coal. The index is highly non-linear, dependent on the moisture- and ash content, metamorphic development (volatile matter), the ultimate-, petrographic-, and mineral composition, and the oxidation of coal and should therefore be used in conjunction with other methods to determine grindability of coal (ACARP, 1998, Miroshnichenko et al., 2019)

Figure 4 below depicts that Victorian brown coal (a specific type of lignite with 60 – 70 % inherent moisture) reaches a plateau for specific surface area when the wet slurry mass-median diameter (D_M) is > 9 µm, while the total porosity reaches a plateau when the wet slurry D_M is > 13.5 µm. A steep decrease of specific surface area and total porosity below a certain mass-mean diameter can be explained by the fact that grinding of lignite destroys (a small) part of the macropores and fills and caps other macropores with colloidal particles. This process is particularly noticeable when the median particle size within the slurry is smaller than 10 µm in diameter, and at this point most micropores (ø < 20 nm) are impervious to CO_2 and He which are used for surface area and true density determination, respectively (Woskoboenko et al., 1991). This tells us that particle size is of importance with regards to nutrient uptake optimization since the extent of nutrient uptake is in part determined by the maximization of specific surface area and porosity to allow for maximum accessibility of sorption sites.

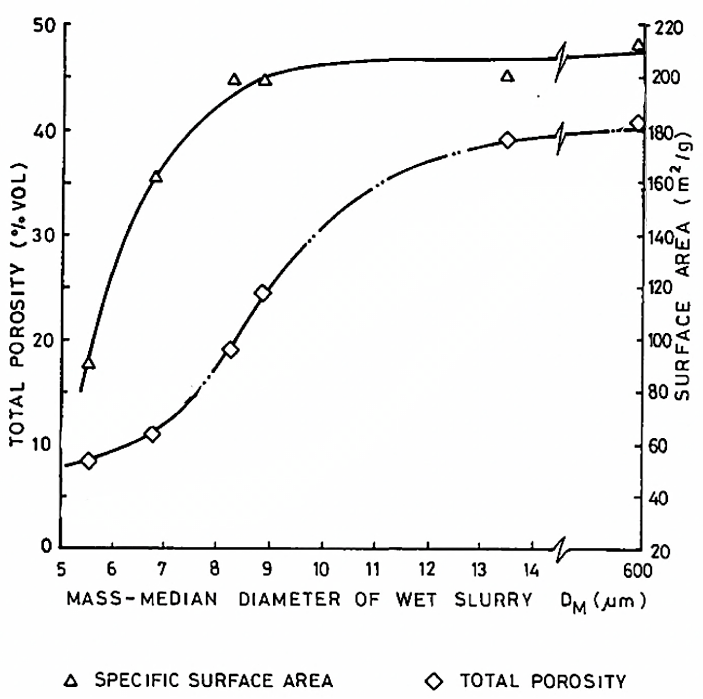

Figure 4 *The effect of wet slurry mass-median diameter (D_M) on total porosity and specific surface area. Source: Woskoboenko (1985) in: Durie (1991). Copyright: Butterworth-Heinemann Ltd. 1991.*

From the **Figure 4** above might follow that particles sizes > 13.5 μm are preferred for attaining maximum nutrient adsorption, but it must be noted that particles with a diameter of < 10 μm are largely responsible for the colloidal characteristics of lignite slurries. Smaller particles increase packing and network structure formation. This means that if the total percentage of these small particles in a slurry drops below a certain critical value the slurry will rapidly settle. A polysized distribution with smaller particles also increases coal loading and will thus foster fertiliser efficiency.

Figure 4 states that above a mass median particle diameter of 10 μm Victorian brown coal has 45 vol. % porosity. In general, the total open pore volume in coal varies by a factor ten, from 0.03 to 0.25 cm^3/gm (Speight, 2005d). According to Speight (2005d) there are two theories regarding the nature of the large pore volume in coal:

- There are large pores, tens of nm's (hundreds of **Å**) in diameter, with small openings that restrict access of molecules for measurement (e.g. nitrogen),
- There is large number of small pores with diameters no larger than 3 nm (30 **Å**).

This means, respectively, that coal has either a large mesopore (2 - 50 nm) volume that cannot be measured accurately because the gas molecules used for the measurements cannot enter the pores, or coal has a large micropore (< 2 nm) volume.

Furthermore, the colloidal stability of lignite slurries is controlled by the oxygen-containing functional groups. Since adsorption of nutrients will alter these groups, a change in slurry viscosity and stability will need to be investigated. To this end, Tu et al. (2019) added anhydrous ammonium chloride (NH_4Cl) and an anionic dispersant (naphthalene sulfonic acid sodium formaldehyde condensate; NSF) to lignite-water-slurries. The addition of an N-species and a dispersant resulted in enhanced stability but also in a significant increase in apparent viscosity, explained by the mechanism displayed in **Figure 5** below.

Figure 5 (a) shows a lignite particle in deionised water. When the NSF dispersant is added it forms a hydration film around the lignite particles (**Figure 5 (b)**). The addition of NH_4^+-N enhances the adsorption of the NSF dispersant onto lignite, causing a thicker and more stable hydration layer (**Figure 5 (c**)). Increased thickness and stabilisation of the hydration film intensifies the interparticle repulsion, preventing agglomeration and sedimentation of particles. Increased thickness of the hydration layer also reduces the amount of free water in the coal-water-slurry, increasing apparent viscosity which is unfavourable for practical slurry applications.

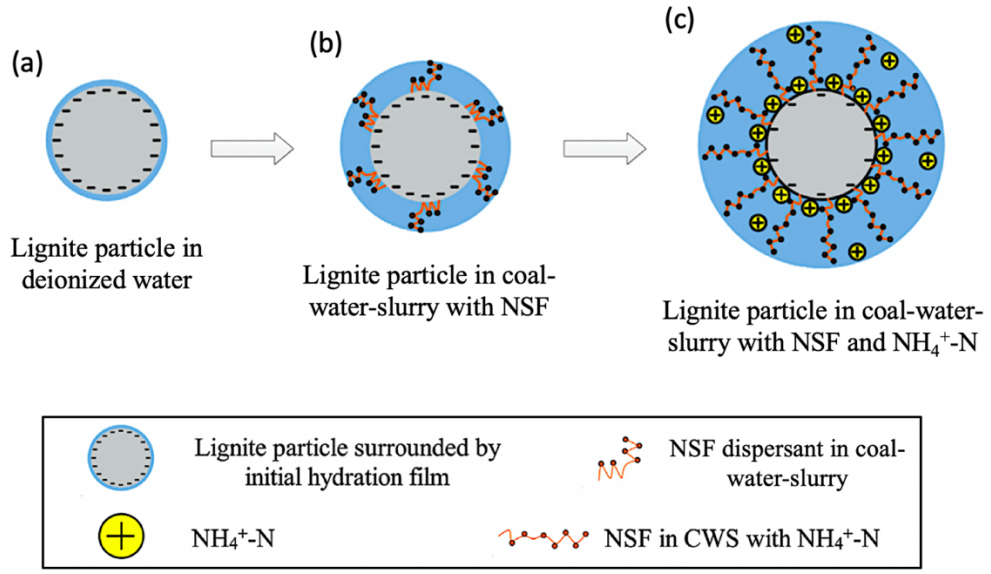

Figure 5 *Schematic diagram showing the mechanism by which NH_4^+-N affects the dispersing and stabilization of lignite particles in a coal-water-slurry with NSF dispersant. With* **(a)** *lignite particle in deionized water,* **(b)** *lignite particle in coal-water-slurry with NSF dispersant, and* **(c)** *lignite particle in coal-water-slurry with NSF and NH_4^+-N. Source: Tu et al. (2019). Copyright: Elsevier Ltd. 2018.*

From the research of Tu et al. (2019) it becomes clear that the increased apparent viscosity and slurry stability of nutrient-infused lignite-water-slurries can negatively affect the applicability in fertiliser spraying systems, and that the addition of dispersants could potentially have a counteractive effect. For the economic viability of lignite-based control-release fertilisers it is therefore crucial to investigate the (interaction) effects of lignite-property manipulations on the rheology of lignite-nutrient slurries. If lignite-property manipulations and additives cannot produce a practical lignite-nutrient-water-slurry, other delivery methods (pellets, granules, etc.) will need to be investigated. Converting the slurry to other delivery methods will require additional preparation, and thus additional manufacturing costs. In order to procure an economically competitive controlled-release fertiliser, a cost-benefit analysis is required to determine the optimal delivery technique.

2.4.4 Potential delivery systems of a lignite-based fertiliser

There are several options for the type of delivery system of a lignite- based controlled-release fertiliser, each with their own advantages and disadvantages. Granules, pellets and

balls (spheres) will all have the associated drying costs (Song et al., 2017), and as mentioned earlier, have to deal with health and safety issues due to its volatility, and can suffer from structural damage. The high water content of slurries is responsible for increased (water)weight for transport and lower nutrient concentration (= lower fertiliser efficiency) and thus increased costs. Slurries will also need to address the potential phase separation (settling of particles) by either an additive in the form of a dispersant, or experimentation with, and careful selection of, different nutrient species and particle size distributions (Tu et al., 2019).

Ultimately, the choice of delivery system will largely depend on the style of agricultural practice. Pumped slurry delivery systems of conventional agriculture, such as band spreading machines, trailing shoe machines and shallow injection, are limited to low viscosities and solids loading (5 – 15 %). Muck spreaders are used for semi-liquids with more than 15 % solids (Misselbrook et al., 2002, Houlbrouke, 2012). Precision agriculture, currently predominantly utilised in high value crops, can potentially use high-tech tailored solutions such as agricultural robots to deliver slurries with high solids loadings. Scaling feasibility studies will need to be conducted in order to find the preferred and most economical delivery system for each type of agriculture.

2.5 Nutrient adsorption by lignite

Fertilisers with a higher nutrient loading are more efficient when it comes to transport, storage and general use of resources, and allow for a lower application rate. That is, if they have a favourable controlled-release character. From this it follows that maximising nutrient adsorption by lignite is an important step in producing economically feasible lignite-based controlled-release fertilisers.

Nutrient and heavy metal uptake by low-rank coal have been studied repeatedly, and it was found that adsorption depends strongly on the following variables: pH (Nazari et al., 2018), the origin of the low-rank coal (Pehlivan and Arslan, 2006), the nature of the ion adsorbed (Pehlivan and Arslan, 2007), and initial concentration (Tu et al., 2019). This chapter discusses the proposed mechanisms by which the variables operate and influence

adsorption, and how manipulation of these variables can potentially foster nutrient adsorption by low-rank coal.

2.5.1 The effects of pH on nutrient adsorption

The pK_a of the carboxylic and phenolic acid groups on the surface of lignite particles is responsible for the acidic nature of the water in lignite, but the pH of raw lignites is governed by the pH and cation composition of the aquifer in which the lignite was located during and after formation (Woskoboenko et al., 1991). When manually lowering the pH of lignite slurries to a value close to the point of zero charge (or the iso-electric point) at pH < 2, all the carboxyl groups of lignite are in their acid form and adsorption is prohibited by electrostatic repulsion (Gupta and Sharma, 2003). A subsequent increase of the pH causes the surface of the particles to become negatively charged (Worch, 2012), allowing for the exchange of cations onto the surface and creating an electrical double layer (Woskoboenko et al., 1991).

Several studies examined the effects of the above mechanisms on adsorption and found varying results for several lignite related or resembling adsorbents:

- Some studies found optimum adsorption to be around pH 4 - 5.5, such as Khan et al. (2011) using $ZnCl_2$ modified lignite granular activated carbon (LGAC) for the removal of nitrate NO_3^-, and Xu et al. (2016) using lignite for the adsorption of quinoline. When Pehlivan and Arslan (2007) investigated the adsorption of heavy metals onto lignite, they found that increasing the pH from 2 to 5 increases adsorption from 10 to 97 % using a solution with a metal ion concentration of $1x10^-3$ M. They did not increase the pH above 5.5 to avoid precipitation of metal ions.
- Tu et al. (2019) studied the adsorption of ammonium-N onto a non-specified lignite in the presence of a dispersant and found the optimum pH to be in the range of 6 - 9.
- Nazari et al. (2018) studied the effects of base treatment on ammonia nitrogen adsorption by Xilin Gol lignite. The lignite was treated with 0.1 M NaOH to convert all acidic functional groups into sodium salts. They observed an optimum ammonium removal of 96 % at pH 12 when using an initial

concentration of 2 mg/L NH_4^+. Doskočil and Pekař (2012) used lignite (Mikulčice, Czech Republic) to adsorb metal ions and found the adsorption of zinc and cadmium to increase over the entire pH range (pH 2 - 8), while lead and copper showed a plateau from pH 3 - 8.

Theories behind pH dependency

The research of Nazari et al. (2018) is of particular interest since they studied the influence of pH, initial NH_4^+ concentration and lignite dose on the adsorption of ammonium from synthetic wastewater. The enhanced adsorption they observed with increasing pH was explained by the base treatment which, at a pH > 8.3, resulted in the liberation of H^+ from carboxylic acid groups, and at a pH > 12.6 caused the liberation of H^+ from phenolic groups. The dissociation of the carboxylic and phenolic groups opened up additional ion-exchange sites that were filled with Na^+. This process replaces strong hydrogen bonds with weaker metallic bonds of sodium and increases ammonium adsorption when NH_4^+ is added to the lignite and substitutes the Na^+. This theory was supported by Malekian et al. (2011) upon investigating the removal of ammonium by zeolite with the addition of NaCl.

That in several other studies adsorption hits a maximum around pH 4 - 5.5 can partially be explained by the effects of pH on the physical characteristics of lignite. **Figure 6** below shows that specific surface area and total porosity decrease drastically for a pH > 5 (Woskoboenko et al., 1988, Xu et al., 2016) and thus negatively influence the availability of sorption sites (functional groups) to the bulk solution containing the cations that are to be adsorbed. Furthermore, at pH > 7 the electrophoretic mobility and zeta potential of the water in lignite decrease. Lower electrophoretic mobility results in a lower electrophoretic velocity (the velocity with which a particle moves in response to the applied electric field) and thus decreases the rate and potential for adsorption. It is not clear if this is controlled by the solubilisation of humic acids or due to the uptake of cations (Quast et al., 1987, Quast et al., 1988, Woskoboenko et al., 1991)

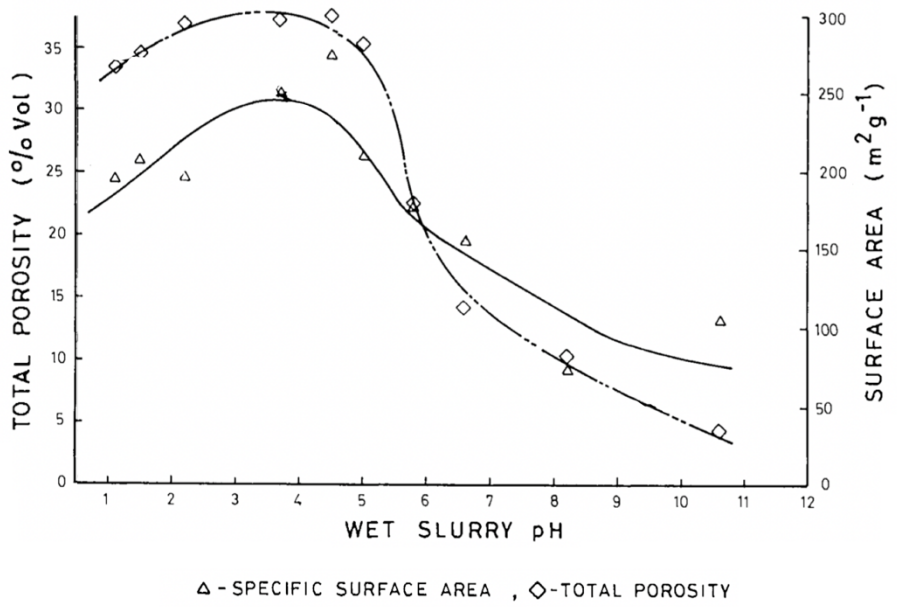

Figure 6 *The effect of wet-slurry pH on specific surface area and total porosity of Morwell (South-East Australia) sundried coal slurry. Source: Woskoboenko et al. (1987) in: Durie (1991). Copyright: Pergamon Press PLC 1985.*

Tu et al. (2019) suggested an acidic environment reduces the cation exchange capacity of the functional sites, while an alkaline environment hydrolyses and thus decreases the availability of ammonium. It must be noted that the study of Tu et al. (2019) used lignite as adsorbent and base material for a coal-water-slurry in combination with the dispersant NSF (naphthalene sulfonic acid sodium formaldehyde condensate). This dispersant had a generally higher affinity for adsorption onto the lignite than the ammonium, which could have impaired ammonium adsorption.

In conclusion, there are contradicting results and theories regarding the effect of pH on the adsorption of ions onto lignite and similar adsorbents. Through kinetic adsorption and equilibrium studies (see Chapter 2.5.3 and 2.5.4) the proposed research will investigate if the addition of a base will open up more adsorption sites and foster nutrient adsorption onto the particular low-rank coals used for the proposed research, or if an increased pH reduces specific surface area and total porosity and what mechanisms could be responsible.

2.5.2 The effects of solvent swelling on nutrient adsorption

As described by Tu et al. (2019), nutrient adsorption onto low-rank coal can be increased through base treatment as this enhances the availability and reactivity of low-rank coal functional groups. Other research found that alcohols and cyclohexanone used as solvents for coal-slurry production have the capacity to open up the coal structure and increase available surface area by breaking hydrogen bonds and swelling coal (Shin and Shen, 2007). Coal swelling has been intensively researched in the past century since it is an integral part in coal energy output optimisation (Hacimehmetoğlu, 2007). One of the hypotheses aimed to be explored in the proposed research is the ability of solvent induced coal swelling to constitute enhanced nutrient uptake. The mechanisms behind coal swelling are discussed below. There are two types of coal swelling: low temperature solvent swelling, that occurs at room temperature under the influence of solvents (Cody Jr et al., 1988), and high temperature swelling, where gasses released during the combustion process get trapped inside the coal structure and constitute pressure build-up (Speight, 2005a). The focus in this research is on low temperature solvent swelling (referred to as "solvent swelling" or "swelling" in the rest of this thesis).

Solvent swelling of coal is determined by two mechanisms: 1) imbibition, or adsorption of a solvent by the cross-linked part of the coal structure, and 2) the partial dissolution of the non-cross-linked part of the coal structure by the solvent (Jones et al., 1991) (Jones et al., 1997). The cross-linked part is made up of micropore walls containing polar functional groups and a micropore structure that is held together by covalent and hydrogen bonds and Van der Waals forces. When a solvent infiltrates the pores these bonds can be cleaved and substituted by coal-solvent bonds. These steric rearrangements result in a weakening, or swelling, of the coal structure (Makitra and Bryk, 2008). Swelling by organic solvents is also established by the dissolution of material that has condensed inside the (micro)pores (the non-cross-linked part of the coal). Since higher rank coals contain less functional groups, have a tighter organic structure and have fewer pores with condensed material, their swelling is less pronounced than for lower rank coals like lignite (Jones et al., 1991, Spears et al., 1991). For illustration purposes, a computer simulation of the swelling of the cross-linked part of Upper Freeport bituminous coal with methanol is shown in **Figure 7** below, where 14 methanol molecules are incorporated onto the system constituting swelling.

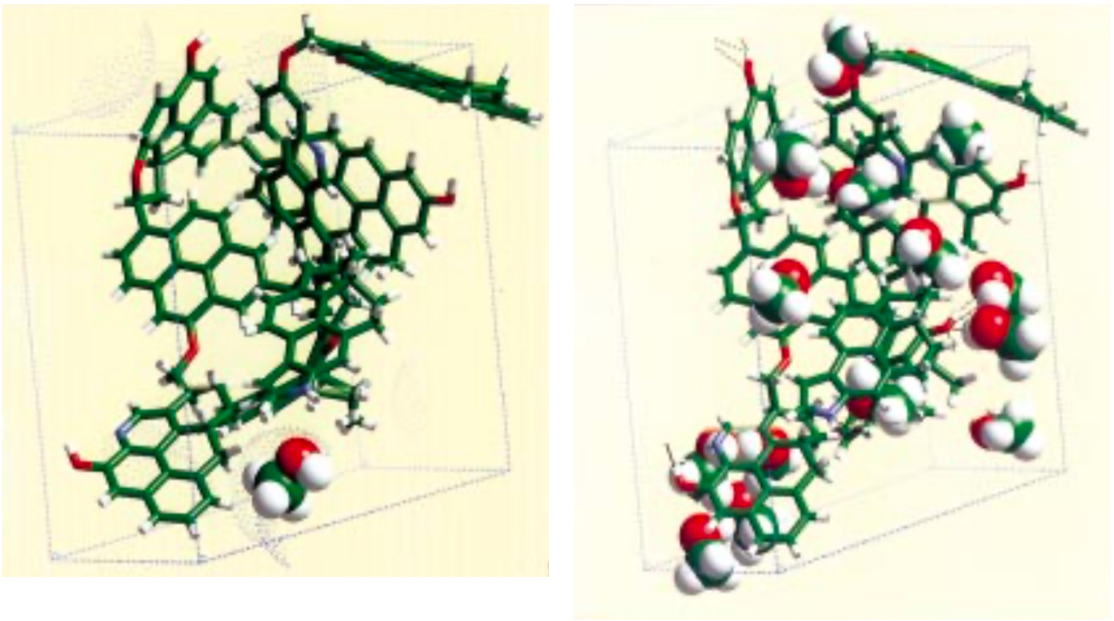

Figure 7 *Computer simulation of the pyridine-insoluble fraction of Upper Freeport bituminous coal with (a) one methanol molecule introduced in the molecular structure and (b) the equilibrium state of swelling with methanol. Source: Takanohashi et al. (1999). Copyright: American Chemical Society 1999.*

Jones et al. (1991) and Jones et al. (1997) stated imbibition of the solvent by coal is at its maximum when the solubility parameter of the solvent is equal to the solubility parameter of the coal. The cross-linked and non-cross-linked part of coal are treated as polymeric and having the same solubility parameter, which is calculated according to **Equation 1** below:

$$\delta = \left(\frac{\Delta U_{vap}}{V_m}\right)^{0.5}$$

Equation 1 *Solubility parameter of coal*

where δ is the Hildebrand solubility parameter ($Pa^{0.5}$), ΔU_{vap} is the energy change accompanying vaporisation ($Jmol^{-1}$) and V_m is the molar volume (m^3mol^{-1}) (Hansen, 2007).

The partial dissolution of the non-cross-linked part of the structure is governed by three solvent characteristics: *1)* the ability of solvent molecules to enter the pores and thus the molecular cross-section of the solvent molecules, *2)* the refractive index, determining the

polarizability of the solvent, and *3)* the dielectric constant, a relative measure of the chemical polarity of the solvent (Makitra and Bryk, 2008).

Mixing of a solvent with pure water can aide both the solubility parameter and the dissolution of the non-cross-linked part of the coal (Jones et al., 1997). Firstly, pure water has a very high solubility parameter which can be used to increase the solubility parameter of organic solvents to match that of the coal. This is done by simply mixing water and a swelling solvent and gives the following solubility parameter δ_{mix} ($Pa^{0.5}$) as described in **Equation 2** below:

$$\delta_{mix} = \gamma_1 \delta(0)_1 + \gamma_2 \delta(0)_2$$

Equation 2 *Solubility parameter of solvent mix*

where δ_1 and δ_2 are the solubility parameters ($Pa^{0.5}$) and γ_1 and γ_2 the volume fractions of solvents 1 and 2 respectively (dimensionless). Secondly, the small molecular cross-section of water allows it to penetrate pores as small as ~ 0.35 nm, while a solvent like acetone can only enter pores with a minimal diameter of ~ 0.6 nm. If coal has many of those smaller micro pores, a large portion of the total coal swelling can be attributed to the enhanced micropore entry by the addition of water.

The increase in coal swelling by both the increased solubility parameter of the mixture and the increased micro pore entry by water addition is shown in **Figure 8(a)** below. The figure shows a swelling spectrum where swelling is plotted against different ratios of an acetone-water mixture. Water has both a higher solubility parameter than acetone, as well as a smaller molecular cross-section. In a swelling series with acetone and water, optimum swelling of 38.5 % was achieved when swelling Bergheim brown coal (Germany) with a mixture of 80 : 20 acetone-water ($\delta_{acetone}$ = 19.6 $Pa^{0.5}$, δ_{water} = 47.4 $Pa^{0.5}$, δ_{mix} = 25.2 $Pa^{0.5}$). According to Jones et al. (1997), the drop in swelling degree when adding more than 20 % water can be explained by the maximum pore entry being accomplished, and the coal imbibes with an acetone-water mixture which has a solubility parameter that is higher than that of the coal and thus constitutes less swelling.

Compare this to the swelling spectrum of **Figure 8(b)** where swelling of the same coal is plotted against different ratios of a methanol-water mixture. Methanol has a smaller molecular cross-section than acetone which should allow it to enter smaller, and thus more, pores than acetone. Yet the maximum swelling attained is less than when using acetone. The lack of an optimum indicates that the solubility constant of the coal is below the range attainable by mixing methanol with water. This is demonstrated by **Figure 8(a)** which shows that the δ_{coal} is around 25 $Pa^{0.5}$ and methanol has a solubility constant higher than that ($\delta_{methanol}$ 29.6 $Pa^{0.5}$) which is only increased by the addition of water (δ_{water} = 47.4 $Pa^{0.5}$).

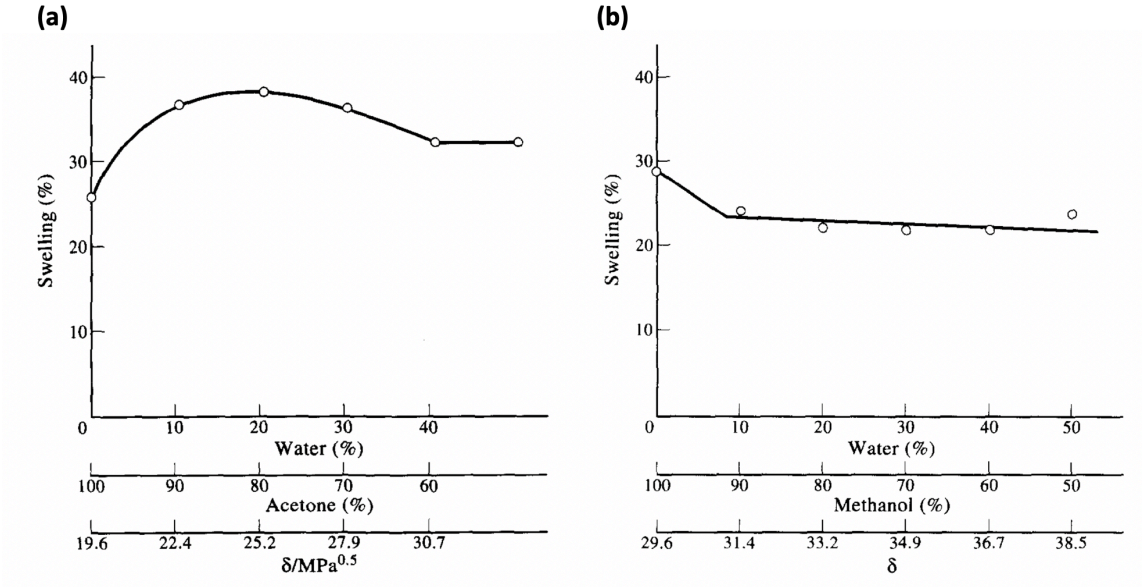

Figure 8 *The swelling spectra of Bergheim brown coal (Germany) for* **(a)** *different acetone-water mixtures and* **(b)** *different methanol-water mixtures. Source: Jones et al. (1997). Copyright: Elsevier Science Ltd. 1997.*

In the study of Suuberg et al. (1994) the researchers indicate that the electron-donating capacity of solvents is an important factor in the swellability of coal, but they also focus heavily on the enthalpy of interaction (heat of immersion and mixing) with surface functional groups, in particular phenolic hydroxyls. Furthermore, they postulate that the magnitude of swelling is predetermined by the number of specific hydrogen-bonding sites present in the coal. However, they also state the possibility that non-specific interactions, such as the dissociation of non-covalent cross-links could be a significant contributor to the swelling process after the available specific bonding sites are filled. This is in line with the theories of Jones et al. (1991) and Jones et al. (1997) above.

The theory of Jones et al. (1991) and Jones et al. (1997) that the alignment of the solubility parameters of coal and solvent is governing a governing factor in swelling was later dismissed by Makitra and Bryk (2008). They stated the Palm basicity of solvents (B) is the crucial factor in determining the degree of swelling of lignites that contain carboxyl and hydroxyl groups. They used an extended Koppel-Palm equation (**Equation 3** below) to predict the degree of swelling (S) and found the equation is only slightly corrected by the solubility parameter (δ). They also found Reichardt electrophilicity (E_T) (or solvent acidity), non-specific solvation (permittivity ε and refractive index n_D) and the cross-sectional area of the solvent to be of little influence. Makitra et al. (2013) revised this theory a few years later, stating the relevance or irrelevance of certain terms in the extended Koppel-Palm equation (**Equation 3**) varies per coal type. It can therefore be hypothesised that when no experimental data is available for a specific coal type, all terms in **Equation 3** must be considered relevant and the equations of. Jones et al. (1991) and Jones et al. (1997) hold their relevance when trying to attain maximum lignite swelling.

$$\log S = a_0 + a_1 f(n^2) + a_2 f(\varepsilon) + a_3 B + a_4 E_T + a_5 \delta^2 + a_6 V_M$$

Equation 3 *Degree of swelling of coal*

Where S is the degree of swelling of coal, n the refractive index of a liquid extractant, ε the permittivity, B the Palm basicity, E_T the Reichardt electrophilicity, δ^2 the squared Hildebrand solubility parameter and V_M the molar volume.

Literature has shown that a temperature increase from 10 °C to 70 °C increased the rate of swelling but not the final percentage of swelling (Aida and Squires, 1985, Otake and Suuberg, 1997, Otake and Suuberg, 1998). For the initial development of a lignite based controlled-release fertiliser it is not important (yet) to increase the rate of swelling. Only after prototype development, when production optimization becomes a topic, might the issue of temperature with regards to swelling need to be revisited.

To conclude, organic polar solvents interact with the covalent and hydrogen bonds, the Van der Waals forces and the functional groups of coal to constitute swelling. The

carboxylic and phenolic acid groups are targeted specifically by some solvents, and the disruption of the micropore bonds increases the number of macropores (Hacimehmetoğlu, 2007). It will need to be investigated if this could have a positive effect on nutrient uptake and release since these interactions have to the best of our knowledge not been investigated yet. If low-rank coal swelling by certain solvents proves to be beneficial to nutrient ad- and desorption, we can focus on optimizing this process by creating a solvent mixture at a particular temperature that provides both maximum swelling and maximum nutrient adsorption for the different types of coal investigated in the proposed research.

2.5.3 Kinetic adsorption studies

Both the rate limiting mechanisms and the most important factors for nutrient uptake by coal can be ascertained by kinetic studies using the data from adsorption experiments. In an adsorption system, the overall adsorption rate is controlled by a specific limiting factor and a specific rate limiting mechanism. Determining this factor and mechanism can help improve the efficiency of the process and are therefore frequently investigated in literature (Xu et al., 2016). Over the years various mathematical models have been developed to aide in this quest. Each of the models depends on a different parameter or mechanism, and when fitting experimental adsorption data, the equation with the best R^2 indicates which parameter or mechanism is rate limiting in the adsorption process. In the proposed research we will be dealing with the adsorption of a dissolved nutrient (solute) onto lignite (solid adsorbent). The most frequently used equations to model this type of adsorption are stated below and are described in detail in Appendix C:

- The Lagergren pseudo first order equation
- The Elovich's equation
- The pseudo second order equation

Initial concentration

Several studies where the pseudo second order equation proved the best fit, found there is an optimum initial concentration that produces the highest rate constant of adsorption (k_2, see Appendix C). Increasing the initial concentration above that optimum value decreases the rate constant of adsorption and thus slows down adsorption. This was found for ammonium adsorption by zeolite (Malekian et al., 2011) and urea adsorption by

activated carbon fibre derived from palm kernel expeller (Ooi et al., 2017). Nazari et al. (2018) studied the removal of ammonium by Victorian brown coal and found that with increasing initial concentration (C_0 = 0 - 65 mg/L) adsorption capacity was heading towards a plateau. In contrast, Kameda et al. (2017) found in their research on urea adsorption onto activated carbon that a higher concentration of urea always resulted in a larger amount of urea adsorbed (C_0 = 50 - 2000 mg/L). The discrepancy in the findings of these studies indicates that, if nutrient adsorption onto various types of low-rank coal is to be maximised, the potential of an optimum initial concentration will need to be examined through kinetic studies.

Diffusion mechanisms

The above kinetic models do not determine which of the three consecutive diffusion mechanisms that occur during the adsorption of nutrients onto low-rank coal, is rate limiting. These diffusion mechanisms are (Gupta and Sharma, 2003, Safwat and Matta, 2018):

1. Film diffusion or external transport; where a nutrient ion moves from the bulk solution to the outer surface of a lignite particle.
2. Intraparticle diffusion or internal transport; where the nutrient ion moves through the internal pore structure of a lignite particle.
3. Adsorption of a nutrient ion onto the surface of a lignite particle.

The overall adsorption rate is determined by the slowest mechanism in the adsorption process. This becomes apparent when a low initial concentration constitutes higher adsorption than with a higher initial concentration in systems with rapid film diffusion. This is because in systems with dilute concentrations, poor mixing or smaller particle sizes, film diffusion is often the rate limiting step. Conversely, in highly concentrated systems or systems with good mixing or large particle sizes, intraparticle diffusion is the rate limiting process (Gupta and Sharma, 2003). To determine which step is rate limiting, the intraparticle diffusion model and Boyd kinetic model can be employed, which are described in detail in Appendix D.

In summary, kinetic studies can identify the rate limiting factors and mechanisms for the adsorption of nutrients onto lignite. They can also produce a value for the optimal initial nutrient concentration.

2.5.4 Equilibrium isotherms for nutrient adsorption

To obtain information on the occurrence of the adsorption process, isothermal equilibrium studies are employed. Experimental data is used to plot adsorption at a constant temperature as a function of initial nutrient concentration, followed by fitting the data to various equilibrium isotherms. These isotherms are based on specific assumptions regarding the nature of the adsorption process. Commonly employed equilibrium isotherms of interest to a low-rank coal-nutrient adsorption study are given below (a description of their suppositions regarding the occurrence of adsorption is given in Appendix E):

- *Langmuir*
- *Freundlich*
- *Redlich-Peterson*
- *Dubinin–Radushkevich*
- *Temkin*
- *Harkins–Jura*
- *Halsey*

The usefulness of equilibrium isotherms is demonstrated by Kameda et al. (2017), who adsorbed urea onto activated carbon. The Halsey isotherm best described the adsorption occurring in their system and this isotherm indicates multilevel adsorption. The apparent rate constant decreased with increasing temperature, which resulted in maximum urea adsorption at a temperature of 10 °C at any given time. Doskočil and Pekař (2012) and Arslan et al. (2007) examined the adsorption of various metal ions onto lignite and lignite derived humic acids, respectively. They found that the adsorption of most metal ions decreased with increasing temperature (from 25 – 45 °C), except for zinc, which showed a 140 % increase in sorbed amount for the same temperature increase (Doskočil and Pekař, 2012).

The discrepancy between the different studies shows that the optimal temperature for adsorption will depend on the specific nutrient species and the specific adsorbent used. To the best of our knowledge, the temperature dependency of ammonium-N adsorption

has only briefly been touched upon by Tu et al. (2019). However, that study was done in the presence of a reactive dispersant and did not investigate an optimum reaction temperature.

2.6 Controlled-release of nutrients by lignite

The controlled release character of fertilisers is examined through nutrient dissolution studies, or desorption studies, in the case of a lignite-based controlled-release fertiliser. Methods to characterise the controlled-release character of fertilisers have been intensively researched over the past decades, and numerous models have been developed to aid in the assessment (Shaviv, 2000). A nutrient dissolution study of particular interest was conducted by Saha et al. (2017), following the method of Dai et al. (2008). As described in Appendix A, Saha et al. (2017) used granulation of brown coal with urea on the basis of C : N ratio and added starch and molasses to the pan granulation process as a binder to increase granule integrity. The dissolution experiment consisted of placing brown coal - urea samples in a mesh bag in deionised water and analysing the water content at specific time intervals. Upon placing the samples in deionized water, Saha et al. (2017) found that urea releases almost 100 % of its urea-N after 3 days. The brown coal granules with a high urea percentage (17.31 - 21.45 % N) released approximately 77 % of their urea-N after 13 days. The brown coal granules with a lower urea concentration (5.74 - 8.33 % N) released only 64 % and 68 % respectively of their urea-N after 13 days.

The release of ammonium-N was also investigated. Urea granules did not result in NH_4^+-N release, while for the urea - brown coal granules the NH_4^+-N release rate increased with the duration of the experiment. This resulted in less than 7 % ammonium-N release for the urea brown coal granules with a higher urea percentage, and less than 2 % NH_4^+-N release for the urea-brow coal granules with a lower urea content. The undesirable release of ammonium-N from the urea-brow coal granules indicates partial hydrolysis of urea, likely caused by the urease inherent to the brown coal structure and brown coal's natural acidity (Saha et al., 2017).

Some form of inhibition of the partial hydrolysis of urea should be an avenue of investigation in order to reduce potential NH_4^+-N losses of lignite-based controlled-release fertilisers. The inhibition could be in the form of a disinfectant; when used as swelling solvent this may prevent or slow down bacterial growth inside the lignite pores. Inhibition could also occur through better regulation of the acidity of lignite-based controlled-release fertilisers. It is also worth exploring if solvent swelling removes part of the urease inherent in low rank coal, and consequently lowers the potential of NH_4^+ release.

The slower release of urea-N from the granules with a lower urea content might be caused by a lower concentration gradient or by oversaturation of the sorption sites in the coal. Increasing the availability and reactivity of the functional groups using solvent interactions might provide a different result to the nutrient release study of Saha et al. (2017), one where a higher N-loading can be accomplished and yet with a release slow enough to be competitive with conventional fertilisers. Coal-solvent (swelling) studies in combination with dissolution studies will therefore need to be conducted in the proposed research to optimise the efficiency of a low-rank lignite-based controlled-release fertiliser.

2.7 Summary of research gaps

From the reviewed literature it can be concluded that conventional fertilisers are inefficient because a discrepancy between fertiliser nutrient release rate and plant uptake results in heavy loss of nutrients. The current slow- and controlled-release alternatives are expensive, cause soil contamination or are otherwise cost-inefficient and inadequate in preventing detrimental environmental effects due to overfertilization. Lignite-based fertilisers could have a considerable advantage over current fertilisers, both economically and environmentally, if they are designed to possess the following characteristics:

a) Consisting of a cheap base material that requires little pre-treatment;
b) Exhibit some form of urease inhibition;
c) Increase P bioavailability;

d) Provide efficient controlled-release of N/P/K that matches plant nutrient requirements, independent of soil and environmental conditions.

The examined body of literature indicates that lignite could be a cheap base material that requires little pre-treatment, has the potential to exhibit some form of urease inhibition and could increase P bioavailability. This leaves the question if lignite can be manipulated to fulfil the most crucial aspect of a feasible new fertiliser strategy; sufficiently and efficiently adsorb and subsequently release N/P/K nutrients in a manner that matches plant nutrient uptake.

From literature, several lignite properties were identified that are likely to play a crucial role in nutrient adsorption and controlled release. How these properties can potentially be manipulated to foster nutrient adsorption and controlled-release, has not been investigated yet. Also, due to the spatial variability of lignite and its inhomogeneous nature, the potentially beneficial property manipulations will need to be assessed for and tailored to individual lignite types. Currently, no investigative feasibility framework exists that contains methods and procedures that allow for a case-by-case assessment of lignite property manipulations to aid the development of lignite-based controlled-release fertilisers. In order to contribute to the alleviation of the environmental problems caused by overfertilization, the lack of such a feasibility framework is the research gap this thesis aims to address.

More specifically, methods will need to be developed to investigate:

1) The extent to which the lignite structure can be mechanically or chemically manipulated to increase the availability of the carboxylic and phenolic functional groups (binding sites) and increase the adsorption of nutrients onto lignite. This is established by investigating the following research gaps:
    - The effects of mechanical comminution on lignite characteristics, focussing on particle size distribution, apparent viscosity, specific surface area, micro and meso pore volume, and nutrient uptake capacity.
    - The effect of swelling solvents on specific surface area, micro and meso pore volume, and nutrient uptake capacity.

- The effect of pH on the availability of adsorption sites, specific surface area and total porosity, and nutrient adsorption onto lignite.

2) The temperature dependency of nutrient adsorption onto lignite.

3) The effect of initial nutrient concentration on nutrient adsorption capacity of lignite.

4) The effect of a variety of N/P/K nutrient species on the nutrient adsorption capacity (and thus nutrient loading) and the controlled-release character of a particular type of lignite.

5) The rate limiting factors and mechanisms of the adsorption of nutrients onto lignite.

6) The effects of the above-mentioned property manipulations on the controlled-release character of a particular type of lignite, and how this controlled-release character compares to conventional slow-or controlled-release fertilisers.

7) The effects of the above-mentioned property manipulations on the apparent viscosity of nutrient-infused lignite slurries, and the consequences of the possible rheological changes for the choice of delivery type of a lignite-based controlled-release fertiliser intended for precision agriculture.

Though points 5 and 6 are research gaps, the methods for investigating those research gaps are well established and thus will not be investigated in this research. After establishing methods for point 1 – 5, filling in the research gaps of 5 and 6 is relatively straight forward, yet some recommendations will be made at the end of the thesis. Methods for point 5 consists of standard desorption studies that are currently employed in academia and industry for comparing the efficacy of controlled-release fertilisers. Methods for point 6 follow from the methods established in point 1.

CHAPTER 3

METHOD DEVELOPMENT AND RESULTS

3.1 Approach to the research and introduction to the feasibility framework

Literature research was used to determine which properties and parameters are of primary importance when developing a lignite-based controlled-release fertiliser and how these properties can potentially be manipulated in favour of sustainable fertiliser development. The literature research showed lignite has a large spatial variability resulting in distinct geographical types of lignite, each with different characteristics that influence its potential as fertiliser matrix. Three main areas of focus were identified for lignite-based fertiliser development: *1)* maximising nutrient adsorption onto lignite through lignite property manipulation, *2)* characterising the subsequent nutrient release *in vitro*, and *3)* evaluating the optimal delivery type for precision agriculture applications.

Next, aims, hypotheses and objectives were formulated to design experiments for a case study that allowed for method development and provided a proof-of-concept of lignite property manipulation, nutrient adsorption and solvent swelling. The experiences obtained during the case study were used to develop best-practice methods and procedures that are suited for any type of lignite.

With the practical knowledge gained from the case study, the initial aims, hypotheses and objectives were tailored towards a more general approach, resulting in a framework with three stages, outlined in the flowchart of **Figure 9**. An exact description of the stages, objectives and hypotheses is given in Chapter 3.2 and Appendix F, and when combined with the recommended methods, they form the complete feasibility framework.

The work presented in this thesis focusses on Stage 1 because that is the area where appropriate and versatile methods are lacking. Each objective of Stage 1 is approached by first describing the general methods chosen to examine the manipulation of a lignite property. This is followed by an account of the exact methods used in the case study, the results and discussion of the scoping experiments, and an evaluation of the methods used. Each objective is concluded by a recommended method and an experimental design for the generalised feasibility framework (highlighted by a grey text box). The result is a set of tools for the case-by-case assessment of lignite property manipulations that are to aide in the development of lignite-based controlled-release fertilisers.

In a separate chapter, recommendations with regards to Stage 2 and 3 are given. In the same chapter, recommendations are made with regards to production, optimisation and potential drawbacks of lignite-based controlled-release fertilisers.

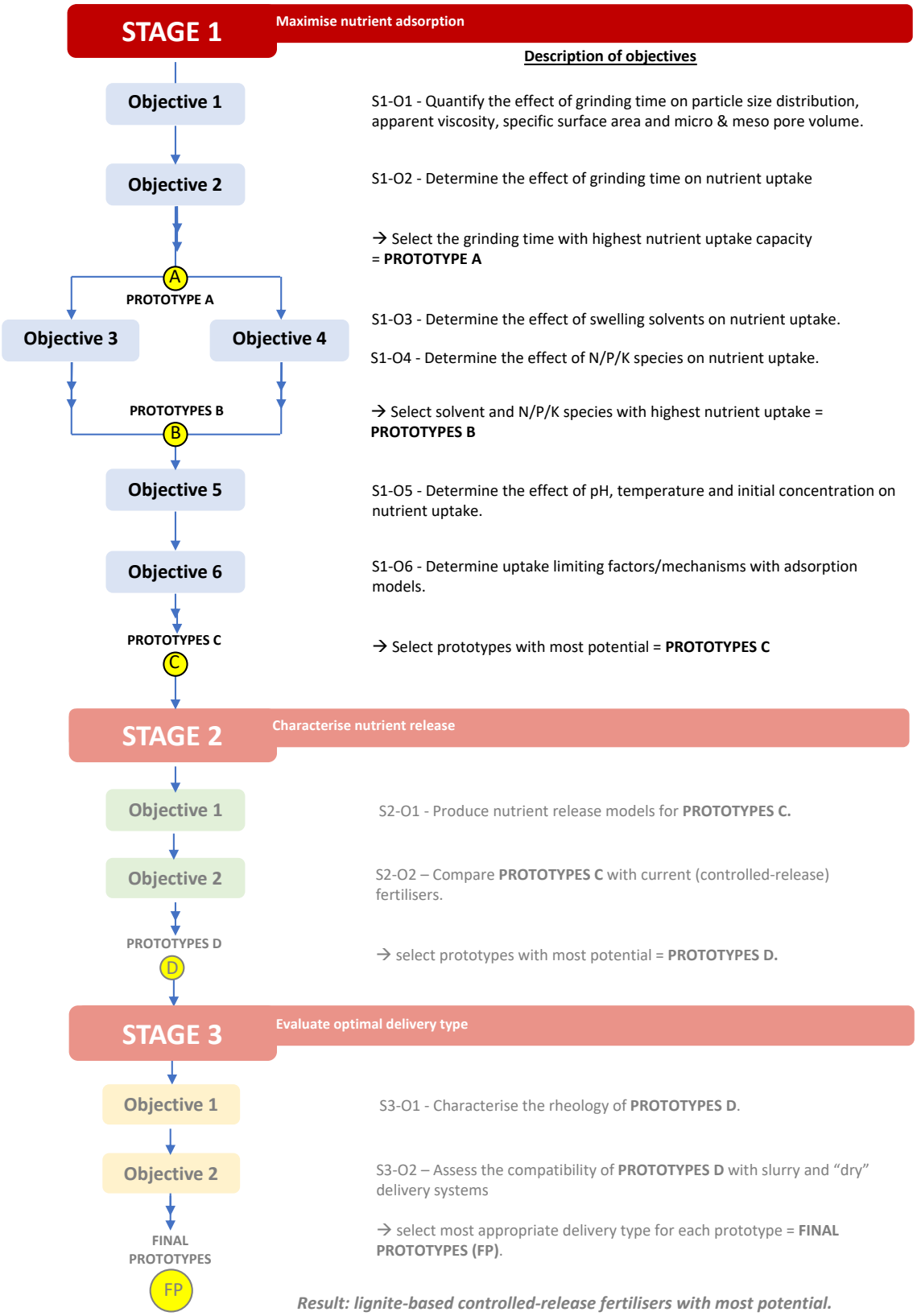

Figure 9 *Flow chart of the feasibility framework for a lignite-based controlled-release fertiliser. Double arrows indicate a prototype selection step. The focus of this thesis is on Stage 1. S = stage, O = objective.*

3.2 Stages and objectives of the feasibility framework

The following three stages have been developed for the feasibility framework that assesses the potential of any type of lignite to act as matrix in a sustainable controlled-release fertiliser:

STAGE 1
Maximise N/P/K nutrient adsorption on to lignite for controlled-release fertiliser development.

STAGE 2
Characterise nutrient release of lignite-based controlled-release fertiliser prototypes and compare to current fertilisers.

STAGE 3
Evaluate the optimal delivery type for deployment in precision agriculture (e.g. slurry, granules, pellets) of the final lignite-based controlled-release fertiliser prototypes.

The objectives to achieve each of the three stages of the framework are listed below. It is emphasised which lignite property or manipulation the objectives investigate. The hypotheses on which the objectives are based are listed in Appendix F.

Objectives (O) to achieve Research Aim 1 (S1):

"Maximise N/P/K nutrient adsorption on to lignite for controlled-release fertiliser development."

- S1-O1 – Quantify the effect of grinding time on lignite particle size distribution (PSD), apparent slurry viscosity, specific surface area, and micro and meso pore volume through experimentation.
- S1-O2 – Following S1-O1, determine the effect of grinding time (and corresponding PSD, specific surface area, micro and meso pore volume) on nutrient uptake capacity, in order to select the grinding time that results in the highest nutrient uptake = PROTOTYPE A.
- S1-O3 – Determine the effects of various swelling solvents on lignite volume, particle size distribution, specific surface area, micro and meso pore volume, and nutrient uptake through a series of swelling experiments, in order to select the solvent that results in the highest nutrient uptake.
- S1-O4 – Determine the effect of different N/P/K species on lignite nutrient uptake through a series of adsorption experiments in combination with varying swelling solvents, in order to select the N/P/K species that results in the highest nutrient uptake. Together with the results from S1-O3 make a selection of the lignite-based controlled-release fertilisers with the most potential = PROTOTYPES B.
- S1-O5 – Determine the effect of pH, temperature and initial nutrient concentration on lignite nutrient uptake using kinetic and equilibrium studies to produce adsorption isotherms.
- S1-O6 – Following S1-O5, determine the adsorption limiting factors and mechanisms of nutrient uptake by lignite, by fitting the produced equilibrium data and adsorption isotherms to a selection of kinetic and isothermal adsorption models, in order to make a selection of the lignite-based controlled-release fertilisers with the most potential = PROTOTYPES C.

Objectives (O) to achieve Research Aim 2 (A2):

"Characterise nutrient release of lignite-based controlled-release fertiliser prototypes and compare to current fertilisers."

- S2-O1 – Quantify the controlled-release nature of PROTOTYPES C with nutrient release models, by performing *in vitro* nutrient release experiments.
- S2-O2 – Compare the nutrient release character and nutrient densities of PROTOTYPES C to that of currently available (controlled-release) fertilisers and select the prototypes that hypothetically compete with current fertilisers and best match nutrient uptake requirements of the intended plant species = PROTOTYPES D.

Objectives (O) to achieve Research Aim 3 (A3):

"Evaluate the optimal delivery type for deployment in precision agriculture (e.g. slurry, granules, pellets) of the final lignite-based controlled-release fertiliser prototypes."

- S3-O1 – Characterise the rheology (apparent viscosity) of PROTOTYPES D.
- S3-O2 – Assess the compatibility of PROTOTYPES D with current fertiliser slurry delivery systems, and assess if additives are required, or if the additional conversion to a "dry" delivery type (e.g. granules, pellets) is an economically advantageous option. The resulting recommended lignite-based controlled-release fertilisers are the FINAL PROTOTYPES.

3.4 Feasibility framework Stage 1: Method development, testing and evaluation

The focus of this thesis is on Stage 1: Maximising nutrient adsorption onto lignite. Though maximised nutrient adsorption onto lignite is not necessarily a prerequisite for a successful controlled-release fertiliser, a nutrient-dense fertiliser is of significant importance from an economic viewpoint. Therefore, high nutrient loading is the starting point for prototype development.

As mentioned earlier, most of the objectives are subdivided into three sections: general methods, Kai Point lignite case study and recommended methods. To reiterate, the scoping experiments of the case study were performed in order to find appropriate methods to evaluate the manipulated properties. The experiments were specifically not conducted to obtain significant results for the local lignite used. A summary and assessment will be given for the results obtained from the case study, but a comprehensive feasibility assessment of Kai Point lignite is not within the scope of this research.

3.4.1 Objective 1 (S1-O1): Determine the effect of grinding time

In order to maximise nutrient adsorption onto lignite, the first objective focusses on manipulating the properties of lignite by varying the solids loading and grinding time of lignite slurries. The objective is to *"Quantify the effect of grinding time on lignite particle size distribution (PSD), apparent slurry viscosity, specific surface area, and micro and meso pore volume through experimentation"*. This objective is achieved by first producing different lignite slurries types by varying the grinding time and solids loading, followed by an analysis of the particle size distribution, apparent viscosity, specific surface area, and micro and meso pore volume of the different slurry types.

3.4.1.1 Lignite slurry production

3.4.1.1.1 Method development for lignite slurry production

In general, lignite slurry is prepared by grinding raw (untreated) lignite and mixing it with water. However, before producing a slurry the raw lignite should be analysed. The conventional methods for analysing any raw coal material are determined by industry standards for proximate (Speight, 2005b) and ultimate analysis (Speight, 2005c) and X-ray fluorescence (XRF). Respectively, the techniques shed light on the elemental composition, the moisture, ash and volatile content, and the ash constituents of a lignite. The ash constituents are important when applying the lignite to agricultural soil in large quantities as the values of the XRF analysis can be used to calculate if the contaminants exceed locally determined legal limits. The proximate, ultimate and XRF values are

usually known for coal from a specific mine, but due to the spatial inhomogeneity of lignite it pays to do these analyses for each batch of lignite obtained.

Grinding of lignite can be done through various comminution techniques, but this research used an attritor (or stirred ball mill) because it is a relatively cheap and simple instrument. When keeping all other parameters the same during the grinding process, the grinding time can be prolonged or shortened to respectively decrease or increase the particle size distribution (PSD) of the lignite particles in the slurry (Woskoboenko et al., 1991). Experiments were set up to investigate if besides grinding time, the solids loading at the start of the grinding process also has an effect on PSD. PSD is an important parameter for nutrient uptake and slurry rheology, and more specifically, apparent viscosity. Apparent slurry viscosity is also affected by the lignite solids loading in a slurry (Goudoulas et al., 2010).

Grinding is a very expensive operation (Tromans and Meech, 2004). For purposes of cost-efficiency it is therefore imperative to find the shortest grinding time that results in a particle size distribution that is favourable for nutrient uptake. Research by Woskoboenko (1985) has shown that a favourable mass-median diameter (= "sweet-spot") of a wet Victorian brown coal slurry is ≥ 13.5 μm, since at this value a plateau is reached for total porosity and specific surface area of the lignite particles. As will be explained below, the equipment used for the analysis of PSD in the case study measures volume-median diameter instead of mass-median diameter. Volume-median diameter can be correlated to a maximum specific surface area just like mass-median diameter. Therefore experiments are designed to determine where the volume-median diameter "sweet-spot" is for a particular type of lignite, and thus inform which grinding time is preferred for maximising nutrient adsorption.

3.4.1.1.2 Kai Point lignite case study: Raw lignite analysis and slurry production

In the case study, Kai Point lignite (Otago, NZ, 45°28'39"S 169°18'24"E) was used as raw material. Ultimate and proximate analysis are shown in **Table 1** below and XRF analysis of the ash constituents in **Table 2** below. It is indicated which industry standards are used for each analysis. The percentages cannot be added because of the different standards used for the analysis (this is the conventional way of representing proximate and ultimate analysis). Kai Point lignite has a considerably lower moisture content than the Victorian

brow-coals described in most literature in Chapter 2.4 and 2.5, and used in the brown-coal fertiliser studies of Rose et al. (2016) and Saha et al. (2017) described in Chapter 2.3.2. The relatively high Al_2O_3 content in the XRF analysis becomes important when considering potential aluminium toxicity further in the development process of lignite-based controlled-release fertilisers.

Table 1 *Proximate and ultimate analysis of Kai Point lignite.*

Constituent	Method	As received basis (%)	Dry Basis (%)
Moisture	ISO 5068	28.0	-
Ash	ISO 1171	5.0	6.9
Volatile	ISO 562	33.4	46.4
Fixed carbon	by difference	33.6	46.7
Sulphur	ASTM D4239	3.8	5.2
Carbon	ASTM D5373	47.7	66.3
Hydrogen	ASTM D5373	3.4	4.8
Nitrogen	ASTM D5373	0.5	0.6
Oxygen	by difference	11.7	16.3

The Al_2O_3 content measured with XRF is of concern since lignites have a low pH (around 4.5) which can result in increased mobility of aluminium (Zheng et al. 2010). Several studies found leaching of aluminium where lignite or lignite fly ash were placed on top of the soil or used as plant growth medium (Ross et al. 2003, Bilski et al. 2014). It is hypothesised, and thus needs further investigation, that XRF Al might also become more available when the properties of lignite are manipulated in order to transform lignite into a controlled-release fertiliser which is subsequently incorporated in agricultural soil with an active soil microbial community. Logic suggests that lignites with a higher aluminium content have a higher probability of leaching toxic amounts of (mobile) aluminium, and thus pose a greater threat to groundwater and the functioning of plant roots than lignites with low Al content. Therefore, if a lignite batch contains a relatively high percentage of Al, this issue could become a serious environmental problem, and further investigation is recommended.

Table 2 *The XRF analysis of ash constituents in Kai Point lignite according to the method ASTM D4326.*

Ash constituents	% (ASTM D4326)
SiO_2	27
Al_2O_3	20.9
Fe_2O_3	7.7
CaO	15.9
MgO	4.6
Na_2O	0.5
K_2O	0.8
TiO_2	0.8
Mn_3O_4	0.3
SO_3	20.1
P_2O_5	0.5

Mechanical particle size reduction was performed by at CRL Energy Ltd., where the raw Kai Point lignite was mixed with tap water and ground in an attritor [CY-SFM-5, Zhengzhou CY scientific instrument co. Ltd] according to the procedure in Appendix G. Both solids loading and grinding time were varied to create nine different slurry types, given the code HS1 - HS9. Due to the nature of the grinding process, the solids loading at the start of the grinding process is rarely identical to the solids loading of the end product. Therefore, the solids loadings of the end products were calculated by weighing a certain amount of Kai Point lignite slurry before and after drying at 40 °C for 5 days, until all free water has evaporated. The values are displayed in **Table 3** below and are the average of duplicate measurements.

Table 3 *Conditions of preparation for the different Kai Point lignite-slurry types HS1-9.*

Slurry name	Lignite (gr)	Water (gr)	Grinding time (min)	Solids loading %	
				Before grinding	*After grinding*
HS1	900	900	5	50	59
HS2	450	1350	10	25	31
HS3	450	1350	15	25	24
HS4	450	1350	20	25	20
HS5	450	1350	30	25	28
HS6	650	1300	10	33	26
HS7	650	1300	15	33	27
HS8	650	1300	20	33	34
HS9	650	1300	30	33	36

3.4.1.1.3 Recommended methods and experimental design for slurry production

Before producing slurries, proximate and ultimate analysis and X-ray fluorescence (XRF) should be used to analyse the specific batch of lignite according to the industry standards listed above. Lignite slurries are produced using one particular type of lignite and (tap) water. Five types of lignite slurries should be produced by varying the grinding time between 1, 3, 5, 10 and 15 minutes, according to the experimental design in Appendix H. Over the course of objective S1-O1 and S1-O2 (S1 = Stage 1, O1 = Objective1 and O2 = Objective 2) this table will be filled in and help identify the effects of grinding time on several lignite characteristics, including nutrient uptake capacity. The filled-in table of Appendix H will inform what grinding time is used for the experiments from Objective S1-O3 onwards.

The slurries are prepared with an initial solids loadings of 50 wt.% raw lignite and the solids loading after preparation should be measured by difference, using oven-drying at 40 °C for 5 days (after 5 days all free water should have evaporated from the lignite slurry) and written down in the experimental design table of Appendix H. The reasoning for the choice of the specific grinding times and solids loading is explained in section 3.4.1.2 below on particle size distribution analysis.

3.4.1.2 Particle size distribution analysis

3.4.1.2.1 Method development for particle size distribution analysis

Particle size distribution (PSD) analysis was performed on the particles in the lignite - water slurries produced the section above, which allowed for the quantification of the effect of grinding time and solids loading on PSD. The equipment used was the Mastersizer 3000 *[Malvern Pananalytical Ltd., Malvern, United Kingdom]*. The output of one measurement of the Mastersizer is the average of a sequence of 5 automated, repeated measurements. To monitor the precision of the used sample- and measurement technique, the experiments were executed in triplicate.

Without requiring any additional data analysis, the accompanying program of the Mastersizer 3000 provides the D10, D50 and D90: indicating the diameter of a sieve that allows respectively 10 %, 50 % and 90 % of the total volume of particles to pass through. D50 is the volume-median diameter (Malvern-Instruments, 2013). The dataset also provides the D[4,3] and D[3,2]. D[4,3] is the volume moment mean (De Brouckere Mean Diameter or volume mean diameter), which reflects the size of those particles which constitute the bulk of the sample volume. It is most sensitive to the presence of large particulates in the size distribution. D[3,2] is the surface area mean diameter (Sauter Mean Diameter or plane mean diameter) which is most relevant where specific surface area is important e.g. for bioavailability, reactivity and dissolution, and is thus most relevant for our nutrient uptake study. D[3,2] is most sensitive to the presence of fine particulates in the size distribution (Malvern-Instruments, 2013).

In order to visualise the data, several types of graphs can be made, emphasising different characteristics of the lignite slurry. Cumulative graphs are appropriate for visualising D10, D50 and D90 and the shift in PSD due to increased grinding time, see **Figure 10** as an example. A normal PSD data plot with log scale X-axis shows the nature of the PSD: monomodal, bimodal or multimodal, see **Figure 11** as an example. Buranasrisak and Narasingha (2012) found that a bimodal PSD can achieve a higher maximum solids loading than a monomodal or multimodal PSD with the same viscosity. A higher

maximum solids loading is favourable for the production of a lignite-based controlled-release fertiliser because it means the lignite slurry can have a higher nutrient loading.

The work of Woskoboenko et al. (1991) suggests a wet slurry mass-median diameter of ≥13.5 μm is beneficial for nutrient adsorption since both the specific surface area and porosity of Victorian brown coal are approaching the optimum. The Mastersizer calculates volume-median diameter (D50) and thus cannot be directly correlated to mass-median diameter. The D50 of the five types of slurries is required to determine the effect of grinding time and PSD on specific surface area (see section 3.5.1.1.5 below). The grinding time that results in the largest specific surface area will likely be the optimum PSD for maximised nutrient uptake and thus inform the most appropriate grinding time. This hypothesis will need to be tested by correlating the nutrient uptake capacity with specific surface area and PSD (D50, D[3,2] and D[4,3]) in the nutrient uptake experiments of section 3.5.1.2.1.

3.4.1.2.2 Kai Point lignite case study: Particle size distribution analysis

Particle size distribution (PSD) analysis was performed on the particles of the nine different lignite - water slurries of **Table 3** above. This allows for the evaluation of the effect of grinding time vs. solids loading on PSD. Equipment used is the Mastersizer 3000 *[Malvern Pananalytical Ltd., Malvern, United Kingdom]*. The PSD of each slurry was measured in triplicate. The output of one measurement sequence is the average of 5 automated measurements (replicates). The used sample and measurement technique proved precise since results were reproducible with an average standard deviation of 0.01-0.06 between triplicates; therefore each curve displayed in **Figure 10** below and each value in **Table 4** is the average of the triplicates.

In order to visualise the data, two types of graphs were made, emphasising different characteristics of the lignite slurry. The cumulative graph of **Figure 10** below is appropriate for visualising D10, D50 and D90 and the shift in PSD due to increased grinding time. The normal PSD data plot with log scale X-axis of **Figure 11** shows the nature of the PSD: monomodal, bimodal or multimodal.

Figure 10 depicts volume % undersize vs. diameter (µm) for Kai point slurries HS1-5, with D10, D50 and D90 indicated by a horizontal line. D represents the diameter of the lignite particles, and D10, D50 and D90 indicate the diameter of the sieve that allows respectively 10 %, 50 % and 90 % of the particle to pass through. D50, the volume-median diameter, is not interchangeable with the mass-median diameter described by Woskoboenko et al. (1991), but without the actual specific surface area values that correspond to the volume-median diameters of the different slurries, the mass-median is used as a rough indicator. This assumption will be tested later in the feasibility framework. When using ≥13.5 µm as a rough estimate of the potentially favourable diameter, **Figure 10** shows that a shorter grinding time is likely a better starting point and that is why the recommended experimental design of S1-O1 and S1-O2 uses relatively short grinding times of 1, 3, 5, 10 and 15 minutes for the production of the lignite slurries.

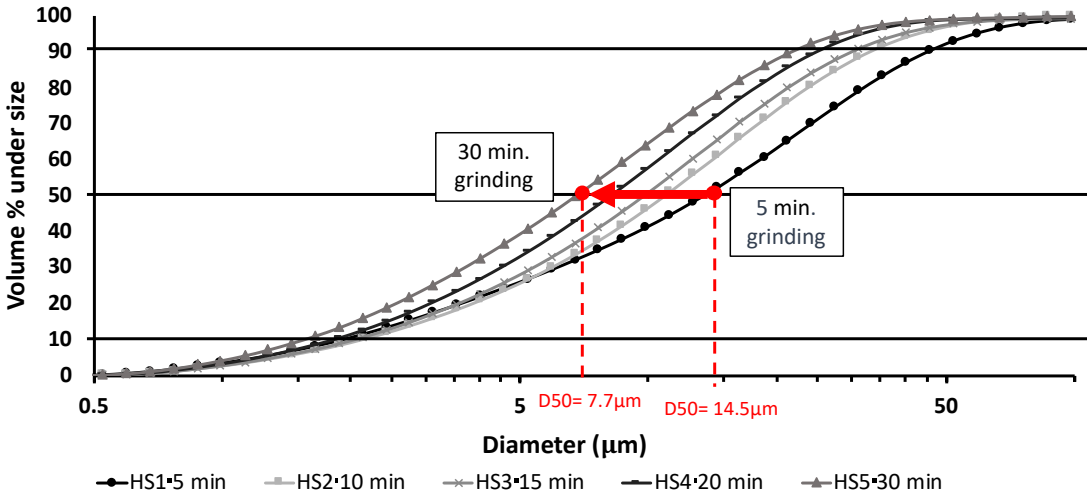

Figure 10 *Volume % undersize vs. size class for Kai Point lignite slurries HS1-HS5, with D10, D50 and D90 indicated by a horizontal line. The trend of decreasing volume-median diameter when grinding time is increased by 25 minutes (from 5 to 30 minutes) is indicated by the red arrow.*

Table 4 *Particle size distribution of Kai Point coal slurries HS1-5 expressed as D50 (volume mean diameter), D[4,3] (De Brouckere mean diameter) and D[3,2] (Sauter mean diameter).*

Sample Name	Grinding time (min.)	D50 (µm)	D[4,3] (µm)	D[3,2] (µm)
HS1	5	14.5	21.8	5.8
HS2	10	11.2	17.2	6.0
HS3	15	9.9	15.5	5.6
HS4	20	8.7	12.3	4.9
HS5	30	6.7	11.3	4.3
HS6	10	12.7	19.2	6.4
HS7	15	9.9	15.5	5.4
HS8	20	8.7	13.1	4.8
HS9	30	6.7	11.0	4.0

The sequential increase in grinding time from 5 min. to 10 min., 15 min., 20 min. and 30 min. is visible in **Figure 10** as a shift to smaller PSDs. Slurries HS6 – HS9 with differing solids loading from HS2 - HS5, are overlapping with the slurries of corresponding grinding time and are due to otherwise cluttered visibility not displayed. However, their almost identical PSDs, a trend also visible in **Table 4** above, tells us that while there is an obvious correlation between grinding time and PSD, there is no clear effect of solids loading on PSD. This lack of connection is why in the experimental design of Stage 1 – Objective1 (S1-O1) and Stage 1 – Objective 2 (S1-O2) solids loading is not a variable when producing lignite slurries; instead, the focus is on varying the grinding time to produce different PSDs and different values for specific surface area.

A short grinding time is preferred from an economic viewpoint since grinding is extremely cost-inefficient (Tromans and Meech, 2004). A short grinding time also results in more favourable coal properties because of the bimodal character of the PSD it produces (see **Figure 11 (a)** below). The bimodal character was observed for the slurry ground for 5 minutes but diminished for longer grinding times (see **Figure 11 (b)** below). Buranasrisak and Narasingha (2012) found that a bimodal PSD can achieve a higher maximum solids loading than a monomodal or multimodal PSD with the same viscosity. A higher maximum solids loading is favourable for the production of a lignite-based controlled-release fertiliser because it means the lignite slurry can have a higher nutrient

loading. This is another reason why the choice was made to shorten the grinding times to 1, 3, 5, 10 and 15 minutes for the recommended experimental design of Appendix H.

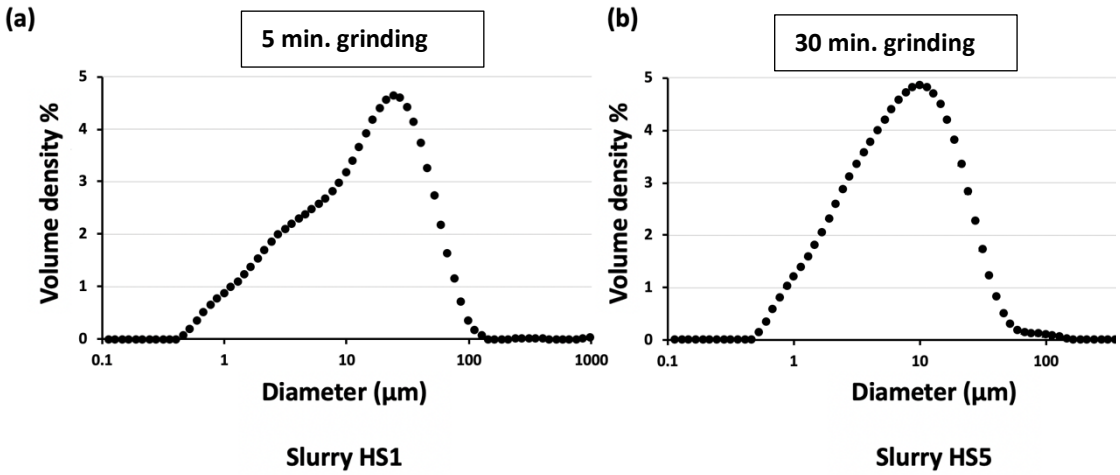

Figure 11 (a) *Bimodal character of the particle size distribution of slurry HS1 (5 minutes grinding, D [3,2] = 5.8µm) and* **(b)** *the unimodal character of the PSD of HS5 (30 minutes grinding, D [3,2] = 4.3µm).*

3.4.1.2.3 Recommended methods and experimental design for PSD analysis

A relatively high solids loading of 50 wt.% is chosen for the production of the lignite slurries of the feasibility framework because the water in the slurry acts as an undesirable diluting factor when adsorbing nutrients onto the lignite particles, which will be further discussed in section 3.4.2.1. A solids loading of 50 wt.% is the maximum attainable solids loading, above which the slurry becomes unmanageable and it is exceedingly difficult to remove the slurry from the attritor or mix the slurry with solvents and transfer it during the subsequent experiments of the framework. The maximum attainable solids loading might deviate for other types of lignite and will need to be assessed on a case by case basis, using 50 wt.% as a guideline.

The five types of slurry listed in Appendix H are analysed on particle size distribution in triplicate, according to the method described above. The values of the D50, D[4,3] and D[3,2] of each measured sample should be written down in the table of Appendix H to allow for comparison with the characteristics of the following sections.

3.4.1.3 Apparent viscosity analysis

Apparent viscosity, or shear viscosity, is a material's resistance to flow. For non-Newtonian fluids this resistance changes with shear rate. Apparent viscosity is an important rheological aspect and is defined by the relationship between shear stress [Pa] and shear rate [1/s].

Throughout the feasibility framework, the apparent viscosity is measured at two different stages. To create a baseline, the apparent viscosity is measured after the production of lignite slurries with varying grinding time (= varying PSD) but with no other lignite property manipulations or additions, and secondly, the apparent viscosity is measured after the production of PROTOTYPES B where most of the property manipulations have already taken place in order to maximise nutrient uptake and match nutrient release to plant uptake (refer to the flow chart of the feasibility framework in **Figure 9**). Apparent viscosity is an important factor when optimizing the lignite-based fertiliser for real-world application systems and assessing the feasibility of the produced prototypes. Apparent viscosity measurements are therefore crucial in achieving Aim 3: Evaluation of the optimal delivery type.

It is important to keep in mind that there are two different "optimal apparent viscosities" with regards to lignite slurries: one for the production process and one for the application of lignite-based controlled-release fertilisers in precision agriculture. During the production process the rheology is not a limiting factor, but when it comes to applying the lignite fertiliser slurry in an agricultural context, the rheological constraints of different slurry application systems determine the optimal apparent viscosity of the fertiliser slurry.

3.4.1.3.1 Method development for apparent viscosity analysis

The apparent viscosity of the nine different slurries listed in **Table 3** was measured in duplicate with a rheometer *[Physica MCR 301, Anton Paar, Graz, Austria]* according to the method below. Rheometers are specifically used for liquids with viscosities that vary with flow conditions (non-Newtonian fluids). The rheometer simulates a sequence of flow conditions and creates a data set of the shear stress in Pascal [Pa] over a predetermined shear rate [1/s] interval, describing the rheological behaviour of the slurry. From this, apparent viscosity [Pa*s] is calculated as follows:

$$Apparent\ viscosity\ = \frac{Shear\ stress}{Shear\ rate}$$

Equation 4 *Apparent viscosity.*

Before each measurement sequence with the rheometer, a conical centrifuge tube *[50 mL Falcon Scientific Ltd., Seaton Delaval, United Kingdom]* was filled with a sample of lignite slurry and tipped over quickly ten times to create a homogeneous sample. Immediately after tipping the tube, approximately 30 mL lignite slurry was poured into the rheometer cup *[CC27, Anton Paar, Graz Austria]* and placed in the rheometer. A rheometer vein *[ST22-4V-40, Part No.: 21015, Serial No.:10809, Anton Paar, Graz Austria]* was inserted in the cup with lignite slurry before starting the measurement.

3.4.1.3.2 Kai Point lignite case study: Apparent viscosity analysis

The apparent viscosity was measured of the nine different types of Kai Point slurry listed in **Table 3 and 4**. Because the slurries settle over time, the conical centrifuge tubes with slurry had to be tipped over ten times and approximately 30 mL slurry was quickly poured into the rheometer cup in order to attain a representative sample.

Findings of the rheological measurements are displayed in **Figure 12** and **Figure 13** below. The data set produced by the rheometer can be graphically represented in various ways, the most common being shear stress vs. shear rate and apparent viscosity vs. shear rate (both types of graphs have a logarithmic scale). **Figure 12** shows all nine slurries divided into two sets, HS1 - H5 above and HS1 + HS6 - HS9 below, to make the results better visible (HS1 is added to both sets to allow for better visual comparison). The graphs on the left display shear stress vs. shear rate, and display an offset at very low shear stresses of all slurry types, as is seen with Bingham plastics (Yavuz and Kucukbayrak, 1998). In the graphs on the right side, apparent viscosity is plotted against shear rate. **Figure 13** explains how rheological information can be extracted from the apparent viscosity vs. shear rate graphs.

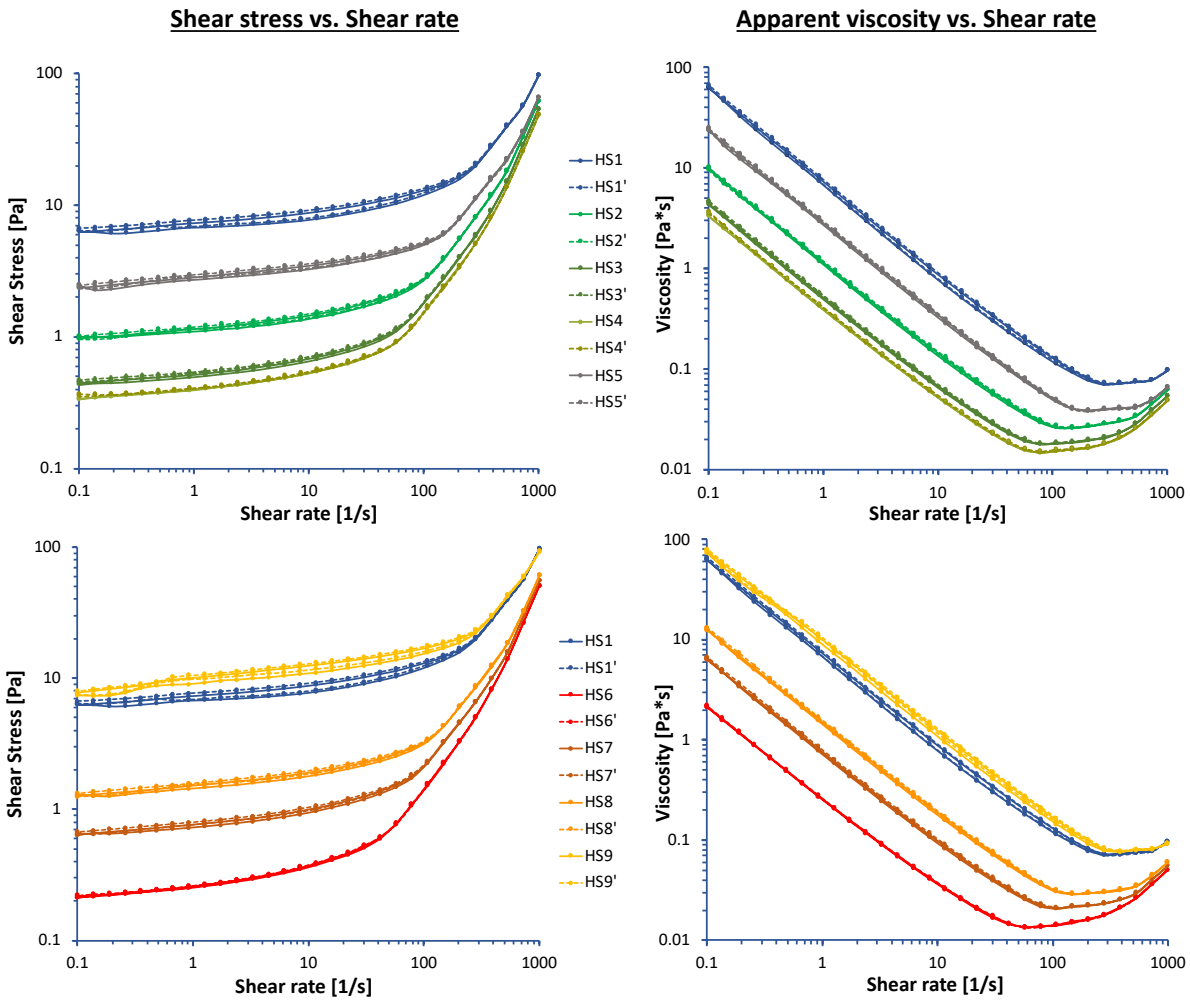

Figure 12 *Results of rheological measurements of shear stress vs. shear rate and apparent viscosity vs. shear rate of the nine different Kai Point lignite slurries HS1-9. (Note the log-log scale)*

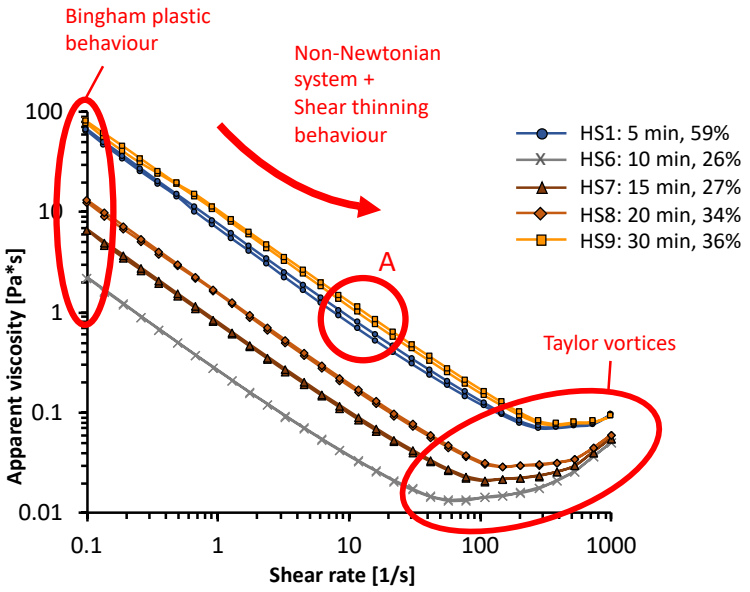

Figure 13 *Apparent viscosity [Pa*s] vs. shear rate [1/s] of HS1 and HS6-9, grinding time 5-30 min. Red circles and text indicate how specific information can be read from the graphs. (Note the log-log scale)*

The apparent viscosity of the slurries decreases non-linearly with increasing shear rate, indicative of shear thinning behaviour (Bahrani et al., 2015). At higher shear rates there is a rate of change in slope which is believed to be the onset of Taylor vortices, introducing turbulent behaviour and instability to the system (Escudier et al., 1995). The slurry with the lowest shear stress displays this Taylor vortex first, at a shear rate of approximately 40/s.

An increase in solids loading as well as an increase in grinding time (= smaller PSD) independently result in a higher apparent viscosity. From A in **Figure 13** can be deducted that the larger PSD of HS1 (grinding time 5 min.) can accommodate a significantly higher solids loading of 59 % compared to HS9 (grinding time 30 min.) with a smaller PSD and 36 % solids loading. This indicates a shorter grinding time is favourable with regards to achieving a slurry with lower viscosity at higher solids loading. Together with the reduced cost and stronger bimodal PSD character produced by a shorter grinding time, this result informed the choice to reduce the grinding time from 5-30 minutes to 1-15 minutes for the slurries of the recommended experimental design of the feasibility framework.

3.4.1.3.3 Recommended methods and experimental design for apparent viscosity analysis

The apparent viscosity of the five different slurries listed in the experimental design in Appendix H should be measured in triplicate with a rheometer *[Physica MCR 301, Anton Paar, Graz, Austria]* according to the method described above. After analysing the rheological behaviour using the type of graphs in **Figure 12**, the apparent viscosity [Pa*s] at shear rate 10/s for each of the five different lignite slurries should be written down in Appendix H for later comparison with the viscosity measurement of Stage 3.

3.4.1.4 Specific surface area, and micro and meso pore volume analysis

Specific surface area is one of the most critical factors for nutrient uptake, as specific surface area determines the extent to which nutrients have access to the pores. A higher specific surface area of the lignite particles means more lignite pores are accessible to the nutrients and thus more binding sites are available for nutrient adsorption, resulting in a higher nutrient uptake capacity of the lignite particles. As described in Chapter 2.4.3, micro and meso pore volume are determining factors in nutrient uptake and will need to be taken into account when choosing swelling solvents and nutrient species.

3.4.1.4.1 Method development for specific surface area and micro & meso pore volume analysis

Specific surface area and micro and meso pore volume analysis of lignite particles can be done with a Brunauer-Emmett-Teller (BET) apparatus (Brunauer et al., 1938). A BET apparatus produces an ad- and desorption isotherm of the physical monolayer adsorption of an inert gas (usually N_2) onto the surface of the particles in a sample. It calculates the specific surface area [m^2/g] of a sample using the BET adsorption isotherm equation. A complete ad- and desorption isotherm and several mathematical models are necessary to evaluate the micropore (< 2 nm) and mesopore (2 - 50 nm) volumes. Due to the versatility and sensitivity of the BET apparatus and the many mathematical models required for data analysis, it is highly recommended that BET apparatus sample preparation, measurement and interpretation is only done by, or with the assistance of, a trained expert.

Sample preparation for BET analysis requires ± 500 mg lignite per sample is oven-dried at 40 °C for 5 days, then the sample is activated at 50 °C under vacuum. In essence, during BET analysis N_2 uptake at -196 °C (77 K) is measured and CO_2 uptake at 0 °C (273 K). BET measurement of a sample takes a long time; therefore duplicates are in most cases the maximum replication that is practically feasible.

The specific surface area, and micro and meso pore volume of each of the slurries analysed with the BET apparatus should be noted in the table of Appendix H for comparison to PSD and grinding time. Grinding can increase specific surface area by fracturing lignite particles and exposing the pores, but when grinding is too long the specific surface area can decrease again. This is due to the destruction of some of the meso pores and capping of other meso pores by finer particles (Woskoboenko et al., 1991). The grinding time, and accompanying lignite slurry PSD, with the highest specific surface area and micro and/or meso pore volume is likely to achieve maximum nutrient adsorption. This theory will be tested in Stage 1 Objective 2 (S1-O2).

Before commencing BET analysis, thermo-gravimetric analysis (TGA) has to be performed to investigate the thermal stability of the sample material and determine the amount of volatiles present. Since water affects TGA measurements, approximately 20 mL lignite slurry sample needs to be dried at 40 °C for 5 days to ensure minimal water content. Equipment required is a TGA analyser *[Jupiter STA449 F1, NETZSCH-Gerätebau GmbH, Selb, Germany]* and the *NETZSCH* Proteus® software *[Version 610, NETZSCH-Gerätebau GmbH, Selb, Germany]*.

Instead of performing costly and time-consuming BET analysis, it has been found that the specific moisture capacity method is an adequate tool for predicting the specific surface area of expansive soils in particular (Khorshidi et al. 2017), meaning it could be explored as a potentially viable option for measuring specific surface area of lignite.

3.4.1.4.2 Kai Point lignite case study: TGA analysis

With the help of Dr Qun Chen (Massey University, School of Food & Advanced Technology) thermogravimetric analysis was performed. The results are required for the sample preparation and profiles of BET measurements. TGA measurements were done in

triplicate on two types of Kai Point lignite slurry: one subjected to 5 minutes grinding and one to 30 minutes grinding. Both slurries had been dried for 5 days at 40°C in an oven *[Series five, Conthern scientific limited, Lower Hutt]* to remove most of the water from the samples.

For the TGA measurement, between 5 - 10 mg dried slurry sample was placed inside the crucible of the TGA. N_2 flow rate was set to 40 mL/min and the temperature regime started at 40 °C. Stage 1 is an increase in temperature of 30 °C/min until 105 °C is reached, here an isotherm is maintained for 1 hour to remove the moisture from the system. In Stage 2 the temperature is further increased by 30 °C/min to 215 °C were another isotherm is maintained for 1 hour. The mass change over Stage 2 is equivalent to the % of light organic volatiles in the sample. Lastly, Stage 3 entails another 30 °C/min increase in temperature, when 900 °C is reached an isotherm is maintained for 45 minutes. The mass change over Stage 3 equals the percentage of other volatiles in the system. A complete measurement sequence, including cooldown, takes approximately 5 hours.

Using the *NETZSCH* Proteus® software *[Version 610, NETZSCH-Gerätebau GmbH, Selb, Germany]* the output graphs can be manually analysed. **Figure 14** below gives an example of such an analyses. The green lines are drawn to get an indication of the mass loss in each of the three stages. The 5.96 % mass change over Stage 1 represents the % moisture in the system, Stage 2 indicates the % of light organic volatiles (sulphur, hydrogen, nitrogen and oxygen), and Stage 3 reveals the % other volatiles of the sample. The results of the TGA analysis of the two different Kai Point lignite slurry samples are given in **Table 5** below. The results indicate (this particular batch of) Kai Point lignite has approximately 5.2 % moisture, 2.1 % light organic volatiles and 40.9 % other volatiles. These values are important when performing subsequent BET analysis, but due to time constraints and limited accessibility to the BET apparatus at Massey University, BET analysis could not be performed in the Kai Point lignite case study.

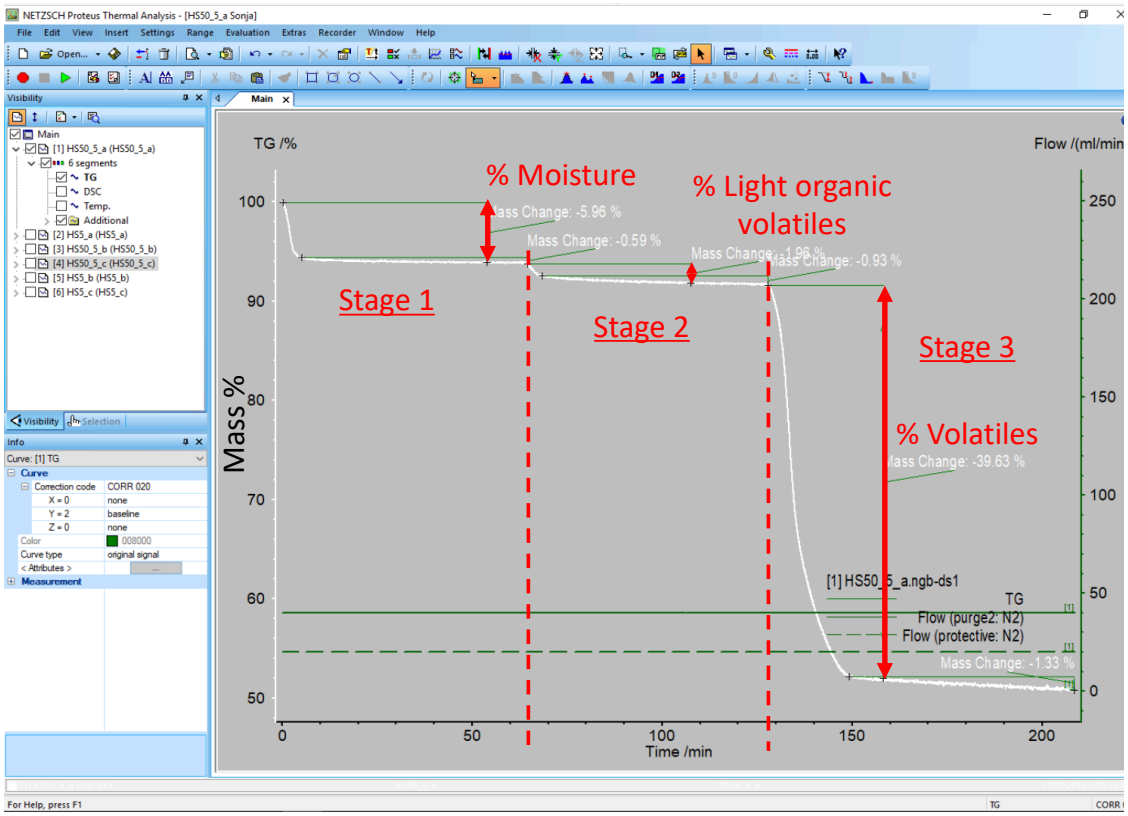

Figure 14 *NETZSCH Proteus® software graphical output of the TGA data from the Kai Point lignite slurry sample with 5 minutes grinding time. The red coloured text and lines are added to indicate how to interpret the graph.*

Table 5 *TGA analysis in triplicate of Kai Point lignite slurry samples with 5 min. grinding time (HS1) and 30 min. grinding time (HS5).*

Lignite sample	Moisture (mass %)	Light organic volatiles (mass %)	Volatiles (mass %)
HS1_a	5.96	1.96	39.63
HS1_b	*	2.20	39.81
HS1_c	5.80	2.01	41.96
HS5_a	4.73	2.17	41.15
HS5_b	5.29	2.21	41.33
HS5_c	4.13	2.17	41.34
Average HS1	5.88	2.06	40.47
Average HS5	4.72	2.18	41.27
Overall average lignite:	5.18	2.12	40.87

*The graph of HS1_b showed an error occurred during the initial phase of Stage 1, which did not affect the other stages of the analysis.

3.4.1.4.3 Recommended methods and experimental design specific surface area analysis

TGA analysis is independent of grinding time or solids loading, therefore only one slurry type needs to be analysed in triplicate. The results are used in the sample preparation and profiles of subsequent BET measurements. For BET analysis all the five slurry types are measured in triplicate, and the results, specific surface area and micro and meso pore volume, are written down in the experimental design table of Appendix H. Now the grinding time that leads to the largest specific surface area can be identified. The next step is confirming if this larger surface area also leads to a higher nutrient uptake capacity, which is done in the next section.

If BET analysis proves too costly and time-consuming, the specific moisture capacity method is worth exploring. It has been found that the specific moisture capacity method is an adequate tool for predicting the specific surface area of expansive soils (Khorshidi et al. 2017), and may be suited for lignite as well.

3.4.2 Objective 2 (S1-O2): Determine the effect of grinding time on nutrient uptake

In order to maximise nutrient adsorption onto lignite, the second objective focusses on the effect of grinding time on nutrient uptake capacity. The objective is to *"Determine the effect of grinding time (and corresponding particle size distribution, specific surface area, micro and meso pore volume) on nutrient uptake capacity, in order to select the grinding time that results in the highest nutrient uptake".* This objective is achieved by performing a nutrient uptake study with the five different types of lignite slurries produced in the previous objective (S1-O1). In the study *1)* a single nutrient species is combined with the lignite slurries, *2)* after an equilibration period the water and solids fraction of the nutrient-infused slurry are separated by filtration, and *3)* the nutrient concentration in lignite is measured to determine the uptake capacity of the lignite. The next step is correlating the uptake capacity to the manipulated properties (particle size distribution, specific surface area, micro and meso pore volume) in order to make an

informed decision on which grinding time to select for PROTOTYPE A, which will be used for the rest of the lignite property manipulations of the feasibility framework.

3.4.2.1 Analysing nutrient uptake capacity

Nutrient uptake capacity is evaluated multiple times within the feasibility framework, namely in Objectives 2 -5 of Stage 1. Described below is the first nutrient uptake study of the framework (performed with only one type of nutrient source: urea (CH_4N_2O)), but the recommended generalised method for nutrient uptake capacity analysis that is described at the end of this section, is employed in all the other objectives of Stage 1, and thus will be referred back to throughout the framework.

3.4.2.1.1 Method development for nutrient uptake capacity analysis

In order to examine nutrient adsorption capacity, samples are prepared by combining lignite slurries subjected to varying grinding times with a measured quantity of urea. Urea contains 46% N and is the most widely used agricultural nutrient-N source. It is theorised that upon dissolving in ultrapure water, urea will diffuse into the lignite pores and attach to the available carboxylic and phenolic binding sites (Saha et al., 2017, Nazari et al., 2018). After mixing lignite slurry with urea, literature was used to estimate how long it would take before an adsorption equilibrium is reached and an adsorption time was chosen that would allow such an equilibrium to establish. During this process, larger lignite particles settle and an interface forms between the settled solids and the liquid. Small volumes of this liquid can be sampled at regular intervals and analysed for total nitrogen with a TNM-L total nitrogen unit. This allows for mapping of the approximated adsorption behaviour of lignite via a relatively non-invasive (indirect) method.

After the adsorption equilibrium is reached, the samples are vacuum filtered through a glass microfibre filter. The solids that remain on the filter are dried for 5 days in an oven at 40 °C to prepare the lignite for elemental analysis, powder X-ray diffraction (PXRD) analysis and attenuated total reflection – Fourier transform infrared spectroscopy (ATR-FTIR). Elemental analysis reveals the total % nitrogen in the lignite that remains on the filter after filtration. Analysis of both total N in the lignite and in the filtrate should theoretically allow for a closed mass balance, identifying where exactly the urea goes when mixed with lignite slurry.

PXRD analysis provides information on the occurrence of nutrient crystals (e.g. urea) on the outside of the dried lignite particles. The occurrence of crystals on the outside is not necessarily detrimental to the development of a controlled-release fertiliser, as some plants have high nutrient demand in the initial stages of development (Römer and Schilling 1986). Crystals are not tightly, or not at all, bound to the lignite surface and readily dissolve in (soil) water, providing a faster release rate right after application. A rinsing step is added to the experimental design to examine if potential crystals can be washed off with a small volume of ultrapure water. If there are crystals on the outside of particles and if rinsing removes them, total nitrogen analysis of the rinsed lignite samples will show if the N in the samples comes only from the crystals on the outside. If total nitrogen analysis reveals nitrogen is present in the sample while PXRD does not indicate the occurrence of crystals, the nutrient-N can be present inside the pores of the lignite particles in the form of urea or other N-species, and the N can be bound in non-crystalline form to the outside of the particles.

ATR-FTIR can be used to elucidate the type of chemical bonds present on the surface of the lignite-urea sample. Combined with the total nitrogen analysis, ATR-FTIR and PXRD can discern if and how the nutrient species in the sample are bound to the surface of the lignite. The combination of the three analysis techniques can also determine if certain property manipulations increase the occurrence or availability of carboxylic and phenolic acid groups and other functional groups in the lignite structure. The three analysis techniques can also determine if the manipulations alter the interactions between various nutrient species and lignite's functional groups, and what effect the altered interactions have on nutrient uptake capacity of lignite.

ATR-FTIR analysis of lignite samples that are only subjected to mechanical comminution and to mechanical comminution and urea, provide a reference for the bonds found in lignite slurries and lignite-urea-slurries. This is useful when studying the effect of interactions between lignite and swelling solvents on the occurrence and availability of binding sites (see Objective S1-O3), and the effect of interactions between lignite and different nutrient species on binding sites (see Objective S1-O4), and the effect of pH changes on the chemical structure of lignite (see Objective S1-O5).

3.4.2.1.2 Kai Point lignite case study: Nutrient uptake capacity analysis

Three experimental designs were tested in order to determine the most appropriate method for measuring nutrient uptake capacity of lignite:

- The first experiment focussed on total nitrogen analysis of the filtrate using a small sample volume.
- The second experiment focussed on: which form of urea to administer to the lignite samples (= nutrient delivery method); the practicality of using a large sample volume to counter inhomogeneity in lignite samples; the ability of elemental, PXRD and ATR-FTIR analysis to determine the nitrogen content of the lignite particles and the nature of the nutrient uptake.
- The third and last experiment focussed on finetuning the sample volume, sample preparation and nutrient delivery method.

Nutrient uptake capacity Experiment 1: Methods and observations

For the first experiment, small volumes (4 - 5 mL) of lignite slurry were mixed with equal parts of a 21 wt.% urea solution in 15 mL conical centrifuge tubes. The lignite-urea slurries were left to settle, gradually creating an interface between the black settled lignite and the liquid on top. After three days there were still fine black particles suspend in the water phase. Centrifuging did not settle the suspended particles, on the contrary, after centrifuging the sample, the lignite – liquid interface was no longer visible and it seemed as if all particles had re-suspended. After the particles were resuspended the settling rate was very slow. In this scoping experiment only the liquid phase and not the solid phase was sampled, diluted and analysed on total nitrogen using a TNM-L total nitrogen unit *[TOC-LCH, Shimadzu, Kyoto, Japan]*. Measurements were done in quadruplets per slurry type.

Measuring the nitrogen concentration of the filtrate is an indirect method for determining the amount of N in the lignite and can be used as a fairly non-invasive technique to measure the N uptake pattern of the lignite in a sample over time. Only a very small volume of filtrate is required for TNM-L analysis since the study uses high concentrations of urea and the TNM-L method used has a low upper detection limit (500 mg N/L) and thus requires strong dilution.

One observation made, is that after a several weeks a gradual reaction became visible: the liquid on top of the settled particles gradually turned from colourless with small black suspended particles into a liquid with a transparent deep orange colour with no visible suspended particles, see Error! Reference source not found. below. The samples with slurries with longer grinding times (15 and 30 minutes) had a darker colour. The discolouration was very stable; even after one year the lignite particles and orange liquid remain optically unchanged. As reference, when adding ultrapure water to a lignite sample, no discolouration is observed after even a prolong period of time. The orange discolouration reaction could be caused by a pH change. It is known that urea increases the pH of a solution, a change that happens more pronounced when adding a higher concentration of urea (Bull et al., 1964). The sample volumes of Experiment 1 are too small to measure pH accurately (pH strips are not accurate enough), therefore a second experiment is conducted with larger sample volumes and pH is monitored throughout the experiment.

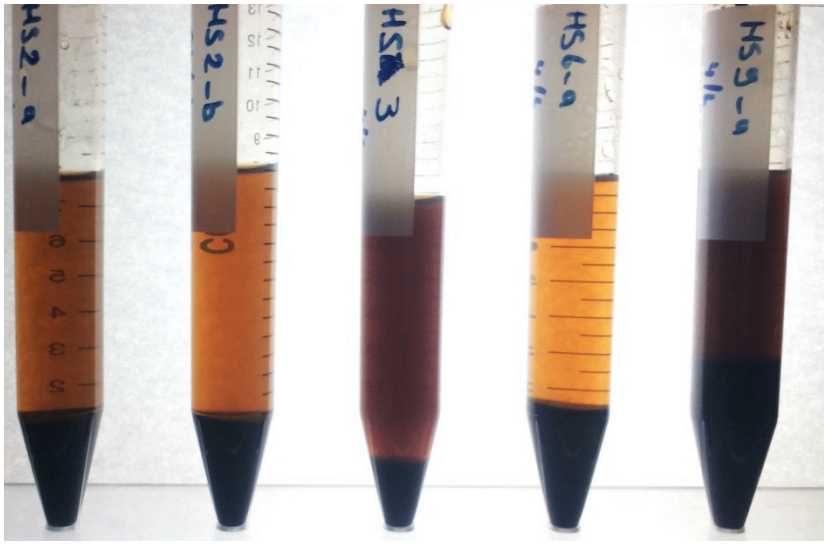

Figure 15 *Several samples of Experiment 1 showing orange discolouration of the liquid on top of the settled lignite.*

Nutrient uptake capacity analysis Experiment 1: Results

The TNM-L analysis of the filtrate gave reproducible results, with a deviation between quadruplets of 0.6 - 3.6 %. The results can be found in **Figure 16** below, wherein **(a)** the concentration of nitrogen in the filtrate is indicated after N-uptake by lignite, and how much the N concentration has decreased compared to the start of the experiment. From

this, it was calculated which percentage of N is theoretically uptaken by the lignite in the duration of the experiment, displayed in **Figure 16 (b)**.

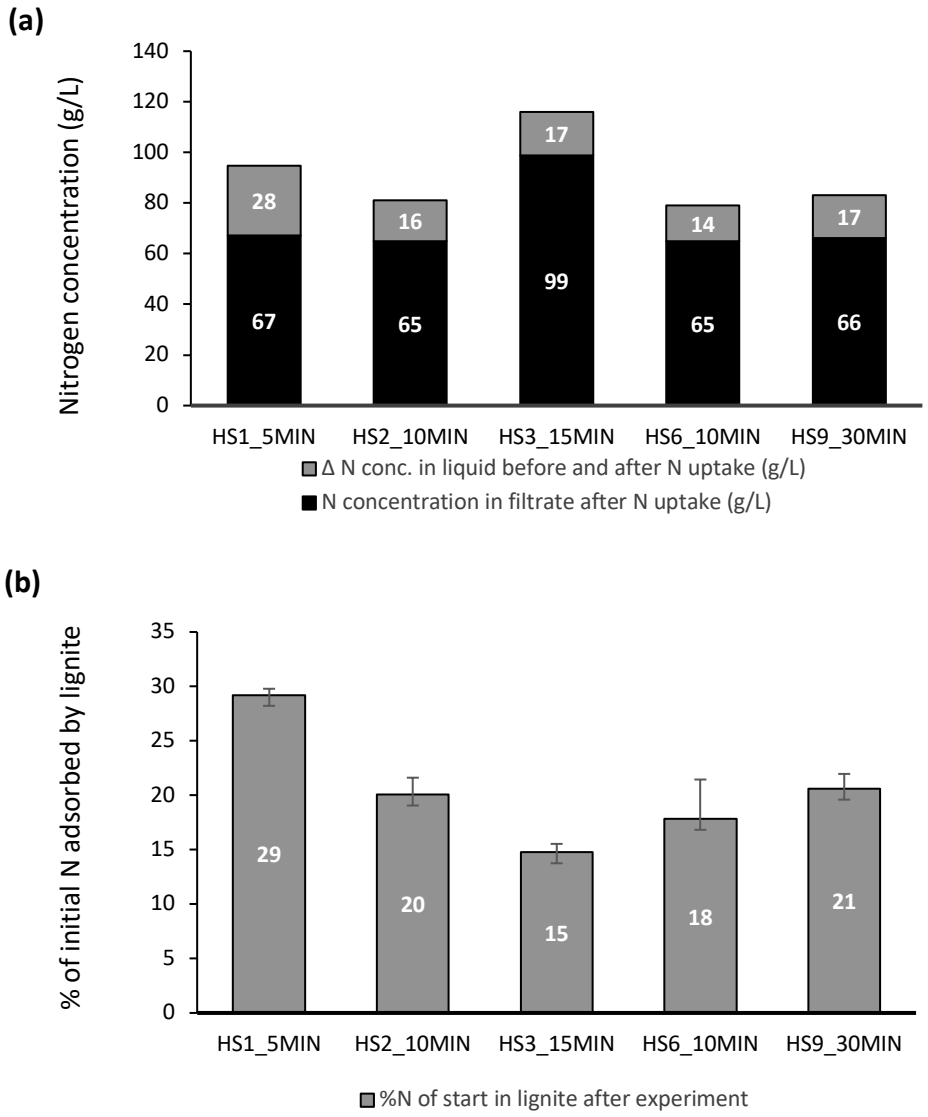

Figure 16 (a) *The amount of nitrogen (g/L) that is in the filtrate after N-uptake by lignite and how much the concentration of nitrogen has decreased compared to the start of the experiment before N-uptake by lignite.* **(b)** *The percentage of the initial amount of nitrogen in the sample that is adsorbed by lignite, with indication of standard deviation.*

From **Figure 16** it follows that the lignite in slurry HS1 (5 min. grinding) has the highest percentage uptake with 29 % of the initial N concentration, even though the samples of HS1 did not have the highest initial N concentration. HS3 had the highest initial N concentration, yet HS3 had an uptake of only 17 % of the initial N concentration. This would indicate that out of all the tested grinding times, a short grinding time of 5 minutes results in the most N uptake. This corroborates the literature findings mentioned in the previous objective (S1-O1), where it was suggested that the optimum specific surface

area is attained when the slurries are ground for only 5 minutes (Woskoboenko et al., 1991).

It is important to note that this method is an indirect way of measuring nitrogen in the lignite of the samples and that direct measurement of nitrogen is necessary to obtain the values of the actual wt.% N in the lignite and verify if the trends ascertained by TNM-L analysis can be generalised.

Nutrient uptake capacity analysis Experiment 2: Methods

In the second experiment, four aspects were investigated:

1. The applicability of elemental analysis, PXRD and ATR-FTIR to directly determine lignite nutrient uptake capacity.
2. The applicability of measuring the urea concentration over time in the separating liquid phase using a refractometer, a conductivity meter and a pH probe.
3. Potential difficulties when handling raw lignite versus lignite slurries in uptake studies.
4. The potential benefit of using relatively large sample volumes.

Sample A consisted of 500g lignite slurry (5 minutes grinding time and ± 23 wt.% lignite), which was mixed in a 2 L Duran bottle with 700 gr of a 50 wt.% urea solution. The urea solution was made with urea in power form *[regent grade, Sigma-Aldrich, Missouri, United States]* and ultrapure water *[Milli-Q®, MilliporeSigma, Burlington, Massachusetts, USA]*. The resulting sample has a hypothetical 116 g raw lignite and 32 wt.% urea solution. Sample B consisted of 500 gr raw, un-sieved lignite, which was mixed with 700 gr 40 wt.% urea solution.

It was hypothesised that the urea concentration in the liquid phase of the slurry would go down over time as urea will diffuse into the pores of the lignite and bind to carboxylic and phenolic acid groups. It was investigated if urea concentration in the liquid phase of a (settled) slurry could be measured using a refractometer or conductivity meter. To test this hypothesis, calibration curves for the different analysis techniques were made with 0, 5, 10, 20 ,30, 40 and 50 wt.% urea solutions. Next, the temperature, pH, conductivity *[pH/Conductivity portable multiparameter meter, Orion Star A325, Thermo Fisher Scientific, Waltham USA]* and refraction *[Pocket refractometer: PAL-1/PAL-3, ATAGO,*

Tokyo Japan, and Multipurpose Automatic Digital Refractometer: RFM 340, Bellingham + Stanley Ltd., Kent, United Kingdom] of the liquid part of the settling slurry were monitored for 5 days (see **Figure 17** below).

Figure 17 *Experimental set up of the second scoping experiment assessing analytical techniques for measuring nutrient uptake capacity of lignite slurry versus raw, un-sieved lignite: Sample A with pH and conductivity probe.*

At the end of the experiment, samples were taken from the settled lignite layer and vacuum filtered through a glass microfibre filter *[grade GF/F 0.7 µm, Whatman, General Electric, Little Chalfont, United Kingdom]*. Part of the lignite on the filter was dried for 5 days in an oven at 40 °C. The rest of the lignite on the sample was subjected to a rinsing step, where the lignite was rinsed with 10 mL ultrapure water under vacuum, and then dried in the same manner as the unwashed lignite. The rinsing step was added to see if this would remove some of the unbound or loosely bound urea (crystals) that could potentially be on the outside of the lignite particles. The dried nutrient-infused lignite was analysed on total nitrogen with a Vario MACRO cube *[Elementar, Langenselbold, Germany]* and the chemical bonds were analysed with ATR-FTIR spectroscopy

[Nicolet™ iS™ with iD7 ATR, Thermo Scientific™*, Waltham USA]*. PXRD analysis *[R-AXIS IV, Rigaku, Tokyo, Japan]* was conducted with scanning speed °2θ sec^{-1}, (Ω = 90°, fixed, ∅ = spin, 6° sec^{-1} and ψ = fixed, o°). Sample A and B were analysed in quadruplet with the Vario MACRO cube and ATR-FTIR spectroscopy, while PXRD analysis was done in duplicate.

Nutrient uptake capacity Experiment 2: Results

Sample A (with lignite slurry and urea) resulted in a settling lignite layer with an opaque, dark brown liquid layer on top with suspended solids. The interface was only visible with correct lightening conditions, see **Figure 18 (a)** below. In Sample B the raw, un-sieved lignite was hydrophobic, resulting in a settled layer of lignite and an 0.5-1 cm thick layer of floating lignite particles that remained on top of a transparent yellow liquid layer in between see **Figure 18 (b)** below. When shaking the bottle again, part of the floating lignite particles were wetted and settled, and the colour of the liquid layer became dark yellow, see **Figure 18 (c)** below. Part of the raw un-sieved lignite particles of Sample B stuck to the glass samples bottle, which was not the case with the lignite slurry of Sample A. The results of the analytical methods used for measuring urea in the liquid and lignite are discussed below.

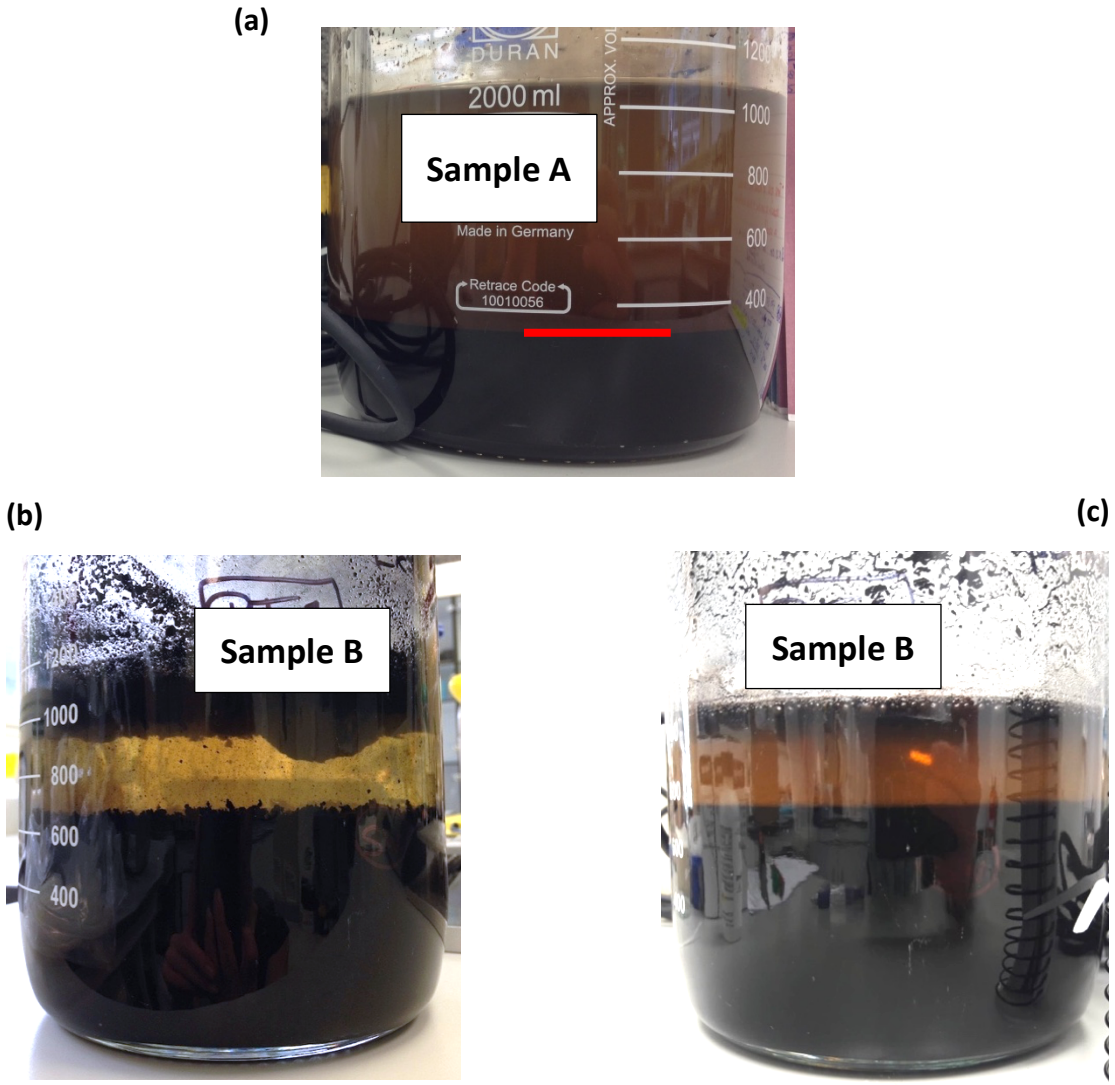

Figure 18 (a) *Sample A with lignite slurry (5 min. grinding time) and 50 wt.% urea solution. The settled lignite – suspended solids interface is indicated with a red line.* **(b)** *Sample B with raw, un-sieved lignite and 40 wt.% urea solution.* **(c)** *Sample B after shaking.*

It was found that both the handheld refractometer, the automatic refractometer and the conductivity meter did not give any meaningful results and it was concluded that refractometry and conductivity is not a suitable method to measure urea concentration in the liquid fraction of a lignite-urea slurry. It is hypothesised that this is caused by the interference from other compounds than urea in the liquid fraction of the settled slurry, such as humic and fulvic acids and small suspended lignite particles.

Distinctive colour differences were observed between the liquids of Sample A and Sample B, see **Figure 18** above. The difference in colour change shows a Kai Point lignite slurry (5 min. grinding time) has much more interaction with a urea 50 wt.% solution than

dry, un-sieved Kai Point lignite with a 40 wt.% urea solution. This can be explained by the smaller particle size distribution of the slurry which results in a larger specific surface area and thus more available functional groups to interact with the urea 50 wt.% solution. The colour difference can also be a result of the difference in pH between Sample A and B. The pH of Sample B increased from 5.31 to 7.35 in 41 days, following a relatively linear trend (R^2=0.828), see **Figure 19 (b)** below, while the pH of Sample A increased from 5.47 to 7.03 in 41 days, not following a linear path (R^2=0.409) see **Figure 19 (a)** below. In Sample A, a steep increase in pH occurred within the first 5 days.

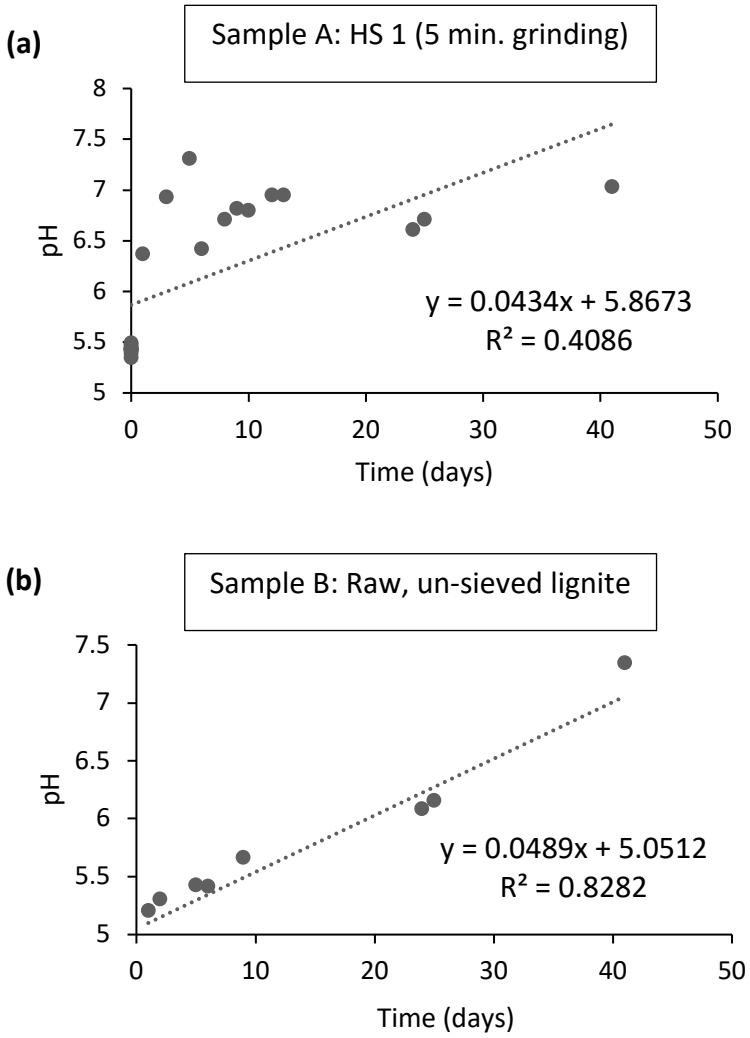

Figure 19 *Development of pH over 41 days in liquid layer of* **(a)** *Sample A (HS1 slurry + 50 et.% urea solution) and* **(b)** *Sample B (dry, un-sieved lignite + 40 wt.% urea solution).*

The results of the elemental total nitrogen analysis, and the PXRD and FT-IR analysis of Experiment 2 are discussed in conjugation with the results of Experiment 3, later in this section.

Nutrient uptake capacity Experiment 2: Discussion

The steady increase of pH in Sample B is likely caused by the slow hydrolysis of urea according to **Equation 5.** Ammonia, carbon dioxide, and subsequently ammonium and hydroxide, are formed which over time increases the pH of the solution. The CO_2 formed in the hydrolysis does not counter the increase in pH since Bull (1964) found that a high concentration of urea, like the 50 wt.% used for our experiments, strongly reduces the activity of H^+.

$$CON_2H_4 + H_2O \rightarrow 2NH_3 + CO_2$$
$$2NH_3 + 2H_2O \rightarrow 2NH_4 + 2OH^-$$

Equation 5 *Two-step hydrolysis of urea*

The yellow colour of the liquid in Sample B could be caused by humic and fulvic acids being released from the lignite (Adey and Loveland, 2007). The opaque brown colour of sample A, on the other hand, cannot be a result of the common mechanism of continued flocculation and subsequent precipitation of humic acids (Canellas et al., 2015). This mechanism only occurs when the pH drops to 1 – 2 (Piccolo, 2002a) and in Sample A the pH increased from 5.47 at the start to a maximum of 7.31.

An explanation for the brown colouration and suspended substances in Sample A could be that urea has the ability to foster the partial dissolution of material that has condensed inside the (micro)pores, similar as to the workings of swelling solvents. Since the condensed material consists primarily of humic and fulvic acids, dissolution of this material could result in yellow and brown colouration, as seen in Sample A and B of the nutrient uptake experiments. Jones et al. (1991) and Jones et al. (1997) described the ability of swelling solvents to dissolve the non-cross-linked part of the coal structure, and it is hypothesised that urea or the resulting hydrolysis into OH^- can constitute a similar

partial dissolution but not to the extent where swelling of the lignite structure occurs, since no obvious swelling of lignite was observed after addition of urea.

The substances causing the yellow and orange colour do not necessarily need to be humic and fulvic acids. Instead, they could be substances that are merely similar to humic acids in appearance and properties (Yilmaz and Deligoz, 1991). However, if the colouration and suspended substances are indeed caused by the release of humic and fulvic acids from the lignite structure into the water phase of the slurry, this could provide an advantage for a lignite-based controlled release-fertiliser. If the humic and fulvic acids released into the slurry have a high bioavailability, literature has shown them to improve soil health and crop yield and are therefore used as commercial fertilisers. Bioavailable humic acids are also instrumental in reducing the bioavailability of xenobiotics (Rice-Evans et al., 1997, de Melo et al., 2016). These added beneficial properties would make a lignite-based controlled-release fertiliser an environmentally and economically superior alternative to conventional fertilisers. Especially since current techniques to extract bioavailable humic and fulvic acids from lignite are elaborate, costly and do not utilise the parent lignite material (Huculak-Mączka et al., 2018, Vlckova et al., 2009). Therefore, further research should investigate if nutrient addition, or urea addition specifically, to lignite slurries can indeed, as hypothesised, foster the release of useful quantities of bioavailable humic and fulvic acids since this discovery would be a novel, more efficient and more beneficial approach to the conventional ways of humic and fulvic acids extraction.

When trying to filter samples of the large bottles of Sample A and B, it became apparent that extracting the settled lignite layer and the liquid layer with suspended particles was difficult in the chosen setup. The volume was too large and the bottle neck opening too small to conveniently extract the settled lignite. This informed the decision for a smaller setup in Experiment 3, with a volume in between that of Experiment 1 and 2.

Nutrient uptake capacity Experiment 3: Methods

The third and last of the nutrient uptake scoping experiments focussed on finetuning the sample volume, sample preparation and nutrient delivery method. In duplicate, 5 g of sieved raw lignite with particle size ≥63<106 µm was placed in a 50 mL conical centrifuge tube, and 30 mL of ultrapure water was added. The tubes were shaken vigorously 40x in an effort to wet the hydrophobic lignite particles. Two additional 50

mL centrifuge tubes were filled with slurry HS1 (5 min. grinding time) and the weight of the slurry in each tube measured. The viscous and sticky nature of the slurry made it difficult to add precisely the same amount to both tubes. All four tubes were left to settle.

After settling, the liquid layer on top was decanted, a measured amount of crystalline urea powder *[reagent grade, Labview, Nelspruit, South Africa]* added, and the tubes were shaken vigorously for 1 minute. The samples were left for 19 hours to allow the urea to dissolve into the pores and potentially attach to binding sites. Next, the samples were vacuum filtered according to the same process as described for Experiment 2 above, using a glass microfibre filter *[grade GF/F 0.7 µm, Whatman, General Electric, Little Chalfont, United Kingdom]*. Half of the sample on the filter was removed and dried for 5 days in an oven at 40 °C. The other half of the filtered sample was subjected to a rinsing step, where the lignite on the filter was rinsed with 10 mL ultrapure water under vacuum. The rinsing step was added to see if this would remove some of the unbound or loosely bound urea (crystals) that could potentially be on the outside of the lignite particles. The dried samples were analysed following the same method as described in Experiment 2.

Nutrient uptake capacity Experiment 3: Observations, results and discussion

When filtering the HS1 slurry samples, transparent cubical crystals became visible in the black lignite. These crystals were also observed in one of the sieved raw lignite samples, but were less pronounced in the duplicate raw sieved lignite sample, where they appeared more like small "glitters" instead of visibly cubical crystals. The rinsing step did not dissolve all the crystals. It is suspected that the transparent cubic crystals are urea crystals that have not completely dissolved when mixed with the lignite, which could indicate there was not enough water in the samples. It is expected that the presence of urea crystals will produce an unreasonably high nitrogen "uptake" percentage, therefore the data points are considered not representative of nutrient adsorption. In future experiments, the issue of undissolved crystals can be avoided by using a concentrated urea solution instead of crystalline urea powder.

Elementar total nitrogen analysis Experiment 2 and 3

The total nitrogen analysis of the samples of Experiment 2, displayed in **Table 6** below, show HS1 (sample A with slurry with 5 minutes grinding time) contained 18.2 % N and the rinsing step removed 28.6 % N. The raw lignite (Sample B) contained 10.1 % N and

the rinsing step removed 24.1 % N. The C : N ratios of the final products were between 2.5 for HS1 and 7.4 for the washed raw lignite. There is minimal variation between replicates, with standard deviations between 0.22 - 1.14, respectively.

Table 6 *Results of the Elementar total nitrogen analysis of the samples from Experiment 2 and 3.*

HS1-U(2/3): Slurry 5 minutes grinding experiment 2/3
HS1-UR(2/3): HS1 rinsed with ultrapure water experiment 2/3
RL-U2: Raw lignite
RL-UR2: RL rinsed with ultrapure water
SRL-U3: Sieved dry lignite with particle size ≥63<108 µm
SRL-UR3: SRL rinsed with ultrapure water

	Lignite sample	Initial C:N	N%	St. dev.	C:N after uptake	Reduction in N% after rinsing
Experiment 2	HS1-U2	0.7	18.2	0.35	2.5	28.6
	HS1-U2R		13.0	1.14	4.0	
	RL-U2	3.9	10.1	0.39	5.3	24.1
	RL-U2R		7.7	0.22	7.4	
Experiment 3	HS1-U3	1.0	39.4*	-	0.5*	7.2*
	HS1-U3R		38.5*	-	0.6*	
	SRL-U3	1.1	23.8*	-	1.6*	8.4*
	SRL-U3R		21.8*		1.8*	
	SRL-U3'	2.0	13.7**	-	3.5**	53
	SRL-U3'R		6.5**		8.4**	

*Crystals present in samples.

**Duplicate with little to no visible crystals.

Also displayed in **Table 6**, are the results of the total nitrogen analysis of Experiment 3. Because of the undissolved urea crystals present in most of the samples of Experiment 3, adsorption values obtained were presumed to be (heavily) overestimated, and therefore the values are indicated with a red colour. Other than comparing the rinsed and unrinsed samples, no other parameters can be compared in the table since more than one parameter was changed at a time to aide in method development.

However, an expectation can be made for the HS1-U3(R) and SRL-U3(R) samples, where initial nutrient concentration was almost identical, and the effect of grinding on nutrient uptake capacity could be analysed. Samples with sieved raw lignite (particle size ≥ 63< 106 µm) had 40% less N than the samples with HS1 slurry. The rinsed samples with sieved raw lignite had 43 % less N than the HS1 samples. However, it is important to note that the results of the scoping experiments have no statistical significance due to the lack of replicates. The role of initial nutrient concentration will be discussed in more detail in Objective S1-A5 and S1-A6, but looking at the results in **Table 6**, several observations can be made. If initial N loading has a stronger effect than particle size distribution, the uptake values of SRL-U3' (13.7 %N) would be between the values of HS1-U2 (18.2) and RL-U2 (10.1 % N), and looking at the values this is indeed the case, but the N % of SRL-U3' is slightly lower than expected.

Both the above-described results could indicate that lignite ground for 5 minutes has a higher uptake capacity than (sieved) raw lignite. This would support the hypothesis that the grinding process makes otherwise inaccessible internal pores of lignite particles available to the bulk solution, thus increasing the specific surface area, and foster nutrient adsorption. This is in contrast to the research of Woskoboenko et al. (1991) that stated there is no change in specific surface area when the mass median diameter of the lignite particles is decreased from 600 µm to 13.5 µm. In future research, the hypothesis can be tested by following the recommended methods that follow from Objective S1-O1 and S1-O2.

PXRD analysis

Looking at the PXRD patterns of Experiment 2 in **Figure 20**, the distinctive peaks of urea crystals are only visible in sample HS1-urea (lignite slurry with 5 min. grinding and urea uptake). Since there are no obvious urea peaks in the pattern of HS1-urea rinsed, it is inferred that the rinsing step removed the urea crystals from the particles of HS1. Saha et al. (2017) used the presence of urea crystals in PXRD analysis to conclude that urea had been loaded into the brown coal structure of their samples and that they thus had incorporated urea into the brown coal structure. However, this assertion is questioned, and it is hypothesised that PXRD only gives information about crystals on the outside of the lignite particles, and no assertion can be made about actual incorporation of N into the lignite structure. This claim is substantiated by the Elementar total nitrogen analysis

in **Table 6**, where all samples of Experiment 2 contain between 7.7 – 18.2 % N, yet only one sample (HS1-urea) displays urea crystallinity in its PXRD pattern. Since there are no urea crystals on the outside of the lignite particles in most samples, the nitrogen must have been incorporated inside the lignite structure in some form. This allows for either or both of the following possibilities:

- The PXRD can only analyse the outside of the lignite particles. The N from the Elementar analysis comes from urea crystals inside the pores, and therefore the urea crystals are not visible in the PXRD patterns.
- There are no urea crystals inside the pores. Instead of being bound to the lignite as crystalline urea, the nitrogen from the Elementar analysis is bound to lignite in other forms such as NH_4^+ (Nazari et al., 2018) or NH_3.

Both of these suggestions explain why the HS1-urea sample has the highest N % according to Elementar analysis. The urea crystals on the outside of the lignite particles account for extra N on top the N that is inside the pores of all samples but is not visible with PXRD analysis. The additional urea crystals on the outside of the lignite particles could even account for the 4.5% more washout that Sample A displayed compared to the samples with raw lignite.

Even though the rinsed HS1-U sample has a higher N % than rinsed RL-U sample, from the Elementar and PXRD analysis it cannot be concluded if lignite slurry with 5 minutes grinding time actually constitutes more N uptake than raw un-sieved lignite. This is because Sample A had a lower C : N ratio (= higher urea concentration) at the start of the experiment, which is likely to strongly contribute to the uptake capacity of lignite. The relation between uptake capacity and initial nutrient concentration is investigated in Objective S1-O5 later in the framework.

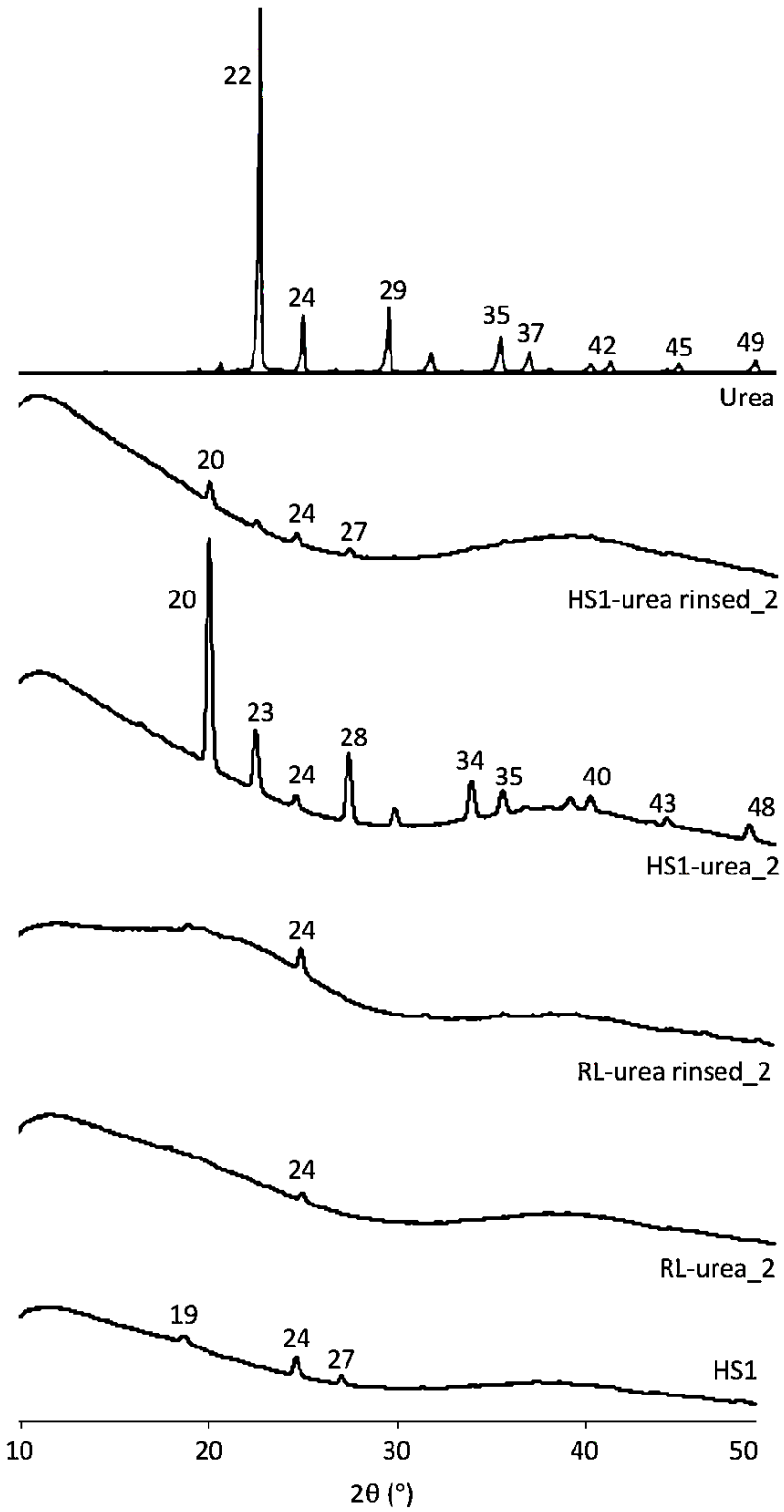

Figure 20 *PXRD patterns of Experiment 2 (bottom to top): lignite (HS1 slurry 5 min. grinding); sieved raw lignite with urea; rinsed sieved raw lignite with urea; HS1 (lignite 5 min. grinding) with urea; rinsed HS1 (lignite 5 min. grinding) with urea; urea.*

ATR-FTIR analysis

Though ATR-FTIR spectroscopy measures transmittance or reflectance, the OMNIC™ software automatically converts the data to an absorbance spectrum. The spectra of the samples form Experiment 2 are given in **Figure 21** and the spectrum of urea in **Figure 22**. The bottom spectrum is pure lignite slurry HS1 (without urea) and acts as a reference for the samples where urea adsorption has occurred. There are several characteristic lignite peaks: the C-H peak at 750 cm^{-1} (Sonibare et al., 2010), which is not visible in the samples with urea; the Si-O peak at 1030 cm^{-1} (Cepus, 2016), which has a high intensity in the lignite sample (HS1) and in the washed raw lignite urea sample (RL-U rinsed) but not in the other urea infused samples; the carboxylic C-O-C peak at 1270 cm^{-1}, visible in all samples; the C-H peak at 1430 cm^{-1} is overshadowed by the 1440 cm^{-1} NH_4^+ peak in the samples with urea (Pironon et al. 2003); the intense C=C and C=O peak at 1600 cm^{-1} (Sonibare et al., 2010), visible in all samples but is accompanied by the C=O bond of urea at 1580 cm^{-1} and 1640 cm^{-1} in the samples with urea; the 1700 cm^{-1} carboxylic C=O bond, only visible in the lignite sample without urea; the "interference" between 1900 - 2365 cm^{-1}, representative of the mineral fraction in lignite, is almost not visible in the (rinsed) HS1-urea samples (Sonibare et al., 2010); the two aliphatic CH_3 peaks at 2845 – 2915 cm^{-1} (Sonibare et al., 2010), visible in all samples but most distinct in the pure lignite sample; and the broad carboxylic and phenolic peak between 3200 – 3400 cm^{-1}, overshadowed in the samples with urea by the 3180 cm^{-1} peak of the NH_4^+ stretching vibrations, the 3330 - 3350 cm^{-1} and 3450 cm^{-1} peaks of the respective symmetric and asymmetric NH_2 vibrations, and another asymmetric NH_2 vibrations peak at 3620 cm^{-1}.

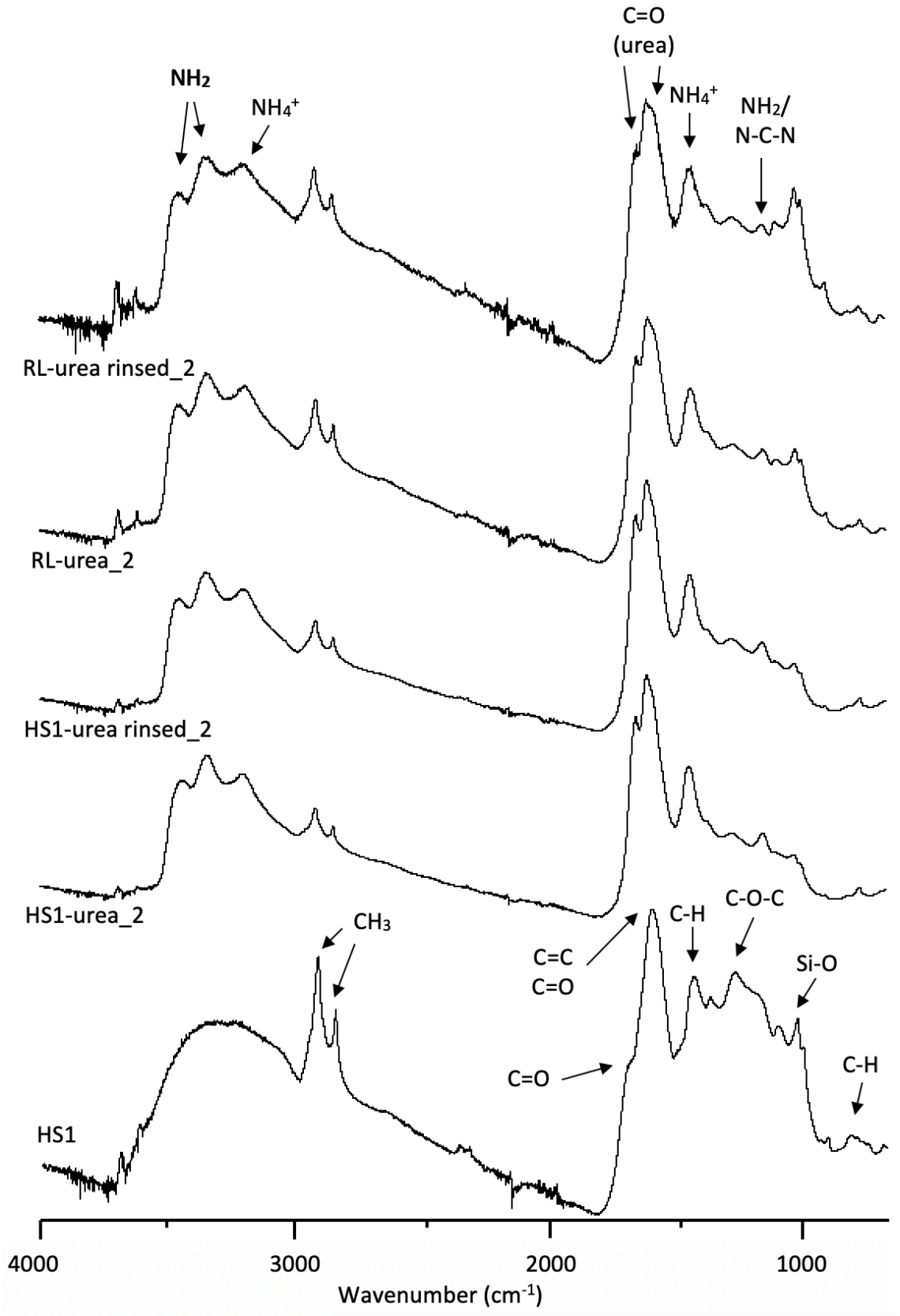

Figure 21 *ATR-FTIR absorption spectra of the samples from Experiment 2: pure lignite (HS1), lignite slurry with urea - rinsed and unrinsed, and raw lignite with urea - rinsed and unrinsed.*

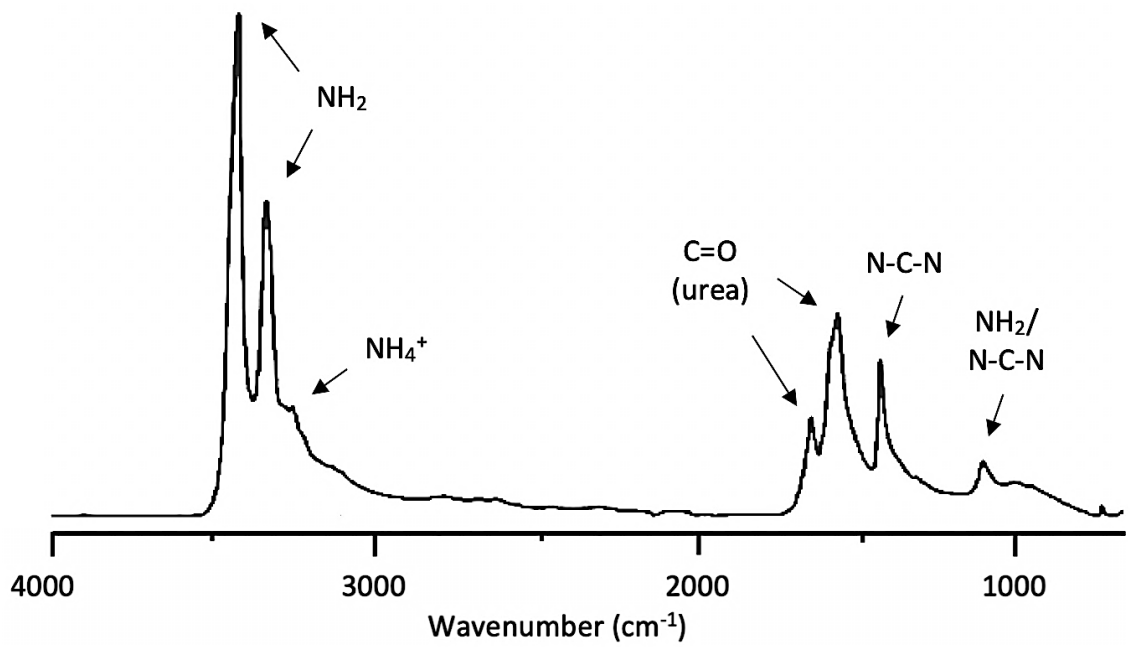

Figure 22 *ATR-FTIR absorbance spectrum of urea.*

The samples consisting of lignite with adsorbed urea display several peaks associated with urea bonds: the 1160 cm^{-1} peak of NH_2/N-C-N (Larrubia et al., 2000); the 1435 – 1440 cm^{-1} peak of the NH_4^+ bending vibrations (Pironon et al. 2003); the 1580 cm^{-1} and 1640 cm^{-1} peaks of the C=O bond of urea; the 3200 cm^{-1} NH_4^+ stretching vibrations; and the symmetric and asymmetric NH_2 bending vibrations around 3330 – 3450 cm^{-1} and 3620 cm^{-1}. The other N-C-N peak, found by Larrubia et al. (2000) at 1460 cm^{-1}, is not observed in the lignite-urea samples. The NH_4^+ stretching vibrations at 3200 cm^{-1} was the most intense peak in the FTIR analysis of Saha et al. (2017), yet they did not recognise it as NH_4^+ stretching vibrations (Pironon et al. 2003). Instead, they saw the peak as a decrease in the phenolic group peak intensities originally at 3369 cm^{-1}. The case can be made that this peak does constitute NH_4^+ stretching vibrations, as this exact peak was also found by Nazari et al. (2018) when adsorbing NH_4^+ onto lignite. The only peak that is visible in the FTIR spectrum of urea but not in the samples from Experiment 2 is the 1460 cm^{-1} N-C-N peak. Instead, the 1435 – 1440 cm^{-1} peak of the NH_4^+ bending vibrations is visible.

The expected OH peak at 3400 cm^{-1} is not visible in any sample, likely because it coincides with the broad carboxylic and phenolic peak between 3200 – 3400 cm^{-1} and the

intense symmetric and asymmetric stretching peaks of NH_2 at 3330 - 3350 cm^{-1}. There was no difference observed in the ATR-FTR patterns of rinsed and unrinsed samples.

The hypothesis that (urea-)N mainly interacts with the carboxylic groups of lignite (Saha et al., 2017) is confirmed because the carboxylic C-O-C peak at 1270 cm^{-1} is very small in the samples were urea was added, the C=O peak at 1700 cm^{-1} is not present at all in the lignite-urea samples, and the broad carboxylic and phenolic peak between 3200 – 3400 cm^{-1} is not visible, mainly due to the high peaks of the symmetric and asymmetric NH_2 vibrations.

The presence of NH_4^+ peaks confirms that one of the hypotheses made in the section above regarding PXRD analysis is proven: the nitrogen found in the samples of Experiment 2 that did not show urea crystallinity in the PXRD pattern can (partly) be attributed to NH_4^+. This does not exclude the possibility that urea crystals are present inside the pore structure of lignite.

It is informative to know some of the urea-N is attached to the lignite structure in the form of NH_4^+ because this predicts that increasing the temperature during the adsorption process will not be beneficial for nutrient adsorption. The adsorption of NH_4^+ onto lignite is an exothermic reaction and decreases entropy, indicating the reaction is not favoured when the temperature is increased (Tu et al. 2019).

In conclusion of the uptake experiments

Urea(-N) binds to the carboxylic and phenolic functional groups of lignite. Rinsing removes part of the urea from the samples, where the samples with urea crystals on the outside of the lignite had a 4.5% higher removal rate. The samples of Experiment 3 had a higher nitrogen content after uptake but also had visible, undissolved urea crystals in the samples due to the low water content of those samples. Lignite slurry with 5 minutes grinding time had more N uptake than sieved and un-sieved raw lignite, but also had a higher N loading at the start of the experiment than the raw lignite samples, which makes a direct comparison not possible. Instead, it introduces the need for additional experiments that focus on initial nutrient concentration, see Objective S1-O5.

For future experiments, a trade-off needs to be made: a urea solution should be used to avoid undissolved crystals, but at the same time the initial C : N ratio should be as small as possible. This requires the use of lignite slurries with high solids loadings and (almost) saturated urea solutions. This trade-off and the implications for the experimental design are described in the next section.

3.4.2.1.3 Recommended methods and experimental design uptake analysis

In order to achieve maximised nutrient adsorption onto lignite, the following methods are recommended for analysing the nutrient uptake capacity of the five different slurry types produced at Objective S1-O1 in order to determine what grinding time is favourable for a lignite-based controlled-release fertiliser.

The nutrient uptake study is designed as follows:

1) A single nutrient species is mixed with the lignite slurries,
2) An adsorption equilibrium is allowed to establish,
3) The water and solid fraction are separated by filtration,
4) The nutrient concentration, chemical bonds and crystallinity of the lignite are measured to determine the uptake capacity of the lignite and the nature of the adsorption.

After the nutrient uptake study, the uptake capacity of the slurries is correlated to the manipulated properties (PSD, specific surface area, and micro and meso pore volume) in order to make an informed decision on which grinding time to use for the rest of the objectives of the framework.

The method described below is designed for studying the uptake capacity of urea-N but can be tailored to study uptake capacity of P and K as well.

From each of the five lignite slurry types produced in Objective S1-O1, three samples (replicates) of 20 g are taken and mixed in equal parts with a 50 wt.% urea solution to make for a lignite-water-urea slurry with 25 wt.% lignite, 25 wt.% urea and 50 wt.% H_2O, see **Figure 23** below. This results in a theoretical 33 wt.% urea solution with raw lignite, where the lignite - urea ratio is 1:1 (C : N = 2.2). A higher initial N concentration can be achieved by using a supersaturated urea solution, but this requires heating of the solution

and would complicate the process. The effect of initial concentration and temperature are studied in Objective S1-O5 later in the framework.

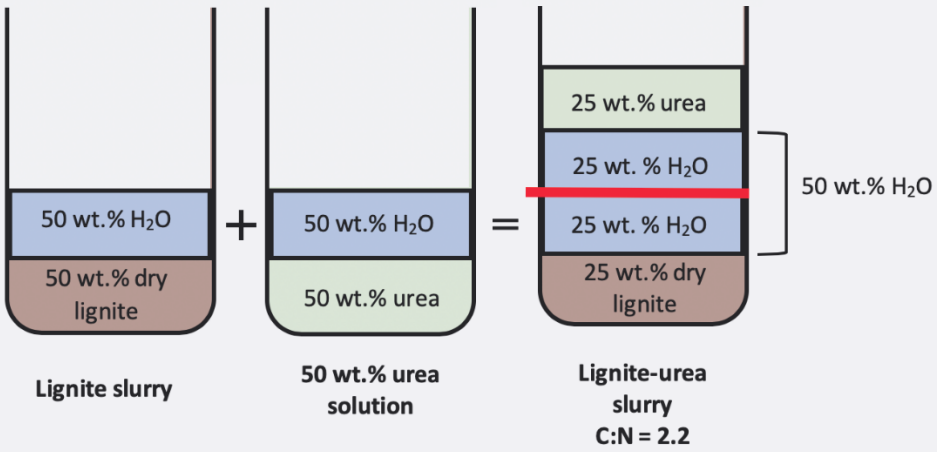

Figure 23 *Illustration of lignite slurry and urea solution used for the recommended urea uptake experiments, and the concentration of the resulting lignite-urea slurry.*

After the urea solution is added to the samples of S1-O1, the newly formed lignite-water-urea slurries are gently shaken/rocked for 24 hours on a shaker table or rocking bed to prevent settling and allow for optimum mixing and interaction between the urea and the lignite. After 24 hours the slurries are vacuum filtered through a glass microfibre filter *[grade GF/F 0.7 µm, Whatman, General Electric, Little Chalfont, United Kingdom]*. The lignite that remains on the filter is dried for 5 days in an oven at 40°C to prepare the samples for elemental, Powder X-ray diffraction (PXRD) analysis and Attenuated Total Reflection – Fourier Transform Infrared spectroscopy (ATR-FTIR).

Total nitrogen of the filtrate (using TNM-L) is not analysed as it is redundant in this experiment where total N of the lignite is the main value of interest. TNM-L is more appropriate for experiments that aim to analyse N uptake over time and will therefore be employed in Objective S1-O5 when studying the kinetics of nutrient adsorption. When phosphorus and potassium adsorption are studied, total P and K of the lignite can be analysed using (P-)XRF.

The rinsing step is not necessary since in this experiment the potential for initial nutrient adsorption by lignite slurries with varying grinding time is investigated. A rinsing step

will be added when characterising the controlled-release nature of PROTOTYPES C in Stage 2. Since plants usually have a high nitrogen demand in the initial stages of growth (Römer and Schilling 1986), a high initial release rate of N due to crystals on the outside of the lignite might be favourable.

The results of the elemental analysis (= the N uptake capacity) and PXRD analysis are written down in the table of Appendix H. Now that the results table is completely filled in, the effect of grinding time can be seen in terms of PSD, specific surface area, micro and meso pore volume, nutrient uptake capacity and crystal occurrence. The assumption can now be verified if, in this particular case, mass-median diameter may be used as a rough indicator for critical volume-median diameter. Also, the hypothesis stated earlier in this chapter, that the grinding time resulting in the largest specific surface area is the optimum grinding time for maximised nutrient adsorption, is either proven or disproven. From the table in Appendix H can also be determined if D[3,2] is indeed a better indicator of nutrient uptake capacity than D50. And lastly, the results in the table indicate if either a larger micro or meso pore volume is preferred when it comes to maximising nutrient uptake. The grinding time that results in the largest N uptake capacity is selected as PROTOTYPE A and is used for all other experiments of the framework.

3.4.3 Objective 3 (S1-O3): Determine the effect of solvent swelling

In order to achieve maximum nutrient loading, this objective focusses on swelling the lignite structure by solvent addition. Objective 3 (S1-O3) states: *"Determine the effects of various swelling solvents on lignite volume, particle size distribution, specific surface area, micro and meso pore volume, and nutrient uptake through a series of swelling experiments, in order to select the solvent that results in the highest nutrient uptake."* This objective is achieved by first selecting potential swelling solvents; the selected solvents are used in experiments that quantify the visible swelling of lignite, followed by an analysis of the samples that constituted the largest amount of swelling to determine which lignite properties were manipulated by the lignite-solvent interactions. The swollen samples that show the most potential for nutrient uptake are used in nutrient uptake studies to determine if solvent swelling increases nutrient adsorption.

Literature describes time-consuming, manual methods for the analysis of swelling behaviour of coal (Nelson et al. 1980, Green et al. 1984). To allow for a comprehensive feasibility assessment, a wide spectrum of solvents and lignite types will need to be analysed. This requires the development of a novel rapid batch analytical technique. The development process of such an analytical technique is described.

3.4.3.1 Solvent selection

3.4.3.1.1 Method development for solvent selection

As described in section 2.5.2 of the literature review, solvent swelling constitutes adsorption of the solvent to the cross-linked part of the lignite structure and dissolution of the non-cross-linked part of the lignite structure. Swelling by the cross-linked part is influenced by the solubility parameter (Jones et al., 1991), while swelling by the non-crosslinked part is primarily determined by the extend of the swelling-solvent contact and thus the compatibility between the porosity and pore size distribution of the coal and the molecular cross-section of the solvent (Makitra and Bryk, 2008). Literature also states that swelling of the cross-linked part of the coal structure is at its maximum when the solubility parameter of the solvent equals the solubility parameter of the coal. From this follows the hypothesis that swelling of a specific type of lignite can be maximised by conducting experiments that identify a solvent with:

- a similar solubility parameter as the lignite type in question,
- a molecular cross-section that allows its molecules to enter most of the pores in the lignite structure.

The Hildebrand solubility parameters of most solvents can be found in literature, while the solubility parameter of a specific lignite sample is usually not known and has to be ascertained experimentally. The required experiments involve systematic swelling of lignite with various solvents and solvent mixes with known solubility parameters and logging the degree of swelling. When optimum swelling is achieved, the solubility parameter of the lignite is found (Jones et al., 1997).

The approximate molecular cross-sectional area of a solvent can be calculated using **Equation 6** below:

$$\sigma = \left(\frac{V_m}{N_0}\right)^{0.667} \times 10^{18}$$

Equation 6 *Approximate cross-sectional area of solvents*

Where the cross-sectional area σ is in nm^2, V_m is the molar volume in m^3mol^{-1} and N_0 is Avogadro's number (Jones et al., 1997). The approximate molecular cross-section can be used in **Equation 7** to estimate of the minimum pore diameter a solvent with a particular molecular cross-section can enter.

$$d = 2\left(\frac{\sigma}{\pi}\right)^{0.5}$$

Equation 7 *Estimation of pore diameter for solvent entry*

Where d is the pore diameter (nm) (Jones et al., 1997). To select appropriate solvents, the minimum pore diameter required for solvent entry can be compared to the micro and meso pore volume of lignite obtained from BET analysis described in objective (S1-O1). For example, a solvent with a minimum pore entry diameter of ≥2 nm is not suited for a lignite type with a large micro pore (< 2 nm) volume. In short, a solvent with a small molecular cross-section will have better pore entry abilities, but if there is too much of a discrepancy between the solubility parameters of the solvent and lignite, the solvent will still not constitute optimum swelling.

The solvents in **Table 7** below are selected from literature as potential swelling solvents. They have medium to strong H-bonding as this has proven to result in more swelling than solvents without H-bonding (Ballice, 2004). The listed solvents have proven to constitute significant swelling in particular lignites. Another important aspect is that they are not toxic when exposed to the environment, contrary to many of the other solvents commonly used for coal swelling. Several of the solvents in **Table 7** are disinfectants which could be favourable in a lignite-based control-release fertiliser. Disinfectants may prevent inherent

microbial activity in lignite pores, and have a potentially urease inhibiting effect, reducing the NH_4^+-N release mentioned by Saha et al. (2017).

Table 7 *Solvents that resulted in large swelling in literature with their respective chemical formulae and Hildebrand solubility parameters.*

Solvent	Chemical formula	Hildebrand solubility parameter δ (MPa0.5)	Strength H-bonding group	Molecular cross-section $\boldsymbol{\sigma}$ (nm^2)	Pore diameter (nm) for entry $\boldsymbol{d = 2\left(\frac{\sigma}{\pi}\right)^{0.5}}$	Reference
Tetrahydrofuran (THF)	C_4H_8O	19.4	M	0.17	0.46	(Dampc et al., 2007)
Acetone	C_3H_6O	20	S/M	0.25	0.56	(Jones et al., 1997)§
Acetaldehyde	C_2H_4O	20.2	M	0.21	0.52	(Barton, 1975)
Diaminoethane (ethylenediamine EDTA)	$C_2H_8N_2$	22.6		0.23	0.54	(Jones et al., 1991)
N,N-Dimethylacetamide	C_4H_9ON	22.7	M			(Barton, 1975)
2-propanol*	C_3H_8O	23.5	S			(Barton, 1975)
Acetonenitrile	C_2H_3N	24.4	S		0.55 (deduced)	(Barton, 1975)
1-propanol*	C_3H_8O	24.5	S			(Barton, 1975)
Coal Jones et al. 1997		*25*		-	-	
Ethanol*	C_2H_5OH	26.5	S	0.22	0.53	(Jones et al., 1991)
Methanol	CH_3OH	29.6	S	0.16	0.45	(Jones et al., 1991)
Ethanolamine	C_2H_7ON	31.5				(Jones et al., 1997)
Water	H_2O	47.8	S	0.10	0.35	(Jones et al., 1997)

* = disinfectant; M = moderate; S = strong; § = differing from Jones et al. 1991.

Table 7 gives the Hildebrand solubility parameters δ (MPa$^{0.5}$) of several of the solvents, the strength of the H-bonding group, the molecular cross-section σ (nm^2; calculated and from literature), and the calculated pore diameter for entry d (nm^2). Solvents that are polar and good hydrogen bond acceptors lead to more swelling than non-polar solvents (Larsen

and Shawver, 1990). However, it is hypothesised that strong H-bonding group might not be preferable because nutrients need to be able to take the place of the solvent molecules at the binding sites. And this might not be possible if the H-bonding is strong. Depending on how much of the solvent remains in the pores after swelling, it is important to assess the solubility of the desired N/P/K nutrient species in the solvents.

Looking at the broader environmental context, it is important to note that the complete removal of swelling solvents from swollen lignite is likely not possible. It is therefore crucial that the swelling solvents are compatible with agricultural and environmental regulations. But besides being safe for agricultural use and having an appropriate solubility parameter and molecular cross-section, solvents can have other properties that make them preferable as swelling solvent in a lignite based controlled-release fertiliser. For example:

- Acetaldehyde is strongly reactive with phenolic compounds, ammonia (a potential nutrient-N source), phosphorus, and strong alkalis and acids. Acetaldehyde is incompatible with oxidising and reducing agents and is miscible with alcohol but not water (NPI, 2018b).

- Acetonitrile dilutes readily in water and air to low concentrations that are harmless to the environment (NPI, 2018a).

- Ethanolamine is crucial for life and can be found in the human body in its free form (Patel and Witt, 2017). It is a medium-strong base that biodegrades or transforms under aerobic and anaerobic conditions to i.a. ammonium, acetate and nitrogen gas (even at concentrations ≥ 1500 mg/kg) (Ndegwa et al., 2004) and is thus expected to be safe for agricultural use. Ethanolamine is also used as a food additive (FDA, 2018).

- Ethylenediamine (EDTA) is used in a variety of medicinal applications, for example, metal chelation therapy and to counter iron deficiency in infants. 4.4 mg day^{-1} per kilogram bodyweight is considered an acceptable daily intake. EDTA is also used as a cleaning agent in the dairy industry. It is found in dairy wastes and either directly discharged into local streams or applied to pastureland through spray irrigation. An extensive study by Xie (2009) found no negative effects of

this EDTA discharge into the environment, with waste streams containing an estimated 5.81 µg EDTA per L.

However, there is the concern that when overtime heavy metals build up in the soil, they are chelated with EDTA and subsequently transported with the EDTA to the groundwater. Literature has extensively described the ability of lignite and lignite-derived humic acids to bind heavy metals and remove them from aqueous solution for remediation purposes (Doskočil and Pekař, 2012, Arslan et al., 2007, Nazari et al., 2018, Tu et al., 2019). When applying an EDTA-swollen lignite-based controlled-release fertiliser to the soil, the soil remediating properties could potentially prevent the transport of EDTA-originated heavy metals to the groundwater.

- Methanol is not persistent in the environment as it readily degrades in air, soil and water, and has no persistent degradation intermediates (IPCS, 1996).

- 1-Propanol and 2-propanol are disinfectants, and at a 70 : 30 propanol-water solution, have the most effective disinfectant properties (Kruse et al., 1963, Kruse et al., 1964). A 70 : 30 propanol-water content can be achieved using the (non-inherent) water content of lignite-slurry.

- Tetrahydrofuran (THF) is a base molecule of the DNA-backbone, a polar solvent and monomer, and sometimes used as a dispersant (Tang et al., 2007). It is often used in literature for coal swelling studies. It is non-ecotoxic, and since it is inherently biodegradable, it is not expected to be environmentally persistent (Fowles et al., 2013).

3.4.3.1.2 Kai point lignite case study: solvent selection

Ideally, a solvent was selected with a solubility parameter close to that of Kai Point lignite, but literature states that the solubility parameter of a molecule is dependent on the prevalence of its functional groups (Hansen, 2007). Even if the group contributions to partial solubility parameters of a “lignite molecule” were known (which is exceedingly difficult for larger molecules), the heterogeneity of lignite would make it impossible to

calculate the σ. Therefore the study of Jones et al. (1997) was used as a reference when selecting the solvent for the scoping experiment that was to examine the ability of solvent swelling by Kai Point lignite.

The Bergheim brown coal used in Jones et al. (1997) had an experimental solubility parameter of about 25 $MPa^{0.5}$. The Kai Point lignite has an inherent moisture content of 28.0 %, which is 29.2 % lower than the moisture content of the Bergheim brown coal used in Jones et al. 1997. From literature it is not clear to what extent the inherent moisture content of a lignite contributes to its solubility parameter. It is postulated that inherent moisture could have a profound effect on the solubility parameter of a lignite since water has a relatively high solubility parameter σf 47.8 $MPa^{0.5}$.

If the inherent moisture does indeed strongly contribute to overall coal σ, Kai Point lignite could have a solubility parameter of up to 29.2 % lower than the 25 $MPa^{0.5}$ found for Bergheim brown coal. If all other attributes of Kai Point lignite were the same as Bergheim brown coal this could theoretically result in a minimum solubility parameter of 17.3 $MPa^{0.5}$ for Kai Point lignite. This seems extremely low and is undermined by the predisposition that the notorious variability of the chemical and physical composition of lignite in general makes it impossible to compare two different types of lignite. The ambiguity of the nature of the molecular structure of a particular lignite sample demands a broad estimate of the solubility parameter of Kai Point lignite. In this case, a margin of 10 $MPa^{0.5}$ around 25 $MPa^{0.5}$ is chosen. This still makes it a case of trial and error with several solvents to find the actual solubility parameter of Kai Point lignite or any other type of lignite.

In order to compare the results of the swelling experiment with those of Jones et al. (1997), acetone, with a solubility parameter of 20 $MPa^{0.5}$, was selected as a swelling solvent. Since the condensed HS1 slurry samples contained 20 % non-inherent water, the addition of acetone created a solvent mixture of 80 : 20 acetone-water. The solubility parameter of the mixture was calculated according to **Equation 2** in Chapter 2.5.2 and was 25.2 $MPa^{0.5}$. This was the exact acetone-water ratio that resulted in maximum swelling of the Bergheim brown coal in Jones et al. (1997), earlier shown in **Figure 8** of the literature review.

3.4.3.1.3 Recommended methods for solvent selection

For the feasibility framework it is recommended to start with a swelling series of lignite with acetone or acetaldehyde if a wet slurry sample is used and 1-propanol or acetonitrile if a dried slurry sample is used. Acetone and acetaldehyde are solvents with a solubility parameter at the lower end of the list **Table 7** making them more suitable to be mixed with water. All the solvents in **Table 7** have resulted in substantial swelling of various coals in the literature (Jones and Prawitasari, 1995, Jones et al., 1997, Takanohashi et al., 1996, Larsen and Shawver, 1990). After making swelling series with either of the two solvents (acetone or acetaldehyde) according to the method in Jones et al. (1997), there are three possible outcomes:

1) The swelling series has an optimum which elucidates the solubility parameter of the lignite, followed by new swelling series with other solvents or solvent mixtures with the target solubility parameter to find the solvent(mixture) that results in the maximum amount of swelling.

2) No optimum swelling is reached, and the direction of the upward trend informs if the solubility parameter of the lignite is lower or higher than tested in the series, followed by new swelling series with a solvent that has a solubility parameter closer to that of the lignite.

3) There is no swelling at all, and the swelling series has to be repeated with a different solvent (a solvent that has a significant swelling effect on one type of coal can have little or no effect on another coal, experimentation is the best way to determine how a solvent affects a specific type of coal).

Once the swelling series has identified the approximate Hildebrand solubility parameter of the lignite, other solvents need to be tested for their ability to optimise swelling of the lignite structure. The table given in Appendix I will help identify potential solvents. The values of the Hildebrand solubility parameters of the solvents from **Table 7** are given, but the solubility parameters of the mixtures (solvent + water from lignite slurry), need to be calculated according to **Equation 2** for the solvents selected for the swelling optimisation experiments. The table should also be used for the subsequent nutrient uptake experiments since it allows for comparison and assessment of the effect of solvent swelling on several lignite characteristics.

3.4.3.2 *Quantifying lignite solvent swelling*

3.4.3.2.1 Method development visual lignite solvent swelling analysis

In the literature, there are two main methods for measuring swelling of coal: a gravimetric and volumetric technique. Green et al. (1984) showed that both give the same results, and therefore the more simple and low-cost volumetric method was chosen for this feasibility framework. The method is based on measuring the height of a coal sample before swelling (h_1) and after swelling (h_2), and calculating the swelling percentage (S) by difference according to **Equation 8** (Jones et al., 1997):

$$S = \left[\frac{(h_2 - h_1)}{h_1}\right] \times 100$$

Equation 8 *Volumetric swelling percentage*

Studies involving solvent swelling of coal for fuel production remove extractable material that is condensed inside the pores before adding the solvent. Since the condensed organic material is likely to possess beneficial attributes for soil health, the material is left inside the lignite pores in this research into a lignite-based controlled-release fertiliser. A downside is that skipping the extraction step is likely to make it more difficult to observe the swelling, as the condensed material can suspend in the solvent, creating a dark liquid difficult to distinguish from the lignite (Green et al., 1984).

The volumetric method is straight forward: tubes are filled with lignite (slurry), the height is measured, a solvent is added, after 24 hours the height is measured again and the degree of swelling calculated. Since lignite is an inhomogeneous material, a large number of replicates will be necessary to assure the accuracy of the conclusions. The visual observation process is automated through the development of a rapid batch analytical method, in order to make the process less labour intensive, to allow for measurement of the swelling behaviour over time, and to standardise the measurement taking process. This method consists of the following steps: the tubes with lignite and solvent are placed inside a lightbox, and a time-lapse recording is started. After 24 hours, the time-lapse

automatically stops and the pictures, who have been uploaded into the cloud, are processed using ImageJ and subsequently analysed using MATLAB. The rate of swelling can provide information on the nature of the swelling process and how long the swelling process takes, potentially allowing for a shortening of the swelling experiments.

As explained in chapter 2.5.2 of the literature review, the effect of temperature on swelling is not investigated as research found only the rate of swelling is affected by temperature, not the extent of swelling (Otake and Suuberg, 1998).

3.4.3.2.2 Kai Point lignite case study: Analysing visual particle swelling

A scoping experiment was conducted regarding the image analysis of visible particle swelling. The aim was to develop a rapid, non-labour-intensive swelling behaviour assessment method that provides reproducible results. Starting with a comparison between the swelling behaviour of dry lignite versus lignite slurry using water and acetone as solvents.

Methods

Eight 50 mL centrifuge tubes were placed in a rack made out of acrylic, specifically designed for the scoping experiments. Four tubes were filled with 5 g of sieved raw lignite (mesh size ≥ 63< 106 µm) and four tubes with approximately 20 g condensed slurry HS1 (5 minutes grinding time). The corresponding volumes were read off the scale on the tubes and noted. The condensed slurry was obtained by letting the slurry settle for one week and scooping a sample from the settled layer of the container. The slurry sample was analysed on solids loading by drying for 5 days at 40 °C and measuring the weight difference (= evaporated unbound water in the sample). The viscous and sticky nature of the slurry made it difficult to add a precise amount in the tube, and the walls of the tubes had to be carefully wiped in order to get a flat surface and thus measurable volume.

The rack with the tubes was placed in a lightbox specifically created for the scoping experiments and an initial picture at "t = ZERO" was taken. The lightbox was made out of sandblasted acrylic and MDF; it was installed with two rulers, a webcam camera *[Logitech C920 HD Pro Webcam, Lausanne, Switzerland]*, backlit with two fluorescent white lights *[18Watt, 6500K Tri-Phosphor, Sylvania Electric Products, Ledvance,*

Ontario, Canada], and connected to a laptop *[MacBook Pro 2009, Apple Inc., Cupertino, USA]*, see **Figure 24** below.

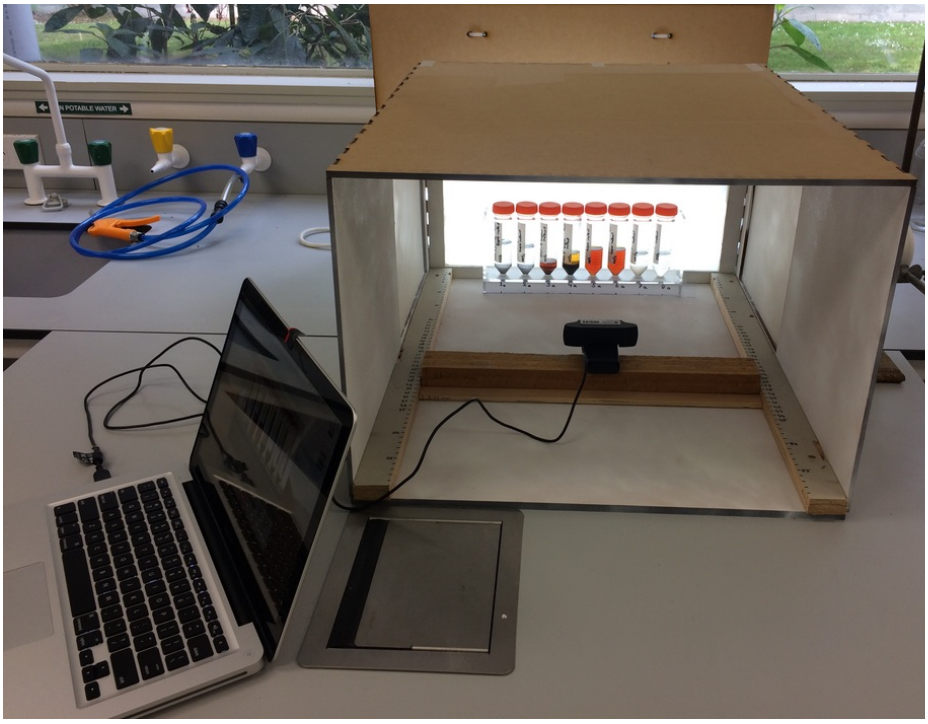

Figure 24 *Lightbox setup with tube rack, webcam and laptop.*

After the initial picture was taken the rack with tubes was taken out of the lightbox, and the solvents were added to the tubes. Two tubes of the sieved dry lignite set and two tubes of the HS1 slurry set were mixed with 30 mL and 20 mL ultrapure water respectively to serve as blank. The other two tubes of each set were mixed with 30 mL and 20 mL acetone respectively *[99.5 % min., analytical reagent grade, LabServ™ Analytical Services, Nelspruit, South Africa]*, resulting in solvent solubility parameters of 16.6 $MPa^{0.5}$ for the samples with sieved raw lignite and 25.2 $MPa^{0.5}$ for the samples with lignite slurry HS1. The lignite-solvent mixtures were stirred with a stainless-steel spatula for 10 seconds, and the lignite slurry was pushed down the wall of the tube to create a flat surface for volume measurement. The height of the lignite-solvent mixtures (h_1) was noted. The rack with the tubes was placed back in the lightbox, and a Python time-lapse code was started. The Python time-lapse code was written to enable a customized image capture sequence that consists of three stages (see Appendix J):

- Stage 1: 1 picture is taken every 60 sec for the first 2 hours.
- Stage 2: 1 picture is taken every 10 min for the following 24 hours.

- Stage 3: 1 picture is taken every hour for the last 48 hours.

After 48 hours, the rack with tubes was taken out of the lightbox, and the heights of the lignite-solvent mixtures (h_2) were noted manually. The swelling was calculated according to **Equation 8**.

Results and discussion

Figure 25 shows the tubes with the lignite samples at the start and end of the time-lapse of the swelling experiment. In **Figure 25 (b)** it is visible that part of the hydrophobic sieved raw lignite particles of tubes nr. 1 and 2 are floating on top of the ultrapure water in samples. This is opposed to the tubes with acetone as solvent, in which all particles are suspended, and hence it is be concluded that lignite is more miscible in acetone than water. It was observed that the samples with sieved raw lignite and ultrapure water settle after approximately 5 minutes, while the samples with slurry HS1 and ultrapure water take approximately 17.5 hours to settle. If gravity outweighs all other forces at play, larger particle size distributions settle faster than smaller particle size distributions, which explains why the settling of tubes with HS1 is 3.5 times slower than the settling of tubes with sieved raw lignite. After 22 minutes, one of the tubes with sieved raw lignite and ultrapure water (SRL-ref) was shaken in an effort to wet all lignite particles and suspend the floating layer.

All the samples with ultrapure water settled much faster than the samples with acetone, indicating there is more interaction between the lignite particles and acetone than with ultrapure water. This is similar to the results of Shin and Shen (2007) who found that alcohols and cyclohexanone used for the preparation of coal slurries formed weak gel structures that increased the stability of the slurries, and thus increased viscosity and slowed down sedimentation. They also stated that the reduced settling rate was favourable for slurry application systems, but the increased viscosity was not.

After approximately 10 hours, the tubes with sieved raw lignite + acetone (tubes nr. 3 and 4) showed settling, and a dark orange liquid layer emerged on top of the black lignite particles. Settling of the tubes with sieved raw lignite + acetone and tube nr. 8 with slurry HS1 + acetone followed several hours later, but their liquid layers were only slightly translucent and were so dark that only hints of orange were visible. Over the course of the experiment, the liquid layers became more transparent and brighter orange, see **Figure**

25 (b) below. Tube nr. 7 with slurry HS1 + acetone displayed hardly any settling, and the liquid layer remained almost opaque dark brown.

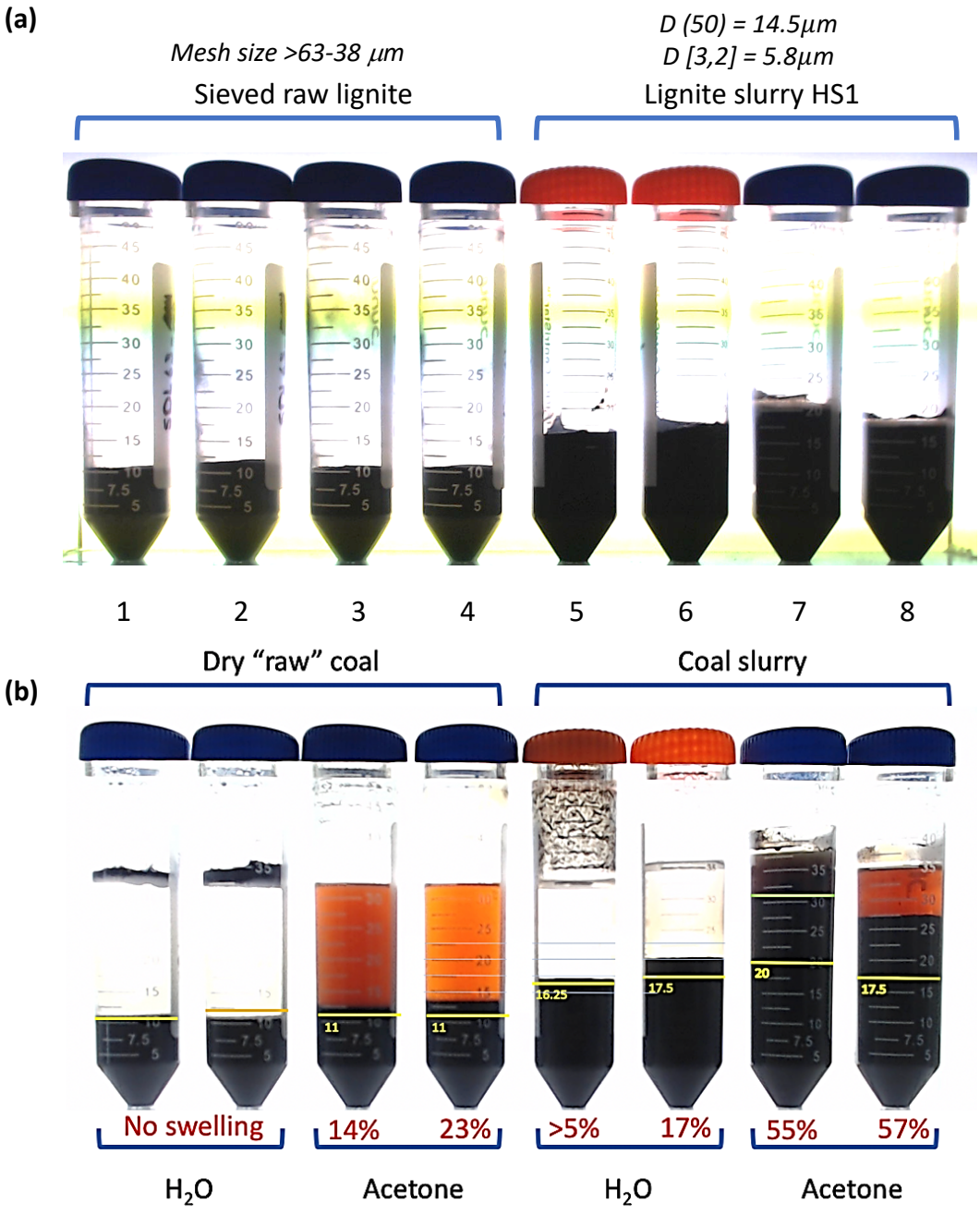

Figure 25 *Centrifuge tubes in the lightbox setup at* **(a)** *the start of the experiment before solvent addition and* **(b)** *the end of the experiment after solvent swelling. The swelling behaviour of sieved raw Kai Point lignite (mesh size ≥ 63< 106 µm) is compared to Kai Point slurry HS1 (5 minutes grinding, D [3,2] = 5.8µm) for two different solvents: water and acetone.*

After 48 hours the heights of the solid lignite beds were measured, and the liquid layer decanted to see if the lignite layer was a solid layer or loose sediment as observed by Shin

and Shen (2007). The lignite bed proved a solid bed in all samples, even in the tube with HS1 + acetone where the interface between the lignite bed and the dark brown liquid layer was hardly visible with the eye. When analyzing the first and last image of the time-lapse, yellow lines were added to **Figure 25 (b)** to indicate the original volume of the lignite (= the volume of the lignite in **Figure 25 (a)**). A green line was added to tube 7 **Figure 25 (b)** to indicate the barely visible liquid – settled lignite interface.

Analysis of the preliminary swelling results indicates that adding ultrapure water to sieved raw lignite (mesh size ≥ 63< 106 µm) does not result in an increase in volume (= no swelling). Adding ultrapure water to a condensed slurry HS1, with D[3,2] = 5.8 µm, results in > 5 – 17 % swelling. This could indicate that the condensed slurry was not saturated with water, otherwise no swelling would have been visible. Adding pure acetone to raw lignite (mesh size ≥ 63< 106 µm) leads to 14 – 23 % swelling. Acetone addition to the dense HS1 slurry results in 55 – 57 % swelling.

As mentioned earlier, the addition of pure acetone to condensed HS1 slurry results in a theoretical lignite – 80 : 20 acetone – water mixture with a Hildebrand solubility parameter of 25.2 $MPa^{0.5}$. The same acetone-water ratio resulted in a maximum of 38.5 % in the swelling spectrum of the Bergheim brown coal used by Jones et al. (1997), earlier shown in **Figure 8** of the literature review. Setting the lack of replicates in this study aside, this indicates that when adding the same 80 : 20 acetone – water solvent mixture to Kai Point lignite and Bergheim brown coal, Kai Point lignite displays 48 % more swelling. This is without having produced a swelling spectrum to ascertain if 57 % is the optimum swelling that can be attained with any given ratio of acetone and water. The 48 % disparity in swelling between the two lignites could indicate that either Kai Point lignite in general swells significantly more than Bergheim brown coal, or Kai Point lignite has more affinity with acetone than Bergheim brown coal. In the latter case, this means Kai Point lignite swells more under the influence of this particular solvent (acetone). It must be noted that the effect of particle size distribution and pre-wetting of lignite in the form of a slurry are parameters not investigated; thus a direct analogy between the swelling behaviour of the two lignites is not possible. If the increased swelling by acetone addition compared to ultrapure water results in higher nutrient adsorption will be examined in the next section.

As was seen in Experiment 1 and 2 of the nutrient uptake capacity experiments, adding urea to lignite (slurries) can also produce a transparent liquid layer with an orange colour or an opaque deep dark brown layer with suspended particles as in the acetone swelling experiment. That, on visual assessment, urea causes the same release of compounds into the liquid of a lignite-solvent slurry, allows for finetuning of the hypothesis made in Chapter 3.4.2.1.2. This hypothesis stated that a highly concentrated urea solution, or the resulting hydrolysis into OH^-, can constitute a similar partial dissolution of (the non-crosslinked part of) the lignite structure as organic polar swelling solvents, but not to the extent where swelling of the lignite structure occurs.

The lack of lignite swelling in a highly concentrated urea solution can now be explained by postulating that urea, being a low-molecular weight solid, is able to enter the micropores of the lignite and dissolve condensed organic matter in those small pores, but that the urea solution does not have a solubility parameter matching Kai Point lignite. This means the urea solution does not fulfil the second requirement to attain lignite swelling, as described in Chapter 3.4.3.1.1 above. The amended postulation is supported when taking a closer look at the Hildebrand solubility parameter of urea and urea's peculiar properties when combined with water. The addition of urea to water has shown to improve the solubility of a range of materials, which has led to the application of urea – water mixtures in processes for swelling and softening of wood, changing wetting behaviour of lithographic stones, and improving wetting of gunpowder particles during grinding (Hansen and Poulsen, 2007).

The Hildebrand solubility parameter of urea is 7.7 $MPa^{0.5}$ (Hansen and Poulsen, 2007), which gives a 50 wt.% urea solution a $\sigma$of 27.7 $MPa^{0.5}$ when applying **Equation 2**. This is higher than the 25.2 $MPa^{0.5}$ of the acetone solution in the swelling experiment, higher than the Hildebrand solubility parameter of the Bergheim brown coal from Jones et al. (1997), and is in the higher end of the range expected to contain the solubility parameter of Kai Point lignite (20 – 30 $MPa^{0.5}$). Combining this knowledge with the result of the acetone swelling experiment, the range of the suspected solubility parameter of Kai Point lignite can be slightly narrowed down to > 20 < 27.7 $MPa^{0.5}$. This new range can inform the solvent selection for subsequent swelling experiments.

3.4.3.2.3 Recommended methods for quantifying solvent swelling

After the swelling experiment of the case study, it is recommended to start the swelling spectra with a condensed slurry. Only if the swelling spectra indicates that a solvent (mixture) with a lower solubility parameter is necessary should an oven-dried (5 days at 40 °C) slurry with the selected grinding time be employed. The duration of the experiment can be reduced to 24 hours. To allow for sufficient replicates, the experimental setup should contain two blanks with lignite and ultrapure water, and six samples with one type of solvent. This gives six replicates, the same amount as employed by Jones et al. (1997).

Due to lignite's inhomogeneity, six replicates are the estimated minimum requirement for making statistically relevant conclusions regarding the effect of various solvents on the swelling behaviour of lignite particles. The suggested methods require a relatively large number of "swelling batches" (= one tube rack with two blanks and six replicates) that need to be analysed to perform a comprehensive analysis of the swelling behaviour of a particular type of lignite subjected to a variety of solvents. A manual assessment would make for a labour intensive and time-consuming endeavour that, in most cases, would not be practically feasibly. Also, manual measurement would require judgement and thus bring subjectivity to the measurements. Therefore, a novel method for automated rapid batch image processing and analysis of lignite swelling was developed, and is described in the sections below. When using the rapid batch method, the resulting swelling percentages of the solvent (mixtures) should be noted in the table in Appendix I "Recommended experimental design and results table solvent swelling S1-O3".

3.4.3.3 A novel method for rapid batch image processing and analysis of lignite swelling

3.4.3.3.1 Method development rapid batch processing and analysis

The image processing and analysis was automated in order to reduce the amount of labour and time required to manually assess the swelling or settling over time, but also to standardise the measurement. This required two consecutive steps: image processing and image analysis. During image processing, one starts with an image and modifies that

image to obtain an "enhanced" image. Image analysis is transforming an image into something else than an image; in this case, information describing pixel height. Repeating the image analysis for many sequential pictures, namely time-lapse of the experiment, provides information on the change in pixel height over time, i.e. the swelling or settling rate and extent.

With the help of Dr Luke Fullard *[lecturer in Mathematics, Massey University, School of Fundamental Sciences]* and using manipulated test images, a MATLAB image analysis code was written, which can be found in Appendix J. Before using the MATLAB code, ImageJ is used to quickly and effectively process the images and prepare them in such a way that the MATLAB code can analyse them as accurately as possible. The preparation process in ImageJ is crucial since this process determines the accuracy and precision of the results.

In ImageJ, one picture is chosen to adjust the brightness and contrast and subtract the background. The extent of the adjustments is decided by the user to make the interface between the solid lignite bed and the liquid as clearly visible as possible. Next, each tube is cropped manually. ImageJ automatically repeats the colour adjusting, background subtracting and cropping process over the entire sequence of pictures, producing and saving individual folders with a time-lapse sequence for each individual tube.

Next, the MATLAB code is run and the user is asked to draw a rectangle inside the lignite bed, see **Figure 26** below. This informs the program what the colour value is of the pixels of the lignite bed. It is crucial that the rectangle is below the minimum height of the lignite bed in every picture of the sequence. It is also important that this area has no white volume indicating lines or numbers, no white label and no glare: the area should only contain the dark pixels representing the lignite bed. Glare is an issue at the round "edges" of the tubes and in the cylindrical bottom of the tubes.

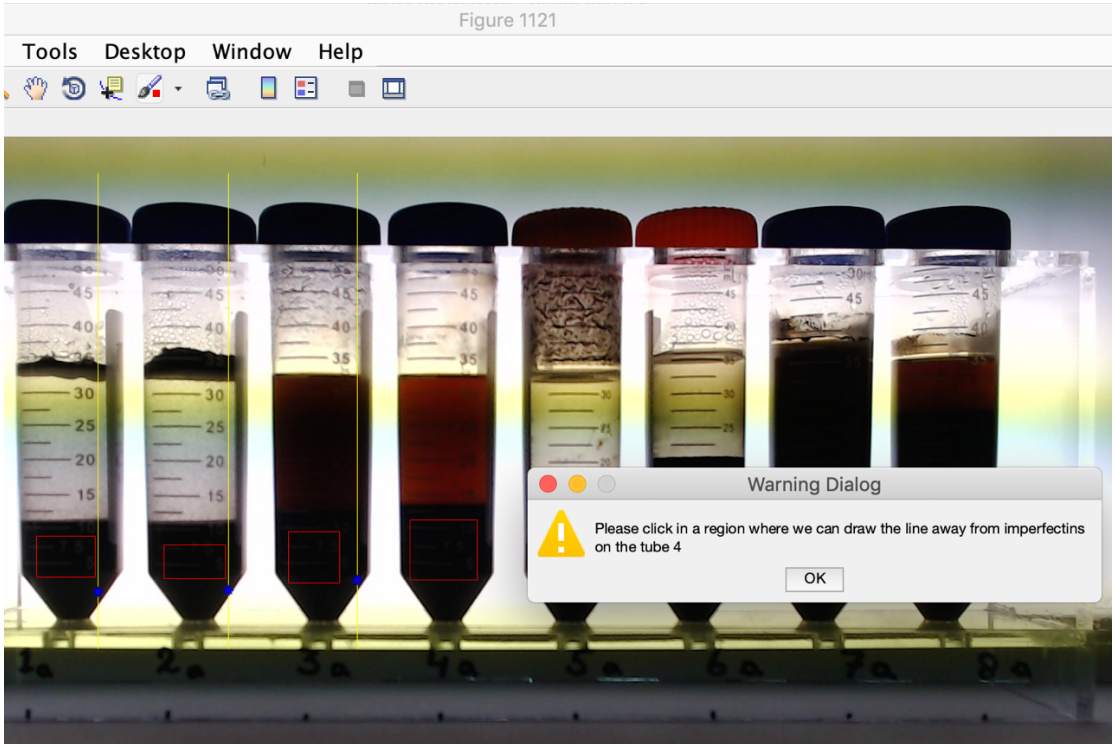

Figure 26 *Screenshot of ImageJ depicting how the threshold value of a lignite bed pixel is selected and where the vertical yellow lines are placed in this example.*

After selecting the pixel value of the lignite bed-pixels, the location of a yellow vertical line is selected along which the pixels need to be counted. This line extends over the whole length of the tube and should not include any white markings or glare. Next, it is selected where the bottom of the lignite bed along the vertical line is located (indicated by a small blue star in **Figure 27**).

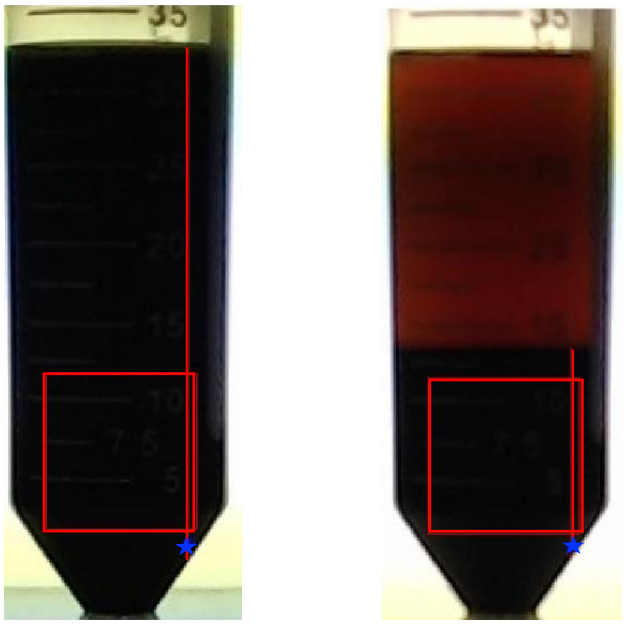

Figure 27 *Two images in the sequence of one tube, analysed by the MATLAB code. The manually drawn red rectangle contains the pixels selected to represent the colour of the lignite bed, the red vertical line indicates which pixels are counted as lignite bed by the MATLAB code (= height).*

A histogram of the selected rectangle is used to determine the maximum colour value a lignite bed pixel is allowed to have; this is known as the threshold value. When the code is stepping and counting along the vertical line, and it detects a pixel with a value larger than the predetermined maximum, the code will stop counting, defining the interface of the lignite bed and the liquid. The MATLAB code puts the lignite bed-pixel counts of each picture in a table and outputs an excel file with eight sheets (tabs), one for each of the eight tubes.

3.4.3.3.2 Kai Point lignite case study: Automated Image analysis

After writing the code, it was run on the time-lapse sequence of the swelling experiment as a test in order to assess where improvements were needed in either the experimental setup or in the code itself. It was found that there were two issues causing noise in the output data and prohibiting proper analysis. Noise in the input data (the images) was caused by a moving horizontal band of lower light intensity originating from the frequency of the fluorescent lights. The dark orange or brown liquid layer was only translucent if it was directly lit from behind which meant that if the fluctuating horizontal, low light intensity band was directly behind the interface, the interface was not visible. In those cases, the value of lignite bed height produced by the code was higher than the

actual value, see **Figure 28** below. A function in the setup of the camera that was supposed to counter the issue of light frequency failed to provide any resolve.

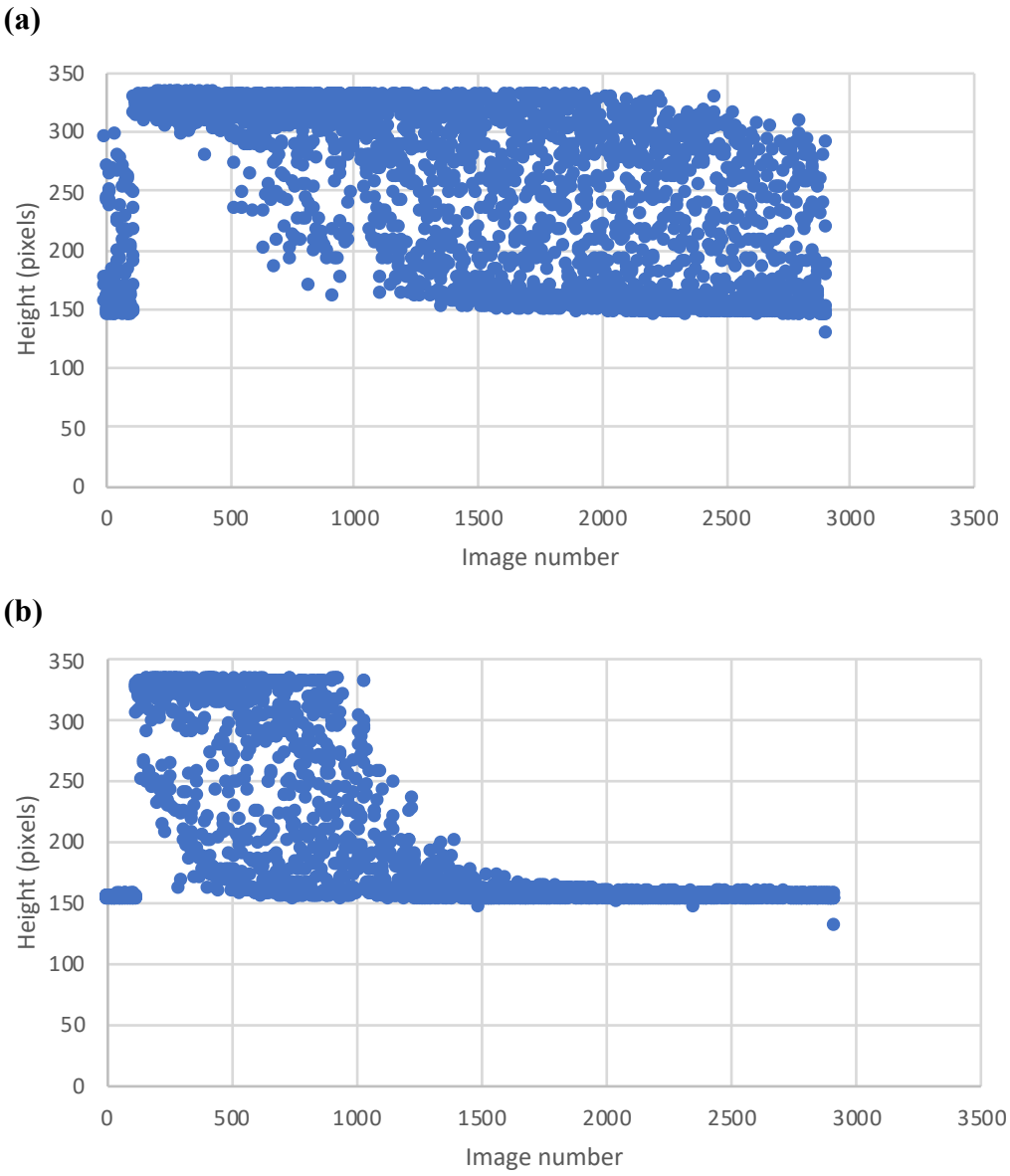

Figure 28 *Test outputs of lignite bed height over time for slurries HS1-ref* **(a)** *and HS1-ref'* **(b)**, *produced by the MATLAB code.*

The other issue causing noise in the data was the result of a flawed experimental setup. The tubes had a white label and white lines and numbers indicating volume. There was also a reflection of light from the glossy acrylic rack onto the cylindrical bottom of the tubes. All of these points made it difficult for the code to detect if a light pixel represented the lignite bed - liquid interface or just noise. The result was an underestimation of the lignite bed pixel height in a significant number of pictures.

3.4.3.3.3 Recommended methods for rapid batch image processing and analysis

In order to remove the noise from the results, a longer exposure time of the camera will need to be employed to remove the band of lower light intensity. Tubes with narrow black lines and numbers indicating volume, and no labels, will limit interference with pixel counting. Having tubes with no lines or numbers is not optimal since this will make it exceedingly difficult to double-check the height results manually. Another improvement would be to design a rack with a matt bottom to prevent reflection of light onto the conical bottom of the tubes. This can be achieved by sandblasting the bottom plate of the acrylic rack. Ones the noise in the data has been minimised, data analysis should constitute taking the log to see if a straight line is produced, and calculating the slope to find the rate of settling or swelling.

3.4.3.4 Analysing the effects of solvent swelling on lignite properties

3.4.3.4.1 Method development for analysing effect of solvent swelling

The solvents that produce the most amount of swelling or display otherwise potentially favourable attributes described in Chapter 3.4.3.1.1 are selected for follow up experiments. The effects of solvent swelling by this selection of solvents are analysed in terms of lignite particle size distribution, specific surface area, micro and meso pore volume, and nutrient uptake capacity. The methods for analysing the above-mentioned lignite properties are described respectively in section 3.4.1.2 and section 3.4.1.4 of Objective S1-O1 and section 3.4.2.1 of Objective S1-O2. The results of the analyses should be noted in Appendix I “Recommended experimental design and results table solvent swelling S1-O3”. As mentioned, this table will enable a comparison between the effects of several solvents and nutrients species (described in the next objective) and informs which combination of solvents and nutrient species should be used for further prototype development.

3.4.3.4.2 Kai Point lignite case study: Effect of solvent swelling on nutrient uptake

Methods

After the swelling experiment described earlier in Chapter 3.4.3.2.2, the samples of that experiment were used for a subsequent nutrient uptake experiment. The scoping experiment was performed to establish a method for assessing the effect of solvent swelling on nutrient uptake by lignite. The experiment was conducted at the same time as Nutrient uptake experiments 2 and 3 (Objective S1-O3) and employed the same methods, described in section 3.4.2.1.2 In short: after the liquid layer was decanted from the samples, a measured weight of urea powder was added, and the samples were stirred with a stainless-steel spatula. Next, the samples were scooped onto a glass microfibre filter and vacuum filtered. Half the volume of the samples was removed from the filter for oven-drying, and the remaining half received an additional washing step with 10 mL ultrapure water. All samples were dried for 5 days at 40 °C before performing total nitrogen analysis and ATR-FTIR analysis. The effect of swelling on other lignite properties such as PSD, specific surface area and micro and meso pore volume was not determined in this scoping experiment.

Results and discussion filtering

30 g of urea powder was added to the first sample, slurry HS1 with 5 min. grinding time + ultrapure water "swelling" + urea (HS1-AU) and it was observed that not all urea crystals dissolved, see **Figure 29 (a)** below. Rinsing the sample washed the finer lignite fraction to the bottom of the sample, revealing more white, transparent urea crystals, see **Figure 29 (b)**. To avoid undissolved crystals, only 23.5 g of urea was added to the next sample, HS-ref'U, reducing the amount of white, transparent crystals in the unrinsed filtered sample (**Figure 29 (c)**) and the rinsed sample (**Figure 29 (d)**).

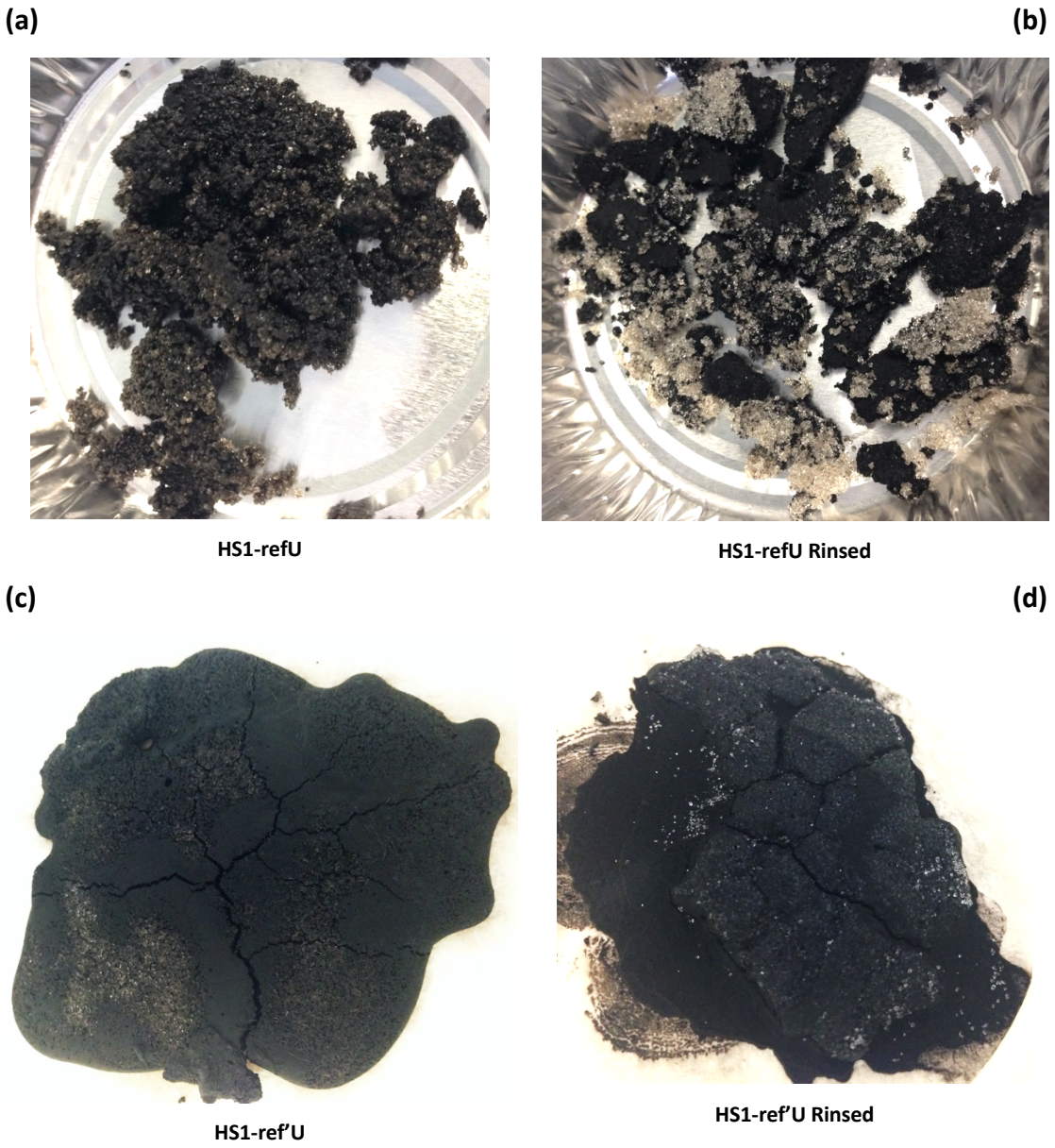

Figure 29 *Filtered HS1 slurry samples subjected to ultrapure water and mixed with urea (a) and (c) unrinsed, (b) and (d) rinsed.*

25 g of urea powder was added to slurry HS1 with 5 min. grinding time + acetone swelling + urea (HS1-AU). The tube became very cold and the slurry very thick. To avoid undissolved crystals, only 19 g of urea was added to the duplicate sample, HS-A'U. When filtering HS1-AU, a black, glossy, fibrous surface appeared (**Figure 30 (a)** below). Rinsing dissolved the glossy and fibrous texture, resulting in a more sand-like texture, see **Figure 30 (b)**. HS1-A'U has white, seemingly amorphous particles (**Figure 30 (c)**) and when rinsed, the sample displayed a clay-like texture and dark brown colour (**Figure 30 (d)**).

This is likely an effect of the acetone swelling that could have release organic matter from the lignite pores that is now visible as a clay-like dark brow structure.

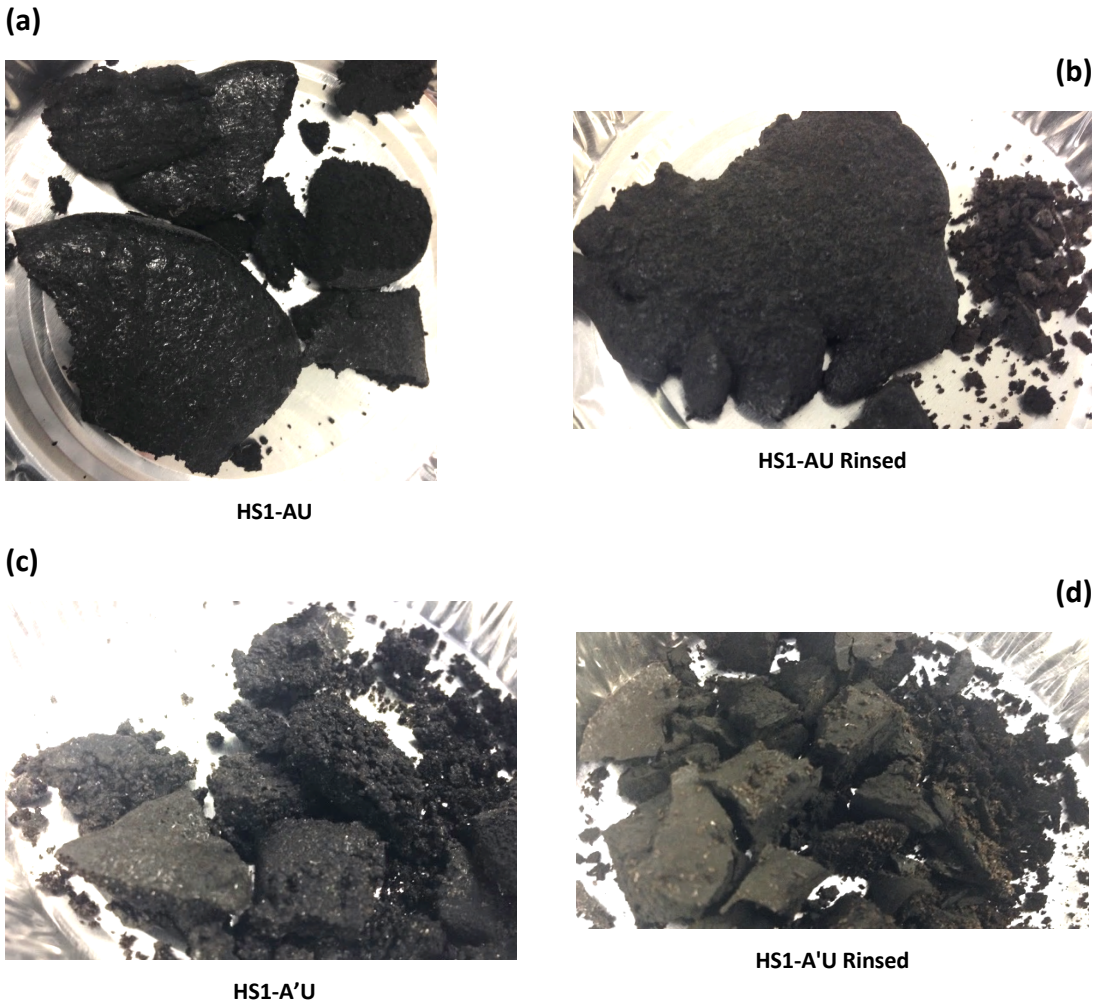

Figure 30 *The filtered samples of slurry HS1 subjected to acetone swelling and mixed with urea:* **(a)** *and* **(c)** *are unrinsed,* **(b)** *and* **(d)** *are rinsed with ultrapure water. The duplicates show a noticeable difference in texture despite the parent samples being subjected to the same manipulations.*

The sample with sieved raw lignite subjected to only ultrapure water (SRL-refU) was able to be mixed with 10 gr urea (**Figure 31 (a)** and **(b)** below), while the sieved raw lignite subjected to acetone, SRL-AU, became very dry upon mixing with urea and an additional 5 mL ultrapure water was added in an attempt to dissolve the crystals. Crystals were not obvious in the unrinsed filtered sample but were exposed after rinsing, see (**Figure 31 (c)** and **(d)**). The replicate of SRL-AU had a strikingly different, soil-like, texture that was littered with white amorphous particles (**Figure 31 (e)**), similar to HS1-A'U Rinsed in

Figure 30 (d) above. The white amorphous particles largely disappeared when rinsing, leaving behind a black soil-like texture (**Figure 31 (f)**).

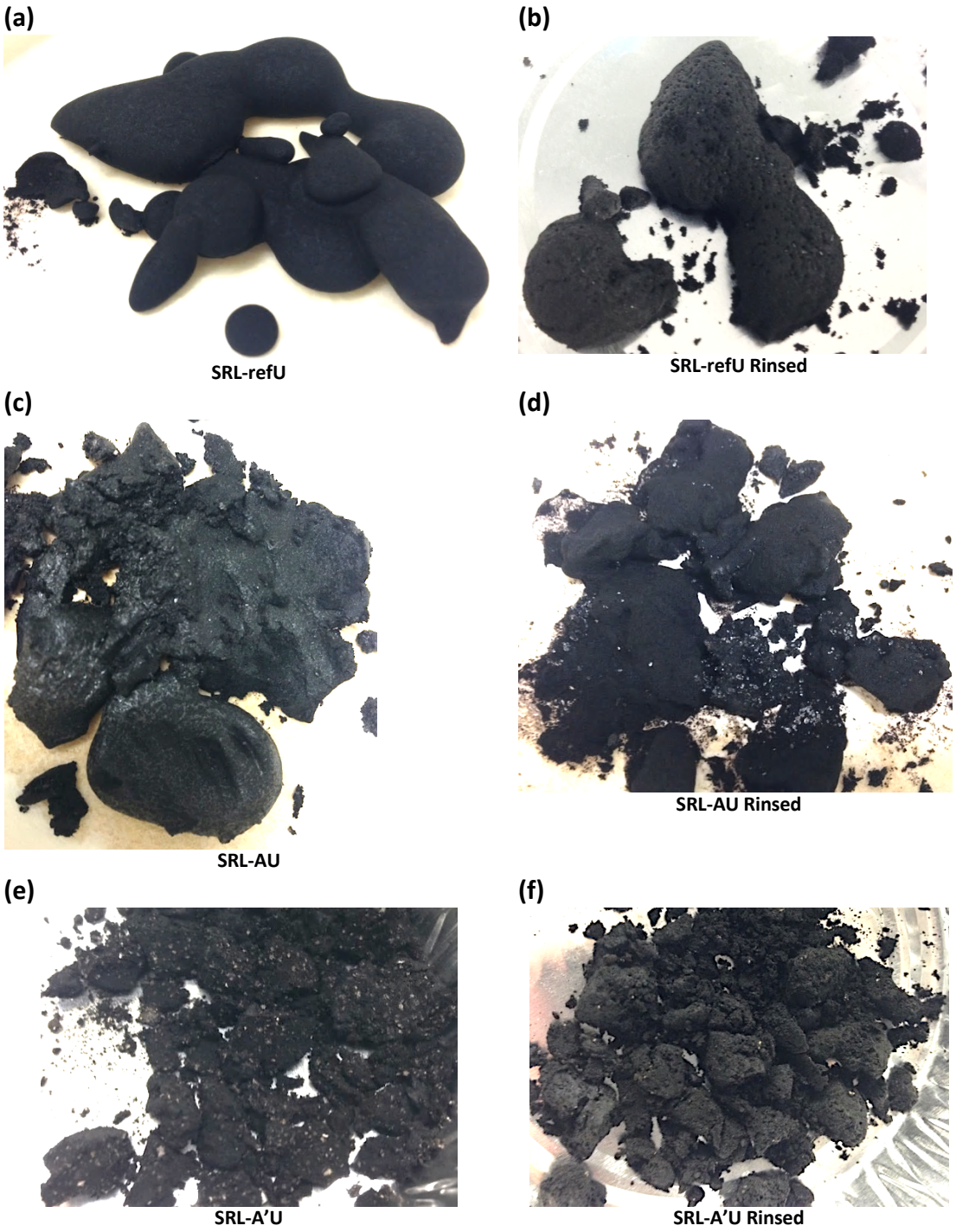

Figure 31 *Filtered samples of sieved raw lignite. Top: "Swollen" with ultrapure water;* **(a)** *unwashed,* **(b)** *rinsed. Middle: swollen with acetone;* **(c)** *unrinsed* **(b)** *rinsed. Bottom: duplicates of swollen with acetone;* **(e)** *unrinsed* **(f)** *rinsed.*

The sieved raw lignite samples were difficult to mix with urea and seemed dry; this could have been caused by acetone's high volatility, meaning a significant portion of the liquid could have evaporated over the course of the experiment, leaving less for the dissolution of urea. Another contributing factor could be the low solubility of urea in acetone, which is approximately 8 g/L at 20 °C (Treivus, 1994). This is more than a factor hundred lower than the solubility of urea in water (1079 g/L 20 °C). Despite the low solubility, urea has not been found to produce phase separation in acetone-water mixtures, unlike dissolving urea in acetonitrile-water mixtures (Loeser et al. 2011). Therefore, adding water to the acetone swollen samples could be a good solution to counter the seemly dry samples.

Since the HS1-ref samples and the SRL-AU(R) samples had a significant percentage of white, transparent urea crystals, it is expected that the total nitrogen analysis will display high percentages of nitrogen for those samples. The observation of crystals makes it clear that part of that nitrogen will not be inside the lignite structure. From the observations described above, the recommendation is made not to use urea powder for the nutrient uptake experiments after swelling, but instead a concentrated urea solution (50 wt.% urea) to deliver the nitrogen to the sample. This will likely eliminate the issues with crystallisation and allow a larger part of the urea to be dissolved in the bulk solution and diffuse into the lignite pores.

Results and discussion total nitrogen analysis

The results of the total nitrogen analysis are shown in **Table 8** below in order to assess the method used to analyse the effect of acetone swelling on nutrient uptake capacity. The solvent swelling percentages obtained in Chapter 3.4.3.2.2 are indicated as well.

As can be seen in **Figure 31**, **Figure 30** and **Figure 31** above, many of the samples contained a significant amount of crystals and white amorphous particles, thought to be urea. This unbound urea is expected to affect the total nitrogen analysis and give an overestimation of how much urea is uptaken by the lignite. Only 30 % of the samples did not contain a significant amount of white crystals or white amorphous particles. It is hypothesised that only samples SRL-refU' (13.7 % N), SRL-refU'R (6.5 % N), SRL-AU'R (12.6 % N), HS1-AU (37 % N), HS1-AUR (36 % N) and HS1-AU'R (29.8 % N) have a representative N %, the other samples are indicated with red colour. In **Table 8**, a negative value for the reduction in N % after rinsing means there was an increase in N % after rinsing. Since

rinsing did not wash out lignite in a significant amount, it is suggested that this illogical result is caused by the large amount of urea crystals present in the samples.

Table 8 *Total nitrogen % of various lignite samples subjected to H_2O or acetone swelling.*

Lignite sample	Swelling %	Initial C:N	N %	C:N after uptake	Reduction in N % after rinsing
HS1-refU	> 5	0.8	43.9*	0.50*	7.2*
HS1-refUR			40.8*	0.61*	
HS1-ref'U	17	1.2	34.8*	0.81*	-4.1*
HS1-ref'UR			36.3*	0.80*	
HS1-AU	55	1.4	37.2	0.74	2.5
HS1-AUR			36.3	0.76	
HS1-A'U	57	1.6	40.0*	0.64*	25.4*
HS1-A'UR			29.8	1.18	
SRL-refU	0	1.1	23.8*	1.56*	8.4*
SRL-refUR			21.8*	1.80*	
SRL-ref'U	0	2	13.7	3.51	53.0
SRL-ref'UR			6.5	8.42	
SRL-AU	14	1.1	18.1*	2.36*	-18.0*
SRL-AUR			21.3*	1.90*	
SRL-A'U	23	4.5	27.3*	1.28*	53.9*
SRL-A'UR			12.6	3.74	

*Samples with undissolved urea crystals or white amorphous particles.

Legend

HS1-refU(R): HS1 (slurry 5 min. grinding) with ultrapure water and urea added, R = rinsed.
HS1-AU(R): HS1 (slurry 5 min. grinding) acetone swollen and urea added, R = rinsed.
SRL-refU(R): Sieved raw lignite (mesh size ≥ 63< 106 µm) with ultrapure water and urea added, R = rinsed.
SRL-AU(R): Sieved raw lignite (mesh size ≥ 63< 106 µm) acetone swollen and urea added, R = rinsed.

In **Table 8**, the samples with no visibly undissolved urea crystals or white amorphous particles attain a minimum nutrient-N content of 6.5 % and a maximum of 37 %. Rinsing lignite slurry HS1 with adsorbed urea results in 2.5 % N loss, while rinsing sieved raw lignite (mesh size ≥ 63< 106 µm) results in 53 % N loss. Though the lack of replicates means the results are not statistically significant, the result could indicate that ground lignite particles retain adsorbed nitrogen better. The tested method resulted in varying initial concentrations. Together with the undissolved urea crystals this means directly comparing the H_2O and acetone swollen samples is not possible. However, predictions

can be made regarding the influence of initial N loading, swelling and N uptake. Rinsed, sieved, raw lignite swollen with acetone (SRL-AU'R) had half the initial nitrogen loading compared to the reference sample SRL-ref'R (0 % H_2O swelling), yet the 23 % acetone swollen sample contained almost twice as much (94 % more) nitrogen as the sample not subjected to acetone.

Results and discussion ATR-FTIR analysis

The ATR-FTIR spectra of the H_2O and acetone swollen samples after urea uptake are displayed in **Figure 32**, together with the spectrum of a pure lignite sample (HS1). The ATR-FTIR spectrum for urea was given earlier in **Figure 22**. The spectra of the samples look very similar to the spectra of the samples from Experiment 2 with one distinct difference, the peaks at 3330 - 3350 cm^{-1} and 3450 cm^{-1} (symmetric and asymmetric NH_2 vibrations) are much more defined in samples HS1-ref'U, HS1-A'U, HS1-A'UR and SRL-A'U. This indicates more urea is present in the samples, which is corroborated by the total nitrogen analysis in **Table 8**, where the higher peaks correspond to a total N % of 27.3 – 40 %, compared to 12.6 and 13.7 % N in the samples with less intense NH_2 peaks. In the sieved raw lignite samples swollen with acetone (SRL-A'U(R)), the Si-O peak at 1030 cm^{-1} and the NH_2/N-C-N peak at 1160 cm^{-1} are connected in a broad set of peaks.

The potential of the rinsing step to remove nitrogen is visible in the FTIR spectra, where the 3330 - 3350 cm^{-1} and 3450 cm^{-1} peaks of symmetric and asymmetric NH_2 vibrations are reduced in intensity after rinsing, as is the 1160 cm^{-1} peak of NH_2/N-C-N (Larrubia et al., 2000) and the 1435 – 1440 cm^{-1} peak of the NH_4^+ bending vibrations (Pironon et al. 2003). What is interesting, is that the 3200 cm^{-1} NH_4^+ stretching vibrations peak does not seem to be as affected by rinsing as the NH_2 vibrations peaks are, and the asymmetric NH_2 vibrations peak is reduced more by rinsing than the symmetric NH_2 vibrations peak. These results indicate that some bonds are easier washed out that others, which can be explained by the fact that NH_2 bonds are found in urea crystals, while the relatively high amount of NH_4^+ peaks in the samples are likely the results of dissociation of urea in the solvent and subsequent interaction with lignite.

In conclusion, there is no obvious effect of acetone swelling on the chemical bonds related to urea adsorption onto lignite. Rinsing samples, the use of raw lignite or slurry with 5 minutes grinding time, and the large amount of urea present in the samples seems to be

more determinant when it comes to the chemical bonds found it the samples. It is postulated that there are effects on the chemical structure when exposing a lignite sample to acetone or any of the other solvents listed in **Table 7**, but this will need to be investigated in the absence of (a high concentration of) nutrients to avoid interference.

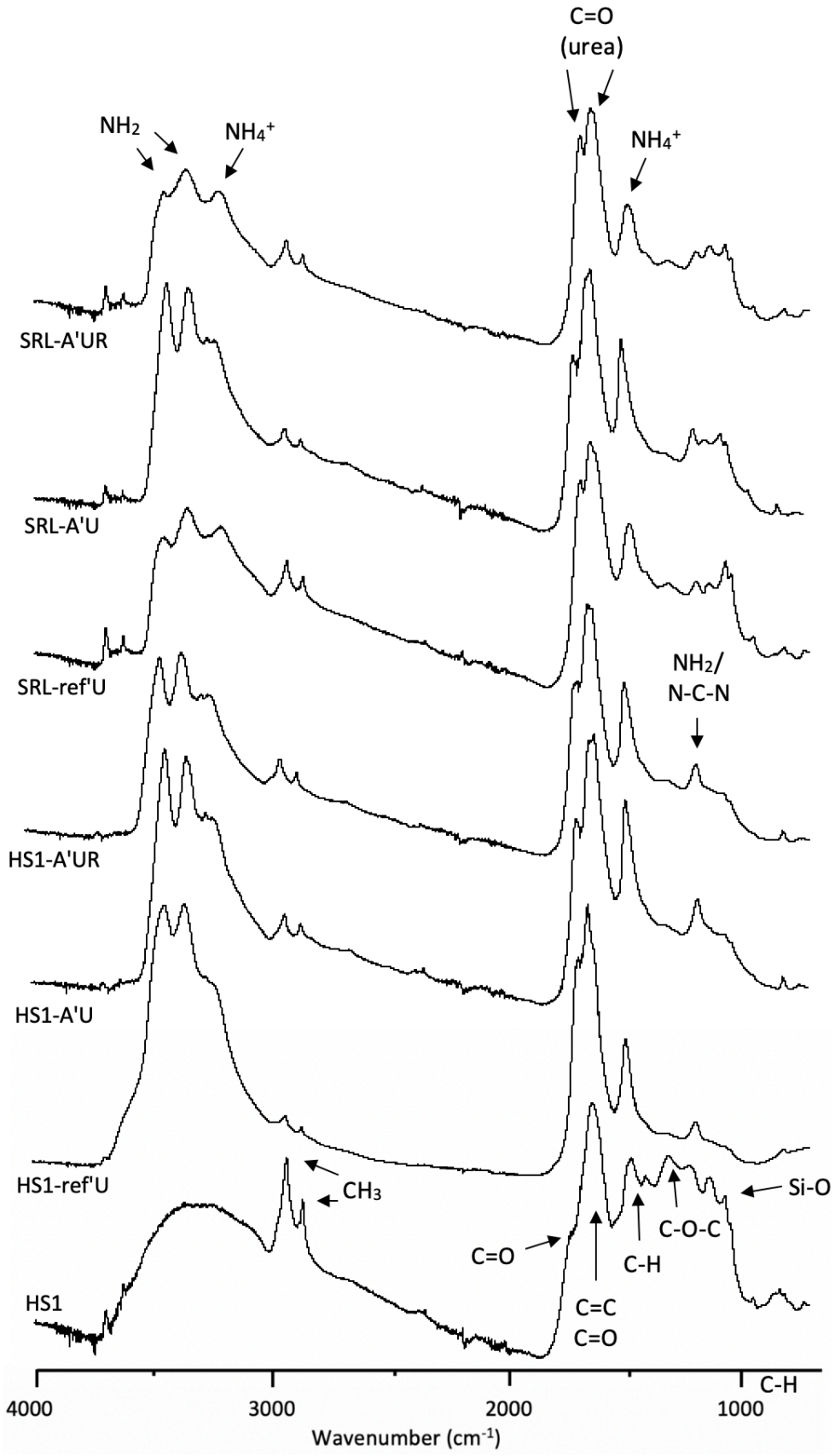

Figure 32 *ATR-FTIR absorbance spectra of the acetone swollen samples, including ultrapure water "swollen" reference spectra and a pure lignite slurry baseline.*

3.4.3.4.3 Recommended methods for analysing the effect of solvent swelling on lignite properties

In order to achieve maximised nutrient adsorption onto lignite, the following methods are recommended for analysing the nutrient uptake capacity of lignite slurries subjected to various swelling solvents. After the swelling experiments, the samples with the solvents that constitute the largest amount of swelling or display otherwise favourable properties, such as interaction with the chosen nutrient species, are used for subsequent nutrient uptake studies. This step is done in conjunction with the next Objective (S1-O4), which informs the choice of nutrients for the nutrient uptake experiments.

The method for particle size distribution analysis is described in Chapter 3.4.1.2, specific surface area, and micro and meso pore volume in section 3.4.1.4, the methods for total nitrogen, PXRD and ATR-FTIR in section 3.4.2.1. Particle size distribution analysis will inform if the swelling solvents constitute chemical comminution and thus particle size reduction. Specific surface area, and micro and meso pore volume analysis, in combination with ATR-FTIR analysis, will shed light on the mechanisms of solvent swelling for a particular solvent; if a rearrangement of the pore structure takes place and if the carboxylic and phenolic functional groups are targeted or if other mechanisms are at play. Total nitrogen and PXRD analysis will inform how much N is in the sample and if the nutrient is in crystalline form or adsorbed into the lignite pores. All the results are noted in Appendix I “Recommended experimental design and results table solvent swelling S1-O3” for comparison.

The large inter-replicate variation seen in the case study emphasises the need for at least six replicates per sample. It was established that in order to prevent issues with undissolved crystals, a concentrated nutrient solution should be used for the uptake experiments, rather than a solid powder. The concentrated solutions can be a solution of ultrapure water and the nutrient, but in some cases, the choice can be made for a solution of the swelling solvent with the selected nutrient, which will be further discussed in the next Objective (S1-O4).

3.4.4 Objective 4 (S1-O4): Determine the effect of nutrient species on nutrient uptake

In order to maximise nutrient adsorption onto lignite, the fourth objective focusses on the nutrient species that is used for adsorption onto lignite in conjunction with a selection of swelling solvents. The objective is to *"Determine the effect of different N/P/K species on lignite nutrient uptake through a series of adsorption experiments in combination with varying swelling solvents, in order to select the N/P/K species that results in the highest nutrient uptake. Together with the results from S1-O3 make a selection of the lignite-based controlled-release fertilisers with the most potential = PROTOTYPES B".* This objective is achieved by first selecting the most likely candidates for an agricultural fertiliser, followed by uptake experiments examining the interaction effects of nutrient species with the swelling solvents stated in **Table 7** of the previous Objective (A-1-O3).

3.4.4.1 Selecting N/P/K nutrients species

3.4.4.1.1 Methods of N/P/K nutrient species selection

A list of the most common agricultural nutrient species is formulated in **Table 9** below. When selecting nutrient species from the list, there are several points to take into account:

1. The micro and meso pore volume of the lignite type used: the selected nutrient species should be able to enter the majority of the pores in order to attain maximum nutrient loading and a more favourable controlled-release character.
2. The solubility of nutrient species in several solvents: a higher solubility enables a larger concentration gradient between outside and inside the lignite pores, which will constitute more adsorption.
3. The interaction effects between the nutrient species and the solvent (mixture), and between the nutrient species and the lignite structure.

For point 1, the BET analyses of solvent swollen lignite samples from the previous objective come into play. Similar as with selecting swelling solvents, the minimum diameter for pore entry needs to be calculated for the nutrient species and compared with the micro and meso pore volume noted in Appendix I "Recommended experimental design and results table solvent swelling S1-03".

Regarding point 2, the choice of nutrient species is very much intertwined with the choice of solvent. Urea, for example, has a decreasing solubility in higher alcohols, but a relatively high solubility can still be attained when using alcohol-water mixtures (Lee and Lathi, 1972, House & House, 2017). Therefore, a comprehensive table should be constructed with the nutrient species from **Table 9** below and their respective solubility in the swelling solvents of **Table 7** in Objective S1-O3 (table not given). The table should include the solubility of the nutrients in the solvents - water mixtures that are created when mixing a lignite slurry (with a given % of water) with a solvent. Such a comprehensive solubility table will be invaluable when selecting a nutrient species that is tailored to nutrient uptake maximisation and will reduce the chance of unnecessary experiments.

A good example of point 3 is the interaction effect between acetonitrile and urea. Loeser et al. 2011 found that when using a wide range of v/v % acetonitrile-water mixtures in the range of 77 - 86 v/v %, the mixtures would divide into two liquid phases when saturated with urea. Such a separation of liquid phases would likely be unfavourable for nutrient uptake optimisation and controlled release. Literature has also described the tendency of urea to form aggregates in higher alcohols. This is caused by the unshared pair of electrons on the oxygen atom and both nitrogen atoms in the urea molecule, which result in multiple sites where urea can form hydrogen bonds with solvent molecules or other urea molecules. The polar urea molecules are predicted to interact more strongly with themselves than with the solvent if the solvent forms weaker hydrogen bonds, has larger molecules and less polar groups (House and House 2017).

Table 9 *Nutrient species suggested for adsorption experiments with nutrient content (%) and approximate solubility (g/L) in water at 20℃.*

Nutrient species	Nutrient content	Solubility in water at 20°C (g/L)
Urea	46.6% N	1080
Thiourea	36.8 %N	137
Anhydrous ammonia	82% N	450*
Ammonium nitrate	33.5% N	1920
Calcium nitrate	15.5% N	1290
Ammonium dihydrogen phosphate (ADP)	11% N, 27% P	368
Diammonium phosphate (DAP)	18% N, 20% P	588
Mono ammonium phosphate (MAP)	11%N, 21-26.6 % P	370
Mono potassium phosphate (MKP)	22.7%P, 28.7%K	230
Calcium ammonium nitrate	27% N	1200
Single superphosphate (SSP)	8.3% P, 10-25% Cl	-
Potassium chloride	52.4% K, 47.6% K	255
Potassium nitrate	13% N, 36.5% K	209

* at 25 °C

3.4.4.1.2 Kai Point lignite case study: Nutrient species selection

In the scoping experiments described in the Objectives above, only one nutrient was investigated: nitrogen. As described extensively in the literature review, N was chosen because the agriculturally related environmental problems with nitrogen are most pressing considering it is applied in the largest quantities of all fertilisers and the losses are most substantial due to the high reactivity and mobility of fertiliser-N (Jackson et al., 2008). The N-nutrient species selected was urea since it is the most prevalent agricultural N-fertiliser, contains a relatively high % N (46 %), and is highly soluble in water. The latter two points allow for a high nutrient loading which is advantageous for maximising nutrient adsorption onto lignite, and thus for the efficiency or a lignite-based controlled-release fertiliser.

3.4.4.1.3 Recommendations for nutrient selection

In order to choose appropriate solvent - nutrient species combinations, the suggested comprehensive table with the nutrient species from **Table 9** and their respective solubility in the swelling solvents of **Table 7** is crucial, as well as an investigation into the interaction effects between nutrient species and solvents, and nutrient species and lignite. This will require extensive literature research and experimental work, but will greatly reduce the number of nutrient uptake studies required to find which combinations of solvents and nutrients result in optimum nutrient adsorption by lignite.

3.4.4.2 Analysing the effect of nutrient species on lignite properties

3.4.4.2.1 Method for analysing effect nutrient species

The effect of nutrient species on nutrient uptake is evaluated through the nutrient uptake studies described in section 3.5.1.3.4. The main focus is on determining N/P/K content, performing PXRD analysis to discover if the nutrients are incorporated into the lignite structure or merely on the outside of lignite particles in the form of crystals, and which chemical bonds are being established or eliminated as a result of nutrient-lignite interactions and nutrient-swelling solvent interactions. The results of the nutrient uptake experiments with various solvents and nutrient species will produce a set of lignite types with particular configurations of particle size distribution, specific surface area, micro and meso pore volume, nutrient species and swelling solvent, culminating in a certain nutrient uptake capacity. The configurations with the most potential to become a lignite-based controlled-release fertiliser are selected as PROTOTYPES B and used for the characterisation and optimisation experiments of the next objective (S1-O5).

3.4.5 Objective 5 (S1-O5): Determine the effect of pH, temperature and initial concentration on nutrient uptake

In order to maximise nutrient uptake and obtain an understanding of the effects of certain combinations of lignite property manipulations, the fifth objective focusses on a more in-

depth study of several of the effective parameters of the adsorption process. The objective states: *"Determine the effect of pH, temperature and initial nutrient concentration on lignite nutrient uptake using kinetic studies and equilibrium studies to produce adsorption isotherms."* This objective is achieved by designing several batch adsorption experiments, each targeting one of the three examined parameters.

3.4.5.1 Methods for assessing effective adsorption parameters

Removal efficiency is determined by measuring the concentration (mg/L) in the nutrient solution before the experiment (C_0) and comparing it to the equilibrated concentration after 48 hours (C_{eq}) (for example using T-NML total nitrogen analysis for N, UV/VIS for phosphate and FES for potassium) according to the following equation (Nazari et al., 2018):

$$Removal\ efficiency\ (\%) = \frac{(C_0 - C_{eq})}{C_0} \times 100\ \%$$

Equation 9 *Nutrient removal efficiency of lignite*

The adsorption capacity of lignite at equilibrium (Q_{eq} in mg/g) is calculated using the initial concentration of the nutrient solution (C_0 in mg/L), the equilibrated nutrient concentration of after 48 hours, the volume of the solution (V in L), and the calculated mass of the dry lignite in the sample (m_{dry} in g) according to the equation (Tu et al. 2019):

$$Q_{eq} = \frac{(C_0 - C_{eq})}{m_{dry}} \times V$$

Equation 10 *Adsorption capacity of lignite*

Equilibrium adsorption is studied at different temperatures to produce adsorption isotherms which inform at which temperature adsorption of nutrients onto lignite is maximised. Tu et al. (2019) showed the adsorption of some nutrient species is favoured at higher temperatures because of the endothermic nature of the adsorption onto lignite. In contrast, the adsorption of other species onto lignite is exothermic and reduces entropy, resulting in weakened adsorption of those nutrients at higher temperatures.

The kinetics of the adsorption process can be studied by measuring the adsorption of a nutrient over time (q_t in mg/g) when using two different initial concentrations: 50 % saturated nutrient solution and a 100 % saturated nutrient solution, and is calculated in a similar manner as q_e according to the equation:

$$q_t = \frac{(C_0 - C_t)}{m_{dry}} \times V$$

Equation 11 *Nutrient adsorption at each time*

In the next objective (S1-O6), the batch experimental data is fitted to kinetic models to study the adsorption kinetics of nutrients onto lignite and determine the governing adsorption mechanism, e.g. physical diffusion or a reaction process. The experimental data will also be fitted to several adsorption isotherms to determine the occurrence of adsorption, e.g. single layer or multi-layer adsorption, and which parameters limit the adsorption of nutrient onto lignite.

3.4.5.2 Kai Point lignite case study: Initial concentration

The scoping experiments of the case study were conducted at room temperature and focussed on the adsorption capacity at equilibrium. They touched upon the use of varying initial concentrations: 40 – 50 wt.% urea solutions or oversaturation with solid urea, or played with adsorbent dosage by varying solids loadings of slurries between 59 - 70 % and by using raw lignite. This resulted in initial C : N ratios of 0.71 – 4.5. However, because in the experiments other parameters were manipulated as well as the initial nutrient concentration (= initial C : N ratio), the resulting total nitrogen concentrations in the lignite samples cannot be directly correlated to the initial nutrient concentration. Instead, a general overview of the nutrient uptake capacities (%) obtained with samples that had (amongst other parameters) different initial nutrient concentrations is given in **Figure 33**. The figure shows that a minimum nutrient-N content of 6.5 % is attaint and a maximum of 37 %. The obtained nitrogen percentages are placed in an agricultural context, indicating where on the line urea is (46 % N) and what N % is required for

vegetable crops (12 % N) and pastures (30 % N). The values for vegetables and pastures are based on the assumption that the nutrient release of the fertilisers exactly matches plant nutrient requirements, and the fertilisers are applied at the same rate as conventional urea fertilisers.

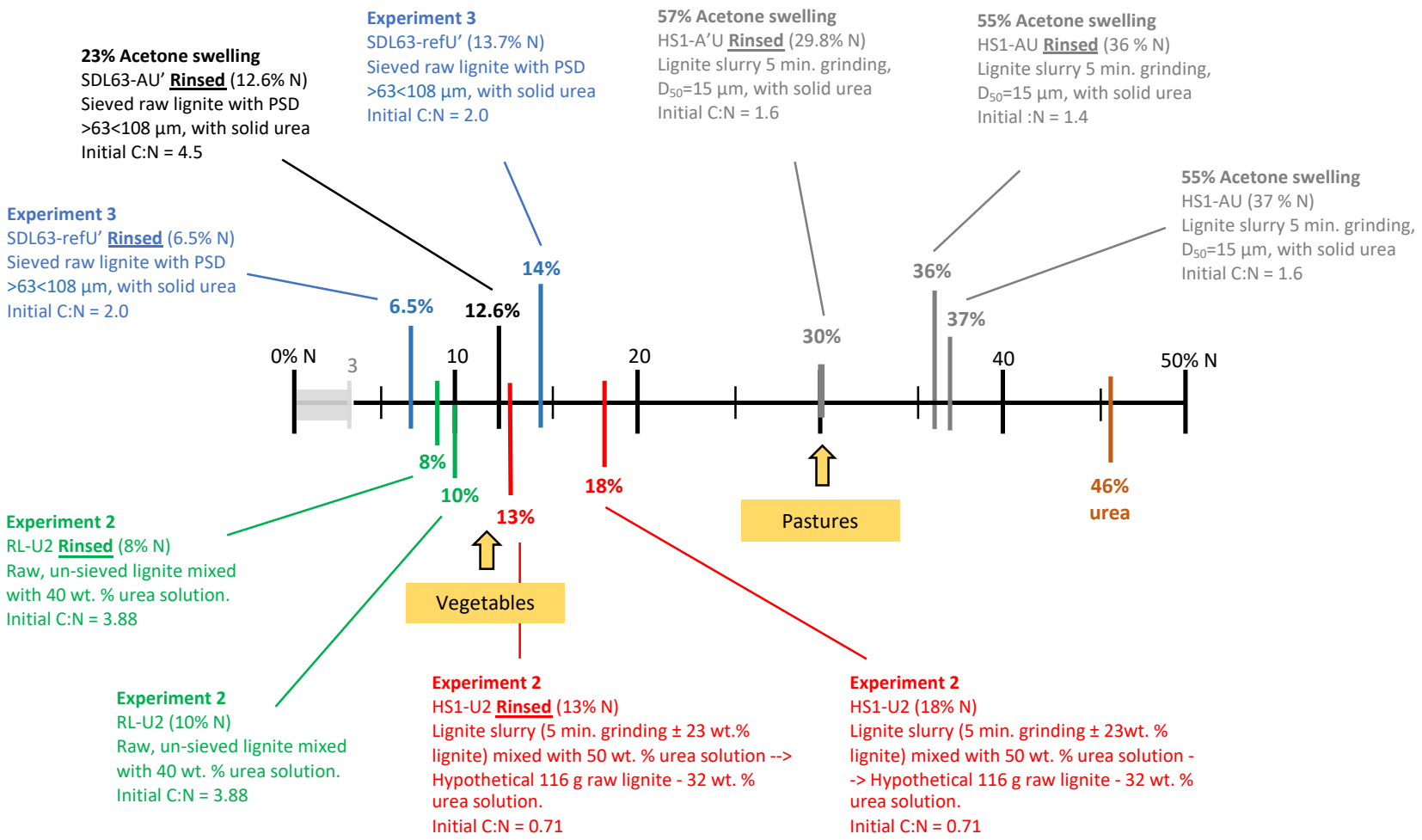

Figure 33 *"Nitrogen uptake line" displaying the total nitrogen % of lignite samples with various particle size distributions, solvent treatments and initial nutrient concentrations (initial C : N). The samples at the top half were mixed with solid urea, the samples at the bottom half with a urea solution. It is indicated if a sample was rinsed.*

3.4.5.3 Recommended methods for accessing the effective parameters in the adsorption process

After the scoping experiments, it is recommended that the first batch experiment should focus on varying the initial nutrient concentration. In objective S1-O3 and S1-O4 are several nutrient-solvent combinations identified that have the most potential for a lignite-based controlled-release fertiliser and are produced with concentrations of 20, 40, 50, 60, 70, 80, 90 and 100% saturation. An equal amount of lignite slurry (grinding time selected in Objective S1-O2 and solvent pre-treatment selected at Objective S1-O3) is mixed with the nutrient solutions of different concentrations and placed on a rocking table for 48 hours. The experiments are conducted in triplicates. The effect of pH is studied by producing adsorption series where a fixed nutrient concentration is mixed with a fixed lignite concentration, and pH is varied over the range 2 – 10 by adding 0.1 M HCl or 0.1 M NaOH. The samples are placed on a rocking table for 48 hours, and again, the experiment is conducted in triplicate. After 48 hours, the nutrient concentration in the solutions is measured, and removal efficiency and adsorption capacity are calculated and plotted against initial concentration and pH. Equilibrium adsorption will need to be studied at different temperatures (isotherms); 20 40 and 60 °C are selected. (Note: Kelvin is the conventional unit, being 293, 313 and 333 K respectively).

3.4.6 Objective 6 (S1-O6): Determine adsorption limiting factors and mechanisms

Using the adsorption data that is to be obtained from objective S1-O5 above, models can be employed to understand and optimise the adsorption process. Therefore Objective 6 (S1-O6) states: *"Following S1-O5, determine the adsorption limiting factors and mechanisms of nutrient uptake by lignite, by fitting the produced equilibrium data and adsorption isotherms to a selection of kinetic and isothermal adsorption models, in order to make a selection of the lignite-based controlled-release fertilisers with the most potential."* The kinetic and isothermal models are extensively described in Chapters 2.5.3 and 2.5.4 of the literature review and Appendix C, D and E.

The results of the model fitting will allow for further optimisation of nutrient adsorption, by predicting optimal reaction temperature, optimal initial nutrient concentration and optimal pH. The results should also provide a deeper understanding of the nature of the adsorption process, which could in turn, provide suggestions as to how manipulation of the properties of lignite can be improved to foster nutrient adsorption. For example, model fitting should provide an answer to the question if an increased pH opens up more adsorption sites and fosters nutrient adsorption onto lignite, or if an increased pH decreases nutrient uptake because it prevents intraparticle diffusion due to a decrease in specific surface area and total porosity.

CHAPTER 4

SUMMARY AND CONCLUSIONS

The work presented in this thesis is based on three aims. The first aim is largely literature-based and identifies crucial aspects that allow for the outline of the feasibility framework. In the second aim, the proposed framework is tested using a case study in which detailed methodologies are established and optimisation is proposed. The third aim incorporates the findings of the first two aims to form the final feasibility framework. The sections below provide a summary of the achievements with regards to each of the three aims.

4.1 Summary of most important properties and parameters

The first aim of the research is to determine which properties and parameters are of primary importance when developing a potential lignite-based controlled-release fertiliser. Literature research reveals three attributes that are prerequisites for an environmentally and economically feasible fertiliser. First, the fertiliser needs to have high nutrient loading to allow for a minimal application rate, contributing to practicality and cost- and resource efficiency. If this has been attained, the fertiliser needs to release the nutrients at a rate that matches plant nutrient uptake requirements, reducing the environmental impact of fertilisation and contributing to cost efficiency. Lastly, the fertiliser needs to have an appropriate delivery type that is compatible with state-of-the-art precision agricultural practices, contributing to both environmental and economic sustainability.

In order to achieve a high nutrient loading onto the lignite structure, several properties have been identified as paramount in nutrient adsorption. The most important property is

the amount of available nutrient-binding sites. In lignite, nutrients attach mainly to carboxylic and phenolic functional groups, and from this, it logically follows that increasing the number of available functional groups will increase nutrient adsorption capacity.

Lignite has a highly porous structure with a vast network of pores. Access to a portion of those pores is restricted by small pore openings, and some pores are completely closed off from the bulk solution and thus not available for nutrient uptake. One way to make more pores accessible, and thus increase specific surface area, is by breaking the lignite particles open. This reduces the particle size and changes the micro and meso pore volume. Grinding is a widely applied method for mechanical comminution (= particle size reduction).

The pH of low-rank coal has also been found to govern adsorption capacity, as have temperature and initial nutrient concentration. It is hypothesised that swelling of the lignite structure through solvent interactions is another method of increasing the availability of binding sites. Lastly, the choice of nutrient species is also a determining factor in the extent of nutrient adsorption since the nutrient content varies per nutrient species, and nutrient species can cause chemical inactions with swelling solvents and the lignite structure.

The properties that are identified as important to the adsorption process are also determinant in controlled-release of nutrients and the choice of fertiliser delivery type. Particle size distribution has a profound effect on lignite slurry viscosity, as does the addition of solvents and nutrients. Viscosity, in turn, is the determining factor in assessing the feasibility of slurry applications.

4.2 Summary and conclusions of Kai Point lignite case study

The second aim of the research is to provide a case study with a proof-of-concept of lignite property manipulation, nutrient uptake and solvent swelling by a type of local lignite. A case study was conducted using Kai Point lignite from New Zealand. Lignite – water slurries were produced with grinding times of 0 – 30 minutes, manipulating particle size distributions. The slurry with 5 minutes grinding time was found to have a slightly bimodal particle size distribution, which is favourable because it can achieve a higher solids loading without viscosity exceeding practical limits. The effect of particle size distribution and solids loading on viscosity was quantified through rheological experiments. It was indeed found that with a shorter grinding time, a higher solids loading could be achieved before viscosity became too high to be practical in an agricultural context.

Next, the effect of grinding time on nutrient uptake was analysed over the range of 5 to 30 minutes grinding in a set of scoping experiments. In these preliminary experiments it was found that the lignite slurry subjected to 5 minutes grinding had the highest percentage nutrient uptake, with 29 % of the initial urea-N concentration being uptaken. Other experiments compared nutrient uptake capacity of lignite slurry with 5 minutes grinding time to raw, unground (sieved) lignite (mesh size $\geq 63 < 106$ µm). Results seem to suggest that lignite ground for 5 minutes has a higher uptake capacity than (sieved) raw lignite. This would support the hypothesis that the grinding process makes otherwise inaccessible internal pores of lignite particles available to the bulk solution, thus increasing the specific surface area and foster nutrient adsorption.

In another experiment, the lignite structure was manipulated by subjecting samples to one of two potential solvents: ultrapure water or acetone. The use of acetone resulted in a maximum of 57 % swelling of the lignite structure. When performing preliminary uptake experiments with the swollen samples, rinsed, sieved, raw lignite swollen with acetone contained almost twice as much nitrogen as the reference samples not subjected to acetone, even though the acetone swollen sample had a lower initial nitrogen loading than

the reference sample. Over the span of all conducted scoping experiments, nutrient uptake capacities of 6.5 % - 37 % total nitrogen were attained for Kai Point lignite. PXRD analysis was used to determine that urea-N was adsorbed by the lignite structure and not attached to the outside of the lignite particles. ATR-FTIR was used to examine which bonds the urea-N formed with the lignite structure.

The scoping experiments provide a proof-of-concept of lignite property manipulation by means of grinding and solvent swelling, and demonstrate that manipulating the properties of lignite has an effect on nutrient adsorption by lignite.

4.3 Summary of feasibility framework methods

The third and last aim of the research brings the first two aims together in the development of detailed methods to examine and characterise the ability of lignite property manipulations to maximise nutrient adsorption onto lignite. **Figure 34** contains a summary of the recommended framework methods informed by the scoping experiments of the case study. Through the case study and literature review, it is also established that the recommended methods allow the most important lignite property manipulations to be tailored to any given type of lignite in order to achieve maximised nutrient adsorption.

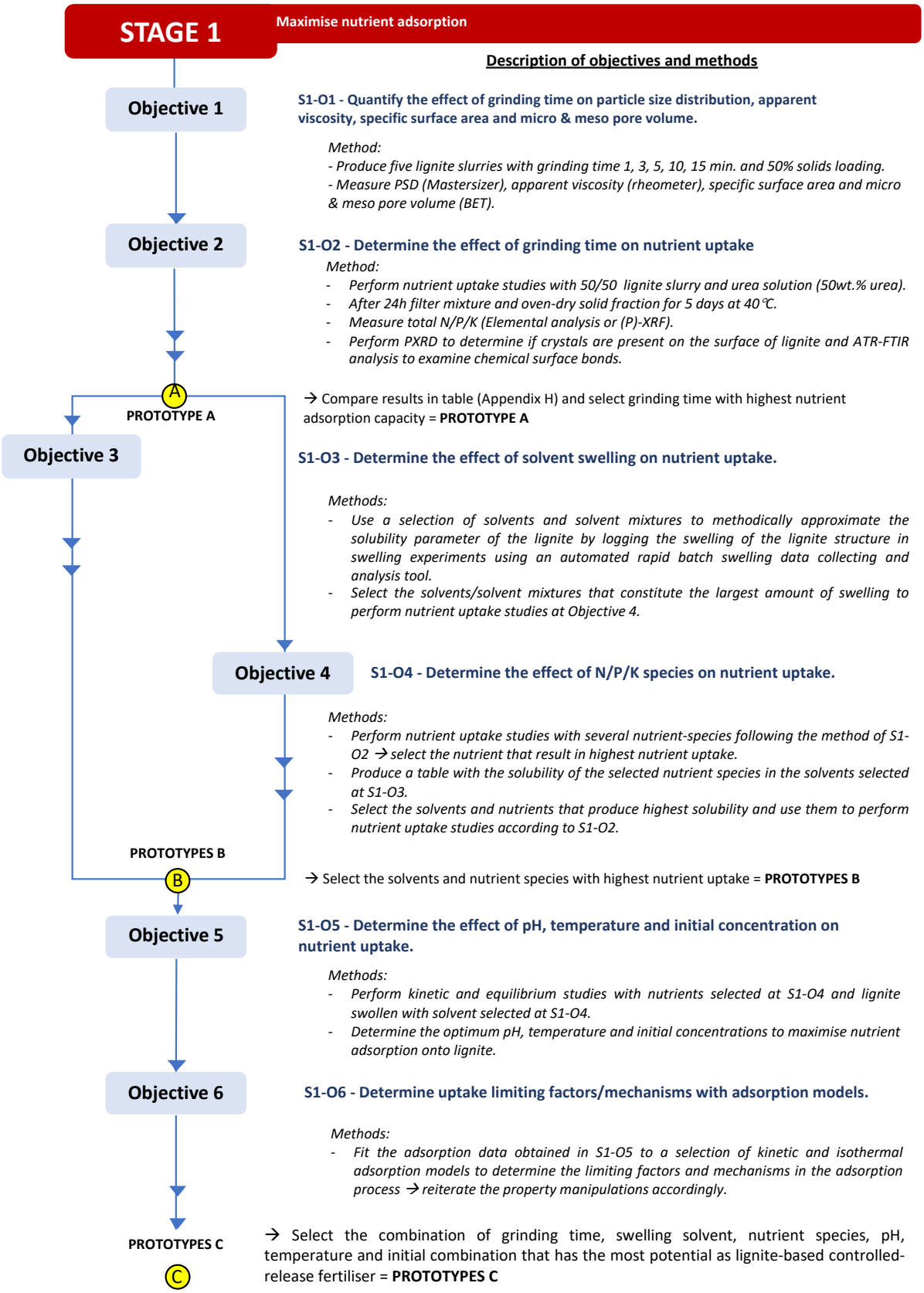

Figure 34 *Summary of the methods established for the feasibility framework. S = Stage, O = Objective*

CHAPTER 5

RECOMMENDATIONS

5.1 Further research

After Stage 1 of the feasibility framework, Stage 2 and 3 focus on matching nutrient release to plant nutrient requirements and application of potential lignite-based controlled-release fertilisers in precision agriculture, respectively.

5.1.1 Stage 2: Characterise nutrient release

Stage 2 is formulated as: *"Characterise nutrient release of lignite-based controlled-release fertiliser prototypes and compare to current fertilisers."* The two accompanying objectives are centred around nutrient release studies of the prototypes developed in Stage 1 and conventional (controlled-release) fertilisers.

5.1.1.1 Objective 1 (S2-O1): Quantify the controlled-release character of prototypes

Stage 2 Objective 1 (S2-O1) states: *"Quantify the controlled-release nature of PROTOTYPES C with nutrient release models, by performing in vitro nutrient release experiments."* The method of Dai et al. (2008) can be employed since Saha et al. (2017) demonstrated the method's applicability for lignite-based fertilisers. Besides testing the prototypes, references will need to be tested as well. These references should consist of raw lignite and lignite with the grinding time selected at S1-O2 infused with the same set of nutrient species selected for prototypes C. This will allow for the evaluation of the effects of lignite property manipulations on the controlled-release character. A large

nutrient uptake capacity of lignite can significantly contribute to fertiliser and resource efficiency, yet it does not necessarily constitute an appropriate controlled release character. Therefore, a carefully selected range of grinding times, nutrient species and swelling solvents will need to be tested in addition to prototypes C of Stage 1. To allow for subsequent comparison with conventional controlled-release fertilisers, the prototypes and other selected lignite – nutrient samples are evaluated on a dry basis, meaning the samples will need to be oven-dried for 5 days at 40 °C.

The method of Dai et al. (2008) consists of batch desorption studies where the oven-dried nutrient-infused and/or solvent swollen lignite samples are placed in mesh bags and submerged in a container with ultrapure water. At specific intervals, the mesh bags with lignite are removed from the container and placed in a new container with water. The nutrient content in the containers is analysed and plotted over time. The experiments are conducted over the range of common soil temperatures.

5.1.1.2 Objective 2 (S2-O2): Compare prototypes to current fertilisers

Stage 2 Objective 2 (S2-O2) states: *"Compare the nutrient release character and nutrient densities of PROTOTYPES C to that of currently available (controlled-release) fertilisers and select the prototypes that hypothetically compete with current fertilisers and best match nutrient uptake requirements of the intended plant species = PROTOTYPES D."* This requires a selection of current (controlled-release) fertilisers to be examined according to the same method as described in S2-O1. Together with information on the nutrient densities, this comparison will determine the competitiveness of the developed lignite-based controlled-release fertilisers.

To tailor lignite-based controlled-release fertilisers to the needs of particular plants, the nutrient release character of the prototypes is compared to plant nutrient requirements during various stages of development, which can be found in literature for a variety of plant species. Besides comparing the dry controlled release character, the wet controlled release character of the lignite - nutrient slurry is also analysed and compared to plant requirements. The suggested method is described in the soil column leaching experiments of Ding et al. (2016). It will be interesting to examine if one of the newly developed

lignite-based fertilisers (dry or wet) matches plant nutrient requirements better than conventional fertilisers, as this will significantly increase the value and feasibility of the lignite-based fertiliser. The prototypes with the most potential are selected as PROTOTYPES D for Stage 3 of the feasibility framework.

5.1.2 Stage 3: Evaluate the optimal delivery type

Stage 3 (S3) is described as: *"Evaluate the optimal delivery type for deployment in precision agriculture (e.g. slurry, granules, pellets) of the final lignite-based controlled-release fertiliser prototypes."* Two objectives are formulated to this aim, focussing on characterisation and compatibility assessment.

5.1.2.1 Objective 1 (S3-O1): Characterise the rheology of PROTOTYPES D

Stage 3 Objective 1 (S3-O1) states: *"Characterise the rheology (apparent viscosity) of PROTOTYPES D."* If slurries prove viable with regards to controlled-release, viscosities and slurry stability will need to be analysed according to the methods developed in S1-O1.

5.1.2.2 Objective 2 (S3-O2): Assess compatibility with delivery systems

Stage 3 Objective 2 (S3-O2) states: *"S3-O2 – Assess the compatibility of PROTOTYPES D with current fertiliser slurry delivery systems, and assess if additives are required, or if the additional conversion to a "dry" delivery type (e.g. granules, pellets) is an economically advantageous option. The resulting recommended lignite-based controlled-release fertilisers are the FINAL PROTOTYPES."* After measuring the viscosities of the potential lignite - nutrient slurries, it is important to compare the viscosities to the requirements of slurry delivery systems. Slurry application is limited by the ability of delivery systems to pump slurries through the system, which means low viscosities are preferred. This conflicts with the expected characteristics of the optimised lignite-based controlled-release fertilisers. The viscosity of PROTOTYPES D will likely be high due

to the choice of high solids loading (to increase nutrient density) and the addition of nutrient species. The addition of environmentally friendly dispersants or other additives may provide a solution. Another option is the development of specialised robots in precision agriculture that can be tailored to delivering lignite – nutrient slurries with high viscosities. However, if a dry lignite type is preferred at S2-O2, granulation or pellet pressing could be options that need to be assessed on their economic viability. The lignite-based controlled-release fertilisers resulting from the compatibility assessments are the FINAL PROTOTYPES.

5.2 Further research outside the scope of the feasibility framework

After the FINAL PROTOTYPES have been developed, the nutrient release rate in soil and the effect on plant growth needs to be examined using lysimeter and field trials. This is outside the scope of the framework but is nonetheless crucial as it will further narrow down the number of prototypes and inform the desired application rate. Any possible effects of residual swelling solvent on plant health and the environment should be investigated in experiments following the feasibility framework. Another issue that will require careful examination is the possibility of fine (< 10 µm) coal dust particles to become airborne when the soil dries in periods of drought. Incorporating certain additives to the dry or wet lignite-based controlled-release fertilisers might provide a resolve.

Biochar used in agriculture causes issues when it washes off into waterways. If lignite is prone to undergo the same fate will need to be investigated, as well as potential issues arising from the relatively high sulphur and aluminium content found in some lignites, and the potential of CO_2 emissions originating from the land-application of a fossil fuel.

It will also need to be investigated if the variability of lignite within quarries is enough to cause issues with the development of a set of property manipulations for one type of lignite. If a high variability cannot be countered by mixing and homogenising lignite from one quarry, it might affect the economic sustainability of lignite-based controlled-release fertilisers and their development.

LIST OF PUBLICATIONS

- Presentation on the rheology of coal slurries at the ***Australasian Particle Technology Student Conference 2018***, 29th September, Queenstown, New Zealand.

- Poster on the rheology of coal slurries at ***CHEMECA 2018***, 1st – 3rd October, Queenstown, New Zealand.

- Patent application for a lignite-based controlled-release fertiliser in progress.

BIBLIOGRAPHY

ACARP. 1998. *The Hardgrove grindebility index*. Sydney, Australia: Australian Coal Association Research Program. Available: https://www.acarp.com.au/Media/ACARP-WP-5-HardgroveGrindabilityIndex.pdf.

Accoe, F., Boeckx, P., Busschaert, J., Van Cleemput, O. & Hofman, G. 2004. Gross N transformation rates and net N mineralisation rates related to the C and N contents of soil organic matter fractions in grassland soils of different age. *Soil Biology and Biochemistry,* 36**,** 2075-2087. Available: 10.1016/j.soilbio.2004.06.006

Adey, W. H. & Loveland, K. 2007. Chapter 6 - The Input of Organic Energy: Particulates and Feeding. *In:* Adey, W. H. & Loveland, K. (eds.) *Dynamic Aquaria (Third Edition).* London: Academic Press. Available: https://doi.org/10.1016/B978-0-12-370641-6.50015-7

Adhikari, K. P., Saggar, S., Hanly, J. A., Guinto, D. F. & Taylor, M. D. 2018. Why copper and zinc are ineffective in reducing soil urease activity in New Zealand dairy-grazed pasture soils. *Soil Research,* 56**,** 491-502. Available: 10.1071/SR17278

Aharoni, C. & Ungarish, M. 1976. Kinetics of activated chemisorption. Part 1.—The non-elovichian part of the isotherm. *Journal of the Chemical Society, Faraday Transactions 1: Physical Chemistry in Condensed Phases,* 72**,** 400-408.

Aida, T. & Squires, T. G. 1985. Solvent swelling of coal 1 - Develepment of an improved method for measuring swelling phenomena. *189th National meeting of the American Chemical Society.* Miami, USA.

Allardice, D. J. 1991. Chapter 3: The Water in Brown Coal. *In:* Durie, R. A. (ed.) *The Science of Victorian Brown Coal: Structure, Properties and Consequences for Utilisation.* Oxford: Butterworth-Heinemann.

Arslan, G., Cetin, S. & Pehlivan, E. 2007. Removal of Cu(II) and Ni(II) from aqueous solution by lignite-based humic acids. *Energy Sources, Part A: Recovery, Utilization, and Environmental Effects,* 29**,** 619-630. Available: 10.1080/009083190957711

Bahrani, S. A., Nouar, C., Neveu, A. & Becker, S. 2015. Transition to chaotic Taylor-Couette flow in shear-thinning fluids. *22ème Congrès Français de Mécanique.* Lyon, France.

Bai, Z., Ma, L., Jin, S., Ma, W., Velthof, G. L., Oenema, O., Liu, L., Chadwick, D. & Zhang, F. 2016. Nitrogen, Phosphorus, and Potassium Flows through the Manure Management Chain in China. *Environmental Science & Technology,* 50**,** 13409-13418. Available: 10.1021/acs.est.6b03348

Ballice, L. 2004. Solvent swelling studies of Soma lignite (Turkey). *Oil Shale,* 21**,** 115-123.

Barceló, J. & Poschenrieder, C. 2002. Fast root growth responses, root exudates, and internal detoxification as clues to the mechanisms of aluminium toxicity and resistance: A review. *Environmental and Experimental Botany,* 48**,** 75-92. Available: 10.1016/S0098-8472(02)00013-8

Barton, A. F. M. 1975. Solubility parameters. *Chemical Reviews,* 75**,** 731-753.

Begeman, S. 2018. *Seeds and Crop Production* [Online]. Farm Journal. Available: https://www.agweb.com/article/inputs-forecast-fertilizer-prices-increase-for-first-time-in-years/ [Accessed 21 May 2019 2019].

Bellarby, J., Surridge, B. W. J., Haygarth, P. M., Liu, K., Siciliano, G., Smith, L., Rahn, C. & Meng, F. 2018. The stocks and flows of nitrogen, phosphorus and potassium across a 30-year time series for agriculture in Huantai county, China. *Science of the Total Environment,* 619**,** 606-620. Available: 10.1016/j.scitotenv.2017.10.335

Berkowitz, N., Schein, H., G. 1951. Heats of wetting and spontaneous ignition of coal. *Fuel,* 30**,** 94-96.

Bilski, J., McLean, K., Soumaila, F., McLean, E. & Kraft, C. 2014. Aluminium in coal fly ash (FA), in plants grown on FA, and in the leachates from FA. *Research Journal of Chemical and Environmental Sciences*, 2(4), 22-26.

Bonhomme, S., Cuer, A., Delort, A.-M., Lemaire, J., Sancelme, M. & Scott, G. 2003. Environmental biodegradation of polyethylene. *Polymer Degradation and Stability,* 81**,** 441-452. Available: 10.1016/S0141-3910(03)00129-0

Bosatta, E. & Ågren, G. I. 1995. Theoretical analyses of interactions between inorganic nitrogen and soil organic matter. *European Journal of Soil Science,* 46**,** 109-114. Available: 10.1111/j.1365-2389.1995.tb01817.x

Braga, D., Grepioni, F. & Shemchuk, O. 2018. Organic–inorganic ionic co-crystals: a new class of multipurpose compounds. *CrystEngComm,* 20**,** 2212-2220. Available: 10.1039/C8CE00304A

Brannon, C. A. & Sommers, L. E. 1985. Stability and mineralization of organic phosphorus incorporated into model humic polymers. *Soil Biology and Biochemistry,* 17**,** 221-227. Available: 10.1016/0038-0717(85)90118-X

Brase, T. A. 2006. *Precision agriculture,* New York, USA, Thomson Delmar Learning.

Brunauer, S., Emmett, P. H. & Teller, E. 1938. Adsorption of Gases in Multimolecular Layers. *Journal of the American Chemical Society,* 60**,** 309-319. Available: 10.1021/ja01269a023

Bull, H. B., Breese, K., Ferguson, G. L. & Swenson, C. A. 1964. The pH of urea solutions. *Archives of Biochemistry and Biophysics,* 104**,** 297-304.

Bull, H. B., Breese, K., Ferguson, G. L., Swenson, C. A. 1964. The pH of Urea Solutions. *Archives of Biochemistry and Biophysics,* 104**,** 297-304.

Buranasrisak, P. & Narasingha, M. H. 2012. Effects of particle size distribution and packing characteristics on the preparation of highly-loaded coal-water slurry. *International Journal of Chemical Engineering and Applications,* 3**,** 31-35.

Burdick, E. M. 1965. Commercial humates for agriculture and the fertilizer industry. *Economic Botany,* 19**,** 152-156.

Cameron, K. C., Di, H. J. & Moir, J. L. 2013. Nitrogen losses from the soil/plant system: a review. *Annals of Applied Biology,* 162**,** 145-173. Available: 10.1111/aab.12014

Camier, R. J. 1977. *Brown coal structure.*, University of Melbourne.

Campbell, R. M., Anderson, N. M., Daugaard, D. E. & Naughton, H. T. 2018. Financial viability of biofuel and biochar production from forest biomass in the face of market price volatility and uncertainty. *Applied Energy,* 230**,** 330-343. Available: https://doi.org/10.1016/j.apenergy.2018.08.085

Canellas, L. P., Olivares, F. L., Aguiar, N. O., Jones, D. L., Nebbioso, A., Mazzei, P. & Piccolo, A. 2015. Humic and fulvic acids as biostimulants in horticulture. *Scientia Horticulturae,* 196**,** 15-27. Available: https://doi.org/10.1016/j.scienta.2015.09.013

Cantarella, H., Otto, R., Soares, J. R. & de Brito Silva, A. G. 2018. Agronomic efficiency of NBPT as a urease inhibitor: A review.

Cayuela, M. L., van Zwieten, L., Singh, B. P., Jeffery, S., Roig, A. & Sánchez-Monedero, M. A. 2014. Biochar's role in mitigating soil nitrous oxide emissions: A review and meta-analysis. *Agriculture, Ecosystems & Environment,* 191**,** 5-16. Available: 10.1016/j.agee.2013.10.009

Cepus, V., Borth, M., Seitz, M. 2016. IR spectroscopic characterization of lignite as a tool to predict the product range of catalytic decomposition. *International Journal of Clean Coal and Energy,* 5**,** 13-22.

Cerofolini, G., Jaroniec, M. & Sokołosvski, S. 1978. A theoretical isotherm for adsorption on heterogeneous surface. *Colloid & Polymer Science,* 256**,** 471-477.

Chassapis, K., Roulia, M., Vrettou, E., Fili, D. & Zervaki, M. 2010. Biofunctional Characteristics of Lignite Fly Ash Modified by Humates: A New Soil Conditioner. *Bioinorganic Chemistry and Applications*. Available: 10.1155/2010/457964

Chen, D., Suter, H., Islam, A., Edis, R., Freney, J. R. & Walker, C. N. 2008. Prospects of improving efficiency of fertiliser nitrogen in Australian agriculture: a review of enhanced efficiency fertilisers. *Soil Research,* 46**,** 289-301.

Chen, J., Lü, S., Zhang, Z., Zhao, X., Li, X., Ning, P. & Liu, M. 2018. Environmentally friendly fertilizers: A review of materials used and their effects on the environment. *Science of the Total Environment,* 613-614**,** 829-839. Available: 10.1016/j.scitotenv.2017.09.186

Chen, S., Yan, Z. & Chen, Q. 2017. Estimating the potential to reduce potassium surplus in intensive vegetable fields of China. *Nutr. Cycl. Agroecosyst.,* 107**,** 265-277. Available: 10.1007/s10705-017-9835-0

Chen, Y. & Stevenson, F. J. 1986. Chapter 5: Soil organic matter interactions with trace elements. *In:* Chen, Y. & Avnimelech, Y. (eds.) *The Role of Organic Matter in Modern Agriculture.* Dordrecht: Martinus Nijhoff Publishers.

Childers, D. L., Corman, J., Edwards, M. & Elser, J. J. 2011. Sustainability challenges of phosphorus and food: Solutions from closing the human phosphorus cycle. *BioScience,* 61**,** 117-124. Available: 10.1525/bio.2011.61.2.6

Cody Jr, G. D., Larsen, J. W. & Siskin, M. 1988. Anisotropic solvent swelling of coals. *Energy & fuels,* 2**,** 340-344.

Dai, J.-j., Fan, X.-l., Yu, J.-g., Liu, F. & Zhang, Q. 2008. Study on the rapid method to predict longevity of controlled release fertilizer coated by water soluble resin. *Agricultural Sciences in China,* 7**,** 1127-1132. Available: https://doi.org/10.1016/S1671-2927(08)60155-8

Dampc, M., Milosavljević, A. R., Linert, I., Marinković, B. P. & Zubek, M. 2007. Differential cross sections for low-energy elastic electron scattering from tetrahydrofuran in the angular range 20°–180°. *Physical Review* 75**,** 042710.

Davidson, D. & Gu, F. X. 2012. Materials for Sustained and Controlled Release of Nutrients and Molecules To Support Plant Growth. *Journal of Agricultural and Food Chemistry,* 60**,** 870-876. Available: 10.1021/jf204092h

de Melo, B. A. G., Motta, F. L. & Santana, M. H. A. 2016. Humic acids: Structural properties and multiple functionalities for novel technological developments. *Materials Science and Engineering: C,* 62**,** 967-974. Available: https://doi.org/10.1016/j.msec.2015.12.001

Dean, S. L., Farrer, E. C., Taylor, D. L., Porras-Alfaro, A., Suding, K. N. & Sinsabaugh, R. L. 2014. Nitrogen deposition alters plant–fungal relationships: linking belowground dynamics to aboveground vegetation change. *Molecular Ecology,* 23**,** 1364-1378. Available: 10.1111/mec.12541

Debska, B., Maciejewska, A. & Kwiatkowska, J. 2002. The effect of fertilization with brown coal on Haplic Luvisol humic acids. *Rostlinna Vyroba,* 48**,** 33-39.

Denne, T. 2014. Coal Prices in New Zealand Markets: 2013 Update. MBIE. https://www.mbie.govt.nz/assets/9b10f9b98c/coal-prices-in-new-zealand-markets-2013.pdf [Accessed: 10 March 2020]

Dodds, W. K., Bouska, W. W., Eitzmann, J. L., Pilger, T. J., Pitts, K. L., Riley, A. J., Schloesser, J. T. & Thornbrugh, D. J. 2009. Eutrophication of U.S. freshwaters: Analysis of potential economic damages. *Environmental Science & Technology,* 43**,** 12-19. Available: 10.1021/es801217q

Dong, L., Córdova-Kreylos, A. L., Yang, J., Yuan, H. & Scow, K. M. 2009. Humic acids buffer the effects of urea on soil ammonia oxidizers and potential nitrification. *Soil Biology and Biochemistry,* 41**,** 1612-1621. Available: 10.1016/j.soilbio.2009.04.023

Doskočil, L. & Pekař, M. 2012. Removal of metal ions from multi-component mixture using natural lignite. *Fuel Processing Technology,* 101**,** 29-34. Available: 10.1016/j.fuproc.2012.02.010

Drury, C., Tan, C., Gaynor, J., Oloya, T. & Welacky, T. 1996. Influence of Controlled Drainage-Subirrigation on Surface and Tile Drainage Nitrate Loss. *Journal of Environmental Quality,* 25**,** 317-324. Available: 10.2134/jeq1996.00472425002500020016x

Durie, R. A. 1991. *The Science of Victorian Brown Coal: Structure, Properties and Consequences for Utilisation.,* Oxford, Butterworth-Heinemann.

Eastman, M., Gollamudi, A., Stämpfli, N., Madramootoo, C. A. & Sarangi, A. 2010. Comparative evaluation of phosphorus losses from subsurface and naturally drained agricultural fields in the Pike River watershed of Quebec, Canada. *Agricultural Water Management,* 97**,** 596-604. Available: 10.1016/j.agwat.2009.11.010

Edmeades, D. C. 2004. *Nitrification and Urease Inhibitors – A Review of the National and International Literature on their Effects on Nitrate Leaching, Greenhouse Gas Emissions and Ammonia Volatilisation from Temperate Legume-Based Pastoral Systems. Environment Waikato Technical Report 2004/22.*

Eisele, T. C., Walqui, H.J. & Kawatra, S. K. 2013. Chapter 9: Coal comminution and sizing. *In:* Osborne, D. (ed.) *The Coal Handbook.* Sawston, United Kingdom: Woodhead Publishing Limited.

Escudier, M. P., Gouldson, I. W. & Jones, D. M. 1995. Taylor Vortices in Newtonian and Shear-Thinning Liquids. *Proceedings: Mathematical and Physical Sciences,* 449**,** 155-176.

Eslamian, F., Qi, Z., Tate, M. J., Zhang, T. & Prasher, S. O. 2018. Phosphorus loss mitigation in leachate and surface runoff from clay loam soil using four lime-based materials. *Water Air Soil Pollut.,* 229. Available: 10.1007/s11270-018-3750-0

Fageria, N. K. & Baligar, V. C. 2005. Enhancing nitrogen use efficiancy in crop plants. *In:* Sparks, D. L. (ed.) *Advances in Agronomy.* Academic Press. Available: https://doi.org/10.1016/S0065-2113(05)88004-6

FDA. 2018. Food additive status list. [Online]. Available: https://www.fda.gov/food/food-additives-petitions/food-additive-status-list#ftnE [Accessed 20 Feb 2020].

Fisher, K. A. 2014. *Urea hydrolysis in soil profile topsequences: mechanisms relevant to nitrogen transport and water quality.* Doctor of Philosophy, University of Maryland.

Fowles, J., Boatman, R., Bootman, J., Lewis, C., Morgott, D., Rushton, E., van Rooij, J. & Banton, M. 2013. A review of the toxicological and environmental hazards and risks of tetrahydrofuran. *Critical Reviews in Toxicology,* 43**,** 811-828. Available: 10.3109/10408444.2013.836155

Freundlich, H. 1906. Über die Adsorption in Lösungen. *Zeitschrift für Physikalische Chemie,* 57U**,** 385-470. Available: 10.1515/zpch-1907-5723

Frimmel, F. H. & Abbt-Braun, G. 2018. Humic matter: basis for life-a plea for humics care. *Journal of Soils and Sediments,* 18**,** 2668-2674. Available: 10.1007/s11368-018-1915-5

Ganesapillai, M. & Simha, P. 2015. The rationale for alternative fertilization: Equilibrium isotherm, kinetics and mass transfer analysis for urea-nitrogen adsorption from cow urine. *Resource-efficient technologies,* 1**,** 90-97. Available: 10.1016/j.reffit.2015.11.001

Gerente, C., Lee, V. K. C., Le Cloirec, P. & McKay, G. 2007. Application of chitosan for the removal of metals from wastewaters by adsorption - Mechanisms and models review. *Critical Reviews in Environmental Science and Technology,* 37**,** 41-127. Available: 10.1080/10643380600729089

González, M. E., Cea, M., Medina, J., González, A., Diez, M. C., Cartes, P., Monreal, C. & Navia, R. 2015. Evaluation of biodegradable polymers as encapsulating agents for the development of a urea controlled-release fertilizer using biochar as support material. *Science of the Total Environment,* 505**,** 446-453. Available: 10.1016/j.scitotenv.2014.10.014

Goudoulas, T. B., Kastrinakis, E. G. & Nychas, S. G. 2010. Preparation and rheological characterization of lignite-water slurries. *Energy Fuels,* 24**,** 496-502. Available: 10.1021/ef900865m

Goulding, K., Jarvis, S. & Whitmore, A. 2008. Optimizing nutrient management for farm systems. *Philosophical Transactions Of The Royal Society Of London. Series B, Biological Sciences,* 363**,** 667-680.

Gray, C. W. 2018. Fluorine in soils under pasture following long-term application of phosphate fertiliser in New Zealand. *Geoderma Regional,* 14. Available: 10.1016/j.geodrs.2018.e00183

Greb, S. 2019. Image Coal_vertical_high. https://www.uky.edu/KGS/coal/coal-diagram-download.php: Kentucky Geological Survey, University of Kentucky, Kentucky, USA.

Green, T. K., Kovac, J. & Larsen, J. W. 1984. A rapid and convenient method for measuring the swelling of coals by solvents. *Fuel,* 63**,** 935-938.

Gupta, V. K., Mohan, D. & Sharma, S. 1998. Removal of lead from wastewater using bagasse fly ash - a sugar industry waste material. *Separation Science and Technology,* 33**,** 1331-1343. Available: 10.1080/01496399808544986

Gupta, V. K. & Sharma, S. 2003. Removal of Zinc from Aqueous Solutions Using Bagasse Fly Ash − a Low Cost Adsorbent. *Industrial & Engineering Chemistry Research,* 42**,** 6619-6624. Available: 10.1021/ie0303146

Hacimehmetoğlu, Ş., Sınag, A., Tekes, A., Misirlioğlu, Z. & Canel, M. 2007. Effect of Various Experimental Parameters on the Swelling and Supercritical Extraction Properties of Lignite. *Energy Sources,* Part A**,** 607-618. Available: 10.1080/00908310500276908

Halsey, G. D. 1951. A new multilayer isotherm equation with reference to surface area. *Journal of the American Chemical Society,* 73**,** 2693-2696. Available: 10.1021/ja01150a076

Haneklaus, S. & Schnug, E. 2006. Chapter 4 - Site-Specific Nutrient Management: Objectives, Current Status, and Future Research Needs. *In:* Srinivasan, A. (ed.) *Handbook of Precision Agriculture.* New York, USA: The Haworth Press, Inc. Available: 10.1300/5627_04

Hansen, C. M. 2007. Chapter 1 - Solubility Parameters - An Introduction. *In:* Hansen, C. M. (ed.) *Hansen Solubility Parameters: A Users Handbook.* Boca Raton, U.S.A: CRC Press.

Hansen, C. M. & Poulsen, T. S. 2007. Chapter 15 - Hansen Solubility Parameters - Biological Materials. *In:* Hansen, C. M. (ed.) *Hansen Solubility Parameters: A Users Handbook.* Boca Raton, U.S.A: CRC Press.

Hardgrove, W. L. & Thomas, G. W. 1982. Conditional formation constants for aluminium-organic matter complexes. *Can. J. Soil Sci.,* 62**,** 571-575.

Harmaen, A., Abdan, K., Hassan, M., Azowa, N., Lee, S. H., Faizal, M. & Rahman, A. 2018. Properties of slow release fertilizer composites made from electron beam-irradiated poly(butylene succinate) compounded with oil palm biomass and fertilizer. *Bioresouces*, 13(4), 8677-8689. Available: 10.15376/biores.13.4.8677-8689

Harmaen, A., Abdan, K., Hassan, M. & Ibrahim, N. 2016. Thermal, morphological, and biodegradability properties of bioplastic fertilizer composites made of oil palm biomass, fertilizer, and poly(hydroxybutyrate-co-valerate). *International Journal of Polymer Science*. Available: 10.1155/2016/3230109

Harvey, G. R., Boran, D. A., Chesal, L. A. & Tokar, J. M. 1983. The structure of marine fulvic and humic acids. *Marine Chemistry,* 12**,** 119-132. Available: 10.1016/0304-4203(83)90075-0

Hautier, Y., Niklaus, P. A. & Hector, A. 2009. Competition for light causes plant biodiversity loss after eutrophication. *Science,* 324**,** 636-638. Available: 10.1126/science.1169640

Ho, Y.-S. 2006. Review of second-order models for adsorption systems. *Journal of Hazardous Materials,* 136**,** 681-689. Available: 10.1016/j.jhazmat.2005.12.043

Ho, Y.-S. & McKay, G. 1999. Pseudo-second order model for sorption processes. *Process Biochemistry,* 34**,** 451-465

Honer, K., Kalfaoglu, E., Pico, C., McCann, J. & Baltrusaitis, J. 2017. Mechanosynthesis of magnesium and calcium salt urea ionic cocrystal fertilizer materials for improved nitrogen management. *ACS Sustainable Chem. Eng.,* 5**,** 8546-8550. Available: 10.1021/acssuschemeng.7b02621

Honer, K., Pico, C. & Baltrusaitis, J. 2018. Reactive Mechanosynthesis of Urea Ionic Cocrystal Fertilizer Materials from Abundant Low Solubility Magnesium- and Calcium-Containing Minerals. *ACS Sustainable Chem. Eng.,* 6**,** 4680-4687. Available: 10.1021/acssuschemeng.7b03766

Houghton, J. T., Jenkins, G. J. & Ephraums, J. J. (eds.) 1990. *Climate Change: The IPCC Scientific Assessment.,* New York: Cambridge Univ. Press.

House, K. A. & House, J. E. 2017. Thermodynamics of dissolution of urea in water, alcohols, and their mixtures. *Journal of Molecular Liquids,* 242**,** 428-432. Available: https://doi.org/10.1016/j.molliq.2017.07.020

Huang, L., Mao, X., Chen, X., Sun, X., Wang, J. & Liao, Z. 2013. Phosphorus availability and fertilizer efficiency of rock phosphate as affected by ultrafine activation. *Acta Pedologica Sinica,* 50**,** 769-777.

Huculak-Mączka, M., Hoffmann, J. & Hoffmann, K. 2018. Evaluation of the possibilities of using humic acids obtained from lignite in the production of commercial fertilizers. *Journal of Soils and Sediments,* 18**,** 2868-2880. Available: 10.1007/s11368-017-1907-x

IPCS. 1996. *International Programme on Chemical Safety, Chapter 1 - Summary, Environmental Health Criteria 196: Methanol*. Geneva, Switserland: World Health Organization. Available: http://www.intox.org/databank/documents/chemical/methanol/ehc196.htm.

Jackson, L. E., Burger, M. & Cavagnaro, T. R. 2008. Roots, Nitrogen Transformations, and Ecosystem Services. *Annual Review of Plant Biology,* 59**,** 341-363. Available: 10.1146/annurev.arplant.59.032607.092932

Jha, S. K., Nayak, A. K. & Sharma, Y. K. 2008. Response of spinach (Spinacea oleracea) to the added fluoride in an alkaline soil. *Food and Chemical Toxicology,* 46**,** 2968-2971. Available: 10.1016/j.fct.2008.05.024

Jha, S. K., Nayak, A. K. & Sharma, Y. K. 2009. Fluoride toxicity effects in onion (Allium cepa L.) grown in contaminated soils. *Chemosphere,* 76**,** 353-356. Available: 10.1016/j.chemosphere.2009.03.044

Johns, R. B., Chaffee, A. L., Harvey, K. F., Buchanan, A. S. & Thiele, G. A. 1989. The conversion of brown coal to a dense, dry, hard material. *Fuel Processing Technology,* 21**,** 209-221. Available: https://doi.org/10.1016/0378-3820(89)90050-7

Jones, C. 2016a. Chapter 1: The Nature of Lignites. *Lignites Their Occurrence Production and Utilisation.* Dunbeath, Scotland, UK: Whittles Publishing.

Jones, C. 2016b. Chapter 1: The Nature of Lignites. *In:* Jones, C. (ed.) *Lignites: Their occurrence, production and utilisation.* Dunbeath, Scotland, UK: Whittles Publishing.

Jones, C. 2016c. Chapter 17: Hazards with lignites. *In:* Jones, C. (ed.) *Lignites Their Occurrence Production and Utilisation.* Dunbeath, Scotland, UK: Whittles Publishing.

Jones, J. C., Boother, M. & Brown, M. 1991. On the solvent-induced swelling of low-rank coals. *Journal of Chemical Technology & Biotechnology,* 52**,** 257-264. Available: 10.1002/jctb.280520212

Jones, J. C., Hewitt, R. G. & Innes, R. A. 1997. Swelling of a German brown coal in acetone-water and methanol-water mixtures. *Fuel,* 76**,** 575-577. Available: 10.1016/S0016-2361(97)00066-5

Jones, J. C. & Prawitasari, B. 1995. Pore entry effects in the solvent-induced swelling of low-rank coals. *Journal of Chemical Technology & Biotechnology,* 64**,** 210-212. Available: 10.1002/jctb.280640216

Kafarski, P. & Talma, M. 2018. Recent advances in design of new urease inhibitors: A review. *Journal of Advanced Research,* 13**,** 101-112. Available: 10.1016/j.jare.2018.01.007

Kameda, T., Ito, S. & Yoshioka, T. 2017. Kinetic and equilibrium studies of urea adsorption onto activated carbon: Adsorption mechanism. *Journal of Dispersion Science and Technology,* 38**,** 1063-1066. Available: 10.1080/01932691.2016.1219953

Kelliher, F. M., Gray, C. W. & Noble, A. D. L. 2017. Superphosphate fertiliser application and cadmium accumulation in a pastoral soil. *New Zealand Journal of Agricultural Research,* 60**,** 404-422. Available: 10.1080/00288233.2017.1363058

Khan, M. A., Ahn, Y.-T., Kumar, M., Lee, W., Min, B., Kim, G., Cho, D.-W., Park, W. B. & Jeon, B.-H. 2011. Adsorption studies for the removal of nitrate using modified lignite granular activated carbon. *Separation Science & Technology,* 46**,** 2575-2584. Available: 10.1080/01496395.2011.601782

Khorshidi, M., Lu, N., Akin Idil, D. & Likos William, J. 2017. Intrinsic relationship between specific surface area and soil water retention. *Journal of Geotechnical and Geoenvironmental Engineering,* 143**,** 04016078. Available: 10.1061/(ASCE)GT.1943-5606.0001572.

Kipton, H., Powell, J. & Town, R. M. 1992. Solubility and fractionation of humic acid; effect of pH and ionic medium. *Analytica Chimica Acta,* 267**,** 47-54. Available: https://doi.org/10.1016/0003-2670(92)85005-Q

Kiss, L. T., Brockway, D. J., George, A. M. & Stacy, W. O. 1984. *Properties of brown coals from the Rosedale, Stradbroke and Gormandale Fields. SECV Research and Development Department Report No. SC/84/85.*: SECV.

Klironomos, J., Zobel, M., Tibbett, M., Stock, W., D., Rillig, M., C., Parrent, J., L., Moora, M., Koch, A., M., Facelli, J., M., Evelina, F., Dickie, I., A. & James, D. B. 2011. Forces that structure plant communities: quantifying the importance of the mycorrhizal symbiosis. *The New Phytologist,* 189**,** 366-370.

Kloth, B. 1996. *RE: Aglukon Spezialdünger GmbH: Reply to the request on controlled-release fertilizers. Personal communication.*

Krajewska, B. 2009. Ureases I. Functional, catalytic and kinetic properties: A review. *Journal of Molecular Catalysis. B, Enzymatic,* 59**,** 9-21. Available: 10.1016/j.molcatb.2009.01.003

Kruse, R. H., Green, T. D., Chambers, R. C. & Jones, M. W. 1963. Disinfection of Aerosolized Pathogenic Fungi on Laboratory Surfaces. I. Tissue Phase. *Applied microbiology,* 11**,** 436-445.

Kulkarni, K., Bhogale, G. M. & Nalawade, R. 2018. Adsorptive removal of fluoride from water samples using Azospirillum biofertilizer and lignite. 35**,** 153-163. Available: 10.1007/s11814-017-0254-3

Kusumastuti, Y., Istiani, A., Rochmadi & Purnomo, C. W. 2019. Chitosan-based polyion multilayer coating on NPK fertilizer as controlled released fertilizer. *Advances in Materials Science & Engineering***,** 1-8. Available: 10.1155/2019/2958021

Kwiatkowska, J., Provenzano, M. R. & Senesi, N. 2008. Long term effects of a brown coal-based amendment on the properties of soil humic acids. *Geoderma,* 148**,** 200-205. Available: 10.1016/j.geoderma.2008.10.001

Langmuir, I. 1918. The adsorption of gases on plane surfaces of glass, mica and platinum. *Journal of the American Chemical Society,* 40**,** 1361-1403. Available: 10.1021/ja02242a004

Larrubia, M. A., Ramis, G. & Busca, G. 2000. An FT-IR study of the adsorption of urea and ammonia over V2O5-MoO3-TiO2 SCR catalysts. *Applied Catalysis B: Environmental,* 27**,** L145-L151. Available: 10.1016/S0926-3373(00)00150-8

Larsen, J. W. & Shawver, S. 1990. Solvent Swelling Studies of Two Low-Rank Coals. *Energy and Fuels,* 4**,** 74-77. Available: 10.1021/ef00019a013

Lee, F.-M. & Lahti, L. E. 1972. Solubility of urea in water-alcohol mixtures. *Journal of Chemical & Engineering Data,* 17**,** 304-306. Available: 10.1021/je60054a020

Lehmann, J., Gaunt, J. & Rondon, M. 2006. Bio-char sequestration in terrestrial ecosystems - A review. *Mitigation & Adaptation Strategies for Global Change,* 11**,** 403-427. Available: 10.1007/s11027-005-9006-5

Lehmann, J. & Kleber, M. 2015. The contentious nature of soil organic matter. Nature, 528(7580), 60-68.

Li, C. Z. 2004. *Advances in the Science of Victorian Brown Coal,* Amsterdam, The Netherlands, Elsevier.

Li, Y., Jia, C., Zhang, X., Jiang, Y., Zhang, M., Lu, P. & Chen, H. 2018. Synthesis and performance of bio-based epoxy coated urea as controlled release fertilizer. *Progress in Organic Coatings,* 119**,** 50-56. Available: 10.1016/j.porgcoat.2018.02.013

Liang, R., Yuan, H., Xi, G. & Zhou, Q. 2009. Synthesis of wheat straw-g-poly(acrylic acid) superabsorbent composites and release of urea from it. *Carbohydrate Polymers,* 77**,** 181-187. Available: 10.1016/j.carbpol.2008.12.018

Ling Ong, H. & Swanson, V. E. 1966. Adsorption of copper by peat, lignite, and bituminous coal. *Economic Geology,* 61**,** 1214-1231.

Liu, X., Liao, J., Song, H., Yang, Y., Guan, C. & Zhang, Z. 2019. A biochar-based route for environmentally friendly controlled release of nitrogen: Urea-loaded biochar and bentonite composite. *Scientific Reports,* 9. Available: 10.1038/s41598-019-46065-3

Liu, X., Yang, Y., Gao, B., Li, Y. & Wan, Y. 2017. Environmentally Friendly Slow-Release Urea Fertilizers Based on Waste Frying Oil for Sustained Nutrient Release. *ACS Sustainable Chem. Eng.,* 5**,** 6036-6045. Available: 10.1021/acssuschemeng.7b00882

Loeser, E., DelaCruz, M. & Madappalli, V. 2011. Solubility of Urea in Acetonitrile–Water Mixtures and Liquid–Liquid Phase Separation of Urea-Saturated Acetonitrile–Water Mixtures. *Journal of Chemical & Engineering Data,* 56**,** 2909-2913. Available: 10.1021/je200122b

Lu, L., Sahajwalla, V., Kong, C. & Harris, D. 2001. Quantitative X-ray diffraction analysis and its application to various coals. *Carbon,* 39**,** 1821-1833. Available: https://doi.org/10.1016/S0008-6223(00)00318-3

Majeed, Z., Ramli, N. K., Mansor, N. & Man, Z. 2015. A comprehensive review on biodegradable polymers and their blends used in controlled- release fertilizer processes. R*eviews in Chemical Engineering,* 31**,** 69-95.

Makitra, R. G. & Bryk, D. V. 2008. Swelling of lignites in organic solvents. *Solid Fuel Chemistry,* 42**,** 278-283. Available: 10.3103/S0361521908050042

Makitra, R. G., Midyana, G. G. & Pal'chikova, E. Y. 2013. Effect of the properties of solvents on the yields of extracts from coals. *Solid Fuel Chemistry,* 47**,** 202-205.

Malekian, R., Abedi-Koupai, J., Eslamian, S. S., Mousavi, S. F., Abbaspour, K. C. & Afyuni, M. 2011. Ion-exchange process for ammonium removal and release using natural Iranian zeolite. *Applied Clay Science,* 51**,** 323-329. Available: 10.1016/j.clay.2010.12.020

Malvern-Instruments 2013. Chapter 5 - Viewing measurement results, page 12. Mastersizer 3000 User Manual, MAN0475 Issue 2.1. Malvern Instruments Ltd. Worcestershire, United Kingdom.

MBIE. 2015. Energy in New Zealand. Available: https://www.mbie.govt.nz/assets/1c22f85721/energy-in-new-zealand-2015.pdf [Accessed 10 March 2020].

McLaughlin, D. & Kinzelbach, W. 2015. Food security and sustainable resource management. *Water Resources Research,* 51**,** 4966-4985. Available: 10.1002/2015wr017053

Meier, D. & Faix, O. 1999. State of the art of applied fast pyrolysis of lignocellulosic materials - A review. *Bioresource Technology,* 68**,** 71-77. Available: 10.1016/S0960-8524(98)00086-8

Meshram, P., Purohit, B.K., Sinha, M.K., Sahu, S.K. & Pandey, B.D., 2015. Demineralization of low grade coal–A review. *Renewable and Sustainable Energy Reviews*, *41*, pp.745-761.

Mikkelsen, R. L. 1994. Using hydrophilic polymers to control nutrient release. *Fert Res.,* 38**,** 53–59.

Miroshnichenko, D. V., Desna, N. A., Koval, V. V. & Fatenko, S. V. 2019. Hardgrove grindability of coal. Part 1- Correlations with composition, structure, and properties. *Coke and Chemistry,* 62**,** 1-4. Available: 10.3103/s1068364x19010058

Misselbrook, T. H., Smith, K. A., Johnson, R. A. & Pain, B. F. 2002. SE—Structures and environment: Slurry application techniques to reduce ammonia emissions: Results of some UK field-scale experiments. *Biosystems Engineering,* 81**,** 313-321. Available: 10.1006/bioe.2001.0017

Modolo, L. V., da-Silva, C. J., Brandao, D. S. & Chaves, I. S. 2018. A minireview on what we have learned about urease inhibitors of agricultural interest since mid-2000s. *Journal of Advanced Research,* 13**,** 29-37. Available: 10.1016/j.jare.2018.04.001

Monoharan, V. T. 1997. *Impacts of phosphate fertiliser application on soil acidity and aluminium phytotoxicity.* Doctor of Philosophy Soil Sciences, Massey University.

Moraes, L. E., Burgos, S. A., DePeters, E. J., Zhang, R. & Fadel, J. G. 2017. Short communication: Urea hydrolysis in dairy cattle manure under different temperature, urea, and pH conditions. *Journal of Dairy Science,* 100**,** 2388-2394. Available: https://doi.org/10.3168/jds.2016-11927

Morgan, C. G., Allen, M., Liang, M. C., Shia, R. L., Blake, G. A. & Yung, Y. L. 2004. Isotopic fractionation of nitrous oxide in the stratosphere: Comparison between model and observations. *Journal of Geophysical Research D: Atmospheres,* 109**,** D04305 1-22.

Mulcahy, M. F. R., Morley, W. J. & Smith, I. W. 1991. Chapter 8: Combustion, gasification and oxidation. *In:* Durie, R. A. (ed.) *The Science of Victorian Brown Coal.* Oxford: Butterworth- Heinemann.

Nardi, P., Neri, U., Di Matteo, G., Trinchera, A., Napoli, R., Farina, R., Subbarao, G. V. & Benedetti, A. 2018. Nitrogen release from slow-release fertilizers in soils with different microbial activities. *Pedosphere,* 28**,** 332-340. Available: 10.1016/S1002-0160(17)60429-6

Nazari, M. A., Pramanik, B. K., Othman, M., Bhuiyan, M. A., Mohaddes, F. & Muster, T. 2018. Application of Victorian brown coal for removal of ammonium and organics from

wastewater. *Environmental Technology,* 39**,** 1041-1051. Available: 10.1080/09593330.2017.1319424

Ndegwa, A. W., Wong, R. C. K., Chu, A., Bentley, L. R. & Lunn, S. R. D. 2004. Degradation of monoethanolamine in soil. *Journal of Environmental Engineering & Science,* 3**,** 137-145. Available: 10.1139/S03-074

Nelson, J. R., Mahajant, O. P., Walker Jr., P. L. 1980. Measurement of swelling of coals in organic liquids: a new approach. *Fuel*, 59, 831-837.

Ni, X., Wu, Y., Wu, Z., Wu, L., Qiu, G. & Yu, L. 2013. A novel slow-release urea fertiliser: Physical and chemical analysis of its structure and study of its release mechanism. *Biosystems Engineering,* 115**,** 274-282. Available: 10.1016/j.biosystemseng.2013.04.001

NPI. 2018a. *Acetonitrile* [Online]. Autralian government - Department of agriculture, Water and the Environment. Available: http://www.npi.gov.au/resource/acetonitrile [Accessed 8 March 2020].

NPI. 2018b. *National Pollutant Inventory, Substances: Acetaldehyde - Overview* [Online]. Australian Government, Department of the Environment and Energy. Available: http://www.npi.gov.au/resource/acetaldehyde [Accessed 29 October 2019].

Ooi, C.-H., Cheah, W.-K., Sim, Y.-L., Pung, S.-Y. & Yeoh, F.-Y. 2017. Conversion and characterization of activated carbon fiber derived from palm empty fruit bunch waste and its kinetic study on urea adsorption. *Journal Of Environmental Management,* 197**,** 199-205. Available: 10.1016/j.jenvman.2017.03.083

Otake, Y. & Suuberg, E. M. 1997. Temperature dependence of solvent swelling and diffusion processes in coals. *Energy & fuels,* 11**,** 1155-1164.

Otake, Y. & Suuberg, E. M. 1998. Solvent swelling rates of low rank coals and implications regarding their structure. *Fuel,* 77, 901-904. Available: 10.1016/S0016-2361(97)00256-1

Pan, J., Zhang, Z., Li, M., Wu, Y. & Wang, K. 2019. Characteristics of multi-scale pore structure of coal and its influence on permeability. *Natural Gas Industry B,* 6**,** 357-365. Available: 10.1016/j.ngib.2019.01.012

Paramashivam, D., Clough, T. J., Carlton, A., Gough, K., Dickinson, N., Horswell, J., Sherlock, R. R., Clucas, L. & Robinson, B. H. 2016. The effect of lignite on nitrogen mobility in a low-fertility soil amended with biosolids and urea. *Science of the Total Environment,* 543**,** 601-608. Available: 10.1016/j.scitotenv.2015.11.075

Patel, D. & Witt, S., N. 2017. Ethanolamine and phosphatidylethanolamine: Partners in health and disease. *Oxidative Medicine and Cellular Longevity*. Available: https://doi.org/10.1155/2017/4829180

PCE. 2013. *Water quality in New Zealand: Land use and nutrient pollution*. Parliamentary commissioner for the environment. Available:

https://www.pce.parliament.nz/media/1275/pce-water-quality-land-use-web-amended.pdf.

Pearson, A. J., Gaw, S., Hermanspahn, N., Glover, C. N. & Anderson, C. W. N. 2019. Radium in New Zealand agricultural soils: Phosphate fertiliser inputs, soil activity concentrations and fractionation profiles. *Journal of Environmental Radioactivity,* 205-206**,** 119-126. Available: 10.1016/j.jenvrad.2019.05.010

Pehlivan, E. & Arslan, G. 2006. Comparison of adsorption capacity of young brown coals and humic acids prepared from different coal mines in Anatolia. *Journal of Hazardous Materials,* 138**,** 401-408. Available: https://doi.org/10.1016/j.jhazmat.2006.05.063

Pehlivan, E. & Arslan, G. 2007. Removal of metal ions using lignite in aqueous solution - Low cost biosorbents. *Fuel Processing Technology,* 88**,** 99-106. Available: 10.1016/j.fuproc.2006.09.004

Piccolo, A. 2002a. The supramolecular structure of humic substances: a novel understanding of humus chemistry and implications in soil science, Chapter 5. Supramolecular associations of self-assembling humic molecules. *Advances in Agronomy,* 75**,** 75-105.

Piccolo, A. 2002b. The supramolecular structure of humic substances: a novel understanding of humus chemistry and implications in soil science. *Advances in Agronomy,* 75**,** 57-134.

Pironon, J., Pelletier, M., De Donato, P. & Mosser-Ruck, R. 2003. Characterization of smectite and illite by FTIR spectroscopy of interlayer NH4+ cations. *Clay Minerals*, 38, 201–211.

Quast, K. B., Hall, S. F. & Readett, D. 1987. Studies on the properties of the lignite/water interface. *In Proceedings of the N.Z. Coal Research Conference R4.3.,* Wellington, New Zealand.

Quast, K. B., Hall, S. F. & Readett, D. 1988. The effect of moisture removal on the surface chemistry of Bowmans and Yallourn coals. *In: Proceedings of the Australian Coal Science Conference 3, A2:1.1-1.7.*, Adelaide, Australia.

Raun, W. R., Solie, J. B., Johnson, G. V., Stone, M. L., Mullen, R. W., Freeman, K. W., Thomason, W. E. & Lukina, E. V. 2002. Improving nitrogen use efficiency in cereal grain production with optical sensing and variable rate application. *Agronomy Journal,* 94**,** 815-820.

Redlich, O. & Peterson, D. L. 1959. A useful adsorption isotherm. *The Journal of Physical Chemistry,* 63**,** 1024-1024. Available: 10.1021/j150576a611

Rice-Evans, C., Miller, N. & Paganga, G. 1997. Antioxidant properties of phenolic compounds. *Trends in Plant Science,* 2**,** 152-159. Available: https://doi.org/10.1016/S1360-1385(97)01018-2

Rodgers, G. A. 1986. Nitrification inhibitors in agriculture. *Journal of Environmental Science & Health, Part A: Environmental Science & Engineering,* 21**,** 701-722.

Römer, W. & Schilling, G. 1986. Phosphorus requirements of the wheat plant in various stages of its life cycle. *Plant and Soil,* 91**,** 221-229. Available: 10.1007/BF02181789

Rose, M. T., Perkins, E. L., Saha, B. K., Jackson, W. R., Patti, A. F., Tang, E. C. W., Hapgood, K. P., Hoadley, A. F. A. & Cavagnaro, T. R. 2016. A slow release nitrogen fertiliser produced by simultaneous granulation and superheated steam drying of urea with brown coal. *Chemical and Biological Technologies in Agriculture,* 3. Available: 10.1186/s40538-016-0062-8

Ross, J. A., Bayer, C. L., Socha, R. P., Sochor, C. S., Fliermans, C. B., McKinsey, P. C., Millings, M. R., Phifer, M. A., Powell, K. R., Serkiz, S. M., Sappington, F. C. & Turick, C. E. 2003. Evaluation of natural and in-situ remediation technologies for a coal-related metals plume. *Waste Management (WM) '03 Conference*, Tucson (AZ), United States, February 23-27.

Rubiera, F., Arenillas, A., Fuente, E., Miles, N. & Pis, J. J. 1999. Effect of the grinding behaviour of coal blends on coal utilisation for combustion. *Powder Technology,* 105**,** 351-356. Available: 10.1016/S0032-5910(99)00158-8

Rudmin, M., Abdullayev, E., Ruban, A., Buyakov, A., & Soktoev, B. 2019. Mechanochemical preparation of slow release fertilizer based on glauconite–urea complexes. *Minerals,* 9. Available: doi:10.3390/min9090507

Rumpel, C., Grootes, P.M., Kögel-Knabner, I. 2001. Characterisation of the microbial biomass in lignite-containing mine soils by radiocarbon measurements. *Soil Biology & Biochemistry*, 33, 2019-2021.

Rumpel, C., Kögel-Knabner, I. 2002. The role of lignite in the carbon cycle of lignite-containing mine soils: evidence from carbon mineralisation and humic acid extractions. *Organic Geochemistry*, 33, 393–399.

Sadler, L. Y. & Sim, K. G. 1991. Reduction of coal-water mixture consistency with soda ash and lime. *Canadian Joumal of Chemical Engineering,* 69**,** 1220-1224.

Safwat, S. M. & Matta, M. E. 2018. Adsorption of urea onto granular activated alumina: A comparative study with granular activated carbon. *Journal of Dispersion Science and Technology,* 39**,** 1699-1709. Available: 10.1080/01932691.2018.1461644

Saha, B. K., Patti, A. F., Rose, M. T., Wong, V. N. L. & Cavagnaro, T. R. 2019. A slow release brown coal-urea fertiliser reduced gaseous N loss from soil and increased silver beet yield and N uptake. *Science of the Total Environment,* 649**,** 793-800. Available: 10.1016/j.scitotenv.2018.08.145

Saha, B. K., Rose, M. T., Wong, V., Cavagnaro, T. R. & Patti, A. F. 2017. Hybrid brown coal-urea fertiliser reduces nitrogen loss compared to urea alone. *Science of the Total Environment,* 601/602**,** 1496-1504. Available: 10.1016/j.scitotenv.2017.05.270

Salmanzadeh, M., Balks, M. R., Hartland, A. & Schipper, L. A. 2016. Cadmium accumulation in three contrasting New Zealand soils with the same phosphate fertilizer history. *Geoderma Regional,* 7**,** 271-278. Available: 10.1016/j.geodrs.2016.05.001

Salmanzadeh, M., Schipper, L. A., Balks, M. R., Hartland, A., Mudge, P. L. & Littler, R. 2017. The effect of irrigation on cadmium, uranium, and phosphorus contents in agricultural soils. *Agriculture, Ecosystems and Environment,* 247**,** 84-90. Available: 10.1016/j.agee.2017.06.028

Sarah, A. G. & Rajanikanth, B. S. 2016. Nox reduction from biodiesel exhaust by plasma induced ozone injection supported by lignite waste adsorption. *IEEE Transactions on Dielectrics and Electrical Insulation,* 23**,** 2006-2014. Available: 10.1109/TDEI.2016.7556472

Sardi, K. & Csitari, G. 1998. Potassium fixation of different soil types and nutrient levels. *Communications in Soil Science & Plant Analysis,* 29**,** 1843.

Sartain, J. B. 2019. *Food for turf: Slow-release nitrogen* [Online]. Penton Media Inc. Available: http://www.grounds-mag.com/mag/grounds_maintenance_food_turf_slowrelease/ [Accessed 18 October 2019].

Schollhorn, R. 1994. Materials and Models: Faces of Intercalation Chemistry. *In:* Muller-Warmuth, W. & Schollhorn, R. (eds.) *Progress in Intercalation Research.* Doordrecht: Springer.

Senna, A. M., Braga do Carmo, J., Santana da Silva, J. M. & Botaro, V. R. 2015. Synthesis, characterization and application of hydrogel derived from cellulose acetate as a substrate for slow-release NPK fertilizer and water retention in soil. *Journal of Environmental Chemical Engineering,* 3**,** 996-1002. Available: https://doi.org/10.1016/j.jece.2015.03.008

Shaviv, A. 2000. Advances in controlled release-fertilizers. *Advances in Agronomy,* 71**,** 1-49. Available: http://dx.doi.org/10.1016/S0065-2113(01)71011-5

Shaviv, A. 2005. Controlled release fertilizers. *In: IFA International Workshop on Enhanced-Efficiency Fertilizers*, Frankfurt, Germany. 28–30.

Shin, Y.-J. & Shen, J. 2007. Preparation of coal slurry with organic solvents. *Chemosphere,* 68**,** 389-393.

Simmler, M., Ciadamidaro, L., Schulin, R., Madejon, P., Reiser, R., Clucas, L., Weber, P. & Robinson, B. 2013. Lignite reduces the solubility and plant uptake of cadmium in pasturelands. *Environmental Science and Technology,* 47**,** 4497-4504. Available: 10.1021/es303118a

Simonne, E. H. & Hutchinson, C. M. 2005. Controlled-release fertilizers for vegetable production in the era of best management practices: Teaching new tricks to an old dog. *Horticulture Technology,* 15**,** 36-46.

Skodras, G., Kokorotsikos, P. & Serafidou, M. 2014. Cation exchange capability and reactivity of low-rank coal and chars. *Central European Journal of Chemistry*, 12(1), 33-43.

Smilek, J., Sedláček, P., Kalina, M. & Klučáková, M. 2015. On the role of humic acids' carboxyl groups in the binding of charged organic compounds. *Chemosphere,* 138**,** 503-510. Available: https://doi.org/10.1016/j.chemosphere.2015.06.093

Song, Z., Yao, L., Jing, C., Zhao, X., Wang, W. & Ma, C. 2017. Drying behavior of lignite under microwave heating. *Drying Technology,* 35**,** 433-443. Available: 10.1080/07373937.2016.1182547

Sonibare, O. O., Haeger, T. & Foley, S. F. 2010. Structural characterization of Nigerian coals by X-ray diffraction, Raman and FTIR spectroscopy. *Energy,* 35**,** 5347-5353. Available: https://doi.org/10.1016/j.energy.2010.07.025

Spears, D. R., Sady, W. & Kispert, L. D. 1991. An investigation of the chemistry of the pore structure of coal in the presence of a swelling solvent using a novel EPR technique. *American Chemical Society Division of Fuel Chemistry,* Reprints 36**,** 1277-1282.

Speight, J. G. 2005a. Chapter 1 - History and Terminology. *In:* Speight, J. G. (ed.) *Handbook of Coal Analysis.* New Jersey, U.S.A: Wiley & Sons, Inc.

Speight, J. G. 2005b. Chapter 5 - Proximate Analysis. *In:* Speight, J. G. (ed.) *Handbook of Coal Analysis.* New Jersey, U.S.A: Wiley & Sons, Inc.

Speight, J. G. 2005c. Chapter 6 - Ultimate Analysis. *In:* Speight, J. G. (ed.) *Handbook of Coal Analysis.* New Jersey, U.S.A: Wiley & Sons, Inc.

Speight, J. G. 2005d. Chapter 7 - Physical Properties. *In:* Speight, J. G. (ed.) *Handbook of Coal Analysis.* New Jersey, U.S.A: Wiley & Sons, Inc.

Sposito, G. & Weber, J. H. 1986. Sorption of trace metals by humic materials in soils and natural waters. *Critical Reviews in Environmental Control,* 16**,** 193-229. Available: 10.1080/10643388609381745

Stafford, A. D., Palmer, A. S., Jeyakumar, P., Hedley, M. J. & Anderson, C. W. N. 2018. Soil cadmium and New Zealand dairy farms: Impact of whole-farm contaminant variability on environmental management. *Agriculture, Ecosystems and Environment,* 254**,** 282-291. Available: 10.1016/j.agee.2017.11.033

Stevens, D. P., Mclaughlin, M. J. & Alston, A. M. 1997. Phytotoxicity of aluminium-fluoride complexes and their uptake from solution culture by Avena sativa and Lycopersicon esculentum. *Plant & Soil,* 192**,** 81-93.

Sun, J., Bai, M., Shen, J., Griffith, D. W. T., Denmead, O. T., Hill, J., Lam, S. K., Mosier, A. R. & Chen, D. 2016. Effects of lignite application on ammonia and nitrous oxide emissions from cattle pens. *The Science Of The Total Environment,* 565**,** 148-154. Available: 10.1016/j.scitotenv.2016.04.156

Suuberg, E. M., Otake, Y., Langner, M. J., Leung, K. T. & Milosavljevic, I. 1994. Coal macromolecular network structure analysis: Solvent swelling thermodynamics and its implications. *Eneryg & Fuels,* 8**,** 1247-1262.

Szalay, A. 1964. Cation exchange properties of humic acids and their importance in the geochemical enrichment of UO2++ and other cations. *Qeochimica et Cosmochimira Acta,* 28**,** 1605-1614. Available: 10.1016/0016-7037(64)90009-2

Szymanska, M., Szara, E., Sosulski, T., Was, A., Van Pruissen, G. W. P. & Cornelissen, R. L. 2019. Struvite—an innovative fertilizer from anaerobic digestate produced in a bio-refinery. *Energies,* 12. Available: 10.3390/en12020296

Tadros, T. F. 2015. Chapter 3 - Electrokinetic phenomena and zeta potential. *Interfacial Phenomena and Colloid Stability: Basic Principles.* Berlin, Germany: De Gruyter.

Tahir, M. M., Khurshid, M., Khan, M. Z., Abbasi, M. K. & Kazmi, M. H. 2011. Lignite-derived humic acid effect on growth of wheat plants in different soils. *Pedosphere,* 21**,** 124–131.

Takanohashi, T., Nakamura, K. & Iino, M. 1999. Computer simulation of methanol swelling of coal molecules. *Energy & Fuels,* 13**,** 922-926.

Takanohashi, T., Yanagida, T. & Iino, M. 1996. Extraction and swelling of low-rank coals with various solvents at room temperature. *Energy & Fuels,* 10**,** 1128-1132.

Tang, X., Qian, J., Huang, J., Wang, H. & Zhu, X. 2007. Application of tetrahydrofuran dispersant in microemulsion for fabricating titania mesoporous thin film. *Journal of colloid and interface science*, *314*(2), pp.584-588.

Tang, Y. & Wang, H. 2019. Experimental investigation on microstructure evolution and spontaneous combustion properties of secondary oxidation of lignite. *Process Safety and Environmental Protection,* 124**,** 143-150. Available: 10.1016/j.psep.2019.01.031

Temkin, M. J. & Pyzhev, V. 1940. Recent modifications to Langmuir isotherms. *Acta Physiochim. URSS,* 12**,** 217–222.

Thirmizir, M. Z. A., Rahim, S., Jani, S. M., Ishak, Z. A. M. & Taib, R. M. 2011. Kenaf-bast-fiber-filled biodegradable poly(butylene succinate) composites: Effects of fiber loading, fiber length, and maleated poly(butylene succinate) on the flexural and impact properties. *Journal of Applied Polymer Science,* 122**,** 3055-3063. Available: 10.1002/app.34046

Thouand, G., Durand, M. J., Maul, A., Gancet, C. & Blok, H. 2011. New concepts in the evaluation of biodegradation/persistence of chemical substances using a microbial inoculum. *Frontiers in Microbiology,* 2. Available: 10.3389/fmicb.2011.00164

Tipping, E., Backes, C. A. & Hurley, M. A. 1988. The complexation of protons, aluminium and calcium by aquatic humic substances: A model incorporating binding-site heterogeneity and macroionic effects. *Water Research,* 22**,** 597-611. Available: 10.1016/0043-1354(88)90061-9

Tran, H. N., You, S.-J., Hosseini-Bandegharaei, A. & Chao, H.-P. 2017. Mistakes and inconsistencies regarding adsorption of contaminants from aqueous solutions: A critical review. *Water Research,* 120**,** 88-116. Available: 10.1016/j.watres.2017.04.014

Tran, K. T. C., Rose, M. T., Cavagnaro, T. R. & Patti, A. F. 2015. Lignite amendment has limited impacts on soil microbial communities and mineral nitrogen availability. *Applied Soil Ecology,* 95**,** 140-150. Available: 10.1016/j.apsoil.2015.06.020

Treivus, E. B. 1994. On the choice of solvent for crystallization. *Journal of Crystal Growth,* 143**,** 369-370.

Trenkel, M. E. 2010a. Chapter 3 - Characteristics and types of slowand controlled-release fertilizers and nitrification and urease inhibitors. *In:* Trenkel, M. E. (ed.) *Slow- and controlled-release and stabilized fertilizers: An option for enhancing nutrient use efficiency in agriculture.* Paris, France: International Fertilizer Industry Association (IFA).

Trenkel, M. E. 2010b. *Slow- and controlled-release and stabilized fertilizers: An option for enhancing nutrient use efficiency in agriculture,* Paris, France, International Fertilizer Industry Association (IFA).

Tromans, D. & Meech, J. A. 2004. Fracture toughness and surface energies of covalent minerals: theoretical estimates. *Minerals Engineering,* 17**,** 1-15. Available: https://doi.org/10.1016/j.mineng.2003.09.006

Tu, Y., Feng, P., Ren, Y., Cao, Z., Wang, R. & Xu, Z. 2019. Adsorption of ammonia nitrogen on lignite and its influence on coal water slurry preparation. *Fuel,* 238**,** 34-43. Available: 10.1016/j.fuel.2018.10.085

van Krevelen, D. W. 1982. Development of coal research — a review. *Fuel,* 61**,** 786-790. Available: https://doi.org/10.1016/0016-2361(82)90304-0

Van Zwieten, L., Singh, B. P., Kimber, S. W. L., Murphy, D. V., Macdonald, L. M., Rust, J. & Morris, S. 2014. An incubation study investigating the mechanisms that impact N2O flux from soil following biochar application. *Agriculture, Ecosystems and Environment,* 191**,** 53-62. Available: 10.1016/j.agee.2014.02.030

Veselovskii, V. S., Vinogradova, L. P., Orleanskaya, G. L., Terpogosova, E. A. & Aleskeeva, N. D. 1967. Scientific principles for the suppression of spontaneous combustion of coal and ores. *Journal of Mining Science,* 3**,** 470-477.

Vinodh, R., Kim, D. K., Ganesh, M., Peng, M. M., Abidov, A., Krishnamurthy, N., Palanichamy, M., Cha, W. S. & Jang, H. T. 2015. Hypercross-linked lignite for NOx and CO2 sorption. *Journal of Industrial and Engineering Chemistry,* 23**,** 194-199. Available: 10.1016/j.jiec.2014.08.015

Vitousek, P. M., Aber, J. D., Howarth, R. W., Likens, G. E., Matson, P. A. & Schindler, D. W. 1997. Human alteration of the global nitrogen cycle: sources and consequences. *Ecological Applications,* 7**,** 737-750.

Vlasak, P. & Chara, Z. 2011. Effect of particle size distribution and concentration on flow behavior of dense slurries. *Particulate Science & Technology,* 29**,** 53-65. Available: 10.1080/02726351.2010.508509

Vlckova, Z., Grasset, L., Antosova, B., Pekar, M. & Kucerik, J. 2009. Lignite pre-treatment and its effect on bio-stimulative properties of respective lignite humic acids. *Soil Biology & Biochemistry,* 41**,** 1894–1901.

von Wandruszka, R. 2000. Humic acids: Their detergent qualities and potential uses in pollution remediation. *Geochemical Transactions,* 2**,** 10. Available: 10.1186/1467-4866-1-10

Wang, X. J., Wang, Z. Q. & Li, S. G. 1995. The effect of humic acids on the availability of phosphorus fertilizers in alkaline soils. *Soil Use and Management,* 11**,** 99-102. Available: 10.1111/j.1475-2743.1995.tb00504.x

Wen, P., Wu, Z., Han, Y., Cravotto, G., Wang, J. & Ye, B.-C. 2017. Microwave-Assisted Synthesis of a Novel Biochar-Based Slow-Release Nitrogen Fertilizer with Enhanced Water-Retention Capacity. *ACS Sustainable Chemistry & Engineering,* 5**,** 7374-7382. Available: 10.1021/acssuschemeng.7b01721

Worch, E. 2012. *Adsorption Technology in Water Treatment: Fundamentals, processes, and modeling,* Berlin/Boston, De Gruyter.

Woskoboenko, F. 1985. *Rheology of brown coal slurries.* PhD Thesis, University of Melbourne.

Woskoboenko, F., Hodges, S. & Krnic, Z. 1987. *Solar drying of low rank coal slurries. Vol. 3. Fundamental Investigations SECV Report ND/87/034.*

Woskoboenko, F., Hodges, S., Krnic, Z. & Brockway, D. J. 1988. Solar drying of low rank coal slurries. Volume 1: summary. SECV Research and Development Department, Report No. ND/87/034. 1.

Woskoboenko, F., Stacy, W. O. & Raisb, D. 1991. Chapter 4: Physical structure and properties of brown coal. *In:* Durie, R. A. (ed.) *The Science of Victorian Brown Coal: Structure, Properties and Consequences for Utilisation.* Oxford: Butterworth-Heinemann.

Wu, L., Liu, M. & Rui, L. 2008. Preparation and properties of a double-coated slow-release NPK compound fertilizer with superabsorbent and water-retention. *Bioresource Technology,* 99**,** 547-554. Available: 10.1016/j.biortech.2006.12.027

Xiao, X., Yu, L., Xie, F., Bao, X., Liu, H., Ji, Z. & Chen, L. 2017. One-step method to prepare starch-based superabsorbent polymer for slow release of fertilizer. *Chemical Engineering Journal,* 309**,** 607-616. Available: https://doi.org/10.1016/j.cej.2016.10.101

Xie, C. Z. 2009. *Environmental impacts of effluent containing EDTA from dairy processing plants.* Doctor of Philosophy, University of Waikato.

Xu, H., Wang, Y., Huagn, G., Fan, G., Lihui, G. & Li, X. 2016. Removal of quinoline from aqueous solutions by lignite, coking coal and anthracite. Adsorption kinetics. *Physicochemical Problems of Mineral Processing,* 52**,** 214-227. Available: 10.5277/ppmp160133

Yang, Y., Ni, X., Zhou, Z., Yu, L., Liu, B., Yang, Y. & Wu, Y. 2017. Performance of matrix-based slow-release urea in reducing nitrogen loss and improving maize yields and profits. *Field Crops Research,* 212**,** 73-81. Available: 10.1016/j.fcr.2017.07.005

Yang, Y., Tong, Z., Geng, Y., Li, Y. & Zhang, M. 2013. Biobased Polymer Composites Derived from Corn Stover and Feather Meals as Double-Coating Materials for Controlled-Release and Water-Retention Urea Fertilizers. *Journal of Agricultural and Food Chemistry,* 61**,** 8166-8174. Available: 10.1021/jf402519t

Yao, Y., Gao, B., Zhang, M., Inyang, M. & Zimmerman, A. R. 2012. Effect of biochar amendment on sorption and leaching of nitrate, ammonium, and phosphate in a sandy soil. *Chemosphere,* 89**,** 1467-1471. Available: 10.1016/j.chemosphere.2012.06.002

Yates, L. M. & Von Wandruszka, R. 1999. Decontamination of polluted water by treatment with a crude humic acid blend. *Environmental Science & Technology,* 33**,** 2076-2080. Available: 10.1021/es980408k

Yavuz, R. & Kucukbayrak, S. 1998. Effect of particle size distribution on rheology of lignite-water slurry. *Energy Sources,* 20**,** 787-794. Available: DOI: 10.1080/00908319808970098

Ye, R. W., Averill, B. A. & Tiedje, J. M. 1994. Denitrification: production and consumption of nitric oxide. *Applied And Environmental Microbiology,* 60**,** 1053-1058.

Yilmaz, M. & Deligoz, H. 1991. Investigation of the formation of humic acids from lignite by using model compounds. *Energy Sources,* 13**,** 211-216.

Zhang, X.-m., Li, Y., Hu, C., He, Z.-q., Wen, M.-x., Gai, G.-s., Huang, Z.-h., Yang, Y.-f., Hao, X.-Y. & Li, X.-y. 2019. Enhanced phosphorus release from phosphate rock activated with lignite by mechanical microcrystallization: Effects of several typical grinding parameters. *Sustainability,* 11**,** 1068. Available: 10.3390/su11041068

Zhang, Y., Li, Y., Ning, Y., Liu, D., Tang, P., Yang, Z., Lu, Y. & Wang, X. 2017. Adsorption and desorption of uranium(VI) onto humic acids derived from uranium-enriched lignites. *Water Science and Technology,* 77**,** 920-930. Available: 10.2166/wst.2017.608

Zheng, S. J. 2010. Crop production on acidic soils: overcoming aluminium toxicity and phosphorus deficiency. *Annals of Botany,* 106**,** 183-184. Available: 10.1093/aob/mcq134

Zhou, F., Cheng, J., Liu, J., Zhou, J. & Cen, K. 2018. Improving physicochemical properties of upgraded Indonesian lignite through microwave irradiation with char adsorbent. *Fuel*, *218*, pp.275-281.

Zhou, T., Wang, Y., Huang, S. & Zhao, Y. 2018. Synthesis composite hydrogels from inorganic-organic hybrids based on leftover rice for environment-friendly controlled-release urea fertilizers. *Science of The Total Environment,* 615**,** 422-430. Available: https://doi.org/10.1016/j.scitotenv.2017.09.084

APPENDIX A RECENT STUDIES ON LIGNITE IN COMBINATION WITH NITROGEN IN AGRICULTURE

A1 Lignite and N co-application

A1.1 Study A: Sun et al. (2016)

Methods

Sun et al. (2016) employed 2-phase application of lignite at a rate of 3 kg/m^2 (phase 1) and 6 kg/m^2 (phase 2) on a feedlot pen and found that NH_3 emissions from the manure in that feedlot pen were reduced by as much as 30 %. Not all the results were positive, nitrous oxide emissions increased by 40 % and 57 % in phase 1 and 2, respectively. Since the N_2 emissions were only < 0.1 % of the total excreted N, the increase in N_2 emissions was insignificant compared to the reduction of indirect N_2O emissions that follow NH_3 volatilisation. Sun et al. (2016) also found that total nitrogen losses due to a combination of leaching, runoff and N_2 emissions were reduced by 90 % compared to a pen that did not receive lignite treatment.

Discussion

It is important to note that their study dealt with very small amounts of N in the manure (1.2-2 % N). Caution must be taken when extrapolating the results found here to systems with higher concentrations of N, such as in systems simulating fertilisers 10 - 50% N. Also, Sun et al. (2016) did not investigate or speculate about the mechanisms by which lignite is able to reduce total nitrogen losses from this particular N source (manure), which

would be valuable knowledge in the development of a lignite-based controlled release-fertiliser.

A1.2 Study B: Paramashivam et al. (2016)

Methods

The study of Paramashivam et al. (2016) is interesting because they compared the NH_4^+ and NO_3^- sorption capacity of three different types of lignite: New Vale lignite (Southland, New Zealand), Charleston lignite (West Coast, New Zealand), Millerton lignite (West Coast, New Zealand). They found ammonium sorption was negligible for the Charleston and Millerton lignites but significant for New Vale lignite. This demonstrates the large variability of physicochemical characteristics amongst lignites and how this manifests itself in vastly different adsorption characteristic, a finding corroborated by (Pehlivan & Arslan, 2007). New Vale lignite displayed the highest cation exchange capacity and was selected for further experiments. No NO_3^- sorption was observed onto either of the lignites, which was due to the negative surface charge of lignite (Simmler et al., 2013). However, it must be said that in earlier research by Khan et al. (2011) NO_3^- sorption by lignite has been accomplished by chemical alteration of the surface and thermal activation.

Results

When studying the effect of pH in the range 4.4 – 6.7, batch sorption experiments showed a pH dependent variable charge on New Vale lignite that resulted in an increased sorption capacity for NH_4^+ with rising pH. Column leaching experiments showed the addition of a higher percentage of New Vale lignite increasingly reduced NH_4^+ leaching from biosolids up to a ratio of 2 : 5 biosolids - lignite, after which the reduction stagnated. In lysimeter experiments, the researchers found no significant reduction in NO_3^- leaching when co-applying Vale lignite with urea. The addition of New Vale lignite had no effect on biomass yield of urea fertilisation but reduced the effectiveness of biosolids fertilisation.

Discussion

On a critical note, Paramashivam et al. (2016) conducted the sorption study with a low concentration (100 mg/L) of $(NH_4)_2SO_4$, and the effect of pH was studied over a narrow range of 4.4 - 6.7. Other research has found that initial nutrient concentration (Tu et al., 2019) and pH (Nazari et al., 2018) can have dramatic effects on the extent of sorption, which is further discussed in Chapter 2.5. These parameters should be investigated in the proposed research to maximise nutrient adsorption onto lignite coal to create an effective controlled-release fertiliser. These issues aside, the seeming lack of increase in biomass yield that Paramashivam et al. (2016) claimed will be an issue when convincing framers to invest in a new lignite-based fertiliser strategy.

A2 Lignite-urea granulation

A2.1 Study C: Rose et al. (2016)

Methods

Rose et al. (2016) attempted to create and assess N-losses from a lignite-urea controlled-release fertiliser in the form of granules. They compared granulation of urea with brown coal by either airdrying or superheated steam drying to create urea - brown coal (UBC) granules. Drum granulation of urea powder and brown coal (50 % moisture, particle size < 3 mm) took 10 min and was followed by 72 h of airdrying. Two different ratios of urea - brown coal granules were produced: with high urea content (UBC-High, 17.1 % N) and granules with low urea content (UBC-Low, 8.7 % N). For the superheated steam drying, granular urea was pre-mixed with brown coal to create granules with an intermediate urea content (UBC-Medium, 10.7 % N). During the production process, they assumed that after 2.5 days the urea granules had dissolved into the intrinsic moisture of the brown coal structure, but concluded this on a visual basis only (urea granules were no longer visible) and did not use any analytical techniques to verify the loading of urea(-N) onto the brown coal structure.

Results

Rose et al. (2016) found that although granulation in combination with superheated steam drying increased large-scale process safety and energy efficiency compared to air drying, it resulted in a similar C : N ratio of the urea - brown coal granules compared to air drying. They also found that varying the temperature of air and superheated steam drying did not affect the C : N ratio of the final product. Moreover, they stated that the effect of superheated steam drying on the retention of urea within the granules was unclear but did not investigate this crucial aspect further.

Instead, only the two air-dried urea - brown coal granule types (UBC-Low and UBC-High) were used in a 42-day leaching and denitrification laboratory column experiment. This experiment compared the two types of urea - brown coal granules to *1)* urea alone, *2)* pure air-dried brow coal granules and *3)* non-treated plots. The fact that the superheated steam dried granules (UBC-Medium) were not incorporated in the leaching and glasshouse plant growth experiments makes it impossible to quantify their potential as controlled-release fertiliser or compare their fertiliser-N efficiency to that of air-dried granules. However, Rose et al. (2016) do imply in their article title that superheated steam drying granules have been proven to act as a slow-release fertiliser, but this has not been proven by any of the experiments described in the article.

Rose et al. (2016) found that in unplanted soil the use of low-N urea - brown coal granules significantly reduced N_2O emissions compared to urea alone, while high-N urea - brown coal granules showed no significant difference compared to urea. They suggested this might occur because low-N urea - brown coal limits nitrate availability, or it implies that low-N urea - brown coal granules limit nitrate availability, potentially by storing nitrate in a zone that inhibits denitrifying bacteria. Cayuela et al. (2014) and Van Zwieten et al. (2014) have postulated that low-N biochar limits nitrate availability because it catalyses the additional reduction of N_2O to N_2.

Discussion

Rose et al. (2016) also hypothesised that the main mechanism for N immobilisation is adsorption of urea and/or mineralised NH_4^+ to the brown coal matrix, and that oversaturation of sorption sites becomes a problem when the urea-N % becomes too high. This means the urea is no longer adsorbed to binding sites but remains in between the particles and readily dissolved out of the granule. Oversaturation of sites has also been

reported by Tran et al. (2015) for their study on lignite adsorption and by Yao et al. (2012) for biochar.

For the success of lignite-based controlled-release fertilisers, it is imperative to overcome the oversaturation of sorption sites since a low N % would decrease the theoretical use-efficiency of a lignite-based controlled-release fertiliser. A way to potentially overcome the oversaturation of the sorption sites is to increase the availability of sorption sites, allowing for a higher nutrient loading onto lignite. The availability of binding sites could potentially be increased by manipulating lignite properties, such as particle size distribution, specific surface area, and micro and meso pore volume. Manipulation of these properties could be instigated by mechanical comminution, solvent swelling, and pH and temperature variations, which will be discussed in Chapter 2.4 and 2.5.

The various experiments of Rose et al. (2016) pointed to the potential of urea adsorption into lignite and several beneficial effects of urea - brown coal fertilisers with varying C : N ratios. However, they did not investigate the nature of the proclaimed “sorption” of urea-N onto brown coal, instead only quantified the total N % of the granules. Neither did they study the uptake mechanisms by means of kinetic and isothermal studies. This meant that they did not have the tools to optimise the lignite-based controlled release fertilisers, nor were they able to assess the full potential of lignite as the matrix of a new fertilisation type.

A2.2 Study D: Saha et al. (2017)

Methods

In another study on lignite-urea granulation, Saha et al. (2017) also hypothesise that brown coal can be used in the development of controlled-release fertilisers. As in the study of Rose et al. (2016) they used granulation of brown coal with urea on the basis of C : N ratio, but Saha et al. (2017) added starch and molasses to the pan granulation process as a binder to increase granule integrity. The granules were subsequently dried in a rotary drum oven at 160 – 200 °C, reducing the moisture content of the granules to 4 - 5 %.

During the granulation and drying process, the C : N ratios of the granules increased compared to the starting ratios.

Saha et al. (2017) fabricated four different urea - brown coal (UBC) granule types with C : N ratios 1.8, 2.7, 5.4 and 10.8 (corresponding to an N content of 21.45, 17.31, 8.33 and 5.74 % respectively). They examined water absorbency of the UBC granules, the dissolution of N from the UBC granules in water, and the (chemical) structure of the granules to determine urea loading onto the brown coal structure. They also performed lab trials to determine the urease activity and water retention capacity of soil amended with the UBC granules, and designed field plot trials to compare the effect of UBC granules on biomass yield and crop N uptake to conventional urea fertilisers.

Results

The lab trials by Saha et al. (2017) demonstrated that the percentage of brown coal in the UBC granules had a rough inverse relationship with the urease activity of the soil, decreasing urease activity by as much as 45 % compared to urea alone when using UBC granules with 8.33 % N. The percentage of brown coal in the granules had a positive relationship with water absorbency, water holding capacity and water retention by soil. This meant the granules with the highest brown coal percentage showed the highest water holding capacity and cumulative water retention of all types of UBC granules and urea alone. The field plot trials resulted in significantly higher grain protein content when fertilising with urea - brown coal granules compared to urea alone, yet no difference was observed between the UBC granules with different C : N ratios.

Discussion

Fourier-Transform Infrared spectroscopy (FTIR) and Nuclear Magnetic Resonance NMR analysis of urea, brown coal and urea - brown coal granules showed that urea binds primarily to carboxylic and phenolic groups (concurring with the theory in Chapter 2.3.1). Saha et al. (2017) postulated that the observation of a lower C : N ratio resulting in a faster release of N is a consequence of the oversaturation of these carboxylic and phenolic sorption sites. However, a lower concentration gradient might be another explanation for the urea - brown coal granules with lower urea concentration showing a slower release of N and NH_4^+, and might not be entirely due to the larger amount of brown coal, as is concluded by Saha et al. (2017).

The results of the four abovementioned lignite-urea studies are summarised in Appendix B **Table 10**. When looking at **Table 10**, it becomes apparent that even though the four studies make strong claims, the data indicates that most of the results do not show a significant difference between the various tested C : N ratios. Even the comparison with urea application alone is not clearly in favour of lignite – urea application. It can be concluded that further study must go into the role of the availability of carboxylic acid and phenolic hydroxyl functional groups with regards to nutrient adsorption and retention. Mechanical and chemical manipulation is suggested as a means to increase the availability of the binding sites, and provide positive results. From the various lignite - urea fertilisation studies described above it also follows that, if there is an optimum C : N ratio for the most efficient controlled-release of N from lignite - urea fertilisers, this will need to be examined through kinetic and isothermal uptake and release studies for different types of lignite.

APPENDIX B OVERVIEW OF LIGNITE - UREA STUDIES

Table *10* *Overview of four lignite - urea controlled-release fertilisers studies and their findings. The various lignite-urea fertiliser types are distinguished by C : N ratio and C and N content. UBC =urea brown coal, BCU = brown coal urea, ns = result is not significant, - = not tested, ^ = no statistical analysis performed, * = significantly better than urea alone but no significant difference between C : N ratios, **Significantly higher activity than two of the four BCU types but still significantly lower than urea*

Author + year	Code	Application rate N (kg/ha)	C : N	C content (%)	N content (%)	Highest yield	Highest N uptake plants	Largest reduction in NH_3 loss compared to urea	Largest reduction in NH_4^+ loss compared to urea	Largest reduction in NO_3^- loss compared to urea	Largest reduction in N_2O compared to urea	Lowest urease activity in soil
Paramashivam et al. 2016	Urea+ lignite	200	67	98.5	1.5	ns	-	ns	-	ns	More loss than urea	-
	Biosolids + lignite	400	33.5	97.1	2.9	ns	-	ns	-	ns	ns	-
Rose et al. 2016	UBC-L	230 mg N/kg soil	3.0	51.5	17.1	ns	ns	ns	ns	ns	x	-
	UBC-M		4.2	45.2	10.7	-	-	-	-	-	-	-
	UBC-H	230 mg N/kg soil	5.3	46.5	8.7	ns	ns	ns	x	x	More loss than urea	-
Saha et al. 2017	BCU 1	70	1.8	39.8	21.5	^	-	-	-	-	-	**
	BCU 2		2.7	45.4	17.3	^	ns	-	-	-	-	*
	BCU 3		5.4	48.4	8.3	^	-	-	-	-	-	*
	BCU 4		10.8	53.8	5.7	^	-	-	-	-	-	*
Saha et al. 2019	BCU 1	50	1.8	39.6	22	ns	ns	*	-	-	ns	-
		100	1.8	39.6	22	ns*	ns*	*			ns*	
	BCU 2	50	2.7	45.9	17	ns	ns	*	-	-	ns	-
		100	2.7	45.9	17	ns*	ns*	*			ns*	

APPENDIX C KINETIC ADSORPTION EQUATIONS

In the proposed research, we will be dealing with the adsorption of a dissolved nutrient (solute) onto lignite (solid adsorbent). The most frequently used equations to model this type of adsorption are described in detail below, including their dependencies:

1. The *Lagergren pseudo first order equation* (**Equation 12** below), which depends on initial concentration of the solute to be adsorbed. It has been noted that this model is reliable only for the first 20-40% of the adsorption capacity (Gerente et al., 2007).

$$q_t = q_{eq}(1 - e^{-k_1 t})$$

Equation 12 *Lagergren pseudo first order equation*

Where q_t is the amount of solute adsorbed (mg/g) at reaction time t (min), q_{eq} is the amount of adsorption (mg/g) at equilibrium, and k_1 is the rate constant of adsorption (min^{-1}) (Xu et al., 2016, Kameda et al., 2017).

2. The *Elovich's equation* (**Equation 13** below) which depends on adsorption capacity of the adsorbent (Ho, 2006). This equation is rather restricted since it is not applicable to the early stages of adsorption (Aharoni and Ungarish, 1976). The equation is usually employed to model the adsorption of gases onto solids but was employed by Safwat and Matta (2018) to model the adsorption of urea onto granular activated carbon.

$$q_t = \frac{1}{\beta} ln(1 + \alpha\beta t)$$

Equation 13 *Elavich's equation*

Where q_t is the amount of solute adsorbed (mg/g) at reaction time t (min), α is the initial rate constant (mg/g*min), and β is the desorption constant (mg/g).

3. The *pseudo second order equation* (**Equation 14** below) which depends on the initial concentration (Ho, 2006). In literature this was the model that provided the best fit with the experimental data obtained from adsorption experiments involving lignite, peat or resembling (Safwat and Matta, 2018, Kameda et al., 2017, Ooi et al., 2017, Ho and McKay, 1999).

$$q_t = \frac{{q_{eq}}^2 k_2 t}{1 + q_{eq} k_2 t}$$

Equation 14 *Pseudo second order equation*

Where q_t is the amount of solute adsorbed (mg/g) at reaction time t (min), q_{eq} is the amount of adsorption (mg/g) at equilibrium, and k_2 is the rate constant of adsorption (min^{-1}) (Ho, 2006).

APPENDIX D DIFFUSION MECHANISM MODELS

To determine which step is rate limiting, the intraparticle diffusion model and Boyd kinetic model can be employed, which are described in detail below:

1. The linear portions in a plot of the *intraparticle diffusion model* (**Equation 15** below) versus $t^{1/2}$ can indicate which step is rate limiting at what point in the adsorption process (Worch, 2012, Safwat and Matta, 2018).

$$q_t = k_p \sqrt{t} + m$$

Equation 15 *Intraparticle diffusion model*

Where q_t is the amount of solute adsorbed (mg/g) at reaction time t (min), k_p is the rate constant of adsorption of the intraparticle diffusion model (mg/g*min$^{0.5}$). The intercept m is a constant that describes the magnitude of the boundary effect of the lignite particles and is positively related to the thickness of the boundary layer (Kameda et al., 2017).

2. Using the *Boyd kinetic model* (**Equation 16** below), differentiation can be made between film diffusion and intraparticle diffusion (Safwat and Matta, 2018).

$$\frac{q_t}{q_{eq}} = 1 - \frac{6}{\pi^2} \exp(-Bt)$$

Equation 16 *Boyd kinetic model*

Where q_t is the amount of solute adsorbed (mg/g) at reaction time t (min), q_{eq} is the amount of adsorption (mg/g) at equilibrium and Bt is a dimensionless function of q_t and q_{eq}. Calculating the Bt values at different times t and plotting them against t gives a plot that, when linear and going through the origin, indicates

intraparticle diffusion is the rate limiting step (Safwat and Matta, 2018, Gupta et al., 1998).

APPENDIX E ADSORPTION EQUILIBRIUM ISOTHERMS

To obtain information on the occurrence of the adsorption process, isothermal equilibrium studies are employed. Experimental data is used to plot adsorption as a function of initial nutrient concentration, followed by fitting the data to various equilibrium isotherms. These isotherms are based on specific assumptions regarding the nature of the adsorption process. Commonly employed equilibrium isotherms of interest to a lignite-nutrient adsorption study are given below, together with a description of their suppositions regarding the occurrence of adsorption:

1. *Langmuir*; the adsorption has a maximum which is determined by the number of accessible sites on the surface of the lignite particles, and all the sites have equivalent energies (Tran et al., 2017, Langmuir, 1918). Using Langmuir, the favourability of the reaction can be calculated according to $R_L = 1/1+bC_o$ (dimensionless), where $R_L << 1$ means the adsorption is very favourable (Gupta and Sharma, 2003).

$$q_e = \frac{q_m K_L C_e}{1 + K_L C_e}$$

Equation 17 *Langmuir adsorption isotherm*

With equilibrium adsorption q_e in mmol/g, equilibrium concentration C_e in mM, maximum adsorption q_m in mmol/g and equilibrium-adsorption constant K_L (Kameda et al., 2017).

2. *Freundlich*, the surface of the lignite is heterogeneous, and adsorption is a multilayer process (Freundlich, 1906).

$$q_e = K_F C_e^{1/n}$$

Equation 18 *Freundlich adsorption isotherm*

With the amount of adsorbed substrate at equilibrium q_e in mmol/g, the equilibrium concentration C_e in mmol/L, Freundlich constant K_F and exponent in the Freundlich isotherm n (Kameda et al., 2017).

3. *Redlich-Peterson*; a three-parameter isotherm that combines the assumptions of the Langmuir and Freundlich isotherms (Redlich & Peterson, 1959).

$$q_e = \frac{K_{RP} C_e}{1 + a_{RP} C_e^{g}}$$

Equation 19 *Redlich-Peterson adsorption isotherm.*

With the amount of adsorbed substrate at equilibrium q_e in mmol/g, the Redlich-Peterson constants K_{RP} in g/L and a_{RP} in $(mg/L)^{-g}$, the equilibrium concentration C_e in mmol/L and the dimensionless g has a value between 1 and 0 (Safwat & Matta 2018).

4. *Dubinin–Radushkevich*; the surface of lignite has a porous structure (Cerofolini et al., 1978).

$$q_e = q_m \exp(-Be^2)$$

Equation 20 *Dubinin-Radushkevich adsorption isotherm*

With the amount of adsorbed substrate at equilibrium q_e in mmol/g, the maximum adsorption capacity q_m in mg/g, $B = \frac{RT}{b}$ (with absolute temperature T and the universal gas constant R) and the Polanyi potential $e = RT\ln\left(1 + \frac{1}{C_e}\right)$ Safwat & Matta, 2018.

5. *Temkin*; there is a linear decrease in heat of adsorption with lignite surface coverage, and binding energies are uniformly distributed over the surface of the lignite particles (Temkin and Pyzhev, 1940). This model provided the best fit for the adsorption of urea onto activated carbon for Safwat and Matta (2018).

$$q_e = \left(\frac{RT}{b}\right)\ln(K_T C_e)$$

Equation 21 *Temkin adsorption isotherm*

With equilibrium adsorption q_e in mmol/g, the ideal gas constant R, absolute temperature T and Temkin constant K_T (Kameda et al., 2017).

6. *Harkins–Jura*; multilayer adsorption occurs on a surface with a heterogeneous pore distribution.

$$\frac{1}{q_e^2} = \left[\frac{B}{A}\right] - \left[\frac{1}{A}\right]\log C_e$$

Equation 22 *Harkins-Jura adsorption isotherm*

With equilibrium adsorption q_e in mmol/g, the Harkins-Jura constants A and B, and the equilibrium concentration C_e in mmol/L (Kameda et al., 2017).

7. *Halsey*; lignite is heterogeneous in nature and adsorption occurs through multilayer adsorption (Halsey, 1951) This model provided the best fit for the adsorption of urea onto activated carbon for Kameda et al. (2017).

$$\ln q_e = \left[\left(\frac{1}{n}\right)\ln k\right] - \left(\frac{1}{n}\right)\ln C_e$$

Equation 23 *Halsey adsorption isotherm*

With equilibrium adsorption q_e in mmol/g, the Halsey constants n and k, and the equilibrium concentration C_e in mmol/L (Kameda et al., 2017).

APPENDIX F HYPOTHESES OF THE FEASIBILITY FRAMEWORK

The following hypotheses are the basis of the research that has to be conducted in order to attain the three stages of the feasibility framework. It is indicated which objectives test the hypotheses.

	Hypothesis	Objectives
H1	Lignite can adsorb N/P/K nutrients.	Stage 1: O1 - O6
H2	Lignite can release adsorbed N/P/K nutrients in a controlled manner.	Stage 2: O1
H3	The properties of lignite can be manipulated to increase N/P/K nutrient uptake capacity:	Stage 1:
H3-a	Increased specific surface area increases N/P/K nutrient uptake capacity of lignite.	O1, O2
H3-b	Lignite particle size distribution (PSD) and pore size distribution affect nutrient uptake capacity.	O1, O2
H3-c	Certain solvents swell lignite and increase the availability of binding sites and thus N/P/K nutrient uptake capacity.	O3
H3-d	Certain nutrient species have more interaction with the lignite binding sites than others.	O4
H3-e	The pH of a lignite slurry affects the availability of binding sites and thus N/P/K nutrient uptake capacity.	O5
H3-f	Lignite N/P/K nutrient uptake capacity is related to temperature and initial nutrient concentration.	O5, O6
H4	There is a specific configuration of the properties described in *H3* that attains maximum nutrient uptake in lignite.	Stage 1: O1 - O6

H5	There is a specific configuration of the properties described in *H3* that allows for controlled-release of nutrients absorbed in lignite, independent of environmental conditions and at a rate that matches plant uptake.	Stage 2: O1, O2
H6	There is a delivery type (e.g. slurry, granules, pellets) that allows for the cheapest and most practical distribution and application of a competitive lignite-based controlled-release fertiliser deployable in precision agriculture.	Stage 3: O1, O2

APPENDIX G PROCEDURE FOR LIGNITE SLURRY PRODUCTION

(Procedure developed by Simon Wang, CRL Energy, Lower-Hut, New Zealand)

Equipment required

Attritor *[CY-SFM-5, Zhengzhou CY scientific instrument co. Ltd].*

Procedure

Pre-checking:

1. Ensure the main power of the attritor switched off.

Loading:

1. Place the 5mm diameter gel ball (grinding media) into the attritor bowl.
2. Weigh out the coal samples and water and record in the workbook
3. Place both coal and water into the attritor bowl.
4. Raise the attritor bowl up until the lid can be secured to the bowl with the 4 lockdown wingnuts, but not high enough to activate the interlock switch.
5. Secure and align the lid and hand tighten the 4 wingnuts evenly to ensure the lid is level. Uneven tightening can result in a non-sealing lid.
6. Turn on the main power of attritor.
7. Raise the bowl up until the interlock switch is activated, the control panel will light up.
8. Turn on the cooling water pump, check inline flow meter is spinning to ensure water is flowing.
9. Turn on cooling unit fan.

Grinding:

10. Check everyone in the grinding lab has hearing protection on
11. Start the attritor motor by pressing the green button and adjust the target RPM to 400 by turning the motor control dial.

12. Allow the attritor to run for a setting grinding time.
13. Shut off the attritor motor by pressing the red stop button.
14. Turn off the cooling water pump and cooling unit fan.

Slurry Extraction:

15. Lower the bowl slightly until the interlock switch cuts off and make sure the panel lights have gone off (after 3 seconds).
16. Turn off the main power.
17. Undo wingnuts on the lid and lower the bowl to the lowest point.
18. Place a clean container under the outlet hose of the extract pump to collect the feedstock slurry.
19. Start the extract pump and push the vacuum hose into the base of the bowl to suck out the slurry.
20. Move the extract hose around the base of the attritor bowl to remove as much slurry as possible.

Attritor clean-up:

21. Add 2L of water to the bowl and start the attritor for ~30 seconds (as described in the sections of loading and Grinding).
22. Using the extract pump, remove the wash water from the bowl and spay the media with water spray until the extract pump outlet runs clear.
23. Turn off the main power of the attritor.
24. Remove the stirrer and lid from the attritor by using a hex key, and wash them with tap water in a sink
25. After cleaning, assemble stirrer and lid, wipe remaining surfaces with a wet-wipe or damp cloth.
26. Spray exposed metallic surfaces with CRC, WD40 or silicone protectant.
27. Leave bowl open so that it can dry.
28. Ensure no feedstock is present on surfaces to become a dust hazard after drying

Hazards:

- **Water/slurry splash** → Slips and trips
  Clean up spills as soon as possible, do not allow slurry to dry – it becomes a dust hazard

- **Electrical** → Water splash possible, cable damage

  Check cables for damage daily, depower single and three-phase when not in operation

  Confirm interlock switch is operating correctly before each run.
- **Rotating parts** → Pinch and catch points

  Ensure guarding is in place, power off attritor prior to cleaning, emptying and refilling
- **Dust** → Fine coal particle

  Clean up spills of wet feedstock prior to drying. Wet down dried material prior to clean-up and place refuse in a sealed plastic bag for disposal.
- **Noise**

  Ensure hearing protection is worn by all staff in the room during attritor operation

APPENDIX H RECOMMENDED EXPERIMENTAL DESIGN AND RESULTS TABLE S1-O1 & S1-O2

Sample code		Grinding time (min.)	Raw lignite (gr)	Water (gr)	Solids loading		Apparent viscosity (Pa*s) at shear rate 10/s	PSD		BET			Elemental analysis: N uptake capacity (N%)	PXRD: Crystals y/-	Total N filtrate (g/L)
Slurry nr.	*Replicate code*				*Before grinding (wt.%)*	*After grinding (wt.%)*		*D50*	*D[3,2]*	*Specific surface area (m^2/g)*	*Micro pore volume (m^2/g)*	*Meso pore volume (m^2/g)*			
S1	a	1	1000	1000	50										
	b	1	1000	1000	50										
	c	1	1000	1000	50										
S2	a	3	1000	1000	50										
	b	3	1000	1000	50										
	c	3	1000	1000	50										
S3	a	5	1000	1000	50										
	b	5	1000	1000	50										
	c	5	1000	1000	50										
S4	a	10	1000	1000	50										
	b	10	1000	1000	50										
	c	10	1000	1000	50										
S5	a	15	1000	1000	50										
	b	15	1000	1000	50										
	c	15	1000	1000	50										

APPENDIX I RECOMMENDED EXPERIMENTAL DESIGN AND RESULTS TABLE SOLVENT SWELLING S1-O3

Solvent	Chemical formula	Hildebrand solubility parameter δ (MPa$^{0.5}$)	Solubility parameter when mixed with water in slurry δ_{mix} (MPa$^{0.5}$)	Strength H-bonding group	Molecular cross-section σ (nm^2)	Pore diameter for entry (nm)	Swelling (%)	PSD D[3,2] (µm)	BET			N%
									Specific surface area (m^2/g)	*Micro pore volume (m^2/g)*	*Meso pore volume (m^2/g)*	
Tetrahydrofuran (THF)	C4H8O	19.4		M								
Acetone	C3H6O	20	25.56	S/M	0.25	0.56	56					
Acetaldehyde	C2H4O	20.2		M	0.21	0.52						
Cyclohexanol	C6H12O	22.4		S								
Diaminoethane (ethylenediamine)	C2H8N2	22.6			0.23	0.54						
N,N-Dimethylacetamide	C4H9ON	22.7		M								
2-propanol*	C3H8O	23.5	25.93	S								
Acetonenitrile	C2H3N	24.4	25.57	S		0.55 (deduced)						
1-propanol*	C3H8O	24.5	26.83	S								
Jones et al. 1997 coal		*25*										
Ethanol*	C2H5OH	26.5		S	0.22	0.53						
Methanol	CH3OH	29.6		S	0.16	0.45						
Ethanolamine	C2H7ON	31.5										
Water	H2O	47.8		S	0.10	0.35						

* = disinfectant; M = moderate; S = strong. Solubility parameters in RED are example values calculated for the case study.

APPENDIX J TIME-LAPSE CODE FOR IMAGE CAPTURE

Equipment used

Computer:	MacBook Pro 2017
Source code editor:	Visual Studio Code *[Version 1.28.2 (1.28.2), Copyright: 2018 Microsoft]*
Programming language:	Python 2.7/3.7
Library:	OpenCV 3.3.0, Installed packages: XCode 10.1 and Homebrew

Purpose of code

The time-lapse code consists of 3 stages:

- Stage 1: 1 picture is taken every 60 sec for 2 hours.
- Stage 2: 1 picture is taken every 10 min for 24 hours.
- Stage 3: 1 picture every hour for 48 hours (This step is removed in the recommended methods).

The pictures are automatically stored in the cloud for processing and analysis.

Python code

```
import cv2
import numpy as np
import time

# stage 1 (1 picture every 60 sec for 2 hours)
intervala = (60*1)
nframes = (intervala*120)

# stage 2 (1 picture every 10 min for 24 hours)
intervalb = (60*10)
```

```
mframes = (intervalb*6*24)

# stage 3 (1 picture every hour for 48 hours)
intervalc = (60*60)
oframes = (intervalc*48)

cam = 0
# Create a VideoCapture object
cap = cv2.VideoCapture(cam)

cap.set(3,2304)
cap.set(4,1536)

# stage 1 (1 picture every 60 sec for 2 hours)
for i in range(nframes):
    # capture
    ret, img = cap.read()
    # save file
    cv2.imwrite('./img1_'+str(i).zfill(4)+'.png', img)
    # wait 60 seconds
    time.sleep(intervala)

# stage 2 (1 picture every 10 min for 24 hours)
for i in range(mframes):
    # capture
    ret, img = cap.read()
    # save file
    cv2.imwrite('./img2_'+str(i).zfill(4)+'.png', img)
    # wait 600 seconds
    time.sleep(intervalb)

# stage 3 (1 picture every hour for 48 hours)
for i in range(oframes):
    # capture
```

```
    ret, img = cap.read()
    # save file
    cv2.imwrite('./img3_'+str(i).zfill(4)+'.png', img)
    # wait 3600 seconds
    time.sleep(intervalc)

# Release the capture
cap.release()
```

APPENDIX K MATLAB IMAGE ANALYSIS CODE

```
clear all
close all
clc
tic
warning off;
SaveImages=1;  % Set this = 1 to save processed images for manual
checking
imagecorrect=0;  %leave as zero for now.
Mean_or_max = 0;  %If this = 1 we use mean +- st dev, if = 0 we use
max

N_std=4;  % Number of standard deviations to use in image processing
NumberOfdigits=num2str(1,'%04.f');   % change this depending on how
many files there are. e.g. if file numbers are like 0001 then set this
= '%04.f', 00001 then set to = '%05.f' ALSO change in the loop
N_Colour_Points=5;    % Number of points to use in colour analysis


%---- Defining the time axis ---------------
%The vector below (ImageTimes) has a very specific structure which is
used to define the time vector.
% There are 2 numbers separated by a ; followed by another two numbers
and a ; and so on
% The first number defines how many images, the second number defines
the
% time (in seconds) between those images.
% So for example, if we had ImageTimes = [60 60; 20 600; 10 172800];
%  Then the first 60 images were taken 60 seconds apart, the next 20
images
%  were taken 600 seconds apart (10 min) and the next 10 images were
taken
%  172800 seconds apart (48 hours?).
ImageTimes = [60 60; 20 600; 10 172800];
Time=[0];
for sss=1:length(ImageTimes)
```

```
    Time = [Time Time(end)+cumsum(ones(1,ImageTimes(sss,1)-
1).*ImageTimes(sss,2))];
end
% return
%-------  Input Prompts ------------------
cd_input = warndlg('Please select the folder where your images are
stored');
waitfor(cd_input);
newdir=uigetdir;
cd(newdir);
if SaveImages==1
    mkdir('Processed_Images')
    Outputdir=[newdir '\Processed_Images'];
end

File_name_answer = inputdlg('Please enter the name of the first image
file without file number (e.g. "image_":');
File_type_answer = inputdlg('Please enter the file type of the first
images (e.g. png, jpeg etc etc):');
prompt_answer = inputdlg('Please enter the number of samples in the
images:');
waitfor(prompt_answer);
N_Samples=str2num(prompt_answer{1});
AllFiles=dir([char(File_name_answer) '*.' char(File_type_answer)]);
A_cell = struct2cell(AllFiles);
NNN=length(A_cell(1,:));

%--------- Read + display first file for box location definition
%----------------
prompt_answer2 = inputdlg('Please enter the image number with the
lowest solids value:');
waitfor(prompt_answer2);
prompt_answer3 = str2num(prompt_answer2{1});
ImageFile=A_cell(1,prompt_answer3); % We want to change A_cell(1,???)
so we can choose which image to test on
Imag1=imread(char(ImageFile));
Imag1c=Imag1;
figure(1121);imshow(Imag1,'InitialMagnification',200)


for jjj=1:N_Samples
```

```
    clear x_box_i y_box_i x_bott_i y_bott_i TestRegion_i
    %---------  Box locations input -------------
    mydlg = warndlg(['Please click in two locations to form a box for
sample number ' num2str(jjj) '. Please make sure the box contains the
black material']);
    waitfor(mydlg);
    [x_box_i,y_box_i] = ginput(2);

    x_box(:,jjj)=x_box_i;
    y_box(:,jjj)=y_box_i;


    y_mid(jjj)=round((max(y_box(:,jjj))+min(y_box(:,jjj)))/2);
    hold on;plot([x_box(1,jjj) x_box(1,jjj)],[y_box(1,jjj)
y_box(2,jjj)],'r')
    plot([x_box(1,jjj) x_box(2,jjj)],[y_box(1,jjj) y_box(1,jjj)],'r')
    plot([x_box(2,jjj) x_box(2,jjj)],[y_box(1,jjj) y_box(2,jjj)],'r')
    plot([x_box(2,jjj) x_box(1,jjj)],[y_box(2,jjj) y_box(2,jjj)],'r')

    mydlg = warndlg(['Please click in a region where we can draw the
line away from imperfectins on the tube ' num2str(jjj)]);
    waitfor(mydlg);
    [x_midddd,y_middd] = ginput(1);
    x_mid(jjj)= x_midddd;
    plot([x_mid(jjj) x_mid(jjj)],[50 700],'y')

    mydlg = warndlg(['Please click on the bottom of test tube number '
num2str(jjj)]);
    waitfor(mydlg);
    [x_bott_i,y_bott_i] = ginput(1);
    x_bott(jjj)= x_bott_i;
    y_bott(jjj)= y_bott_i;
    plot(x_mid(jjj),y_bott_i,'b*')

    max_x(jjj)=max(x_box(:,jjj));min_x(jjj)=min(x_box(:,jjj));
    max_y(jjj)=max(y_box(:,jjj));min_y(jjj)=min(y_box(:,jjj));
    TestRegion_i=Imag1(ceil(min_y(jjj)):floor(max_y(jjj)),ceil(min_x(j
jj)):floor(max_x(jjj)),:);
    TestRegion{jjj}=double(TestRegion_i);
    pause(1)
end
```

```
if imagecorrect==1
    mydlg2 = warndlg(['Please click To the right of each sample to
help correct the image']);
    waitfor(mydlg2);
    [x_corrector,y_corrector] = ginput(N_Samples);
    hold on
end

close(1121)
figure(1121);imshow(Imag1c,'InitialMagnification',200)
for jjj=1:N_Samples
    clear x_box_c_i y_box_c_i
    mydlg = warndlg(['Please click in two locations in sample number '
num2str(jjj) ' to form a box for the colour analysis. Please make sure
the box DOES NOT contain the black material']);
    waitfor(mydlg);
    [x_box_c_i,y_box_c_i] = ginput(2);
    x_box_c(:,jjj) = x_box_c_i;
    y_box_c(:,jjj) = y_box_c_i;

    hold on; plot([x_box_c_i(1) x_box_c_i(2)],[y_box_c_i(1)
y_box_c_i(1)],'r');
    plot([x_box_c_i(1) x_box_c_i(1)],[y_box_c_i(1) y_box_c_i(2)],'r');
    plot([x_box_c_i(1) x_box_c_i(2)],[y_box_c_i(2) y_box_c_i(2)],'r');
    plot([x_box_c_i(2) x_box_c_i(2)],[y_box_c_i(2) y_box_c_i(1)],'r');
    min_x_c(jjj) = ceil(min(x_box_c_i));
    max_x_c(jjj) = floor(max(x_box_c_i));
    min_y_c(jjj) = ceil(min(y_box_c_i));
    max_y_c(jjj) = floor(max(y_box_c_i));
end
pause(3)

%-------  Pre-allocating matrix sizes ----------------
Cell_Lower_M = zeros(NNN,N_Samples);
Cell_Upper_M = Cell_Lower_M;
Colours_RGB = zeros(NNN,3,N_Samples);
%--------------------------------------------

%-----------   Iterating over all of the images  ----------------
for iii=1:NNN
```

```
    Time_Left = NNN - iii
    clear ImageFile Imag1 Imag1c Imag1col TR_mean TR_median TR_std
TR_range Line1 L_upper cell_upper L_lower cell_lower fig1 Sorted
IndexSort
    ImageFile = A_cell(1,iii);
    Imag1=imread(char(ImageFile));
    Imag1col = Imag1;
    figure(1121);imshow(Imag1)

  % -----   Bit that needs to go in a loop: START ------------------
  for jjj=1:N_Samples
    %--------  New colour bit -----------------
    clear Sorted IndexSort Imag1c Imag1c_Red Imag1c_Green Imag1c_Blue
TR_mean TR_median TR_std TR_range Line1  L_upper cell_upper L_lower
cell_lower Line1  TestRegion_R TestRegion_G TestRegion_B  TR_mean_R
TR_median_R TR_std_R TR_range_R  TR_mean_G TR_median_G TR_std_G
TR_range_G
    clear Line1_R Line1_G Line1_B L_upper_R L_upper_G L_upper_B
L_lower_R L_lower_G L_lower_B
    Imag1c =
Imag1col([min_y_c(jjj):max_y_c(jjj)],[min_x_c(jjj):max_x_c(jjj)],:);
    Imag1c_Red = Imag1c(:,:,1);
      Imag1c_Green = Imag1c(:,:,2);
        Imag1c_Blue = Imag1c(:,:,3);
    [Sorted,IndexSort] = sort(Imag1c_Red(:));
    Colours_RGB(iii,1,jjj)=mean((Imag1c_Red(IndexSort(end -
N_Colour_Points + 1:end))));
    Colours_RGB(iii,2,jjj)=mean((Imag1c_Green(IndexSort(end -
N_Colour_Points + 1:end))));
    Colours_RGB(iii,3,jjj)=mean((Imag1c_Blue(IndexSort(end -
N_Colour_Points + 1:end))));
    %-----------------------------------------------
%---- NOTE:  If this piece of code is present then we evaluate the
%histogram at each time/image. If not then is based on 1st image
averages;
    clear TestRegion
    Imag1_temp = Imag1;
    if imagecorrect==1
        clear Diff_Image_R Diff_Image_G Diff_Image_B
Multiplier_Image_correct_R Multiplier_Image_correct_G
Multiplier_Image_correct_B
```

```
        Multiplier_Image_correct_R =
255./Imag1(:,round(x_corrector(jjj)),1);
        Multiplier_Image_correct_G =
255./Imag1(:,round(x_corrector(jjj)),2);
        Multiplier_Image_correct_B =
255./Imag1(:,round(x_corrector(jjj)),3);
        clear Imag1_temp
        Imag1_temp = Imag1;
        Imag1_temp(:,:,1) =
Imag1_temp(:,:,1).*repmat(Multiplier_Image_correct_R,1,length(Imag1(1,
:,1)));
        Imag1_temp(:,:,2) =
Imag1_temp(:,:,2).*repmat(Multiplier_Image_correct_G,1,length(Imag1(1,
:,1)));
        Imag1_temp(:,:,3) =
Imag1_temp(:,:,3).*repmat(Multiplier_Image_correct_B,1,length(Imag1(1,
:,1)));
    end

    TestRegion_R{jjj}=double(Imag1_temp(ceil(min_y(jjj)):floor(max_y(j
jj)),ceil(min_x(jjj)):floor(max_x(jjj)),1));
    TestRegion_G{jjj}=double(Imag1_temp(ceil(min_y(jjj)):floor(max_y(j
jj)),ceil(min_x(jjj)):floor(max_x(jjj)),2));
    TestRegion_B{jjj}=double(Imag1_temp(ceil(min_y(jjj)):floor(max_y(j
jj)),ceil(min_x(jjj)):floor(max_x(jjj)),3));
%-----------------------------------------------
    TR_mean_R=mean(TestRegion_R{jjj}(:));
    TR_median_R=median(TestRegion_R{jjj}(:));
    TR_std_R=std(TestRegion_R{jjj}(:));

    if Mean_or_max==1
        TR_range_R=[TR_mean_R-
N_std*TR_std_R,TR_mean_R+N_std*TR_std_R];
    else
        TR_range_R=[0 max(TestRegion_R{jjj}(:))];
    end

        TR_mean_G=mean(TestRegion_G{jjj}(:));
    TR_median_G=median(TestRegion_G{jjj}(:));
    TR_std_G=std(TestRegion_G{jjj}(:));
    TR_range_G=[TR_mean_G-N_std*TR_std_G,TR_mean_G+N_std*TR_std_G];
```

```
        TR_mean_B=mean(TestRegion_B{jjj}(:));
    TR_median_B=median(TestRegion_B{jjj}(:));
    TR_std_B=std(TestRegion_B{jjj}(:));
    TR_range_B=[TR_mean_B-N_std*TR_std_B,TR_mean_B+N_std*TR_std_B];

    Line1_R=double(Imag1_temp(:,x_mid(jjj):x_mid(jjj),1));
    Line1_R(find(Line1_R<min(TR_range_R)))=255;
    Line1_R(find(Line1_R>max(TR_range_R)))=255;
    Line1_R(find(Line1_R<=max(TR_range_R) &
Line1_R>=min(TR_range_R)))=0;

    Line1_G=double(Imag1_temp(:,x_mid(jjj):x_mid(jjj),2));
    Line1_G(find(Line1_G<min(TR_range_G)))=255;
    Line1_G(find(Line1_G>max(TR_range_G)))=255;
    Line1_G(find(Line1_G<=max(TR_range_G) &
Line1_G>=min(TR_range_G)))=0;

    Line1_B=double(Imag1_temp(:,x_mid(jjj):x_mid(jjj),3));
    Line1_B(find(Line1_B<min(TR_range_B)))=255;
    Line1_B(find(Line1_B>max(TR_range_B)))=255;
    Line1_B(find(Line1_B<=max(TR_range_B) &
Line1_B>=min(TR_range_B)))=0;

    L_upper_R=Line1_R(y_mid(jjj):-1:3) + Line1_R(y_mid(jjj)-1:-1:2) +
Line1_R(y_mid(jjj)-2:-1:1);
    L_upper_G=Line1_G(y_mid(jjj):-1:3) + Line1_G(y_mid(jjj)-1:-1:2) +
Line1_G(y_mid(jjj)-2:-1:1);
    L_upper_B=Line1_B(y_mid(jjj):-1:3) + Line1_B(y_mid(jjj)-1:-1:2) +
Line1_B(y_mid(jjj)-2:-1:1);

    L_upper = L_upper_R;% + L_upper_G + L_upper_B;

    cell_upper=y_mid(jjj) - min(find(L_upper>0));

    L_lower_R=Line1_R(y_mid(jjj):1:end-2) +
Line1_R(y_mid(jjj)+1:1:end-1) + Line1_R(y_mid(jjj)+2:1:end);
    L_lower_G=Line1_G(y_mid(jjj):1:end-2) +
Line1_G(y_mid(jjj)+1:1:end-1) + Line1_G(y_mid(jjj)+2:1:end);
    L_lower_B=Line1_B(y_mid(jjj):1:end-2) +
Line1_B(y_mid(jjj)+1:1:end-1) + Line1_B(y_mid(jjj)+2:1:end);
```

```
    L_lower = L_lower_R + L_lower_G + L_lower_B;
%     pause
    cell_lower=y_mid(jjj) + min(find(L_lower==3*255*3));

    if isempty(cell_lower)
        cell_lower = y_bott(jjj);
   end

     if isempty(cell_upper)
        cell_upper = y_bott(jjj);
    end

    Cell_Lower_M(iii,jjj)=cell_lower;
    Cell_Upper_M(iii,jjj)=cell_upper;

    fig1=figure(1121);hold on;plot([x_mid(jjj) x_mid(jjj)],[cell_lower
cell_upper],'r')
    plot(x_mid(jjj),y_bott(jjj),'b*')
    hold on;plot([x_box(1,jjj) x_box(1,jjj)],[y_box(1,jjj)
y_box(2,jjj)],'r')
    plot([x_box(1,jjj) x_box(2,jjj)],[y_box(1,jjj) y_box(1,jjj)],'r')
    plot([x_box(2,jjj) x_box(2,jjj)],[y_box(1,jjj) y_box(2,jjj)],'r')
    plot([x_box(2,jjj) x_box(1,jjj)],[y_box(2,jjj) y_box(2,jjj)],'r')

  end

    % -----   Bit that needs to go in a loop: END -----------------

    if SaveImages==1
        cd(Outputdir);
        saveas(fig1,['OutputImages' num2str(iii,'%04.f') '.jpg'])
        cd(newdir);
    end
    close all

end

ManualBottom=ones(size(Cell_Upper_M)).*y_bott;
```

```
cd(Outputdir);
HeightsFinal=abs(Cell_Upper_M-ManualBottom);

display('Writing xlsx file...')
display('Writing xlsx file...')
display('Writing xlsx file...')
display('Writing xlsx file...')
display('Please wait')
for jjj=1:N_Samples
    N_Samples-jjj
    xlswrite('HeightsOutputNew.xlsx',{'Time (seconds)'},['Sample '
num2str(jjj)],'A1')
    xlswrite('HeightsOutputNew.xlsx',Time',['Sample '
num2str(jjj)],'A2')

    xlswrite('HeightsOutputNew.xlsx',{'Height'},['Sample '
num2str(jjj)],'B1')
    xlswrite('HeightsOutputNew.xlsx',{'Mean colour: Red'},['Sample '
num2str(jjj)],'C1')
    xlswrite('HeightsOutputNew.xlsx',{'Mean colour: Green'},['Sample '
num2str(jjj)],'D1')
    xlswrite('HeightsOutputNew.xlsx',{'Mean colour: Blue'},['Sample '
num2str(jjj)],'E1')
    xlswrite('HeightsOutputNew.xlsx',HeightsFinal(:,jjj),['Sample '
num2str(jjj)],'B2')
    xlswrite('HeightsOutputNew.xlsx',Colours_RGB(:,1,jjj),['Sample '
num2str(jjj)],'C2')
    xlswrite('HeightsOutputNew.xlsx',Colours_RGB(:,2,jjj),['Sample '
num2str(jjj)],'D2')
    xlswrite('HeightsOutputNew.xlsx',Colours_RGB(:,3,jjj),['Sample '
num2str(jjj)],'E2')
end

display('FINSHED!')
display('FINSHED!')
display('FINSHED!')
display('FINSHED!')
toc
```